Friedrich-Schiller-Universität Jena
seit 1558

MOLEKULARE ANALYSEN DES AKTINZYTOSKELETTS UND DES POLAREN WACHSTUMS IN *ASHBYA GOSSYPII* UND *CANDIDA ALBICANS*

DISSERTATION

zur Erlangung des akademischen Grades
doctor rerum naturalium
(Dr. rer. nat.)

vorgelegt dem Rat der Biologisch-Pharmazeutischen Fakultät
der Friedrich-Schiller-Universität Jena

von Andrea Walther
geboren am 25.04.1979 in Frankenberg/Sachsen

Gutachter:

1. _____
2. _____
3. _____

Tag des Rigorosums:

_____

Tag der öffentlichen Verteidigung:

_____

Inhalt |

Zusammenfassung

1. Zusammenfassung

Pilze wachsen entweder in einer zelligen Form wie z.B. die Bäckerhefe *Saccharomyces cerevisiae* oder in filamentöser Form wie z.B. *Aspergillus nidulans* oder *Ashbya gossypii*. Einige humanpathogene Pilze wie *Cryptococcus neoformans* und *Candida albicans* sind dimorphe Pilzen, die einen Wechsel von der Hefe- in die Hyphenphase vollziehen können.
Ziel dieser Arbeit war die vergleichende molekulare Untersuchung solcher Wachstumsprozesse sowohl in *A. gossypii* als auch in *C. albicans*, um ein besseres Verständnis über die morphogenetischen Netzwerke, die polares Zellwachstum steuern, zu erzeugen.

Zunächst wurden Module zur gerichteten Veränderung von Genen erzeugt, um die Funktionsanalyse von Genen in diesen Modellorganismen zu erleichtern. Mit diesen Modulen können durch PCR spezifische Kassetten erzeugt werden, die die exakte Deletion von offenen Leserastern ermöglichen. Ebenso gelingt damit die Expression von Genen durch regulierbare Promotoren wie auch die Fusion mit dem Gen, das für das grün fluoreszierende Protein (GFP) kodiert. Mit den entsprechenden Fusionsproteinen kann die subzelluläre Lokalisierung des Zielproteins bestimmt werden. Der zusammengesetzte Aufbau der Module erlaubt es in einfacher Weise, Markergene oder GFP-Varianten auszutauschen, um neue Module herzustellen. Die Module können mit einer minimalen Anzahl an Oligonukleotid-Primern amplifiziert werden, um das gesamte Spektrum der Kassetten zu erzeugen. Mit Verwendung der etablierten PCR-Technologie konnte eine große Zahl von Transformanten in *C. albicans* mit den gewünschten Veränderungen erzeugt werden, wenn die Länge der benutzen flankierenden Sequenzen 100bp betrug.

Polares Zellwachstum, insbesondere in filamentösen Pilzen, erfordert eine stark polarisierte Organisation des Aktinzytoskeletts. Das Aktinzytoskelett wird durch GTP-bindende Proteine der Rho-Familie reguliert. Rho-Proteine sind molekulare Schalter, die mit Hilfe von Guanin-Nukleotid Austauschfaktoren (GEFs) und GTPase-aktivierenden

Proteinen (GAPs) zwischen aktivierten (GTP-gebundenen) und inaktiven (GDP-gebundenen) Zuständen wechseln können. Aktivierte G-Proteine leiten Signale an Effektorproteine weiter, die wie im Fall des konservierten Cdc42-Proteins, die Aktinassemblierung regulieren und damit die Etablierung von Zellpolarität und deren Beibehaltung kontrollieren.
Das *A. gossypii* Genom enthält mit *RHOH* eine zusätzliches Rho-Gen, das in *S. cerevisiae* nicht vorkommt. *RHOH* ist ein Paralog des *A. gossypii RHO1* Gens und entstand durch lokale Genduplikation. RhoHp besitzt zumindest überlappende Funktionen mit Rho1p bei der Aufrechterhaltung von Zellpolarität.

Das Hauptziel dieser Arbeit war die Durchführung tiefer gehender Analysen zur Funktion der Wiskott-Aldrich-Syndrom Protein- (WASP)-Homologen in *A. gossypii* und *C. albicans*. In beiden Organismen spielen die entsprechenden Homologen *WAL1*-Gene eine Schlüsselrolle für die Beibehaltung der Zellpolarität und der Positionierung des kortikalen Aktins (der sog. Aktinpatches). In einer vorangegangenen Arbeit konnte gezeigt werden, dass die Deletion von *WAL1* in *C. albicans* die Hyphenbildung inhibiert, während eine *A. gossypii* WASP Mutante langsames Wachstum und angeschwollene Hyphen aufweist.
Durch die Verwendung der *in vivo* Fluoreszenz-Zeitraffer-Mikroskopie konnte die Aufnahme des lipophilen Farbstoffes FM4-64 beobachtet werden. Dabei konnte die Verteilung und die Bewegung kleiner Endozytosevesikel und größerer Vakuolen durch hochauflösende Mikroskopie sichtbar gemacht werden. Es zeigte sich, dass hochmobile Vesikel in den Hyphenspitzen des *A. gossypii* Wildtyps vorhanden waren, die in der *A. gossypii ⊿wal1* Mutante gänzlich fehlten. In der *A. gossypii ⊿wal1* Mutante erscheinen solche Vesikel in subapikalen Hyphenabschnitten. Dies zeigt, dass die Position der Aktinpatches, die sich ebenfalls in diesem subapikalen Bereich befinden, mit der Position von Endozytoseereignissen zusammenfällt. Dies spricht für eine Rolle von Wal1p bei der Positionierung der Aktinpatches in der Hyphenspitze.
Die Bewegung von großen Vakuolen, die im Wildtyp leicht als zytoplasmatische Strömung sichtbar ist, war in *A. gossypii ⊿wal1* Hyphen sehr langsam und erschien unkoordiniert. Interessanter Weise wurden Mitochondrien im Gegensatz zu den Endosomen in den Hyphenspitzen der *⊿wal1* Mutante ebenso wie im Wildtyp gefunden. Dies belegt, dass es unterschiedliche Transportmechanismen für beide Organellen geben muss.
Ähnliche Ergebnisse bezüglich des Endozytosedefektes wurden auch für die *C. albicans ⊿wal1* Mutante erhalten. Die starke Verzögerung bei der Aufnahme des Farbstoffes wurde

von Defekten in der Vakuolenmorphogenese begleitet, die in *A. gossypii* nicht beobachtet werden konnten. Statt einer einzigen großen Vakuole enthielten *C. albicans ⊿wal1* Zellen oftmals viele kleinere.

Keine der hypheninduzierenden Bedingungen, die bei *C. albicans wal1* Mutante getestet wurden, resultierte in einer Hyphen- bzw. Myzelbildung. Hyphenbildung bei *C. albicans* hängt von der Ras1-GTPase ab, die zwei Signalkaskaden, eine MAP-Kinase Kaskade und den cAMP-Weg, aktiviert. Integration eines konstitutiv aktiven *RAS1*-Allels in einen Wildtyp-Stamm resultiert in Hyphenwachstum auch unter nichtinduzierenden Bedingungen. Trotzdem war dieses konstitutiv aktive *RAS1*-Allel in der *⊿wal1* Mutante nicht in der Lage, die Hyphenbildung anzuregen.

In einem *in vivo* Mausmodell einer systemischen *C. albicans* Infektion zeigte der *C. albicans wal1* Stamm verglichen mit Wildtypstämmen eine reduzierte Virulenz. Dieses Verhalten wurde mit einem *in vitro* Modell unter Verwendung von Schweinedarm-Epithel verglichen. Zellen des Wildtyps zeigten sehr starke Adhärenz an dieses Epithel und wurden zu einer intensiven Hyphenbildung angeregt. Im Gegensatz dazu zeigten *⊿wal1* Zellen nur eine schwache Adhäsion und waren auch unter diesen Bedingungen nicht in der Lage, Hyphen zu bilden. Dies zeigt, dass zwei Faktoren, die die Virulenz von *C. albicans* beeinflussen können, von einer Deletion des *WAL1* Gens beeinflusst werden.

Die vorgelegte Arbeit belegt, dass WASP-Homologe eine entscheidende Rolle bei der Koordinierung von Endozytose und polarem Zellwachstum in zwei unterschiedlichen Pilzsystemen spielen. Dies zeigt, dass polares Wachstum nicht nur einen intakten sekretorischen Weg benötigt, sondern auch von der korrekten Positionierung des kortikalen Aktins an den Stellen der Endozytose in der Hyphenspitze abhängt.
In *C. albicans* konnten selbst starke hypheninduzierende Stimuli den *wal1* Defekt nicht supprimieren. Damit konnte gezeigt werden, dass die Signalwege zum Aktinzytoskelett und die Aktinassemblierung essentiell an der Hyphenmorphogenese in *C. albicans* und *A. gossypii* beteiligt sind.

Summary

2. Summary

Fungi grow either in a cellular form as, for example, the baker´s yeast *Saccharomyces cerevisiae* or in filaments as, e.g. *Aspergillus nidulans* or *Ashbya gossypii*. Some human fungal pathogens like *Cryptococcus neoformans* or *Candida albicans* are dimorphic and are able to switch between yeast and filamentous stages.
The aim of this thesis was a comparative molecular analysis of growth processes in both the filamentous fungus *A. gossypii* and the dimorphic pathogen *C. albicans* to elucidate morphogenetic networks that regulate polarized cell growth.

Initially, a number of gene targeting modules were constructed to facilitate the functional analysis of genes of these model organisms. With these modules PCR-generated cassettes allow the precise deletion of open reading frames, their expression under the control of regulatable promoters, as well as fusions to the green fluorescent protein encoding gene (GFP) to monitor subcellular localization of the corresponding proteins. Modular set up of these cassettes allows the facile exchange of markers or GFP-variants to construct new modules. All of these modules can be amplified with a minimal set of primers to generate the whole array of specific cassettes. Using the established PCR-based gene targeting technology generated a large amount of correctly targeted transformants in *C. albicans* when using terminal target homology regions of 100bp.

Polarized cell growth, particularly in filamentous fungal cells, requires a strongly polarized organization of the actin cytoskeleton. The actin cytoskeleton is regulated by GTP-binding proteins of the Rho-GTPase-family. Rho-proteins are molecular switches that cycle between GTP-bound ‘on’- and GDP-bound ‘off’-states with the help of guanine-nucleotide exchange factors (GEFs) and GTPase-activating proteins (GAPs). Activated G-proteins relay signals to effector proteins, which in case of the conserved Cdc42p regulate actin assembly and thus controls cell polarity establishment and the maintenance of polarized cell growth.

The *A. gossypii* genome contains an additional Rho-gene, *RHOH*, which is not present in *S. cerevisiae*. *RHOH* is paralogous to *AgRHO1* and originates from a local gene duplication event. RhoHp shares at least partial overlapping functions with Rho1p in the maintenance of cell wall integrity.

The major goal of this thesis was the detailed analysis on the function of Wiskott-Aldrich Syndrome Proteins (WASPs) in *A. gossypii* and *C. albicans*. The corresponding *WAL1* gene homologs of both organisms play key roles in the maintenance of cell polarity and the positioning of cortical actin patches. Previously, deletion of *WAL1* in *C. albicans* was shown to abolish mycelial formation whereas the *A. gossypii* WASP mutant showed slow growth and swollen hyphae.
With the use of *in vivo* fluorescence time lapse microscopy the uptake of the lipophilic dye FM4-64 could be monitored. The distribution and movement of small endocytic vesicles and larger vacuoles could be visualized by high resolution microscopy. These analysis demonstrated the presence of highly motile vesicles at the hyphal tips in the *A. gossypii* wild type which were completely absent in the *Agwal1* mutant. In *wal1* hyphae endocytotic vesicles appeared in subapical regions indicating that the positioning of cortical actin patches which also accumulated subapically correlates with sites of endocytosis in *A. gossypii* and that Wal1p plays a key role in the apical positioning of actin patches. Movement of larger vacuoles, easily visible as cytoplasmic streaming in the wild type, was very slow and appeared uncoordinated in *wal1* hyphae. Strikingly, the absence of endosomes in the tips of *wal1* hyphae was contrasted by the apical wild type-like localization of mitochondria indicating that different transport mechanisms exist for both organelles.
Similar results were obtained by analyzing endocytosis in *C. albicans wal1* cells. The strong delay in dye uptake was accompanied by defects in vacuolar morphogenesis which were not easily detectable in *A. gossypii*. Instead of one large vacuole, *C. albicans wal1* cells contained a larger number of smaller vacuoles.

None of the hyphal inducing cues tested resulted in hyphae formation and mycelial growth in *C. albicans wal1* cells. Hyphal growth in *C. albicans* depends on signalling via the Ras1p-GTPase which activates two signal transduction pathways, a MAP-kinase cascade and the cAMP-pathway. Integration of a constitutively active *RAS1*-allele results in hyphal

growth under non-inducing conditions in the wild type. However, such a constitutively active *RAS1*-allele was not able to trigger hyphal development in *C. albicans wal1* cells.

In an *in vivo* mouse model of systemic infection the *C. albicans wal1* strain exhibited reduced virulence in comparison to wild type strains. This was compared with an *in vitro* model using porcine intestinal epithelium (PIE). Wild type cells adhered strongly to the PIE and readily developed filaments. In contrast, *wal1* cells showed only weak adherence and were unable to generate hyphae. This indicates that two factors which may affect the virulence of *C. albicans* are affected by the deletion of *wal1* in *C. albicans*.

This work could show that WASP proteins play an important role in coordinating endocytosis and polarized cell growth in two different fungal systems. This demonstrates that polarized morphogenesis not only requires an intact secretory pathway but also depends on correct positioning of cortical actin patches at sites of endocytosis at the hyphal apex. In *C. albicans* even strong inducers of filamentation cannot suppress a defect in *WAL1.* Together these results demonstrate that signalling to and assembly of the actin cytoskeleton is essential for polarized hyphal morphogenesis in *C. albicans* and *A. gossypii*.

Einleitung

3. Einleitung

Das Wachstum von Pilzen kann in einzelliges, hefeartiges und filamentöses Wachstum unterschieden werden. Einzelliges Wachstum findet man zum Beispiel bei der Bäckerhefe *Saccharomyces cerevisiae* oder der Spalthefe *Schizosaccharomyces pombe*. Hefezellen von *S. cerevisiae* bilden durch Knospung Tochterzellen aus, die sich nach erfolgter Mitose von ihren Mutterzellen durch Zytokinese und Septenbildung abtrennen. Kolonien bestehen daher bei Hefen aus Einzelzellen, die jedoch über ins Medium abgegebene Stoffe, zum Beispiel Ammoniumionen bei *S. cerevisiae* miteinander kommunizieren können (Vachova und Palkova, 2005). Filamentöses Wachstum, wie bei den Ascomyzeten *Ashbya gossypii*, *Neurospora crassa* oder *Aspergillus nidulans*, oder bei den Basidiomyzeten *Schizophyllum commune* und *Coprinus cinereus* ist im Gegensatz dazu durch schlauchförmig elongierte und aneinander gereihte Zellen gekennzeichnet, die durch Septen voneinander getrennt sind und ein verzweigtes Myzel bilden. Ferner sind dimorphe Pilze, wie *Ustilago maydis*, *Candida albicans* oder *Holleya sinecauda*, in der Lage, unter bestimmten Umweltbedingungen vom einzelligen zum filamentösen Wachstum zu wechseln (Wendland, 2001).

Bei *Candida albicans* unterliegt der Wechsel von der Hefe- in die Hyphenphase einer Quorum-sensing Kontrolle, die über die Produktion von Farnesol bei einer hohen Zelldichte (>10^6 Zellen/ml) den Wechsel in die Hyphenphase blockiert (Kruppa *et al.*, 2004, Hornby *et al.*, 2001).

Für den humanpathogenen Pilz *C. albicans* kann der Wechsel vom einzelligen hefeartigen Wachstum zum filamentösen Wachstum einen wichtigen Faktor darstellen, um *C. albicans* Zellen einen entscheidenden Vorteil bei der Besetzung von Wirtsnischen zu verschaffen. Dabei spielen Adhäsion der Hyphen an humane Epithelien, Penetration dieser Epithelien und die Evasion der zellulären Immunantwort eine wichtige Rolle in der Pathobiologie von *C. albicans* (Odds, 1994, Gantner *et al.*, 2005). Der Pilz tritt in der Bevölkerung häufig als Kommensale des Gastro-Intestinal Traktes, der Mundschleimhaut oder der Haut auf. Neben Vaginalinfektionen und Oberflächenmykosen auf der Haut, verursacht *C. albicans*, insbesondere bei immunsupprimierten Patienten, systemische Infektionen, die zum Befall

der inneren Organe und zur Sepsis führen, wenn der Erreger in die Blutbahn eingeschwemmt wird (Berman und Sudbery, 2002; Lott *et al.*, 2005). Bedeutend für die Ausbildung einer *C. albicans* Infektion sind Virulenzfaktoren, die eine entscheidende Rolle für die Pathogenese von *C. albicans* spielen (Casadevall und Pirofski, 2001). Virulenzfaktoren sind definiert als Eigenschaften, die für die Etablierung einer Erkrankung notwendig sind. Dabei spielt insbesondere die Wirt-Pathogen Interaktion eine wichtige Rolle (Odds *et al.*, 2001).

Histoplasma capsulatum, der Verursacher der Histoplasmose, ist ein weiterer fakultativer, intrazellulärer, dimorpher Pilzpathogen. Im Boden kommt er in seiner filamentösen Form vor und produziert asexuelle Sporen. Durch Inhalation von Mikrokonidien oder Myzelfragmenten gelangt *H. capsulatum* in die Lunge. Von dort wird er von alveolaren Makrophagen aufgenommen und tritt in die pathogene Hefephase über. Die Vermehrung erfolgt intrazellulär und die Hefezellen können sich auf die inneren Organe wie Leber und Milz ausbreiten (Eissenberg und Goldman, 1991; Hwang *et al.*, 2003; Newman, 2005).

Der wichtigste pathogene Pilz, der über die Luft verbreitet wird, ist jedoch *Aspergillus fumigatus* (Brakhage und Langfelder, 2002). Für *A. fumigatus* steht derzeit ebenso wie für *C. albicans* kein sexueller Zyklus für klassische genetische Experimente zur Verfügung. Unter den Basidiomyzeten tritt insbesondere *Cryptococcus neoformans* als wichtiger Pathogen in Erscheinung. *C. neoformans* ist ein Heterobasiodiomyzet. Haploide Hefen können zu Heterokaryen verschmelzen, die Filamente bilden. An den Enden solcher Filamente entstehen Basidien, in denen Kernfusion, Meiose und Sporenentwicklung erfolgt (Lengeler *et al.*, 2000). Interessanter Weise sind MATα-Zellen bei *C. neoformans* in der Lage, sexuelle Reproduktion in Abwesenheit eines MATa-Paarungspartners durchzuführen (Lin *et al.*, 2005). Diese Art der sexuellen Fortpflanzung hat weitreichende Konsequenzen für die Populationsdynamik und liefert Möglichkeiten, genetische Informationen auszutauschen in einem Wirt-Pathogen Verhältnis, dass hauptsächlich auf der klonalen Verbreitung von Zellen innerhalb eines Wirtes beruht.

Um eine Infektion im menschlichen Wirt zu verursachen, muss *C. albicans* dem Immunsystem des Wirts entkommen und sich im Wirt verbreiten und vermehren können. Einer der ersten Schritte während einer Infektion ist die Adhäsion des Pilzes an Wirtsgewebe, in die Proteine der ALS-Familie (Agglutinin-like sequences) involviert sind (Hoyer, 2001; Kamai, 2002). ALS-Gene zeichnen sich durch interne repetitierte Elemente aus, deren Zahl in verschiedenen Isolaten variierte und damit eine phänotypische

Variabilität in der Adhäsion herbeiführte (Oh *et al.*, 2005). Neben der Adhäsion an Wirtsepithelien haben diese Proteine entscheidende Bedeutung bei der Adhäsion von *C. albicans* an medizinische Geräte und der Bildung von Biofilmen (Chandra *et al.*, 2001; O'Connor *et al.*, 2005; Abbildung 1).

Einen weiteren bedeutenden Virulenzfaktor stellen Proteinasen wie die sekretierten Aspartylproteinasen (Saps) dar, die von der 10 Gene umfassenden SAP-Familie codiert werden (Naglik *et al.*, 2003). Diese Gene werden während der Infektion unterschiedlich exprimiert. Die Sap1-3 Proteine tragen dabei entscheidend zur Gewebeschädigung und Invasion oraler Epithelien bei, während Sap4-6p bei systemischen Infektionen von Bedeutung sind (Schaller *et al.*, 1999; Schaller *et al.*, 2000; Sanglard *et al.*, 1997; Felk *et al.*, 2002).

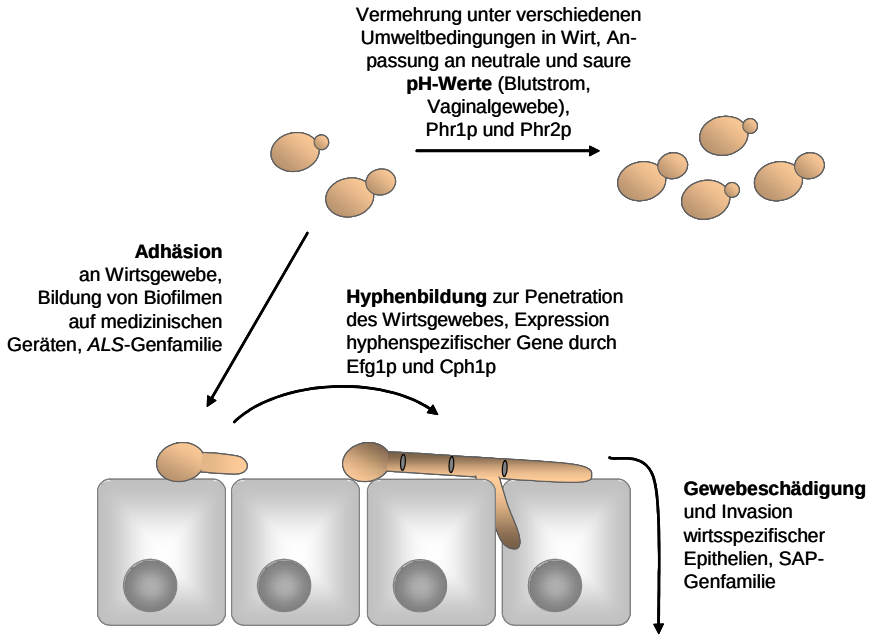

Abbildung 1 | Schematische Übersicht über Virulenzfaktoren, die für die Pathogenität von *C. albicans* von Bedeutung sind.

C. albicans kann, im Gegensatz zu *S. cerevisiae*, zwischen Hefeform und filamentösen Wachstum wechseln. Die Bäckerhefe *S. cerevisiae* zeigt jedoch unter stickstoff-limitierten Bedingungen einen Wechsel von hefeartigem zu pseudohyphalem Wachstum (Gimeno *et al.*, 1992). Zu den Genen, die für den Wechsel zum pseudohyphalen Wachstum von

Bedeutung sind, gehören die Transkriptionsfaktoren Ste12p und Phd1p, welche durch den MAP-Kinase-Weg (MAP mitogen-activated protein kinase) bzw. die Aktivität der Ras2-GTPase aktiviert werden (Gimeno und Fink, 1994; Roberts und Fink, 1994). Homologe von Ste12p und Phd1p konnten in *C. albicans* als Cph1p und Efg1p identifiziert werden (Liu *et al.*, 1994; Stoldt *et al.*, 1997). Analog zu den Ergebnissen in *S. cerevisiae* werden diese Transkriptionsfaktoren durch die MAP-Kinase-Kaskade, die in *S. cerevisiae* die Pheromonantwort weiterleitet, bzw. die Ras1-GTPase aktiviert. Dies führt zur Induktion hyphenspezifischer Gene und letztlich zur Ausbildung filamentösen Wachstums (Leberer *et al.*, 2001). Es konnte gezeigt werden, dass eine Δ*efg1*/Δ*cph1* Mutante nicht mehr in der Lage ist, unter induzierenden Bedingungen Hyphen auszubilden und avirulent im Tierexperiment ist (Lo *et al.*, 1997).

Morphogenese, die Ausbildung von unterschiedlichen Zellformen und Transportprozesse sind abhängig von einer dynamischen Organisation des Aktinzytoskeletts. Defekte in einem zentralen Regulatormodul, angetrieben von der Rho-GTPase Cdc42p, führen zu ungerichtetem isotropem Wachstum. Die Deletion von *CDC42* führt in *S. cerevisiae* zum Verlust der Fähigkeit, Tochterzellen ausbilden zu können und zum Zelltod. Intrazellulär kommt es zu weiteren Kernteilungen, so dass multinukleäre Zellen entstehen. In ähnlicher Weise erlaubt die Deletion von Cdc42p in *A. gossypii* das Keimen von Sporen. Auch hier werden mehrere Kernzyklen durchlaufen, aber die Bildung eines Keimschlauches findet nicht statt (Johnson und Pringle, 1990; Wendland und Philippsen, 2001).
Auch für die Ausbildung von Hyphen in *C. albicans* ist die Organisation des Aktinzytoskeletts von zentraler Bedeutung (Woo *et al.*, 2003, Bassilana *et al.*, 2003; Bassilana *et al.*, 2005).
Um den morphogenetischen Wechsel von der Hefe- in die Hyphenphase auf molekularer Ebene zu verstehen, ist es notwendig, die Prozesse, die zur Etablierung und Aufrecherhaltung polaren Wachstums beitragen, zu analysieren.
Die frühe Phase der Knospenbildung von Hefezellen ist bei *S. cerevisiae* und *C. albicans* durch eine polare Wachstumsphase gekennzeichnet, in der die eigentliche Wachstumszone auf einen kleinen Bereich an der Spitze der neuen Tochterzelle beschränkt ist. Erreicht die Tochterzelle eine bestimmte Größe, geht dieses polare Wachstum in isotropes Wachstum über (Lew und Reed, 1993). Vorraussetzung für die Ausbildung des stark polarisierten Wachstums in filamentösen und dimorphen Pilzen ist neben der Etablierung einer Zellpolarität an einer Hyphenspitze insbesondere die

Aufrechterhaltung von gerichteten Transportprozessen in die Hyphenspitze, um kontinuierliches Wachstum der Hyphenspitze zu ermöglichen. Hierbei könnte neben dem Mikrotubulizytoskelett das Aktinzytoskelett eine wesentliche Rolle spielen. GTP-bindende Proteine der Rho-Familie (Ras-Homologie) beeinflussen dabei als Regulatoren die Organisation des Aktinzytoskeletts und bestimmen über Effektorproteine die Zell- und Wachstumsformen eukaryotischer Zellen (Hall, 1998). Rho-GTPasen treten in zwei unterschiedlichen Zuständen auf, einer aktiven, GTP- beladenen Form und einer inaktiven, GDP-beladenen Form. Durch Nukleotid-Austauschfaktoren (GEFs – guanine nucleotid exchange factor) werden G-Proteine mit GTP beladen und aktiviert, GTPase aktivierende Proteine (GAPs – GTPase activating protein) katalysieren dagegen die Hydrolyse von GTP zu GDP durch die GTPase und führen diese in eine inaktive Form zurück. Die GTPase und ihre spezifischen GEF- und GAP-Proteine bilden Module, bei denen die GTPase durch ihre Regulatoren Zyklen der Aktivierung und Inaktivierung druchlaufen kann (Schmidt und Hall, 1998). Störungen dieser Module durch Deletion eines regulatorischen Proteins oder durch konstitutive Aktivierung der GTPase können zu Veränderungen in der Signalwirkung des entsprechenden Moduls führen und daraus beispielsweise für das Cdc42-Modul zu aberranten Prozessen bei der Knospenbildung, der Länge polaren Wachstums und der Septierung führen. Die Deletion der GTPase Rho1p in *S. cerevisiae* führt andererseits zu Defekten in der Zellwandbiosynthese, die durch die fehlende Aktivierung der β-(1,3)-Glukansynthase durch Rho1p verursacht werden (Cabib *et al.*, 1998).

Die räumliche und zeitliche Kontrolle von Wachstums-, Morphogenese- und Zytokineseprozessen setzt ein intaktes und komplexes Netzwerk von Proteinen voraus. Dabei werden ausgehend von GTPase-Modulen, wie Cdc42p, Informationen an Effektorproteine weitergegeben, die an der Organisation des Aktinzytoskeletts beteiligt sind. Solche Proteine sind z.B. Forminhomologe aber auch Proteine der Wiskott-Aldrich-Syndrom-(WASP)- oder IQGAP-Proteinfamilie, welche zu drei konservierten Proteinfamilien, die in eukaryotischen Organismen an der Assemblierung des Aktinzytoskeletts beteiligt sind, gehören.

Das Aktinzytoskelett kann in drei hauptsächliche Strukturen unterteilt werden, an der jeweils eine Effektorproteinfamilie beteiligt ist. Kortikales Aktin (Aktinpatches) enthält das Wiskott-Aldrich Syndrom Protein, lineare Aktinfilamente werden von Formin-Homologen gebildet und IQGAP / *CYK1* ist in *S. cerevisiae* an der Bildung von Aktinringen beteiligt. In *S. cerevisiae* ist der Arp2/3-Komplex an der Polarisierung und Bewegung kortikalen

Aktins sowie der Endozytose beteiligt (McCollum *et al.*, 1996; Moreau *et al.*, 1996; Moreau *et al.*, 1997; Winter *et al.*, 1997; Winter *et al.*, 1999). An Aktinfilamenten findet der gerichtete Transport von Vesikeln, Molekülen oder Zellwandkomponenten über Myosin-Motorproteine statt (Pruyne *et al.*, 2004).

Für die meisten an der Aktinassemblierung beteiligten Proteine bei *S. cerevisiae* finden sich entsprechende Homologe in filamentösen oder dimorphen Pilzen. Einige dieser Proteine, wie Abp1p, Pan1p und Las17p/Bee1p, welches für das *S. cerevisiae* Homologe des humanen Wiskott-Aldrich Syndrom Proteins (WASP) kodiert, sind Aktivatoren des Arp2/3-Komplexes (Winter *et al.*, 1999; Duncan *et al.*, 2001; Goode *et al.*, 2001, Kaksonen *et al.*, 2003). Die Aktivierung des Arp2/3-Komplexes führt zur Assemblierung kortikalen Aktins und zur Bildung von verzweigten Aktinfilamenten (Madania *et al.*, 1999; Engqvist-Goldstein und Drubin, 2003). Las17p/Bee1p interagiert mit Myo3p bzw. Myo5p, den zwei Typ-I Myosinen in *S. cerevisiae* (Evangelista *et al.*, 2000). Die Deletion beider Gene, *MYO3* und *MYO5*, in *S. cerevisiae* führt zu gravierenden Wachstumsdefekten der Zellen. Beide Proteine werden durch Phosphorylierung durch die PAK-ähnlichen Kinasen Ste20p oder Cla4p aktiviert (Wu *et al.*, 1996; Wu *et al.*, 1997) Damit kann die Aktivierung des Arp2/3-Komplexes durch Cdc42p und dessen Effektorproteine Ste20p und Cla4p und deren Wechselwirkungen mit dem Myo3/5-Las17/Bee1p-Komplex stattfinden.

Die funktionelle Analyse dieser Homologen in filamentösen Pilzen ist daher von Bedeutung für das Verständnis von Endozytose in diesen Organismen. Trotz anfänglicher Zweifel am Vorkommen und der Bedeutung von endozytotischen Prozessen in filamentösen Pilzen (Torralba und Heath, 2002) gibt es nun - auch durch diese Arbeit - überwältigende Beweise für das Auftreten von Endozytose in verschiedenen Pilzen, wie *Magnaporthe grisea*, *Aspergillus nidulans* und *A. gossypii* (Yamashita und May, 1998; Atkinson *et al.*, 2002; Walther und Wendland, 2004b).

Die Familie der Forminhomologen ist in eukaryoten Zellen an der Assemblierung linearer Aktinfilamente beteiligt (Sagot *et al.*, 2002a, b; Kobielak *et al.*, 2004). *S. cerevisiae* besitzt zwei Forminhomologe, Bni1p und Bnr1p, während SEPA das einzige Formin von *Aspergillus nidulans* darstellt (Harris *et al.*, 1997; Imamura *et al.*, 1997). Formine enthalten eine N-terminale GTPase-Bindedomäne (GBD), durch die sie direkt mit Cdc42p interagieren können, gefolgt von einer FH3-Domäne (formin homology) und einer C-terminalen FH1-FH2-DAD-Domäne (Diaphanous autoinhibitory domain), die an der Assemblierung von linearen Aktinfilamenten beteiligt ist, sowie autoinhibitorische Funktionen hat (Moseley *et al.*, 2004).

WASP-ähnliche Proteine vom Menschen aber überraschender Weise auch der Basidiomyzeten *Ustilago maydis* und *Cryptococcus neoformans* besitzen eine GTPase-Bindedomäne, so dass eine direkte Interaktion mit Cdc42p oder Rac-Proteinen möglich ist. Dagegen haben WASP-Homologe von Ascomyzeten wie *S. cerevisiae*, *A. gossypii* oder *C. albicans* keine solche Domäne und können damit nicht direkt mit Cdc42p interagieren. Für das *C. albicans* WASP-Homologe Wal1p sowie das *A. gossypii* Wal1p konnte in dieser Arbeit gezeigt werden, dass diese Proteine eine wichtige Funktion bei der Vakuolenmorphologie, der Endozytose sowie für das polare Hyphenwachstum aufweisen.

Neben Aktinpatches und Aktinfilamenten stellen Aktinringe, die während der Zytokinese gebildet werden, die dritte strukturierte Form von Aktin in der eukaryoten Zelle dar. Die Zytokinese stellt den abschließenden Schritt des Zellzyklus während der mitotischen Vermehrung von Zellen dar und kann in drei wesentliche Schritte unterteilt werden, die die Auswahl einer Teilungsstelle, die systematische Assemblierung von Proteinkomplexen an diese Stelle und die dynamische Kontraktion des Aktinringes und damit verbundene Bildung eines Septums beinhalten (Walther und Wendland, 2003b). In einzelligen Hefen erfolgt die Trennung von Mutter- und Tochterzelle durch die partielle Hydrolyse des chitinreichen Septums durch Chitinasen der Tochterzelle. In filamentösen Pilzen bleibt das Septum als Abtrennung zweier Zellkompartimente bestehen und wird nicht durch Chitinasen degradiert. Zudem trennt das Septum die Zytoplasmen beider Zellen nicht vollständig, sondern erhält eine Septenpore aufrecht, die beide Zytoplasmen miteinander verbindet und die Bildung multizellulärer Myzelien ermöglicht. Die Zytokinese setzt weitere Prozesse wie die DNA-Replikation und Mitose voraus, die der Trennung von Mutter- und Tochterzelle vorangehen und eine gleichmäßige Verteilung des genetischen Materials auf beide Zellen realisieren. Während der Anaphase werden die Kerne entlang von Mikrotubuli mittels minusende-gerichteter Motorproteine transportiert. Zytoplasmatisches Dynein ist ein solches Motorprotein, dessen Deletion in *S. cerevisiae* und *C. albicans* zu fehlerhafter Kernverteilung führt und daraus in einem Defekt der Zelltrennung resultiert (Li *et al.*, 1993; Martin *et al.*, 2004).

Ergebnisse und Diskussion

4. Ergebnisse und Diskussion

4.1. Konstruktion von pFA-Modulen zur Funktionsanalyse von *A. gossypii*- und *C. albicans*-Genen

4.1.1. pFA-Module in *C. albicans*

Für die diploide Hefe *C. albicans* erfordert die Funktionsanalyse von Genen die Deletion beider allelischer Kopien eines Gens. Bisherige Verfahren zur Erzeugung von Disruptionsmutanten gingen von der Klonierung von Deletionskassetten aus. Für die Deletion mehrerer Gene wurde dafür das URA-Blaster-System etabliert. Dieses System basiert auf der Verwendung eines Δ*ura3* Ausgangsstammes (z.B. CAI-4, Δ*ura3*), der mit einer *URA3*-Kassette transformiert wird, die an beiden Enden durch direkte Sequenzwiederholungen und Homologieregionen zum Zielgen flankiert werden (Alani und Kleckner, 1987; Fonzi und Irvin, 1993). Zunächst erfolgt hier eine Selektion der integrativen Transformanten auf Uridin-Mangelmedien. Durch die direkten Sequenzwiederholungen, die das *URA3*-Gen flankieren, kann eine homologe Rekombination über diese direkten Sequenzen zum Verlust des *URA3*-Markergens und einer der direkten Sequenzwiederholungen führen. Um diese zufälligen Ereignisse aufzufinden und Δ*ura3* Zellen zu identifizieren, die die gewünschte Gendeletion tragen, kann eine negative Selektion verwendet werden. Zellen, die ein funktionelles *URA3*-Gen besitzen, wandeln 5FOA (5-Fluororotsäure) in eine zytotoxische Substanz um und können damit negativ selektiert werden. Die Selektion von Δ*ura3* Mutanten bewirkt, dass nur Mutanten mit defektem oder über Rekombination deletiertem *URA3*-Gen wachsen können. Auf diese Weise kann in beliebig vielen Wiederholungen dieser Selektionsmarker mehrfach verwendet werden. Ein solches System ist vorteilhaft, da für *C. albicans* kein vollständiger sexueller Zyklus bekannt ist, so dass keine Kreuzungsexperimente durchgeführt werden können, die zu Mutanten mit bestimmten Markerkombinationen führen würden.

Durch das Candida Genom Projekt steht nun das nahezu vollständige Genom dieses Pilzes zur Verfügung und eröffnet die Möglichkeit, eine Vielzahl von Genen zu charakterisieren. Jüngste Veröffentlichungen beschrieben eine Funktionsanalyse von Genen, die auf einem PCR-basierenden Verfahren beruht. Dabei wurde versucht, ein Verfahren zur Gendisruption nach dem erfolgreichen Muster von *S. cerevisiae* zu etablieren (Wach *et al.* 1994). Es wurde gezeigt, dass mit 50-60bp Homologieregion zum Zielgen flankierend zum Selektionsmarker erfolgreich Gene in *C. albicans* deletiert werden können, allerdings mit einer nur geringen Effizienz. Um die Deletion beider Allele eines Gens beschleunigen zu können und nicht notwendiger Weise die URA-Blaster Kassetten einsetzen zu müssen, wurde ein neuer Stamm konstruiert, BWP17, der die Verwendung dreier Auxotrophiemarker erlaubt (Wilson *et al.*, 1999; Wilson *et al.*, 2000). In einer weiterführenden Arbeit wurden Module konstruiert, die die Amplifikation von

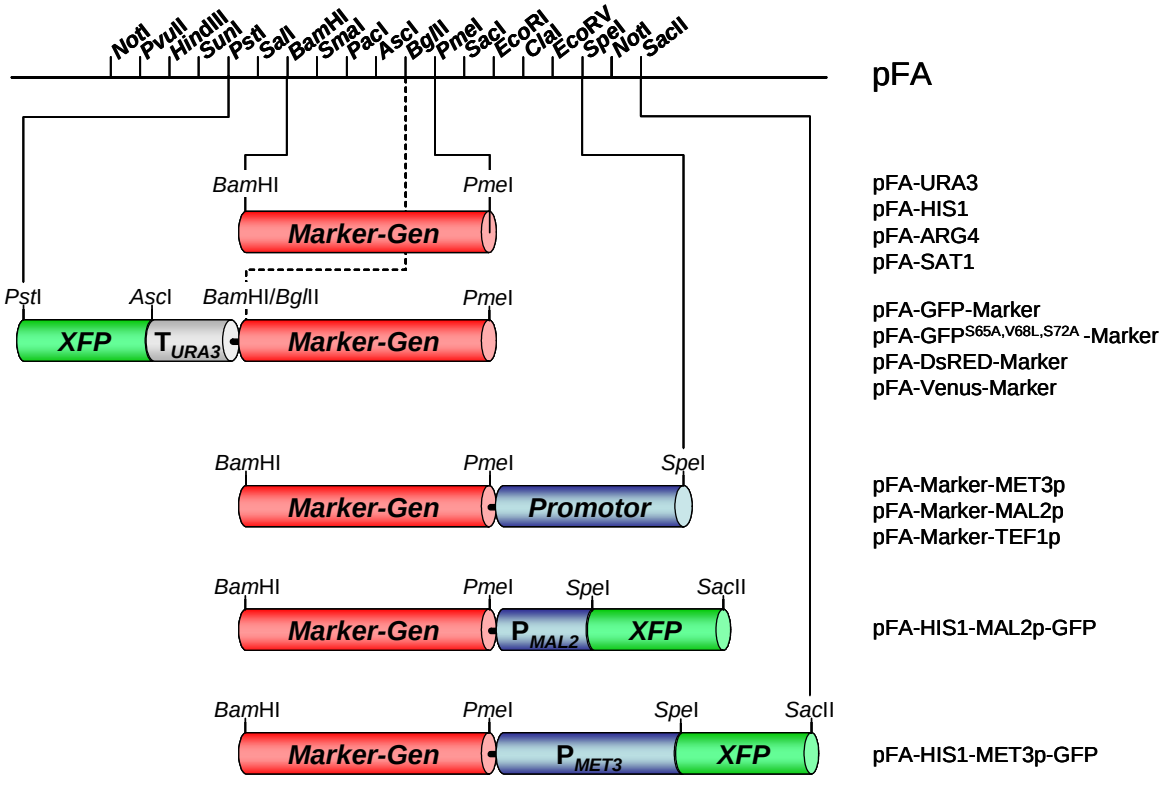

Abbildung 2 | Übersicht und Nomenklatur der klonierten *C. albicans* Module in den pFA-Vektor. Restriktionsstellen, die für die Klonierung verwendet wurden, sind an den Modulen dargestellt. *URA3*, *HIS1*, *ARG4* und *SAT1* wurden als Markergene verwendet. Vier Varianten fluoreszierender Proteine bzw. die drei Promotoren *MAL2*p, *MET3*p und *TEF1*p wurden mit den Markergenen kombiniert. Zusätzlich wurde ein Modul für die N-terminale Fusion eines Proteins mit GFP konstruiert.

Markergenen mit einem kleinen Set an Oligonukleotidprimern ermöglichte. Die hier verwendeten Homologieregionen an beiden Seiten des Markergens betrugen etwa 70bp (Gerami-Nejad *et al.*, 2001; Gerami-Nejad *et al.*, 2004). Die in den Arbeiten dieser Gruppen verwendeten Plasmide und PCR-Kassetten waren mit 3-4kb ziemlich groß und mitunter schwierig zu amplifizieren. Um die Transformationseffizienz zu steigern und die Deletion von Genen zu beschleunigen, wurde in unserer Arbeitsgruppe eine große Zahl von Modulen zusammengestellt, die auf dem für *S. cerevisiae* verwendeten Standardvektor pFA basieren. Vorteil dieser Module ist, dass nur eine geringe Zahl an Oligonukleotiden notwenig ist, um sowohl die Deletion eines Gens als auch dessen Fusion mit GFP oder den Austausch des endogenen Promotors gegen einen regulierbaren Promotor zu realisieren.

In Experimenten mit Oligonukleotiden, die etwa 70bp Homologie zum Zielgen aufwiesen, wurden nur sehr geringe Transformantenzahlen erhalten. Zudem war die korrekte Integration der Disruptionskassette nicht nachweisbar. Um die Zahl der Transformanten mit korrekter Integration des Selektionsmarkers zu steigern, wurde die Länge der den Selektionsmarker flankierenden Sequenzen erhöht. Bei einer Länge von 100bp Homologieregion konnten erfolgreich Transformanten isoliert werden, die mittels PCR auf die korrekte Integration des Selektionsmarkers überprüft wurden. Diese verlängerten Oligonukleotide konnten eine hohe Transformationseffizienz und korrekte Integration der Disruptionskassette sicherstellen. Die 120bp langen Oligonukleotide sind zusammengesetzt aus etwa 100 Basen, die homolog zum Zielgen sind, gefolgt von 20 Basen, die homolog zu den pFA-Modulen sind und die Amplifikation der Module mittels PCR ermöglichen (Abbildung 2). Unter Verwendung eines verbesserten Transformationsprotokolls basierend auf der Lithiumacetat-Methode von *S. cerevisiae* konnte die Transformationseffizienz deutlich gesteigert werden (Walther und Wendland, 2003a). Hierbei erwiesen sich zwei Parameter als entscheidend. Die Inkubation der Zellen in Lithiumacetat wurde über 20 Stunden statt nur 30 Minuten durchgeführt und die Hitzeschocktemperatur wurde für *C. albicans* auf 44°C anstelle von 42°C bei *S. cerevisiae* erhöht.

Für die Funktionsanalyse von Genen in *C. albicans* wurde der Stamm BWP17 ausgewählt, der aus CAI-4 entstanden ist, aber neben der Deletion des *URA3*-Gens zusätzlich Deletionen im *HIS1*- und *ARG4*-Gen besitzt. Außerdem wurde zusätzlich der dominante Marker *SAT1* in die pFA-Module eingefügt, der die Selektion von Nourseothricin (cloNAT)-resistenten *C. albicans* Mutanten erlaubt. Damit stehen vier

Selektionsmarker zur Verfügung. In einer neueren Arbeit wurde gezeigt, dass der BWP17-Stamm durch die Deletion des *HIS1*-Gens eine Chromosomenaneuploidie erzeugt wurde durch den Verlust der Gene zwischen *HIS1* und dem Telomer des Chromosoms V (Selmecki *et al.*, 2005). Dieses Problem tritt nicht in der Konstruktion eines neuen Stammes auf, in dem neben den drei Auxotrophiemarkergenen, die auch in BWP17 Verwendung fanden (*HIS1*, *URA3* und *ARG4*) auch beide Kopien des *LEU2*-Gens deletiert wurden (Noble und Johnson, 2005).

Neben den zwei Varianten des grün-fluoreszierenden Proteins wurde zusätzlich zu den bisherigen pFA-Modulen noch eine Variation des gelb-fluoreszierenden Proteins (Venus) hinzugefügt, die eine höhere Stabilität bei 37°C besitzt und damit die Lokalisierung von Proteinen unter hypheninduzierenden Bedingungen ermöglichen kann (Abbildung 2).

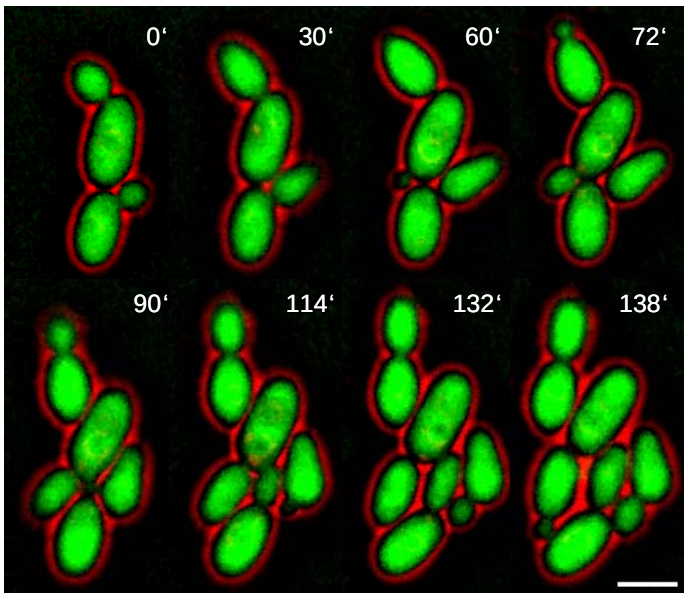

Abbildung 3 | *In vivo* Fluoreszenz-Zeitraffer-Aufnahmen einer *C. albicans TEF1/tef1::TEFp-GFP-HIS1* Mutante.
Die Zellen wurden bis zur exponentiellen Phase in YPD-Vollmedium inkubiert, anschließend gründlich gewaschen und auf ½ CSM-Agar mikroskopiert. Die Bildaufnahme erfolgte in einem Intervall von 3 Minuten. Der vollständige Film M01 befindet sich im CD-Anhang der Dissertation. Der Größenbalken entspricht 5µm.

In den pFA-Modulen wurden zwei regulierbare Promotoren verwendet. Dabei ist der Promoter des *MET3*-Gens abschaltbar durch Zugabe der Aminosäuren Methionin und

Cystein im Medium während der Promoter des *MAL2*-Gens nur unter Verwendung von Maltose als Kohlenstoff-Quelle aktiviert wird (Care *et al.*, 1999; Backen *et al.*, 2000; Gola *et al.*, 2003). Als konstitutiver Promotor sollte nun auch der *TEF1*-Promotor verwendet werden. In einer ersten Untersuchung zur Stärke der Expression wurde das grün-fluoreszierende Protein mit diesem Promotor fusioniert. Die daraus entstandene Mutante ist in Abbildung 3 dargestellt, das GFP leuchtet zytoplasmatisch. Dieser Stamm kann zukünftig als Ausgangsstamm für genomische N-terminale GFP-Fusionen von Zielgenen verwendet werden, so dass die daraus resultierenden Proteine in der Zelle lokalisiert werden könnten.
Die Verwendung des *URA3*-Gens als Selektionsmarker wurde verschiedentlich kritisiert, da der Status der *URA3*-Expression einen Einfluss auf die Ergebnisse von Virulenztests haben kann. Deletionsmutanten, z.B. der Ausgangstamm BWP17 sind aufgrund des Fehlens des *URA3*-Genproduktes avirulent in Mausversuchen (Bain *et al.*, 2001; Cheng *et al.* 2003; Sharkey *et al.*, 2005). Ein möglicher Ausweg ist die Erhöhung der *URA3*-Expression durch die Reintegration von *URA3* in das *RPS10*-Gen (Brand *et al.*, 2004). Allerdings könnte auch die Verwendung des pFA-URA3-MX dieses Problem lösen. In dieser Kassette steht das C. albicans *URA3*-Gen unter der Kontrolle des *A. gossypii TEF1* Promotors, der in *C. albicans* funktionell ist (Goldstein *et al.*, 1999).

4.1.2. pFA-Module in *A. gossypii*

PCR-basierende Verfahren zur Deletion von Genen wurden auch für den filamentösen Ascomyzeten *A. gossypii* eingeführt (Wendland *et al.*, 2000). In der vorliegenden Arbeit wurden, basierend auf den Modulen für *C. albicans*, weitere PCR-Module konstruiert, um das Spektrum an verfügbaren Markergenen zu erhöhen.
A. gossypii ist ein filamentöser Pilz, der durch laterale Verzweigungen im jungen Myzel und dichotome Verzweigungen im gereiften Myzel gekennzeichnet ist (Abbildung 4). Aus einer Transformation von *A. gossypii* entstehen Mutanten, die heterokaryotisch sind, also neben transformierten Kernen auch untransformierte Wildtyp-Kerne in einem Zellkompartiment besitzen. Durch Sporulation und selektive Keimung der Sporen ist es bei *A. gossypii* aber möglich, homokaryotische Myzelien zu erhalten (Abbildung 4).

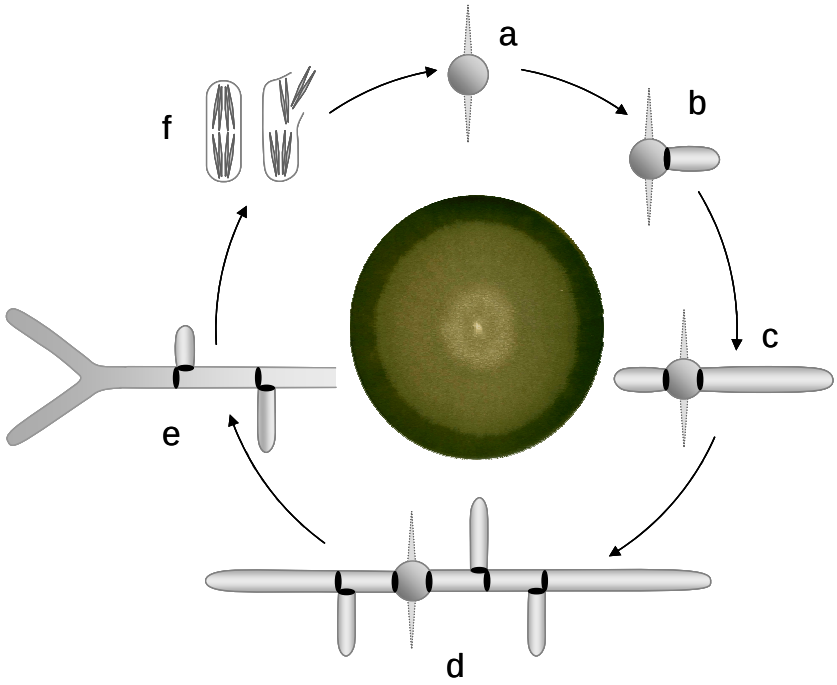

Abbildung 4 | Lebenszyklus von *A. gossypii*.
Im Zentrum ist eine *A. gossypii*-Kolonie gezeigt, welche zentral angeimpft wurde und für eine Woche bei 30°C inkubiert wurde. Die gelbe Farbe wird durch die hohe Riboflavinproduktion des Pilzes verursacht. Der innere hellere Ring des Myzels ist die Sporulationszone des Pilzes. Charakteristische Wachstumsphasen (a-f) sind dargestellt: (a) Sporenkeimung durch Ausbildung einer Keimblase, (b) Ausbildung einer ersten Keimhyphe, (c) bipolares Verzweigungsmuster, (d) juveniles Myzel, (e) dichotome Verzweigungen an den Hyphenspitzen, (f) Sporulation.

Damit lassen sich phänotypische Untersuchungen an mutanten Stämmen durchführen oder terminale Phänotypen nach der Deletion von essentiellen Genen bestimmen (Wendland und Philippsen, 2001). Neben den bereits bekannten Selektionsmarkern *LEU2* und *GEN3* steht auch für *A. gossypii* ein Nourseothricin-Resistenzmarker *NAT1* zur Verfügung (Abbildung 5).

Ein Ziel dieser Arbeit war es, unter Verwendung der pFA-Module gezielt Mutanten zu erzeugen und mit diesen dynamische Wachstumsprozesse mit Hilfe der Zeitraffer-Fluoreszenzmikroskopie zu untersuchen, um so Einblicke in wichtige zelluläre Prozesse, wie Vakuolendynamik und Endozytose von *C. albicans* und *A. gossypii* zu erhalten. Die Ergebnisse dieser Arbeiten werden in den folgenden Kapiteln ausführlich erläutert.

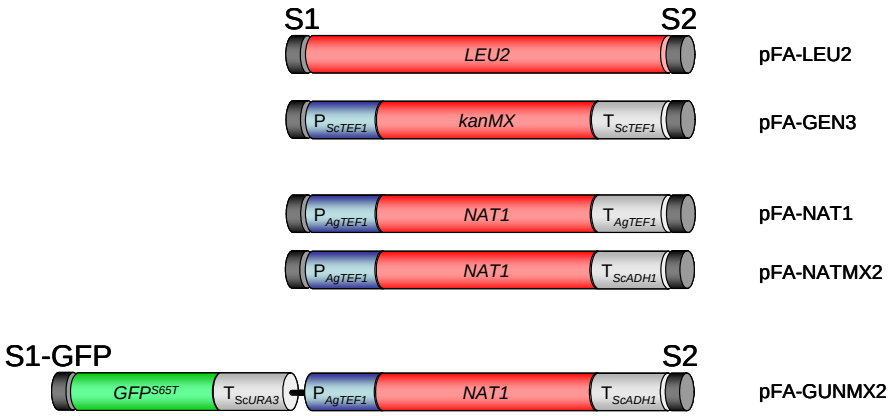

S1 Homologie-Region: 5‘-GAAGCTTCGTACGCTGCAGGTC-3‘
S2 Homologie-Region: 5‘-TCTGATATCATCGATGAATTCGAG-3‘
S1-GFP Homologie-Region: 5‘-GGTGCAGGCGCTGGAGCTG-3‘

Abbildung 5 | Übersicht und Nomenklatur der *A. gossypii* Module im pFA-Vektor.
Für die Deletion von Genen in *A. gossypii* stehen drei Marker zur Verfügung. Das pFA-NATMX2-Modul und das pFA-NAT1-Modul unterscheiden sich in ihrem Terminator. Für genomische C-terminale GFP-Fusionen wurde das Modul pFA-GUNMX2 konstruiert, welches aus GFP, dem *ScURA3*-Terminator sowie dem Selektionsmarker *NATMX2* zusammengesetzt ist. Die Homologieregionen der S1- und S2-Oligonukleotid-Primer sind identisch mit denen der *C. albicans*-Module.

Daneben wurde auch für den dimorphen Pilz *H. sinecauda* versucht, dieses PCR-basierte Transformationssystem zu etablieren. Aus rDNA-Sequenzvergleichen ist bekannt, dass *H. sinecauda* phylogenetisch eng verwandt ist mit *A. gossypii*, aber im Gegensatz zu *A. gossypii* zu den dimorphen Pilzen gehört (Holley *et al.*, 1984; Prillinger *et al.*, 1997; Wendland *et al.*, 1999). Die enge Verwandtschaft und die unterschiedliche Morphologie machten diesen Pilz zu einem interessanten Organismus für genetische Untersuchungen. Dazu war es notwendig, ein Transformationssystem zu entwickeln, welches die gezielte Deletion von Genen in *H. sinecauda* ermöglicht. Da sich *H. sinecauda* sensitiv gegenüber dem Antibiotikum Geneticin/G418 verhält, wurden zunächst die Transformation frei replizierender Plasmide, die den Resistenzmarker *kanMX* tragen, versucht. In *A. gossypii* und *S. cerevisiae* können frei replizierende Plasmide mit hoher Effizienz transformiert werden. Die autonome Replikation dieser Plasmide benötigt ein ARS-Element (ARS autonom replizierende Sequenz). Dabei zeigte sich, dass ARS-Elemente aus *S. cerevisiae* in *A. gossypii* funktionell sind (Wright und Philippsen, 1991; Wendland und

Philippsen 2002). Für *H. sinecauda* wurden verschiedene ARS-Elemente aus *A. gossypii* und *S. cerevisiae* verwendet und zusätzlich mit Zentromerregionen dieser Organismen kombiniert, die eine stabile Verteilung der Plasmide auf Mutter- und Tochterzelle gewährleisten. Eine Transformation nach dem *A. gossypii* Elektroporationsprotokoll erwies sich hier als effizienteste Methode. Nach 2-3 Tagen wurden Kolonien transformierter Zellen für jedes verwendete Konstrukt gefunden, die sich aber in ihrer Größe unterschieden. Es zeigte sich nach Überimpfen der Kolonien auf neue Selektionsplatten, dass Zellen, die mit pFA-AgCEN5-AgARS-kanMX oder pFA-AgARS-kanMX transformiert wurden, stabile Kolonien bildeten. Dagegen konnten Transformanten mit dem *S. cerevisiae* ARS nach Überimpfung auf neue Selektivplatten nicht wieder angezogen werden. Obwohl ARS-Elemente aus *S. cerevisiae* in *A. gossypii* und anderen Hefespezies, wie *Schwanniomyces occidentalis*, funktionell sind, waren diese erstaunlicherweise in *H. sinecauda* nicht in der Lage, eine effiziente Replikation der Plasmide zu erzielen (Janatova *et al.*, 2000; Wendland und Philippsen, 2000; Wendland und Philippsen, 2001; Wright und Philippsen, 1991). Dagegen zeigte sich, dass das *A. gossypii* ARS-Element aus der Zentromerregion des Chromosom V (CEN5) in *H. sinecauda* aktiv ist. Ebenso konnte gezeigt werden, dass das *A. gossypii* CEN5 in der Lage ist, die gleichmäßige Verteilung und die Plasmidstabilität unter nichtselektiven Bedingungen in *H. sinecauda* zu erhöhen. Diese heterologe Funktion von *Ag*CEN5 in *H. sinecauda* unterstreicht auch die nahe Verwandtschaft dieser beiden Organismen (Schade *et al.*, 2003).

Die Übertragung des PCR-basierten Transformationsverfahrens auf *H. sinecauda* war nicht erfolgreich, da die Länge der flankierenden Homologieregionen nicht ausreichend für die exakte Integration der Disruptionskassette ins Zielgen war. Daher wurde für eine erste genomische Deletion eine Disruptionskassette kloniert. Ausgehend von einem 0,5kb-Fragment des *HsLEU2*-Gens, welches mit Hilfe degenerierter Oligonukleotide amplifiziert werden konnte, wurde der *kanMX3*-Selektionsmarker, dessen *kanMX*-Gen von direkten Sequenzwiederholungen flankiert wird, in das *HsLEU2*-Fragment integriert. Die resultierende Disruptionskassette, die 180bp und 350bp flankierende Homologieregion zum *H. sinecauda LEU2* am 5'- und 3'-Ende besaß, wurde aus dem Vektor mittels Restriktionsenzymen herausgeschnitten und direkt für die Transformation verwendet. Auf diese Weise konnte eine erste Geneticin (G418)-resistente integrative Transformante für *H. sinecauda* hergestellt werden. Durch Sporulation dieses Stammes und selektive Keimung der Sporen konnte anschließend ein *H. sinecauda* Δ*leu2* Stamm isoliert werden,

der nach Rekombination über die direkten Sequenzwiederholungen des *kanMX3* Selektionsmarkers auch Geneticin (G418) sensitiv war. Damit steht für *H. sinecauda* ein Stamm zur Verfügung, der mit zwei Markergenen transformiert werden kann und damit Deletions- und Komplementierungsanalysen erlaubt.

4.2. Etablierung der *in vivo* Fluoreszenz-Zeitraffer-Mikroskopie

Die eukaryotische Zelle ist strukturell ein komplexes System, in dem Wachstumsprozesse durch simultane hochdynamische Vorgänge erzeugt werden. Dazu zählen insbesondere Prozesse wie der gerichtete Vesikeltransport an Stellen polaren Wachstums, der Transport von endozytotischen Vesikeln sowie der Transport von Organellen wie z.B. Vakuolen und Mitochondrien in die Tochterzelle bzw. an die Hyphenspitze bei filamentösen Pilzen. Neben dem Transport kommt es auch zu Fusionen von Vesikeln und Teilungen von Organellen, die insbesondere für die Vererbung bei Vakuolen und Mitochondrien von Bedeutung sein können.
Die Bedeutung dieser Dynamiken für polares Hyphenwachstum und möglicherweise für die Virulenz von *C. albicans* ist bisher nicht untersucht. Bisherige Untersuchungen GFP-markierter Proteine von *C. albicans* beschränkten sich auf Aufnahmen eines einzigen Zeitpunktes einer Zelle, welche mit maximaler UV-Belichtung und beliebig langer Aufnahmezeit gemacht werden können, da ein Weiterleben der Zelle nicht unbedingt erforderlich war. Die Beobachtung dynamischer Prozesse *in vivo* erfordert aber zunächst die Etablierung geeigneter Verfahren, um mikroskopische Untersuchungen über längere Zeiträume durchführen zu können.

Bildaufnahme und Bildbearbeitung: Im Rahmen meiner Diplomarbeit wurden bereits Verfahren für die Präparation von Wachstumskammern im Format von Objektträgern angewendet, die eine zentrale Vertiefung besitzen, in die Festmedium eingefüllt werden kann (nach Hoepfner *et al.*, 2000). Diese Objektträger konnten für die Beimpfung mit *A. gossypii* oder *C. albicans* und anschließende Hellfeld-Zeitraffer-Aufnahmen verwendet werden. In der Regel wurden dafür Vollmedien verwendet (YPD für *C. albicans* und AFM für *A. gossypii*).
Für die *in vivo* Fluoreszenz-Zeitraffer-Mikroskopie ist diese Form der Objektträger-Präparation aufgrund der starken Eigenfluoreszenz des Mediums nicht geeignet. Daher mussten alternative Medien ausgewählt werden, die aber das Wachstum des jeweiligen

Pilzes in seiner Wachstumsgeschwindigkeit und Zellmorphologie nicht verändern sollten. Dafür erwies sich ein Medium, welches zu gleiche Teilen aus 3,4%igem Wasseragar und CSM-Medium (complete supplement mixture) bestand, als geeignet. Diesem Medium wurde zusätzlich Aminosäurelösungen zugeben, sofern der untersuchte Stamm entsprechende Aminosäureauxotrophien aufwies.

Außerdem mussten Möglichkeiten gefunden werden, die eine geringe UV-Belichtung und hochauflösende, detailgenaue Bilder miteinander vereinen. Die bisher zur Verfügung stehenden GFP-Varianten zeigten in *C. albicans* nur bei stark exprimierten Genen eine ausreichende Fluoreszenzintensität, was die Realisierung der *in vivo* Mikroskopie zusätzlich erschwert. Daher wurden zunächst Aufnahmen mit einer *C. albicans HHF1-GFP* Mutante durchgeführt, die mit einer auf 25% reduzierten UV-Belichtung und einer Aufnahmezeit von 800ms bei einer Vergrößerung von 630fach durchgeführt wurden. Mit diesen Voreinstellungen konnten qualitativ hochauflösende Bilder aufgenommen werden. Es zeigte sich aber, dass die Zellen bei dieser UV-Intensität schon nach wenigen Minuten ihr Wachstum einstellten und damit unter diesen Bedingungen kein vollständiger Teilungszyklus aufgenommen werden konnte. Offenbar war hier die UV-Belastung der Zellen zu hoch, so dass weitere Versuche mit geringerer UV-Intensität und verlängerter Belichtungszeit durchgeführt wurden. Im Ergebnis dieser Versuche erwies sich eine Reduzierung der UV-Intensität auf 5% verbunden mit einer Belichtungszeit von 1000-1500ms als günstig, um das Wachstum der Zellen über bis zu 10 Stunden fluoreszenzmikroskopisch verfolgen zu können. Durch die Verlängerung der Belichtungszeit konnten auch bei der reduzierten UV-Intensität hochauflösende Bilder produziert werden. Um die Zellgrenzen im Zeitraffer-Film sichtbar zu machen, wurde zu jedem Zeitpunkt neben der GFP-Aufnahme eine zusätzliche Phasenkontrastaufnahme gemacht. Beide Bilder entstanden dabei direkt aufeinander folgend mit einem maximalen Zeitabstand von zwei Sekunden. Das Zeitintervall zwischen zwei Aufnahmepunkten variierte zwischen ein und drei Minuten. Innerhalb dieser Zeit wurde eine geringe Absenkung des Objekttisches beobachtet, die allerdings groß genug war, dass die beobachteten Zellen nicht mehr in der Fokusebene lagen. Um die Absenkung des Objekttisches vor jeder Aufnahme zu korrigieren, wurde mittels Autofokussierung die korrekte Bildebene neu bestimmt und anschließend Fluoreszenz- und Hellfeldaufnahme gemacht. Diesen Prozess konnte ich durch die Programmierung spezieller Journale automatisieren und realisierte so eine funktionsfähige vollautomatische

Mikroskopsteuerung, Bildaufnahme und Abspeicherung der aufgenommenen Daten über beliebige Zeitintervalle.

Die Bearbeitung der Einzelbilder erfolgte im Anschluß mit Hilfe der Metamorph 4.6 bzw. 6.3 Software (Universal Imaging Corporation). Kontrastverstärkung und Unschärfe konnten mit Hilfe von Dekonvolutions-Filtern realisiert werden. Nachdem die Einzelbilder in Stapel verarbeitet wurden, konnten Phasenkontrast- und GFP-Stapel miteinander überlagert und in Falschfarben dargestellt werden. Für die Analyse der Zeitraffer-Aufnahmen wurden die Bilddateien in Videodateien konvertiert (Metamorph 6.3, Universal Imaging Corp.; TMPGEnc 2.5, Pegasys Inc.).

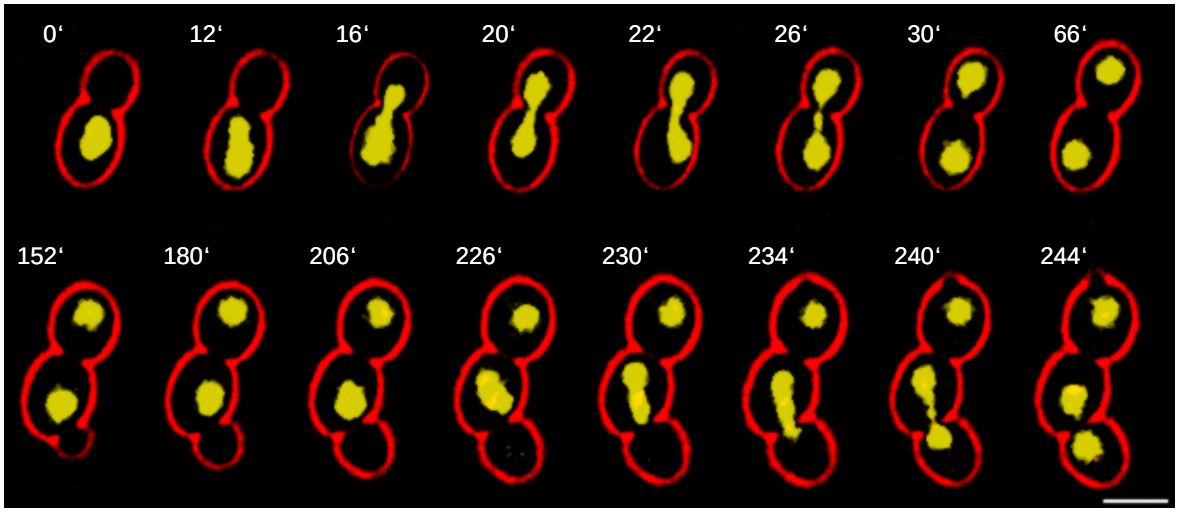

Abbildung 6: Dynamik der Kernteilung und Kernbewegung in *HHF1-VENUS* markierten BWP17 Zellen von *C. albicans*, die mit Hilfe der *in vivo* Fluoreszenz-Zeitraffer-Mikroskopie aufgenommen wurden.
(0‘) Während der Entstehung der Tochterzelle ist der Zellkern zufällig in der Mutterzelle lokalisiert. (12‘) Erreicht die Tochterzelle eine bestimmte Größe, wird die Spindel in der Mutterzelle elongiert. (16‘-26‘) Sobald die Spindel entlang der Mutter-Tochter-Achse orientiert ist, wandert ein Kern in die Halsregion zwischen Mutter- und Tochterzelle ein. Zum Beginn der Anaphase B erfolgen die Elongation des Kerns, bei der sich der Spindelapparat nahezu über die gesamte Mutter-Tochter-Länge ausdehnt und die Einwanderung eines Kerns in die Tochterzelle. (30‘-66‘) Nach der vollständigen Trennung der Kerne erfolgt die Zytokinese. (152‘-240‘) Zweite Knospung der Mutterzelle. (244‘) Erste distale Knospenbildung der Tochterzelle. Der vollständige Film M02 befindet sich im CD-Anhang der Dissertation. Der Größenbalken entspricht 5µm.

Herstellung von *CaHHF1-VENUS*: Anschließend wurde in gleicher Weise wie für den *CaHHF1-GFP* Stamm eine *C. albicans HHF1-VENUS* Mutante unter Verwendung des PCR-Verfahrens konstruiert. Venus ist eine YFP-Variante, die im Vergleich zum GFP eine beschleunigte Oxidation der chromophoren Gruppe aufweist, was den limitierenden Schritt der Reifung eines GFPs darstellt. Damit sollte Venus insbesondere in Temperaturbereichen um 37°C besser geeignet sein als GFP, das hier bedeutend schlechtere Reifungseigenschaften aufweist. (Nagai *et al.*, 2002).

Damit wurden Untersuchungen ermöglicht, die aufzeigen sollten, welches der fluoreszierenden Proteine unter hypheninduzierenden Bedingungen besser für *C. albicans* geeignet ist. Vergleichbar zu Aufnahmen der *CaHHF1-GFP* Mutante konnten mit der VENUS-Variante Kernteilungen über mehrere Zellzyklen beobachtet werden (Martin *et al.*, 2004; Abbildung 6). Dabei erfolgt die erste Spindelelongation zunächst in der Mutterzelle, anschließend wird die Spindel entlang der Mutter-Tochter-Achse ausgerichtet. Ist die Spindel in der Mutter-Tochter Ebene in der Höhe des Knospungshalses zentriert, erfolgt die Kernteilung. Die Fluoreszenzmarkierung der VENUS-Mutante erwies sich als sehr stabil und erlaubte erstmals auch *in vivo* Fluoreszenz-Aufnahmen der Hyphenphase, die bisher an der Leuchtintensität oder einem aberranten Hyphenwachstum der verwendeten *HHF1-GFP* markierten Stämme scheiterten (Abbildung 7).

Dazu wurde der *CaHHF1-VENUS* Stamm in Vollmedium bei 30°C bis zur logarithmischen Wachstumsphase angezogen. Anschließend wurden die Zellen zweimal mit destilliertem Wasser gewaschen, um Mediumbestandteile zu entfernen, und auf vorbereitete Agar-Objektträger, die 10% Serum enthielten, getropft. Eine dauerhafte Inkubation der Zellen bei 37°C unter dem Mikroskop konnte durch eine Heizplatte gewährleistet werden, die durch ein Wasserbad temperiert wurde.

Deutlich erkennbar ist in den Zeitraffer-Aufnahmen, dass der Kern der Mutterzelle in die neu entstehende Keimhyphe einwandert, dort eine mitotische Teilung durchführt und einer der beiden Tochterkerne zurück in die Mutterzelle einwandert. Die erste Kernteilung bei der Hyphenentwicklung findet also nicht in der Mutterzelle statt, sondern in der Keimhyphe. In der Keimhyphe ergibt sich auch eine veränderte Anordnung des ersten Septums der Hyphe. Dieses befindet sich 6-20µm von der Hyphenbasis entfernt (Martin *et al.,* 2004). Analog zur Kernteilung in der Hefephase findet auch in der Hyphenphase die Kernteilung an Stellen zukünftiger Septierung statt. Anders als in der Hyphenphase erfolgt bei einzelligen Hefen aber die vollständige Trennung von Mutter- und Tochterzelle voneinander.

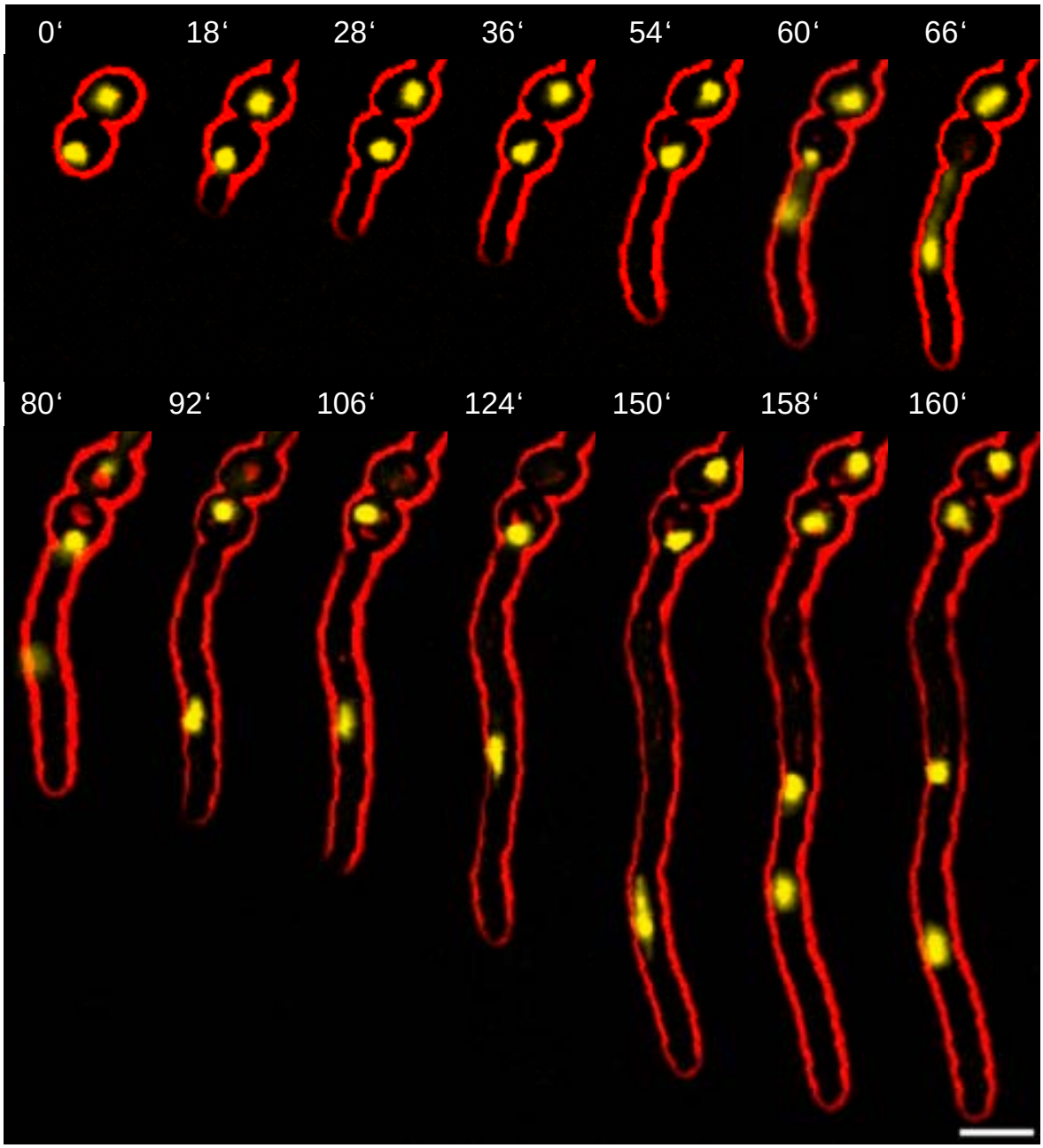

Abbildung 7 | Dynamik der Kernteilung und Kernbewegung in *HHF1-VENUS* markierten BWP17 Zellen von *C. albicans* in der Hyphenphase.
(0‘) Nicht-induzierte Zellen zum Beginn der Induktion. (18‘-54‘) Durch die Induktion mit Serum beginnen die Zellen eine erste Hyphe auszubilden. Der Kern verbleibt zunächst in der Mutterzelle bis die Hyphe etwa die dreifache Länge der Keimzelle erreicht hat. (60‘-66‘) Der Kern wandert in die Keimhyphe ein, elongiert und trennt sich. (80‘) Beide Kerne sind voneinander getrennt. Einer der Kerne wandert zurück in die Keimzelle. (92‘-124‘) Der Kern wandert entlang der wachsenden Hyphe. (150‘) Zweite Kernteilung in der Hyphe. (158‘-160‘) Einer der Kerne wandert erneut zurück in den ersten Hyphenabschnitt. Der vollständige Film M03 befindet sich im CD-Anhang der Dissertation. Der Größenbalken entspricht 5µm.

Die Lokalisierung des ersten Septums in der Hyphe ist ein entscheidendes Merkmal zur Abgrenzung echter Hyphen von Pseudohyphen (Sudbery, 2001). Daneben bleibt der Durchmesser der Hyphen am Septum gleich dem der gesamten Hyphe und wird nicht eingeschnürt wie in Pseudohyphen.

Um die Fluoreszenzintensität der verschiedenen *CaHHF1*-Mutanten zu messen, wurden alle Kulturen bei 30°C oder 37°C in Vollmedium (YPD) angezogen, gründlich mit destilliertem Wasser gewaschen und anschließend mikroskopisch ausgewertet. Um die Fluoreszenzintensität der Stämme miteinander vergleichen zu können, wurden alle Aufnahmen bei gleicher UV-Intensität und Belichtungszeit in 16bit Graustufen abgespeichert. Anschließend wurde von den aufgenommenen Zellkernen der maximale Helligkeitswert ermittelt. Dabei konnte eine maximale Helligkeit von 65535 (=weiß)

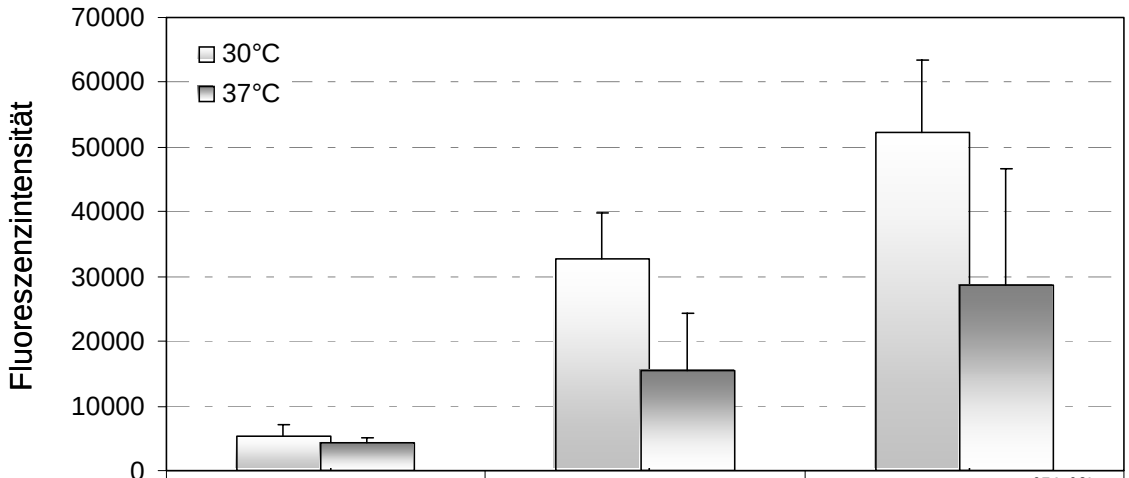

	HHF1-Venus	HHF1-GFP	HHF1-GFP $^{65A\ 68L\ 72A}$
30°C	5220	32739	52295
37°C	4194	15478	28619

Abbildung 8 | Analyse der Fluoreszenzintensität von drei verschiedenen *HHF1-GFP* oder *–VENUS* Stämmen.
Die Kulturen wurden in YPD-Vollmedium bei 30°C oder 37°C angezogen, zweimal mit Wasser gewaschen und anschließend mikroskopiert. Die Aufnahme der Zellen erfolgte mit gleicher Belichtungszeit und Fluoreszenzintensität in 16bit-Graustufen. Mit Hilfe der Metamorph-Software wurde für jeden aufgenommenen Zellkern die Fluoreszenzintensität als maximaler Helligkeitswert bestimmt (Minimum=0 entspricht schwarz; Maximum=65535 entspricht weiß).

erreicht werden, der Wert = 0 entsprach einem schwarzen Bildpunkt. Alle Werte zwischen 0 und 65535 beschreiben einen Grauwert, wobei mit zunehmender Zahl die Helligkeit des Grauwertes steigt. Demnach entsprechen große Zahlenwerte einer hohen Fluoreszenzintensität. Anhand der bestimmten Messwerte (n>165 für jede Mutante bei 30°C; n>220 für jede Mutante bei 37°C) wurden für die *HHF1-GFP*$^{S65A,\ V68L,\ S72A}$ Mutante die höchste Fluoreszenzintensitäten sowohl bei 30°C als auch 37°C gemessen, die geringste für die *HHF1-VENUS* Mutante.

Dagegen ist die Intensitätsabschwächung durch die Inkubation bei 37°C bei dieser Mutante am geringsten, sie beträgt weniger als 20%. Die größte Reduzierung der Fluoreszenzintensität von über 50% wurde für die *HHF1-GFP* Mutante festgestellt.

Die GFP$^{S65A,\ V68L,\ S72A}$-Variante erwies sich in diesen Untersuchungen als äußerst stabil bei 30°C und besaß bei 37°C die höchste Fluoreszenzintensität, obwohl diese um fast 50% reduziert war. Allerdings konnten bei 37°C auch deutliche Veränderungen der markierten Strukturen festgestellt werden (Abbildung 9). Neben sehr hell fluoreszierenden Zellkernen wurden aber auch Zellkerne beobachtet, die keine oder nur eine sehr geringe Fluoreszenz besaßen. Die Streuung der Messwerte um den Mittelwert nahm deutlich zu.

Hhf1-Venus zeigte in *C. albicans* nur eine vergleichsweise geringe Fluoreszenzintensität. Zwar wurde das Protein mit nur etwa 10% der Intensität des GFP$^{S65A,\ V68L,\ S72A}$ gemessen, war aber in 37°C-Versuchen sehr stabil und behielt über 80% seiner Leuchtkraft. Zudem verringerte sich die Streuung der Fluoreszenzintensität des *HHF1-VENUS* sogar bei 37°C, so dass alle Kerne einer Fokusebene mit annähernd gleicher Intensität gemessen

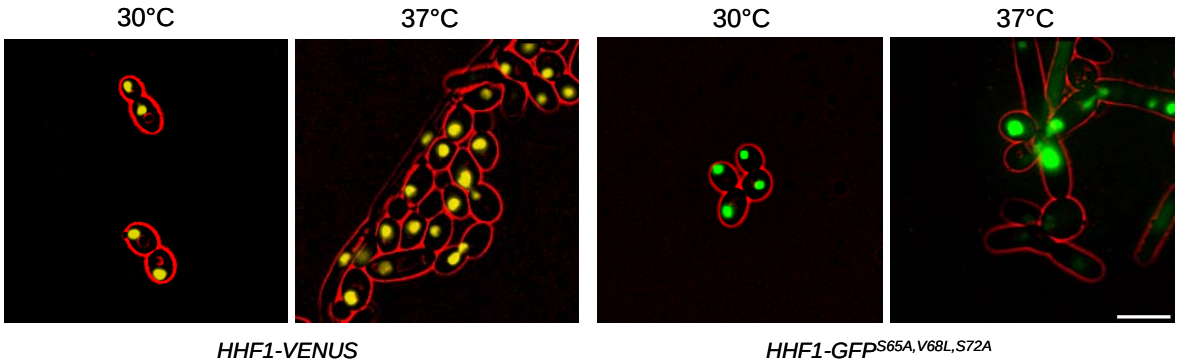

Abbildung 9 | Analyse der Fluoreszenzintensität von *HHF1-VENUS* und *HHF1- GFP*^{S65A,V68L,S72A} bei unterschiedlichen Temperaturen.
Die Stämme wurden bei 30°C oder 37°C in YPD-Vollmedium angezogen, gewaschen und mit gleichen Mikroskop-Einstellungen aufgenommen. *HHF1-VENUS* zeigte bei 37°C eine ähnliche Fluoreszenzintensität aller Kerne. Dagegen schwanken die Helligkeiten der *HHF1-GFP*^{S65A,V68L,S72A}-markierten Zellkerne einer Fokusebene.

werden konnten. Damit stellt die Venus-Variante des GFP eine für *C. albicans* besonders gut geeignete GFP-Form dar, die sowohl in Hefezellen als auch während einer Hypheninduktion die Detektierung von GFP-Signalen erlaubt. In weiterführenden Untersuchungen könnten Venus-Varianten mit an *C. albicans* angepasstem Codon-Gebrauch konstruiert werden, um so zu versuchen, eine höhere Fluoreszenzintensität durch ein möglicherweise verbessertes Expressionsniveau zu erreichen. Damit sollen zukünftig neben den derzeit verwendeten GFP-Varianten alternative Fluoreszenzproteine zur Verfügung stehen, die eine stabile Fluoreszenz bei 37°C besitzen und damit zur Charakterisierung der Hyphenphase von *C. albicans* beitragen.

Die mikroskopische *in vivo* Analyse fluoreszenzmarkierter *C. albicans* Mutanten bedarf auch weiterhin einer speziellen Anpassung von UV-Intensität und Belichtungszeit an das jeweilige markierte Protein und kann nicht unverändert von den *HHF1*-Aufnahmen übertragen werden.

4.3. Bedeutung der Endozytose für das polare Hyphenwachstum

Mit Hilfe moderner Methoden der molekularen Zellbiologie gelingt es uns, neue Einblicke in zelluläre Prozesse, wie polares Wachstum, Differenzierung und Entwicklung zu erhalten.

Filamentöse Pilze bieten aufgrund ihrer leichten Handhabbarkeit und guten genetischen Manipulierbarkeit die Möglichkeit, auf einfache Weise Mutanten zu generieren und stellen ein ausgezeichnetes System dar, um zelluläre Differenzierungsprozesse auf molekularer und zellbiologischer Ebene zu untersuchen (Wendland und Walther, 2005). Die Kontrolle über die Ausbildung und Aufrechterhaltung polaren Wachstums bei filamentösen Pilzen wird von einer kleinen Zahl konservierter, GTP-bindender Proteine der Ras/Rho-Familie sowie deren Regulatoren ausgeübt, die die dynamische Organisation des Aktinzytoskeletts steuern (Wendland und Philippsen, 2001; Bauer *et al.*, 2004). Apikal konzentriertes Wachstum an der Hyphenspitze erfordert darüber hinaus die Koordinierung des Transports von sekretorischen Vesikel entweder über das Aktin- oder Mikrotubuli-zytoskelett.

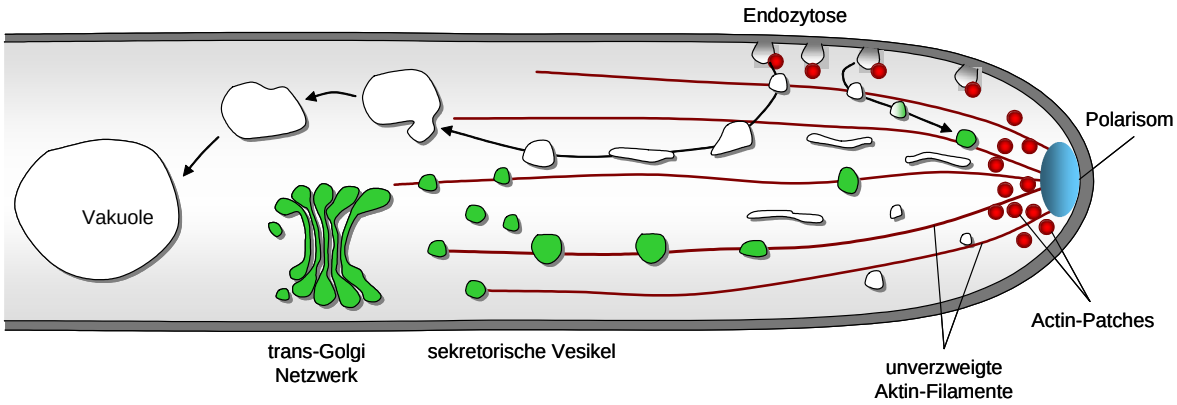

Abbildung 10 | Schematische Übersicht über den Vesikeltransport in die Hyphenspitze und zu den Vakuolen filamentöser Pilze.
An der Hyphenspitze werden ausgehend vom Polarisom-Komplex lineare Aktinfilamente gebildet. Sekretorische Vesikel des Golgi-Apparates werden an Aktinfilamenten oder Mikrotubuli (nicht abgebildet) transportiert. Endozytotische Vesikel werden entweder an die Hyphenspitze oder zu Vakuolen transportiert, mit denen sie fusionieren.

In dieser Arbeit wurde die Frage untersucht, inwieweit Endozytose das polare Wachstum der Hyphenspitze beeinflusst. Endozytose beschreibt den generellen Prozess der Plasmamembraneinstülpung und der Bildung intrazellulärer Vesikel oder Endosomen. Dieser Prozess wird für eine Reihe unterschiedlicher Aufgaben, wie die Aufnahme extrazellulärer Partikel und Moleküle (Phagozytose) oder Flüssigkeiten (Pinozytose) sowie für die Internalisierung von plasmamembranständigen oder zellwandassoziierten Proteinen verwendet (Engqvist-Goldstein und Drubin, 2003). Die aufgenommenen Partikel und Membranen werden nun zu spezifischen zellulären Kompartimenten transportiert (Abbildung 10). Vesikeltransport, Vesikelsortierung und der zelluläre Membranfluss stellen hochdynamische Prozesse dar, die durch das Aktinzytoskelett oder Mikrotubuli gesteuert werden. Die Regulation und die dynamische Organisation des Aktinzytoskeletts können somit wichtige Schaltstellen für den gerichteten Ablauf des Vesikelflusses darstellen.

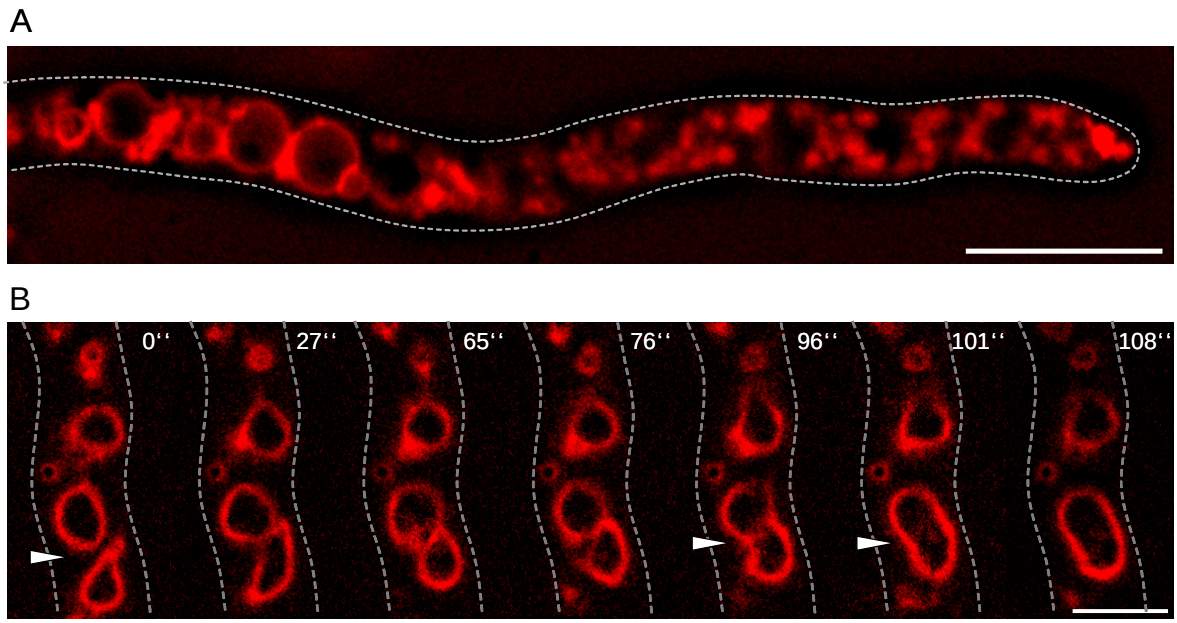

Abbildung 11 | Vakuolenverteilung und Endozytose in *A. gossypii*
(a) Aufnahme einer *A. gossypii* Hyphe, die 30 Minuten vor der Mikroskopie mit dem lipophilen Farbstoff FM4-64 (2µM) gefärbt wurden. (b) *In vivo* Fluoreszenz-Zeitraffer-Aufnahmen einer Vakuolenfusion in *A. gossypii*. Zwei Vakuolen im unteren Teil des Hyphenabschnittes, die zum Zeitpunkt 0'' deutlich getrennt voneinander vorliegen, sind nach 108 Sekunden miteinander fusioniert. Der vollständige Film M04 befindet sich im CD-Anhang der Dissertation. Der Größenbalken entspricht 10µm.

In jüngsten Studien wurde die Existenz der Endozytose in filamentösen Pilzen allerdings in Frage gestellt (Cole *et al.*, 1998; Torralba und Heath, 2002). Durch die Aufklärung pilzlicher Genomsequenzen sowie Mutantenanalysen und Fluoreszenz-Zeitrafferaufnahmen, die die Aufnahme des membranselektiven lipophilen Farbstoffes FM4-64 zeigten, konnten endozytotische Prozesse auch in filamentösen Pilzen nachgewiesen werden (Yamashita und May, 1998; Fischer-Parton *et al.*, 2000; Atkinson *et al.*, 2002; Read und Kalkman, 2003; Walther und Wendland, 2004b).
Die Verwendung hochauflösender *in vivo* Zeitraffer-Mikroskopie in filamentösen Pilzen stellt dabei eine wichtige Möglichkeit dar, die Aufnahme- und Transportprozesse in Hyphen sowie den Transport und die Fusion von Vesikeln oder Zytoplasmaströmungen zu analysieren (Abbildung 11).

In *A. nidulans* wird das einzige Typ-I Myosin durch das Gen *myoA* codiert. MYOA lokalisiert an kortikale Aktinpatches besonders an der Hyphenspitze und Stellen zukünftiger Septierung (Osherov *et al.*, 1998, Yamashita *et al.*, 2000). *myoA* ist ein essentielles Gen in *A. nidulans* und gehört zu einer Gruppe von Myosinen, die entweder einen Serin- oder Threonin-Rest in ihrer schweren Kette an einer bestimmten Position (TEDS-Stelle, Ser371 in MYOA) besitzen (McGoldrick *et al.*, 1995). Die Phosphorylierung an diesem konservierten Serin- oder Threonin-Rest durch eine Kinase der PAK-Familie (p21-activated kinase) ist für die Aktivierung der aktin-aktivierten Mg^{2+}-ATPase notwendig. In einer *myoA* Mutante, die an der TEDS-Stelle statt Serin an Position 371 Glutaminsäure (S371E) besitzt und damit eine Phosphorylierung nachahmt, konnte konstitutive Endozytose durch die Aufnahme von FM4-64 und die Anhäufung intrazellulärer Membranen gezeigt werden (Yamashita und May, 1998). Darüber hinaus konnte nachgewiesen werden, dass dieser Prozess F-Aktin abhängig ist und *MYOA* als Motor für die Membraninternalisierung fungiert.
Eine analoge Mutation des *C. albicans MYO5*-Gens, bei der Serin an Position 366 durch Asparaginsäure (S366D) ersetzt wird, zeigte polares Hyphenwachstum selbst in Abwesenheit kortikaler Aktinpatches an der Hyphenspitze. Hier führte eine Behandlung mit Cytochalasin A zur Inhibierung der Hyphenbildung, so dass eine Beteiligung von Aktinstrukturen an der Ausbildung und Aufrechterhaltung polaren Wachstums nachgewiesen werden konnte. Die Deletion des gesamten Gens lieferte lebensfähige Mutanten, die jedoch nicht in der Lage waren Hyphen auszubilden (Oberholzer *et al.*, 2002; Oberholzer *et al.*, 2004). Die Deletion des WASP-Homologen *WAL1* in *C. albicans*

führte zu einem ähnlichen Phänotyp wie die Deletion des *CaMYO5*-Gens (Walther und Wendland, 2004a). Neben einem Endozytosedefekt, der sich in der zeitlich stark verzögerten Aufnahme von FM4-64 ausdrückte, zeigte die Δ*wal1* Mutante auch Defekte in der Vakuolenmorphologie und Vakuolenfusion. Dies führte zur Anhäufung zahlreicher kleinerer Vakuolen statt wie im Wildtyp zur Ausbildung einer großen Vakuole. Insbesondere das Fehlen der Hyphenbildung bei der Δ*wal1* Mutante unter induzierenden Bedingungen zeigte die offensichtliche Bedeutung endozytotischer Prozesse für polares Zellwachstum filamentöser Pilze.

Die Bedeutung des WASP-Homologen für die Hyphenbildung bei *C. albicans* sowie das Fehlen einer Hyphenphase bei der *Cawal1* Mutante führten dazu, dass ich die Analyse der Endozytose auch auf einen filamentösen Ascomyzeten ausdehnte. Hierzu wurde die in meiner Diplomarbeit entstandene *Δwal1* Mutante von *A. gossypii* verwendet. In den Hyphen der *Agwal1* Mutante zeigten sich Defekte in der Endozytose noch viel stärker als in *C. albicans* Zellen. Durch die *in vivo* Fluoreszenz-Zeitraffer-Mikroskopie wurde die Aufnahme und der Vesikeltransport unter Verwendung des lipophilen Farbstoffes FM4-64 untersucht. In Wildtyp Hyphen konnten hochbewegliche Endosomen in der Hyphenspitze festgestellt werden. In subapikalen Hyphenabschnitten wurden tubuläre Strukturen ausgebildet, die miteinander fusionierten. In weiter hinten gelegenen Abschnitten wurden große Vakuolen gebildet (Walther und Wendland, 2004b; Abbildung 11a). Die Bildung von großen Vakuolen in zurückliegenden Hyphenabschnitten ist ein sehr charakteristisches Merkmal während des polaren Hyphenwachstums bei Pilzen (Cole *et al.*, 1998; Ohneda *et al.*, 2002; Barelle *et al.*, 2003; Veses *et al.*, 2005).
Die Färbung von Wildtyp-Endosomen an der Hyphenspitze war dabei effizient und lieferte stark fluoreszierende Vesikel. Im Gegensatz dazu erfolgte die Aufnahme des Farbstoffs in der *Agwal1* Mutante deutlich schlechter und lieferte diffuse intrazelluläre Signale. Zudem waren nur sehr wenige Endosomen in den Hyphenspitzen der *Agwal1* Mutante sichtbar, die nahezu leer von Vesikeln waren. In subapikalen Hyphenregionen konnte eine Vielzahl von Vesikeln auch in der *Agwal1* Mutante beobachtet werden, die verringerte aber ähnliche Beweglichkeit wie Vesikel im Wildtyp aufwiesen und tubuläre Strukturen ausbildeten (Abbildung 12). Die Deletion von *WAL1* resultierte zudem in einer Akkumulation von Aktinpatches in subapikalen Hyphenregionen, nicht aber in der Hyphenspitze wie im Wildtyp. Aktinpatches lokalisieren also ebenso wie

Endozytosevesikel nicht an die Hyphenspitze. Dies führte außerdem zu einem geschwollenen, isotropen Wachstum und einer veränderten Hyphenmorphologie.

Die Fehllokalisierung der Aktinpatches der *Agwal1* Mutante weist darauf hin, dass ebenso wie in *S. cerevisiae* durch die Lokalisierung der Patches die Position der Endozytose bestimmt wird (Irazoqui *et al.*, 2005; Stefan *et al.*, 2005). Das Fehlen von *WAL1* führt zu einer starken Reduzierung der Wachstumsgeschwindigkeit.

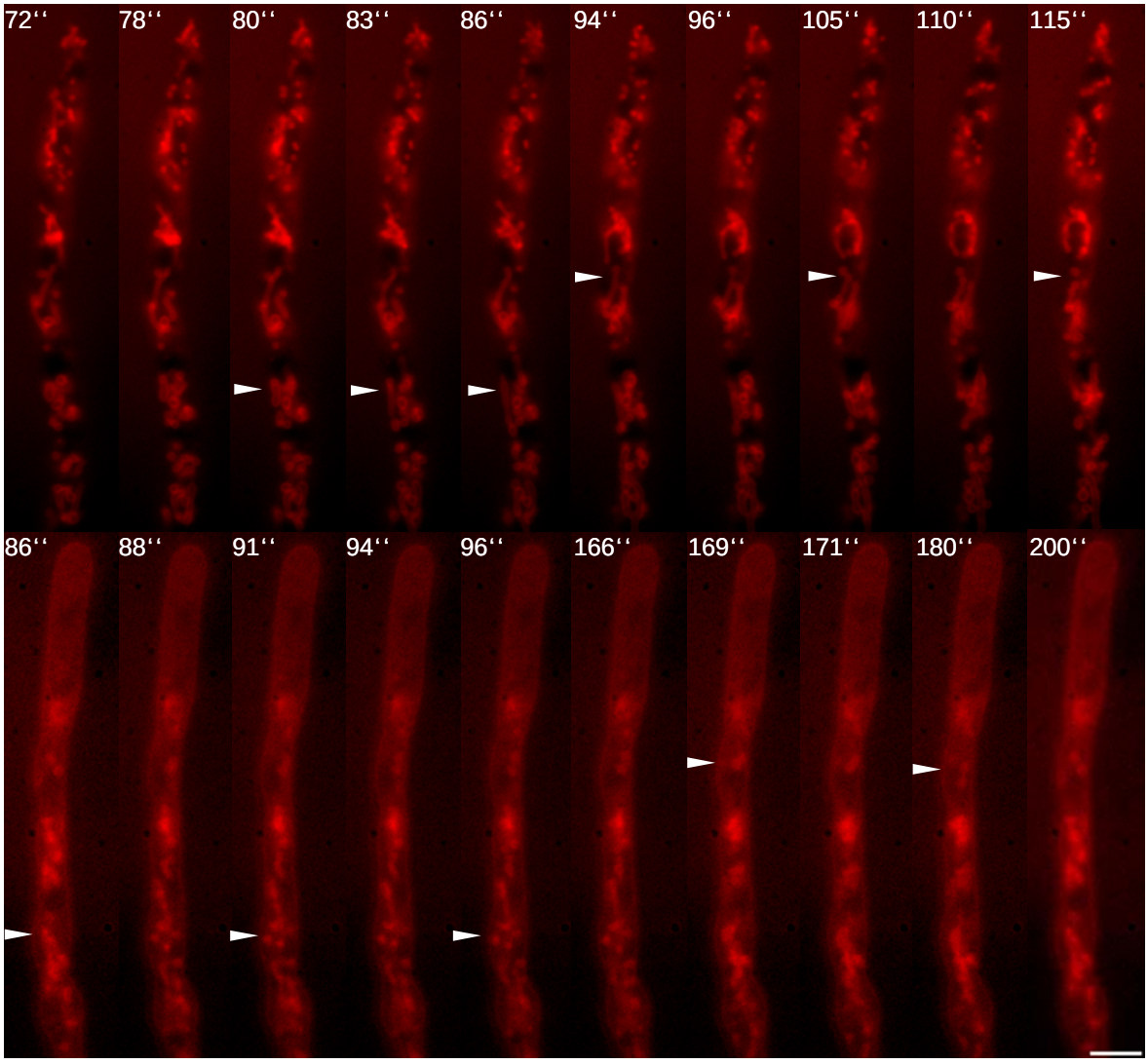

Abbildung 12 | Analyse der Endozytose in *A. gossypii* und *Agwal1* Mutante
Durch die Verwendung des lipophilen Farbstoffes FM4-64 wurden die frühen Stadien der Endozytose an der Hyphenspitze mittels *in vivo* Fluoreszenz-Zeitraffer-Mikroskopie sichtbar gemacht. Die Hyphenspitze der *Agwal1* Mutante ist im Gegensatz zum Wildtyp nicht mit Endosomen gefüllt, welche tubuläre Strukturen ausbilden können. Die Pfeile markieren Vesikelfusion oder –abtrennung. *Agwal1* Hyphen wiesen eine reduzierte Beweglichkeit auf, so dass Fusions- und Trennungsereignisse seltener zu beobachten waren. Der vollständige Film befindet sich im CD-Anhang der Dissertation (06_tip_Agwt-wal1_vacuoles_Fig8AB.mpg). Der Größenbalken entspricht 5µm.

Aus Analysen von Zeitrafferaufnahmen konnte die Wachstumsgeschwindigkeit des Wildtyps im juvenilen und älteren Myzel sowie der *Agwal1* Mutante bestimmt werden. Danach hatte der Wildtyp vom Zeitpunkt der Keimung bis zur Entwicklung der ersten dichotomen Verzweigungen eine Wachstumsgeschwindigkeit von etwa 20µm/h, im älteren Myzel steigt diese auf bis zu 170µm/h an. In der *Agwal1* Mutante wurden während ihres gesamten Wachstums Geschwindigkeiten von nur etwa 15µm/h gemessen. Dies entspricht also etwa der Wachstumsgeschwindigkeit, die der Wildtyp zu Beginn seiner Myzelbildung aufweist. Diese minimale polare Wachstumsgeschwindigkeit in *Agwal1* zeigt den deutlichen Beitrag von Wal1p für polare Wachstumsprozesse. Der zentrale Defekt für diese Wachstumsinhibierung ist derzeit nicht bekannt. Dieser könnte in der Störung vakuolärer Prozesse beispielsweise durch verlangsamte Transportprozesse von Stellen der Endozytose bis zu den Vakuolen liegen. Ebenso könnte das Recycling von Vesikeln an die Hyphenspitze ein wichtiger Prozess bei der Aufrechterhaltung des polaren Wachstums sein.

4.4. Einfluss von GTPase-Modulen auf das polare Hyphenwachstum

Der morphologische Wechsel von *C. albicans* als Reaktion auf Serum und 37°C oder andere hypheninduzierende Stimuli ist ein charakteristisches Merkmal für diesen humanpathogenen Pilz. Unter diesen Bedingungen vollzieht *C. albicans* eine Wechsel von hefeartigem einzelligen Wachstum zum filamentösen Wachstum verbunden mit der Bildung von Keimschläuchen und Hyphen. Die Ausbildung von Hyphen stellt einen wichtigen Aspekt in der Virulenz dieses Pilzes bezüglich der Adhäsions- und Penetrationsfähigkeit sowie der Immunevasion dar.

Die molekulare Grundlage für den Wechsel zum filamentösen Wachstum in *C. albicans* basiert auf der Aktivierung der Ras1-GTPase durch extrazelluläre Signale. Dadurch werden zwei nachfolgende Signalkaskaden, der MAP-Kinase-Weg und der cAMP-Weg, aktiviert. Über diese Signalkaskaden werden die Transkriptionsfaktoren Efg1p und Cph1p aktiviert, die ihrerseits die Expression hyphenspezifischer Gene einleiten (Abbildung 13). Der cAMP-Weg hat auch eine wichtige Funktion in der Morphogenese anderer filamentöser oder dimorpher Pilze. Im phytopathogenen dimorphen Pilz *Ustilago maydis* wird die Transition von einzelligen zum filamentösen Wachstum und damit vom saprophytischen zum parasitischen Wachstum durch eine cAMP-abhängige Proteinkinase reguliert (Dürrenberger, 1998; Gold *et al.*, 1994) Dabei wird durch die Aktivität der Adenylatzyklase *uac1* und in Gegenwart von cAMP filamentöses Wachstum unterdrückt. Die Deletion des Adenylatzyklase Gens *uac1* führt bei *U. maydis* zu filamentösem Wachstum (Gold *et al.*, 1994). Suppressoren dieses filamentösen Wachstums der *uac1* Mutante wurden in den *ubc3, ubc4* und *ubc5* Genen gefunden, die Komponenten des MAP-Kinase Wegs darstellen, der in *S. cerevisiae* die Pheromonantwort vermittelt (Mayorga und Gold, 1999; Andrews *et al.*, 2000).

Ebenso ist im Reispathogen *Magnaporthe grisea* die cAMP-abhängige katalytische Untereinheit der Proteinkinase (*CPKA*) für Morphogenese und Virulenz erforderlich (Mitchell *et al.*, 1995; Xu und Hamer, 1996). Neben *CPKA* wurden andere Gene, die in den cAMP-Weg involviert sind, charakterisiert. Wie die *cpkA*-Mutante weist auch eine

Adenylatzyklase-Mutante, die durch Deletion von *MAC1* entstand, einen Verlust der Appressorienbildung auf, der die Penetration der Keimlinge ins Pflanzengewebe verhindert, so dass die Mutanten avirulent sind. Externe Zugabe von cAMP hebt diesen Defekt auf, so dass diese Mutanten wieder Läsionen im Blattgewebe erzeugen konnten (Xu *et al.*, 1997; Choi *et al.*, 1997).

In einem anderen humanpathogenen Pilzsystem, bei *Penicillium marneffei*, erfolgt wie in *C. albicans* ein temperaturabhängiger Morphologiewechsel. Allerdings bildet *P. marneffei* bei 25°C Myzelien aus, während bei 37°C der Prozess der Arthrokonidienbildung und der Zerfall der Hyphen einsetzt und Vermehrung als Hefezellen erfolgt (Boyce *et al.*, 2003). Neben Ras1p und dem *CDC42*-Homolog *cflA* ist in *P. marneffei* ein weiteres G-Protein, das Rac-ähnliche *cflB* an der Kontrolle des Aktinzytoskeletts und der Morphogenese beteiligt (Boyce *et al.*, 2003, Boyce *et al.*, 2005).

S. cerevisiae besitzt zwei *RAS*-Gene *RAS1* und *RAS2*, deren Genprodukte die cAMP-Produktion über die Adenylatzyklase regulieren. Ras2p reguliert zusätzlich die Aktivität des MAP-Kinase-Weges während des filamentösen Wachstums. Das *U. maydis* Genom enthält ebenfalls zwei *RAS*-Gene. Dabei vermittelt Ras1p die Pheromonantwort, während Ras2p das filamentöse Wachstum induziert (Lee und Kronstad, 2002; Müller *et al.*, 2003).

Die Ras1-GTPase ist in *C. albicans* essentiell für den morphologischen Wechsel nicht aber für das vegetative Wachstum (Feng *et al.*, 1999; Leberer *et al.*, 2001). Die Deletion von *RAS1* oder den beiden Transkriptionsfaktoren *EFG1* und *CPH1* führt zu lebensfähigen Mutanten, die allerdings nicht in der Lage sind, Hyphen auszubilden und darüber hinaus im Tierversuch apathogen sind. Dagegen sind Einzeldeletionen von *EFG1* oder *CPH1* unter bestimmten Bedingungen in der Lage, Hyphen zu bilden, woraus eine übergeordnete Rolle von *RAS1* als Regulator zweier Signalwege für die Hyphenentwicklung, der MAP-Kinase-Kaskade und dem cAMP-Weg, geschlossen werden kann. Auf der anderen Seite führt eine konstitutive Aktivierung von *RAS1* unter Verwendung des $RAS1^{G13V}$ Allels zu einer Verstärkung filamentösen Wachstums auch unter nicht induzierenden Bedingungen.

Die Rolle des Aktinzytoskeletts für das filamentöse Wachstum wurde bereits durch die Deletion des Gens für das Wiskott-Aldrich Syndrom Protein Homologe *WAL1* in *C. albicans* gezeigt (Walther und Wendland, 2004a). Eine *Cawal1* Mutante ist nicht in der Lage unter induzierenden Bedingungen Hyphen auszubilden. Zwar werden in dieser Mutante zunächst Keimhyphen ausgebildet, aber das polare Wachstum wird nicht aufrechterhalten und es entstehen Pseudohyphen.

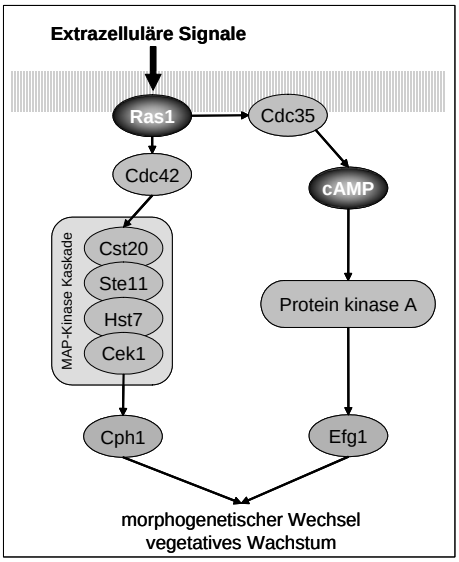

Abbildung 13 | Modell für Funktion von Ras1p in *C. albicans.*
Ras1p fungiert als Verbindung zwischen Umweltsignalen und morphogenetische Prozessen, die entweder über die MAP-Kinase Kaskade oder den cAMP-abhängigen Signalweg Filamentbildung induzieren (nach Leberer *et al.*, 2001).

Darauf aufbauend sollte geklärt werden, ob eine konstitutive Aktivierung von *RAS1* dazu führen kann, den Δ*wal1* Defekt in der Hyphenmorphogenese zu supprimieren. Dazu wurden in die homozygote *Cawal1* und die heterozygote *CaWAL1/wal1* Mutante jeweils entweder das konstitutiv aktive *RAS1*^{G13V}-Allel sowie das dominant negative *RAS1*^{G16A}-Allel oder das *RAS1*-Wildtyp-Allel gerichtet in den *ADE2*-Lokus integriert (Abbildung 14). Dafür wurden integrative Kassetten verwendet, die den *URA3*-Selektionsmarker und die verschiedenen *RAS1*-Allele unter der Kontrolle des regulierbaren *MAL2*-Promotors enthielten. Flankiert werden diese Kassetten durch Sequenzen von 0,95kb am 5'-Ende und 0,7kb am 3'-Ende, die homolog zum *ADE2*-Gen von *C. albicans* sind. Unter induzierenden Bedingungen (37°C und Serum) sowie Maltose als Kohlenstoff-Quelle zeigte sich jeweils starke Hyphenentwicklung im Wildtyp SC5314 sowie den Stämmen *WAL1/wal1, MAL2pRAS1*^{GV13} und *WAL1/wal1, MAL2pRAS1* sowohl in Flüssigkultur als auch auf Festmedien. Dagegen war die *WAL1/wal1 MAL2pRAS1*^{GV16A} Mutante auch unter induzierenden Bedingungen nicht in der Lage, Keimhyphen zu bilden.

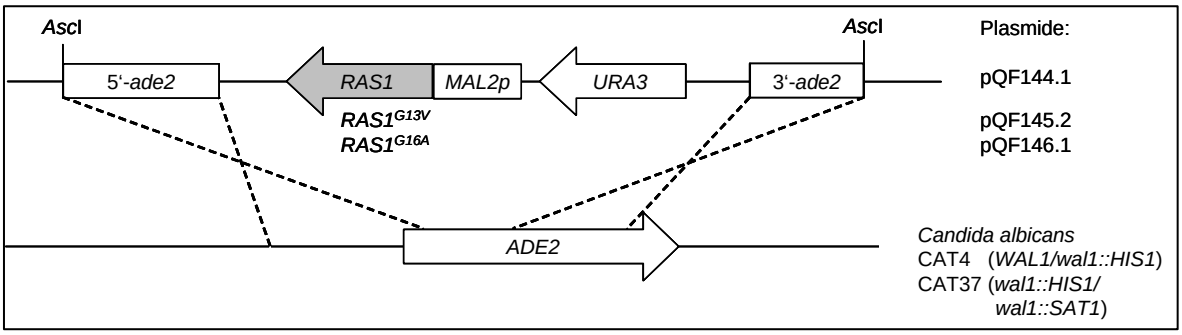

Abbildung 14 | Konstruktion der *C. albicans* Stämme.
Durch Restriktion der jeweiligen Plasmide mit *Asc*I wurden die Disruptionskassetten aus den Plasmiden herausgeschnitten und konnten in CAT4 (*WAL1*/ *wal1::HIS1*) und CAT37 (*wal1::HIS1/ wal1::SAT1*) transformiert werden.

Die Expression der drei verschiedenen *RAS1*-Allele im Δ*wal1* Hintergrund zeigte jeweils den Δ*wal1* Phänotyp und lieferte keine morphologischen Veränderungen, so dass diese Mutanten nicht befähigt waren, Hyphen auszubilden. Daraus kann geschlossen werden, dass weder durch das Maltose-induzierte *RAS1*-Allel noch durch die konstitutive Aktivierung von Ras1p der Hyphendefekt der Δ*wal1* Mutante supprimiert werden kann. Damit konnte belegt werden, dass endozytotische Prozesse eine wesentliche Rolle für polares Wachstum bei *C. albicans* spielen.
Weiterhin wurden die Stämme, die neben der Deletion des *WAL1* Genes eines der *RAS1*-Allele trugen, durch Zugabe von cAMP in Glukose-Medium induziert. Auch hier zeigte sich, dass eine Aktivierung der Signalkaskade unterhalb von Ras1p ebenfalls nicht in der Lage ist, den Δ*wal1*-Defekt in der Hyphenbildung zu umgehen (Abbildung 15).
Anhand der *C. albicans* Δ*wal1* Mutante konnte der Einfluss von *WAL1* auf die Endozytose und auf die Hyphenentwicklung, sowie die Funktion des Proteins bei der Aufrechterhaltung polaren Wachstums nachgewiesen werden. Der Verlust von *WAL1* führt zu einer Fehllokalisierung von Aktinpatches und Defekten in der Hyphenbildung, die auch nicht durch die konstitutive Aktivierung von Ras1p umgangen werden können. Im Gegensatz zu humanen WAS-Protein besitzt das pilzliche Homolog in *C. albicans* keine GTPase-Bindedomäne und kann daher nicht direkt mit GTPasen interagieren. Dagegen wurde im WASP-Homologen von *U. maydis* eine GTPase-Bindedomäne gefunden, die

direkt mit Cdc42p interagieren kann. Phänotypische Untersuchungen einer *Camyo5* Mutante zeigten ähnliche Phänotypen wie die der *Cawal1* Mutante. Zusätzlich konnte in der Bäckerhefe *S. cerevisiae* die Interaktion von Myo5p mit dem WASP-Homologen Las17p/Bee1p nachgewiesen werden. Myo5p und Wal1p interagieren mit dem Arp2/3-Komplex und führen zur Bildung verzweigter Aktinfilamente und Aktinpatches, die für Transportprozesse und Endozytose in der Zelle gebraucht werden.

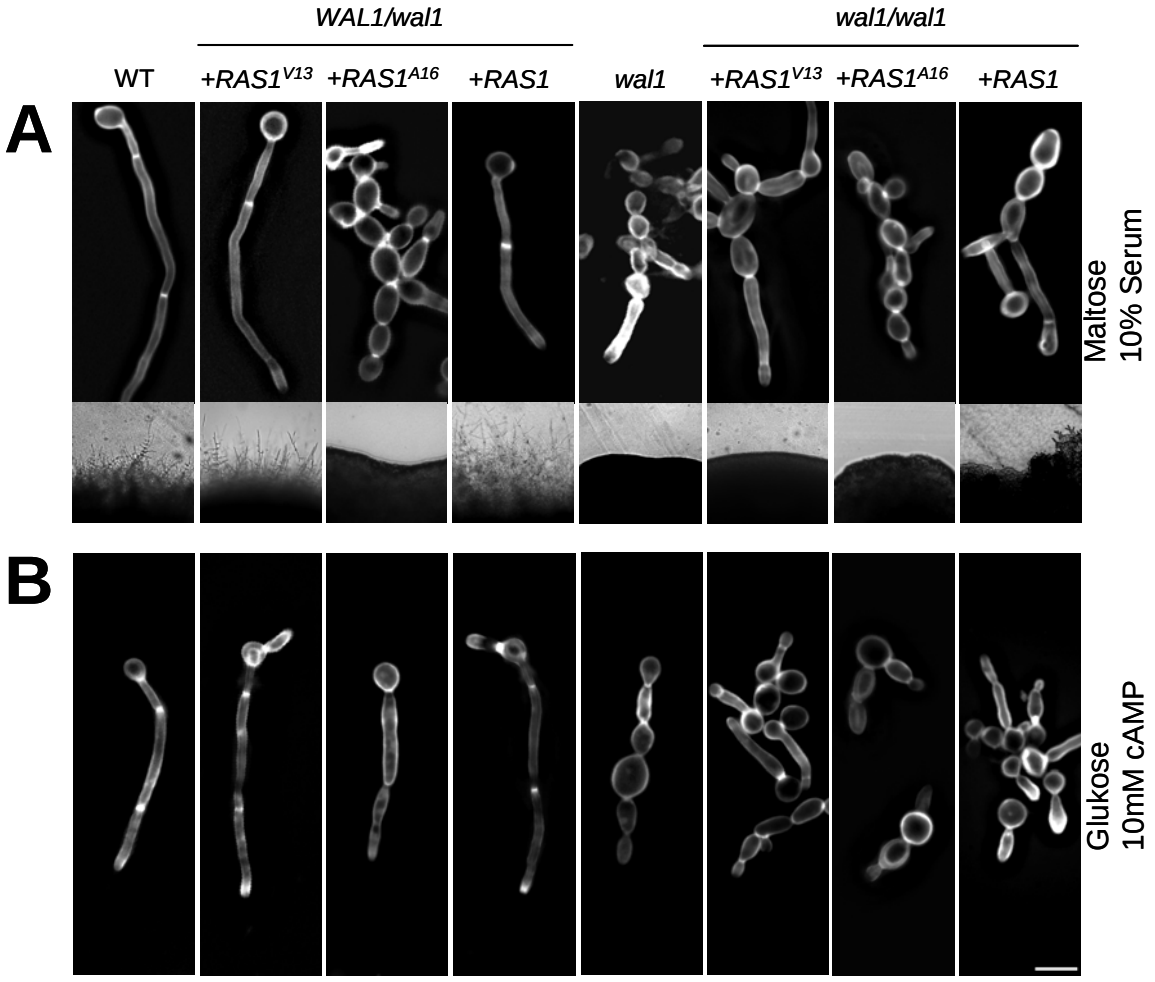

Abbildung 15 | Hypheninduktion in verschiedenen *C. albicans* Stämmen.
Die Kulturen wurden über Nacht in Minimalmedium mit Maltose als C-Quelle angezogen. Die Induktion erfolgte über drei Stunden entweder mit 10% Serum in Maltose-Medium (A) oder in Glukose-Medium und 10mM cAMP (B) bei 37°C. Die Zellen wurden vor der Mikroskopie mit Calcofluor gefärbt. In (A) sind Bilder von Maltose-Platten mit 10% Serum abgebildet, die Kolonieränder nach 3-5 Tagen Inkubation zeigen.

4.5. Virulenz- und Adhäsionstests

C. albicans gehört neben *C. dubliniensis*, *C. parapsilosis, C. krusei* und *C. glabrata* zu einer Gruppe fakultativ humanpathogener Pilze, die als Kommensalen vorkommen und hauptsächlich bei Menschen mit geschwächtem Immunsystem zu schweren Mykosen führen (Marr, 2004). Der Pilz tritt saprophytisch auf der Haut im Gastro-Intestinaltrakt und Schleimhäuten auf und kann daher in immungeschwächten Patienten zu endogen verursachten Infektionen führen. Weiterhin kann eine intensive Antibiotikatherapie zu einer Besiedelung des Darmepithels und im Folgenden zur Invasion des befallenen Gewebes und zur systemischen Ausbreitung, das heißt zum Befall der inneren Organe, führen.
Um die Pathogenität verschiedener *C. albicans* Mutanten zu untersuchen, wird ein Mausmodell verwendet. Hierbei wird eine systemische Infektion durch Injektion von Blastosporen direkt in die Schwanzvene der Maus herbeigeführt. Dieses Verfahren ist eine der wichtigsten Standardmethoden für die Beurteilung der Virulenz eines mutanten Stammes.

Etablierung des *in vitro* Porcine Intenstinal Epithelium (PIE)-Assays: Um die frühe Kolonisierungsphase epithelialen Gewebes durch *C. albicans* zu untersuchen, wurde ein neuartiges *in vitro* System entwickelt, welches der *in vivo* Situation im humanen Wirt möglichst ähnlich sein sollte. Zusätzlich sollte das System einfach handhabbar und das Gewebe unbegrenzt verfügbar sein. Da das Darmepithel einen der wichtigsten Eintrittsorte für systemische *C. albicans* Infektionen darstellt, wurde ein System unter Verwendung von Dickdarmepithel des Schweins etabliert. Dieses Gewebe ist unbegrenzt verfügbar von frisch geschlachteten Schweinen und kann mehrere Stunden für eine Ko-Kultivierung mit *C. albicans* verwendet werden.

Durchführung des PIE-Assays: Für den PIE-Assay wurde nur Dickdarmepithel verwendet, da *C. albicans* unter kommensalischen Lebensbedingungen hier am ehesten zu finden ist. Um das Schweinedarmepithel für den Versuch vorzubereiten, wurden

zunächst Nahrungsreste vom Gewebe entfernt und die Darmoberfläche mit Wasser gewaschen. Anschließend wurde der Darm in etwa gleich große Stücke geteilt (ca. 25cm²) und in Petrischalen, die Ringerlösung enthielten, eingelegt. Auf das so vorbereitete Gewebe wurde 1ml Flüssigkultur eines jeweiligen *C. albicans* Stammes, der über Nacht in Vollmedium (YPD) angezogen worden war, aufgetragen. Dabei wurde eine Zelldichte von $1x10^6$ bis $1x10^7$ Zellen/cm² angestrebt. Diese Ansätze wurden für ein bis sieben Stunden bei 37°C inkubiert. Anschließend wurde das Epithel gründlich gespült, um nicht-adhärente Zellen von der Epitheloberfläche zu entfernen. Die oberste Zellschicht des Darmepithels wurde daraufhin abgenommen, zerteilt und mit Calcofluor (Fluorescent Brightener 28) inkubiert, um spezifisch die Zellwand der *C. albicans* Zellen zu färben und diese gegenüber verbliebenen Epithelzellen mittels Fluoreszenzmikroskopie zu unterscheiden.

Analyse der *Cawal1*-Mutante im PIE-Assay: Um direkt die Adhäsionsfähigkeit der Δ*wal1*-Mutante zu prüfen, wurde dieser Stamm zusammen mit dem Wildtyp SC5314 sowie dem Ausgangsstamm BWP17 im PIE-Assay getestet. Dabei konnte gezeigt werden, dass der Wildtyp SC5314 sehr schnell zur Hyphenbildung induziert wurde und nach kurzer Zeit beinahe alle Zellen Hyphen gebildet hatten. Die Hyphenbildung ging einher mit einer starken Agglomeration der Hyphen und einer ausgeprägten Adhäsion an das Darmepithel (Abbildung 16). Im Gegensatz dazu war die Adhärenz der BWP17-Zellen auf der Epitheloberfläche sehr schwach ausgeprägt. Zellen dieses Stammes bildeten zudem kaum Hyphen. Für die *C. albicans* Δ*wal1*-Mutante wurde bereits durch verschiedene *in vitro* Versuche zur Hypheninduktion ein Defekt in der Hyphenentwicklung festgestellt. Hierzu wurde z.B. Serum oder Spider-Medium verwendet. Spider-Medium ist ein synthetisches Medium, welches durch seine alternative Kohlenstoffquelle bei 37°C *C. albicans* zur Hyphenbildung induziert. Auch auf dem Darmepithel zeigte sich, dass Δ*wal1*-Zellen nicht in der Lage waren, Hyphen auszubilden. Lediglich einige Pseudohyphen konnten beobachtet werden. Damit entspricht das Verhalten von *Cawal1* im PIE-Assay den *in vitro* Untersuchungen zur Hypheninduktion. Dennoch konnte auf dem Darmepithel eine stärkere Adhärenz der Δ*wal1*-Zellen beobachtet werden als für den apathogenen Stamm BWP17, der unter diesen Bedingungen nur sehr wenige Hyphen bildete. Allerdings war die Adhäsion von Δ*wal1*-Zellen deutlich geringer als für den Wildtyp SC5314, der unter diesen Bedingungen abundant filamentierte.

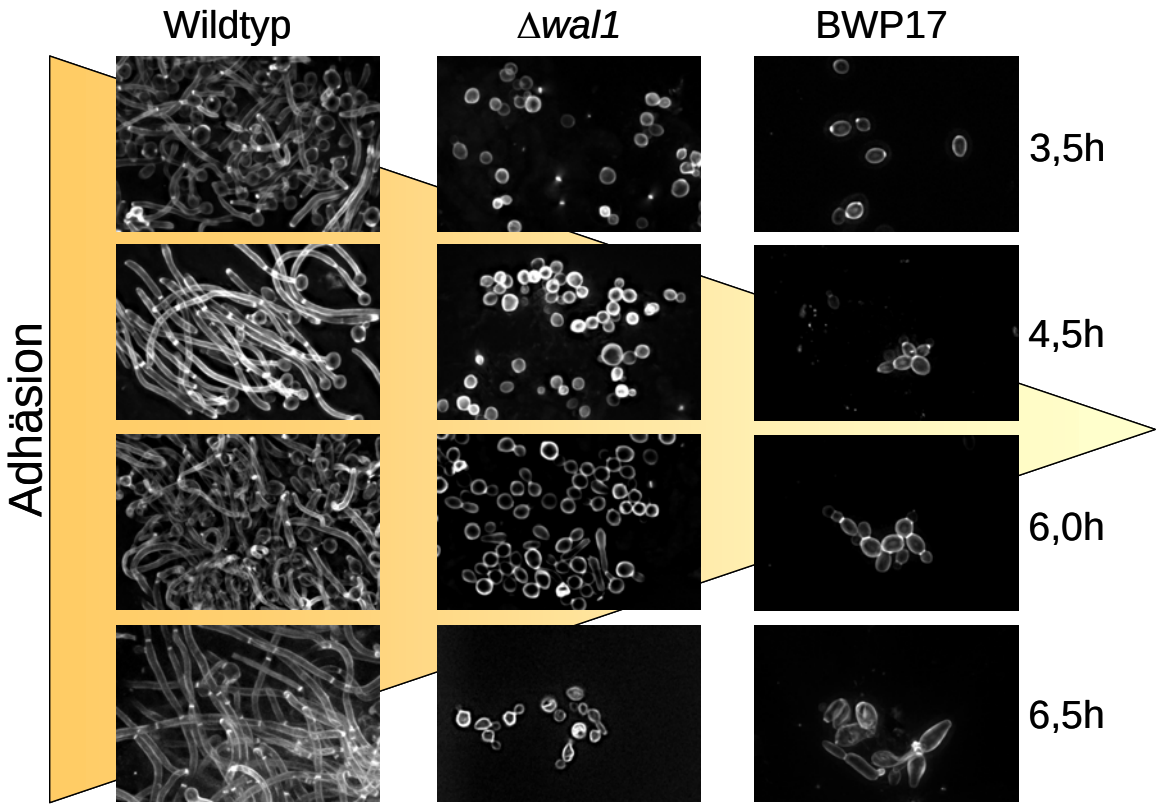

Abbildung 16 | Analyse verschiedener *C. albicans* Stämme im PIE-Assay.
Hefekulturen des Wildtyps SC5314, der homozygoten *Cawal1* Mutante und des Ausgangsstammes BWP17 wurden auf Schweinedarm-Epithel inkubiert. Das Epithel wurde nach den angegebenen Zeitpunkten gewaschen, danach wurde die obere Zellschicht des Epithels mit den adhärierenden *C. albicans* Hyphen entfernt und die Pilzzellen selektiv mit Calcofluor gefärbt.

Um die Rolle der Hyphenbildung für die Adhäsionsfähigkeit näher zu untersuchen, wurden ein Vergleich zwischen dem Wildtyp, der *Cawal1* und der afilamentösen Δ*efg1*/Δ*cph1* Mutante im PIE-Assay vorgenommen. Alle Stämme wurden auf den Darmepithelien inkubiert und nach verschiedenen Zeitpunkten auf ihre Hyphenbildung und Adhäsion untersucht (Abbildung 17).

In den Waschlösungen beider Stämme konnten überwiegend Hefezellen gefunden werden, teilweise waren Pseudohyphen bei der Δ*efg1*/Δ*cph1* Mutante zu beobachten. Auf den Epithelien dagegen, die mit dem Wildtyp beimpft worden waren, wurden ausschließlich Hyphen diagnostiziert, die stark an die Oberfläche adhärierten und auch durch intensives Waschen nicht entfernt werden konnten. Die Δ*efg1*/Δ*cph1* Mutante war

nicht in der Lage, die Bildung von Hyphen zu initiieren und an dem Darmepithel zu adhärieren. Auf der Epitheloberfläche konnten daher nur sehr wenige Zellen beobachtet werden. Deutlich mehr Zellen und teilweise auch Pseudohyphen wurden auf Darmepithelien mit *Cawal1*-Zellen beobachtet.

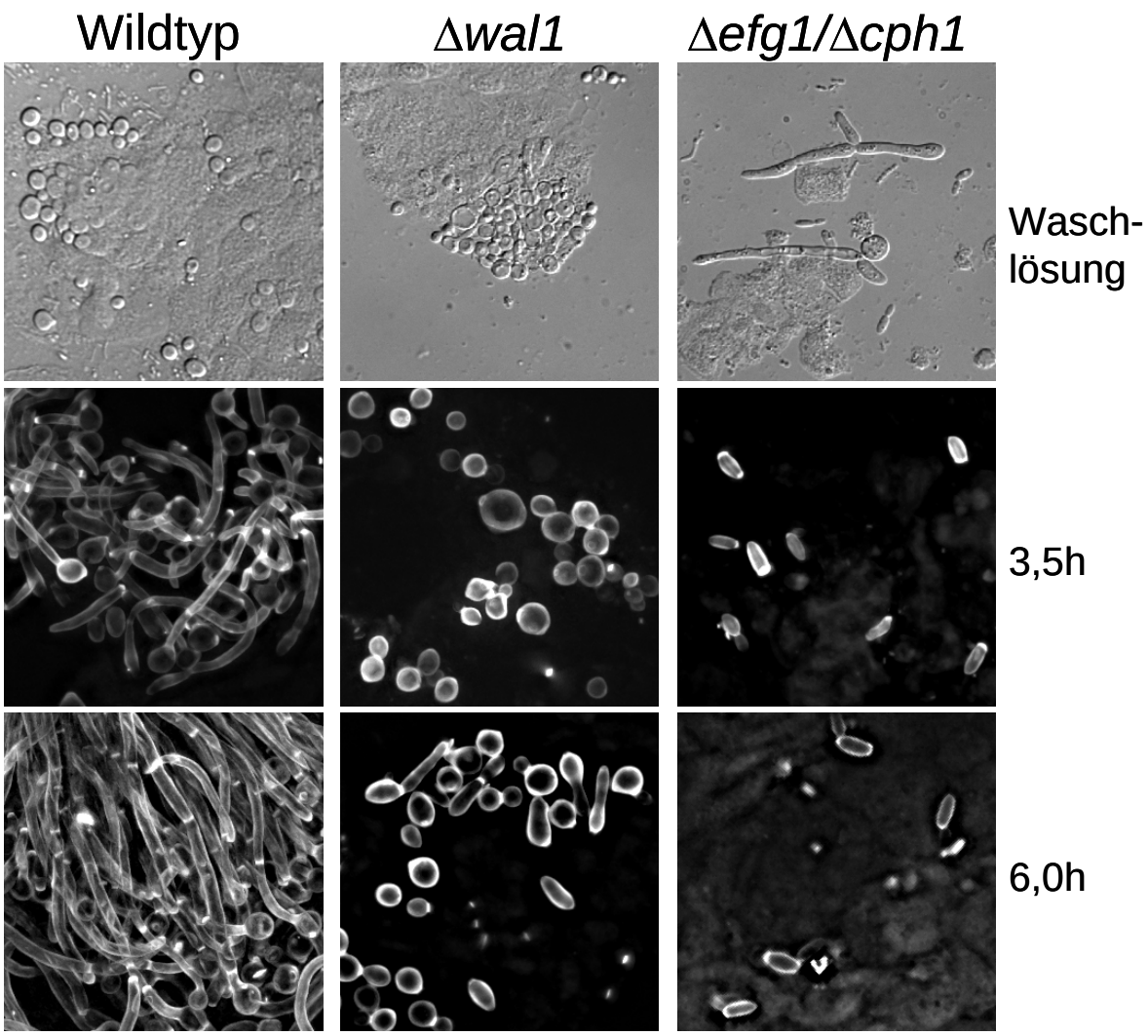

Abbildung 17 | Analyse der Rolle von *EFG1* und *CPH1* für die Adhäsion und Hyphenmorphogenese im PIE-Assay.
Wildtyp, *C. albicans* Δ*wal1* und die Δ*efg1*/Δ*cph1* Mutante wurden auf Darmepithel inkubiert. In den Waschlösungen wurden vor allem nicht-adhärente Hefezellen gefunden, bei der Δ*efg1*/Δ*cph1* Mutante waren teilweise Pseudohyphen zu finden.

Untersuchungen zur Virulenz der *Ca*Δ*wal1*-Mutante im Mausmodell (in Zusammenarbeit mit Nir Osherov, Tel Aviv University, Israel): Um die Daten aus dem PIE-Assay mit einem *in vivo* Modell für systemische Infektion vergleichen zu können, wurden *C. albicans* Stämme, die entweder eine heterozygote (CAT5: *WAL1/wal1::URA3*) oder homozygote (CAT6: *wal1::HIS1/wal1::URA3*) Deletion des *WAL1*-Gens tragen, mit dem Wildtyp SC5314 und BWP17, der als Ausgangsstamm für die Deletion von *WAL1* diente, in ihrer Virulenz im Mausmodell untersucht. Dazu wurden verschiedene Zellkonzentrationen dieser Stämme in die Schwanzvene der Mäuse injiziert.

Die heterozygote Mutante zeigt dabei bei allen injizierten Zellkonzentrationen eine mit dem Wildtyp vergleichbare Virulenz. Dieser Versuch zeigte auch, dass nach der Komplementierung des *ura3*-Defektes im BWP17-Ausgangsstamm die Virulenz dieses Stammes wiederhergestellt werden konnte. Wie in Abbildung 18 gezeigt wird, ist der Verlauf der Sterberate zwischen Wildtyp und CAT5 ähnlich. Die homozygote Δ*wal1*-Mutante CAT6 allerdings zeigt eine deutliche Reduktion in ihrer Virulenz, so dass die Mehrzahl der Mäuse auch bei steigenden Zellkonzentrationen bis zum Ende des Experiments überlebte und keine sichtbaren Krankheitssymptome zeigte. Erst bei sehr hohen Zellkonzentrationen konnten bei der Mehrzahl der Mäuse Krankheitssymptome festgestellt werden. Der Ausgangsstamm BWP17 ist aufgrund seines Genotyps *(*Δ*ura3*, Δ*his1*, Δ*arg4*) apathogen, so dass bei allen Zellkonzentrationen alle Mäuse überlebten. Entscheidend für die fehlende Virulenz ist dabei das Fehlen des *URA3*-Gens, welches für eine Orotidinmonophosphat-Decarboxylase codiert und den letzten Schritt in der *de novo* Biosynthese von Uridinmonophosphat katalysiert. Alle anderen Stämme, die im Mausmodell verwendet wurden, tragen mindestens eine Kopie des *URA3*-Gens, so dass eine reduzierte Virulenz nicht auf das Fehlen des *URA3*-Gens zurückgeführt werden kann.

Um die Virulenz mutanter *C. albicans* Stämme zu beurteilen, werden verschiedene Modellsysteme herangezogen. Dabei stellt das Mausmodell die am weitesten verbreitete Methode dar. Allerdings sind Tierversuche eine zeit- und kostenintensive Methode, mutante *C. albicans* Stämme zu testen. Daher wurde in den letzten Jahren intensiv nach alternativen Testmethoden gesucht, die anstelle des Mausmodells verwendet werden könnten. Neuere *in vitro* Methoden untersuchen das Ausmaß der Gewebeschädigung und die Expressionsprofile bereits identifizierter Virulenzgene bei *C. albicans* anhand von rekonstituierten, humanen Epithelien, z.B. von Vaginalepithelien (Schaller *et al.*, 2003).

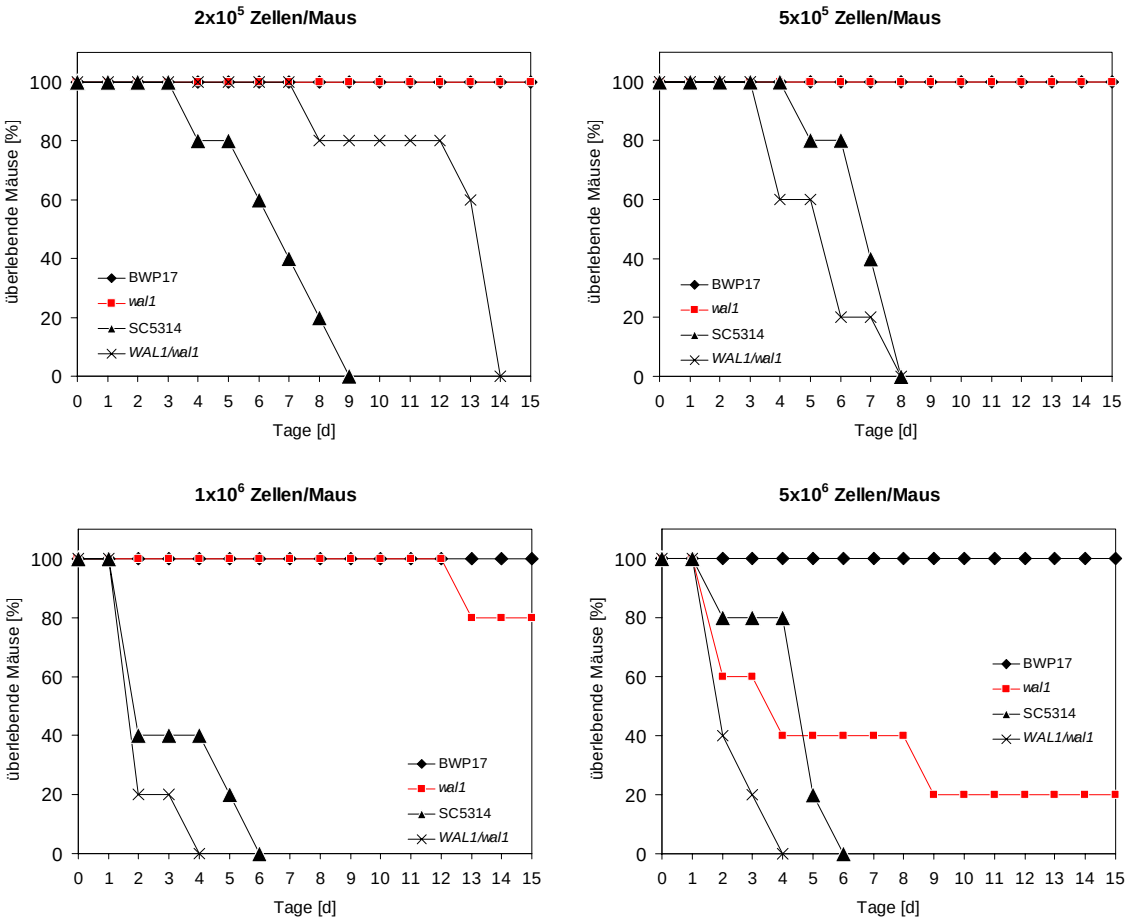

Abbildung 18 | Analyse verschiedener *C. albicans* Stämme im Maus-Modell.
Hefekulturen des Wildtyps SC5314, der homozygoten *Cawal1* Mutante sowie der heterozygoten *CaWAL1/wal1* Mutante und des Ausgangsstamms BWP17 wurden in bestimmten Zellkonzentrationen in die Schwanzvene von Mäusen injiziert. 5 Mäuse je Stamm und Experiment wurden verwendet. In den Grafiken ist die Sterberate der Mäuse dargestellt.

Eine Untersuchung der sekretierten Aspartylproteasen (SAPs) zeigte, dass in einer initialen Kolonisierungsphase während der ersten 6 Stunden die Gene *SAP2, SAP9* und *SAP10* angeschaltet wurden. In einer darauf folgenden Phase (bis 12h), die mit der Zerstörung des Gewebes einherging, wurden weitere Gene dieser Genfamilie, *SAP1, SAP4* und *SAP5* aktiviert und erst deutlich später auch die *SAP6* und *SAP7* Gene (Schaller *et al.,* 2003). In weitergehenden Untersuchungen wurde die Produktion von Cytokinen als proinflammatorische Antwort des Epithels auf eine *C. albicans* Infektion untersucht (Schaller *et al.,* 2005). *In vitro* Rekonstruktionen von Haut und Darmepithelien

zeigten die Bedeutung der Transkriptionsfaktoren Cph1p und Efg1p für die Adhäsion und Invasion (Dieterich *et al.,* 2002). *C. albicans* besitzt eine Genfamilie von ALS-Proteinen, die pflanzlichen Lektinen ähnlich sind und als „Agglutinin-Like Sequences“ bezeichnet werden. In Untersuchungen mit rekonstituierten Oral-Epithelien wurden der Beitrag verschiedener ALS-Proteine bei der Adhäsion bestimmt und die Fähigkeit zur Invasion des Epithels untersucht (Bartie *et al.*, 2004; Zhao *et al.*, 2005). Die rekonstituierten humanen Epithelien enthalten allerdings nur einen Teil der Vielzahl unterschiedlicher Zelltypen, die in einem natürlichen Gewebe vorkommen und können daher nur bedingt die *in vivo* Situation einer *C. albicans* Infektion simulieren. Mit Hilfe dieser rekonstituierten Epithelien kann jedoch die Gewebezerstörung durch *C. albicans* bewertet und quantifiziert werden.

Eine weitere Möglichkeit für die Untersuchung der Virulenz stellen Zellkulturen menschlicher Zellen dar. Diese Zellen sind leicht zu kultivieren und nahezu unbegrenzt verfügbar, so dass standardisierte Testsysteme entwickelt werden können. Nachteilig kann sich hierbei jedoch die Notwendigkeit der Passagierung von Zellkulturen auswirken, denn im Laufe der Zeit können zellspezifische Eigenschaften verloren gehen, die wesentlich für die biologische Funktion dieser Zellen *in vivo* sein können, was den Vergleich einer Ko-Kultivierung dieser Zellkulturen mit *C. albicans* mit *in vivo* Modellen erschwert. Weiterhin können diese Zellkulturen nicht als intakte Gewebe fungieren, so dass die Adhäsions- und Penetrationsfähigkeit von *C. albicans* Stämmen schwierig zu bewerten ist. Ein Vorteil solcher Zellkulturen und rekonstituierter Epithelien liegt in der Möglichkeit, die Adhäsions- und Penetrationsprozesse mikroskopisch verfolgen zu können. Dabei könnten *in vivo* Zeitraffer-Aufnahmen bei der Charakterisierung von Mutanten eingesetzt werden.

Eine weitere Möglichkeit eines *ex vivo* Modells ist, die Reaktion von *C. albicans* Zellen auf Makrophagen zu analysieren und damit die ersten Schritte der Wirt-Pathogen Interaktion zu charakterisieren. Werden einzellige, hefeförmige *C. albicans* Zellen durch Makrophagen aufgenommen, können diese Zellen zur filamentösen Hyphenform differenzieren und damit den Makrophagen entkommen. Die Aufnahme und Freisetzung der *C. albicans* Zellen kann so in einem *in vitro* System in Echtzeit beobachtet werden. Allerdings stellt sich hierbei die gleiche Problematik wie bei Zellkulturen, dass die Zellen durch die fortlaufende Vermehrung *in vitro* ihre Differenzierungsfähigkeit verlieren können ebenso wie die Fähigkeit, beispielsweise reaktive Sauerstoff-Spezies zu produzieren, um die *C. albicans* Zellen oxidativem Stress auszusetzen (Lorenz *et al.*, 2004).

Ziel der Versuche dieser Arbeit war es, ein alternatives Infektionsmodell zu finden, welches weniger aufwendig als bisherige Verfahren, wie Mausmodell oder rekonstituierte Gewebe, ist aber auch möglichst nahe an der *in vivo* Situation im Wirt ist. Dafür wurde der auf Schweinedarm-Epithel basierende PIE-Assay entwickelt. Dieses Gewebe ist in Aufbau und Beschaffenheit dem des menschlichen Darmgewebes sehr ähnlich. Über mehreren Schichten Bindegewebe, die mit Epithelzellen besetzt sind, befindet sich eine Mukosa aus N-Acetylglukosamin, welches auch *in vitro C. albicans* zur Induktion von Hyphen führen kann.

Um die Ergebnisse des PIE-Assays bewerten zu können, wurde dieser dem Mausmodell gegenübergestellt. Dabei zeigt der Wildtyp SC5314 bereits nach wenigen Stunden eine starke Kolonisierung des Darmgewebes sowie eine starke Hyphenbildung. Im Mausmodell einer systemischen Infektion verursachte der Wildtyp eine vollständige Letalität nach wenigen Tagen. Beide Modelle ermöglichen zusammen die Analyse der frühen Kolonisierungsphase im PIE-Assay sowie die langfristigen Auswirkungen einer systemischen Infektion durch die zu testenden Stämme hinsichtlich ihrer Virulenz. Für die Δ*wal1* Mutante wurde im Mausmodell eine verminderte Virulenz festgestellt. Im PIE-Assay wurde für Δ*wal1* Zellen eine reduzierte Adhäsionsfähigkeit und fehlende Hyphenbildung festgestellt. Der PIE-Assay lieferte neben den *in vitro* Daten zusätzlich Aussagen über die Adhäsionsfähigkeit der Mutante sowie die morphologische Differenzierung auf der Epitheloberfläche. Die verminderte Adhäsion an Epithelien sollte zu einer reduzierten Fähigkeit der *Cawal1* Zellen führen, über das Epithel in den Wirt einzudringen und über den Blutstrom verbreitet zu werden. Somit kann der PIE-Assay als alternatives Modell für die Beurteilung der Adhäsions- und Penetrationsfähigkeit verschiedener *C. albicans*-Stämme verwendet werden, nicht jedoch für Aussagen über die Virulenz eines Stammes, die nur im Mausmodell eindeutig beurteilt werden kann.

4.6. Abschließende Bemerkungen

Viele der heute verwendeten Medikamente gegen *C. albicans* besitzen Nebenwirkungen oder sind aufgrund von Resistenzen ineffektiv gegen pilzliche Infektionen. Dazu gehört das Polyen Amphotericin B, das Ergosterole in der Pilzmembran bindet und dadurch die Permeabilität der Zellmembran verändert, so dass das Zytoplasma ausläuft und zum Zelltod führt. Allerdings verursacht Amphotericin B als Nebenwirkung bei vielen Patienten Nierenschädigungen. Azolverbindungen sind antifungale Substanzen, die die 14-α-Lanosterol-Demethylase inhibieren. Diese wird in *C. albicans* durch das *ERG11*-Gen kodiert. Das entsprechende Protein wird für die Ergosterolbiosynthese benötigt. Damit wirken die beiden wichtigsten antifungalen Substanzen auf die Ergosterolbiosynthese. Diese unterscheidet sich von der Cholesterolbiosynthese im Menschen, so dass ein pilzspezifischer essentieller Vorgang betroffen ist. Ein weiterer Aspekt in der Pilzbiologie ist der Aufbau einer Zellwand, die tierischen Zellen fehlt. Hierbei dient für einen antifungalen Angriff insbesondere die Chitinsynthese und Glukansynthese. Als Substanzen stehen dabei Polyoxin D, Nikkomycin und Caspofungin zur Verfügung (Kim *et al*., 2002; Schmidt, 2004; Stevens *et al*., 2004).

Die Zunahme an pilzlichen Infektionen und ein sich vergrößerndes Erregerspektrum in den letzten Jahren lässt es notwendig erscheinen, neue effektive antifungale Substanzen zu finden, die möglicherweise andere Signalwege in Pilzen treffen als die bisher von antifungalen Substanzen genutzten. Ein Weg, um neue Substanzgruppen und damit wirksame Medikamente zu entwickeln, ist es, zunächst die Mechanismen der Virulenz von *C. albicans* zu verstehen. Ein weitere, dazu komplementäre Methode ist, neue Naturstoffe zu isolieren und auf ihre antifungale Wirksamkeit zu untersuchen.

C. albicans ist ein opportunistischer, kommensalischer Pilz auf Schleimhäuten insbesondere des Gastro-Intestinaltraktes. Bei Patienten mit beeinträchtigtem Immunsystem kann es daher zu *C. albicans* Infektionen kommen, die durch die Kolonisierung und Invasion von Wirtsgewebe hervorgerufen werden. Ein wichtiger Aspekt in der Virulenz von *C. albicans* ist die Fähigkeit, zwischen hefeartigem und filamentösem Wachstum zu wechseln (Liu, 2001; Odds, 1985). Dieser Wechsel ist verbunden mit einer

Vielzahl extrazellulärer Stimuli und wird von einem Netzwerk an Proteinen koordiniert, die polares Wachstum aufrechterhalten. In der pilzlichen Zelle spielt die GTPase Ras1p eine zentrale Rolle für diesen morphogenetischen Wechsel. Ras1p aktiviert zwei nachgeordnete Signalwege, eine MAP-Kinase-Kaskade und den cAMP-Weg. Dadurch erfolgt die Aktivierung der Transkriptionsregulatoren Efg1p und Cph1p und die Aktivierung hyphenspezifischer Gene (Berman und Sudbery, 2002; Leberer *et al*., 2001).

Die regulatorische Funktion von Cdc42p auf die Ausbildung einer Zellpolarität und damit auf die Form des Aktinzytoskeletts während der Hefe- und der Hyphenphase von *C. albicans* konnte in früheren Arbeiten bereits belegt werden (Bassilana *et al*., 2003; Hazan und Liu, 2002; Ushinsky *et al*., 2002). Signale dieser Rho-Protein-Module werden auf Effektorproteine übertragen, die die Assemblierung von Aktinfilamenten regulieren. Dazu gehören Proteine hochkonservierter Familien wie die IQGAP-, Formin- und Wiskott-Aldrich Syndrom-Protein- (WASP)-Familien. Durch die Funktionsanalyse des WASP-Homologen *WAL1* in *C. albicans* konnte dessen Funktion in der Zelle aufgeklärt werden. Eine Δ*wal1* Mutante weist deutliche Defekte in der Morphologie und in der Zellpolarität der Hefezellen auf, was durch das gehäufte Auftreten großer, rundlicher Zellen und deren zufälliges Erscheinen neuer Knospungsstellen auf der Zelloberfläche sichtbar wurde. Defekte in der Organisation des kortikalen Aktinzytoskeletts und eine verzögerte Aufnahme des lipophilen Farbstoffes FM4-64 stellen intrazelluläre Defekte dieser Mutante dar, die durch Fluoreszenz-Mikroskopie aufgedeckt werden konnten. Die Vakuolenmorphogenese war in der Δ*wal1* Mutante gestört und führte zu stark fragmentierten Vakuolen. Unter hypheninduzierenden Bedingungen konnte in Δ*wal1* Zellen polares Wachstum initiiert aber nicht aufrechterhalten werden und führte daher zu pseudohyphalem Wachstum (Walther und Wendland, 2004a). Ähnliche Phänotypen wurden in der *C. albicans* Δ*myo5* Mutante festgestellt, so dass beide Proteine in *C. albicans* möglicherweise in einem Proteinkomplex agieren (Oberholzer *et al*., 2002). In *S. cerevisiae* konnte eine Interaktion der Typ-I Myosine Myo3p und Myo5p über deren SH3-Domänen mit der prolinreichen Domäne von Las17p/Bee1p, dem WASP-Homologen von *S. cerevisiae,* gezeigt werden (Machesky, 2000). Beide Proteinklassen, Typ-I Myosine und WASP besitzen zudem eine C-terminale saure Domäne, die für die Aktivierung des Arp2/3-Komplexes verantwortlich ist (Lechler *et al*., 2000; Madania *et al*., 1999). Durch die Charakterisierung von *C. albicans WAL1* und die Ergebnisse der *MYO5* Arbeiten konnten ähnliche Phänotypen beschrieben werden, die darauf schließen, dass beide Proteine für eine Aktinassemblierung während der Endozytose benötigt werden.

Diese Aktinassemblierung wird für einen wesentlichen Schritt während des Endozytoseprozesses benötigt, da die Deletion des *C. albicans WAL1* Gens eine deutliche Verzögerung in der Aufnahme von FM4-64 und damit bei dem Internalisierungsschritt von Zellmembranen lieferte. Ähnliche Defekte wurden auch in Säugerzellen beschrieben, in denen die Beeinträchtigung der Aktivität von WASP zur Anhäufung von Endozytosevesikeln und zu Endozytosedefekten führte (Da Costa *et al*., 2003). Darüber hinaus lieferte der Befund von fragmentierten Vakuolen bei *C. albicans ⊿wal1* Zellen einen weiteren Hinweis darauf, dass Wal1p an Fusionsprozessen von Endozytosevesikeln beteiligt ist. Eine weitere Rolle von Wal1p könnte im Transport von Vesikeln liegen, um diese von ihrem Entstehungsort an der Plasmamembran ins Zellinnere zu befördern. Interessanterweise benutzen einige bakterielle intrazelluläre Pathogene wie *Shigella flexneri* und *Listeria monocytogenes* WASP zur Generierung von Aktinstrukturen, den sog. „comet tails“, die ihnen zur Beweglichkeit innerhalb von Wirtszellen und zur Infektion neuer Zellen verhelfen (Gouin *et al*., 1999; Suzuki *et al*., 2002).

Die Deletionen der *C. albicans* und *A. gossypii WAL1* Gene belegten, dass WASP-Homologe bei Pilzen einen entscheidenden Beitrag für die polare Wachstumsphase leisten. Die Beeinträchtigungen in der Organisation des Aktinzytoskeletts in der *C. albicans ⊿wal1* Mutante, führten dazu, dass Aktinpatches nicht wie beim Wildtyp hauptsächlich in die entstehende Tochterzelle lokalisiert werden. Dieser Defekt könnte in direktem Zusammenhang mit einem verstärkten isotropen Wachstum der Mutterzellen stehen. Die Fehlverteilung der Aktinpatches in *C. albicans ⊿wal1* Zellen könnte dabei durch das nicht polarisierte Wachstum dazu beitragen, dass *C. albicans* die Fähigkeit verliert, polare Wachstumsrichtungen beizubehalten, die für die Hyphenmorphogenese essentiell sind. Im Gegensatz zu den Aktinpatches ist die Assemblierung linearer Aktinfilamente in den mutanten Zellen nicht gestört. Diese Aktinfilamente reichen bis in die Spitze der entstehenden Tochterzellen hinein (oder gehen von dort aus). Aus Arbeiten in *S. cerevisiae* ist bekannt, dass die Assemblierung dieser Aktinfilamente von dem Formin Bni1p abhängig ist (Evangelista *et al*. 2002; Evangelista *et al*. 2003; Pruyne *et al*., 2002; Sagot *et al*., 2002). Formine stellen neben der konservierten Gruppe der WASP-Homologen die zweite wichtige Klasse von Effektorproteinen des Aktinzytoskeletts dar. Die Assemblierung von linearen Aktinfilamenten erfolgt dabei in einem Arp2/3-unabhängigen Prozess (Sagot *et al*., 2002).

In *A. nidulans* lokalisiert das Formin SEPA an die Hyphenspitze sowie an Stellen zukünftiger Septierung (Sharpless und Harris, 2002). Die Lokalisierung in die Hyphenspitze gleicht der Position des Spitzenkörpers. Der Spitzenkörper ist eine Struktur an der Hyphenspitze filamentöser Pilze, die im Phasenkontrast beobachtet werden kann und für die Wachstumsrichtung der Hyphenspitze verantwortlich ist (Bartnicki-Garcia *et al*., 1995; Girbardt, 1957; Harris *et al*., 2005). Der Spitzenkörper stellt dabei ein „Vesicle Supply Center" dar, d.h. eine Ansammlung endozytotische Vesikel auf dem Weg zum Einbau in die Hyphenspitze. Inwieweit der Spitzenkörper auch eine Kontrollfunktion für das polare Wachstum hat, ist umstritten. Allerdings kann durch eine Veränderung der Position des Spitzenkörpers, z.B. mit Hilfe eine Lasers, auch die Wachstumsrichtung von Hyphen beeinflusst werden (Harris *et al*., 2005).

Mit Hilfe des Farbstoffes FM4-64 kann auch in *C. albicans* eine dem Spitzenkörper ähnliche Struktur angefärbt werden (Crampin *et al*., 2005; Martin *et al*., 2005, in Revision). Unmittelbar nach der Inkubation der Hyphen mit FM4-64 akkumuliert der Farbstoff in der Hyphenspitze. *C. albicans* Bni1-GFP zeigt eine Kolokalisierung mit diesem Spitzenkörper und ist außerdem an Septierungsstellen, wie auch in *A. nidulans*, zu finden (Martin *et al*., 2005 in Revision). In *S. cerevisiae* wurde Bni1p als Teil des Polarisom-Komplexes zusammen mit Spa2p, Bud6p und Pea2p identifiziert (Sheu *et al*., 1998).

Mit der Charakterisierung von *WAL1* konnte gezeigt werden, dass neben den sekretorischen Prozessen, an denen z.B. Formine wie Bni1p eine wichtige Rolle spielen, auch die Endozytose einen wesentlichen Anteil am polaren Zellwachstum besitzt (Abbildung 19). Damit kommt dem Aktinzytoskelett von *C. albicans* eine essentielle Bedeutung für die Hyphenmorphogenese zu. Dies könnte in Zukunft weitere Zielgene liefern, deren Protein an der Aktinzytoskelett-Assemblierung beteiligt sind und die sich damit als Zielstrukturen für die Suche nach antifungalen Substanzen eignen könnten.

C. albicans ist ein dimorpher Pilz der unter bestimmten Bedingungen, wie 37°C und Serum, in der Lage ist, Hyphen auszubilden. Die *C. albicans* Δ*wal1* Mutante war unter allen getesteten Bedingungen nicht mehr in der Lage, Hyphen zu bilden. Daher war die Analyse von hyphenspezifischen Defekten durch die Deletion von *WAL1* in *C. albicans* nicht möglich. Aus diesem Grund wurde die Deletion und Charakterisierung des WASP-Homologen *WAL1* im filamentösen Ascomyzeten *A. gossypii* durchgeführt. Die *A. gossypii* Δ*wal1* Mutante wies temperatursensitives Wachstum auf und zeigte damit einen ähnlichen Phänotyp wie die *bee1/las17* Mutante bei *S. cerevisiae* (Li, 1997).

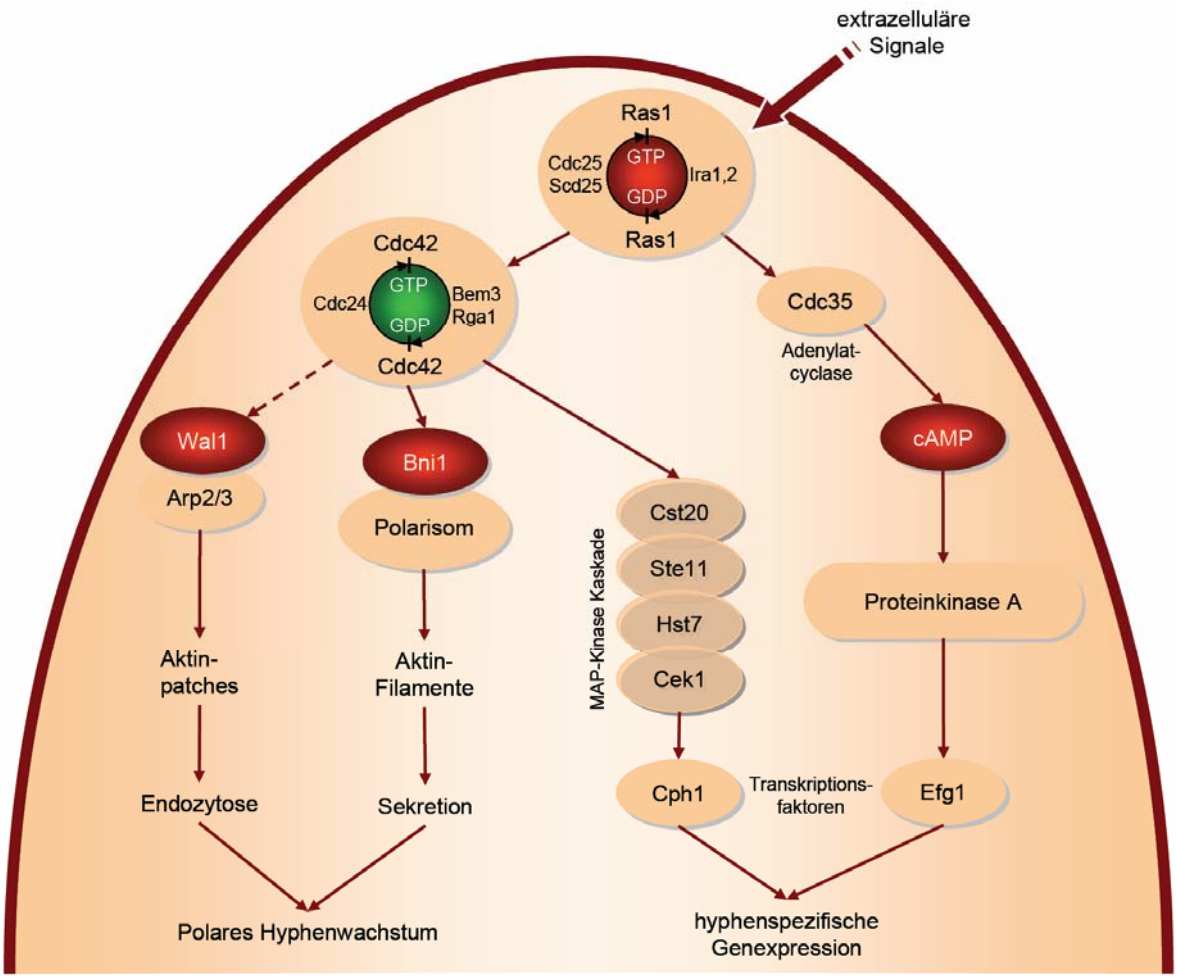

Abbildung 19 | Das Aktinzytoskelett als Teil der Signaltransduktionskaskade zur Ausbildung filamentösen Wachstums.
Dargestellt ist ein Modell, welches die Strukturen des Aktinzytoskeletts und ihre Funktionen der Endozytose und Sekretion beinhaltet. Durch Ras1p werden über zwei alternativen Signalwege Transkriptionsfaktoren aktiviert, die die Expression hyphenspezifischer Gene einleiten. Durch die Aktivierung von Cdc42p werden Proteine direkt oder über Adapterproteine induziert, was zur Bildung von Aktinfilamenten führt.

Das polare Hyphenwachstum in *A. gossypii* war nach der Deletion von *WAL1* drastisch reduziert und ähnelte dem der *Agbem2* und *Agcla4* Mutanten. Cla4p wird in *A. gossypii* für einen Prozess, der als „hyphal maturation“ bezeichnet wird, gebraucht (Ayad-Durieux *et al*., 2000). Dieser Prozess beschreibt die Zunahme der Wachstumsgeschwindigkeit während der Myzelbildung bei *A. gossypii*. Junges Myzel ist durch laterale Verzweigungen

gekennzeichnet, die mit etwa 20µm/h wachsen. Beim Übergang dieses Verzweigungsmusters zu dichotomen Verzweigungen des maturierten Myzels steigt die Wachstumsgeschwindigkeit auf nahezu den zehnfachen Wert an. Die Geschwindigkeit dieses polaren Wachstums ist abhängig von Transport sekretorischer Vesikel zur Hyphenspitze und dort von der Insertion dieser Vesikel in die Zellmembran. Mit Hilfe von Zeitrafferaufnahmen konnte gezeigt werden, dass das schnelle Hyphenwachstum gleichzeitig mit dem Erscheinen großer Vakuolen in subapikalen Hyphenregionen auftritt. Anhand dieser Vakuolen, die lichtmikroskopisch sichtbar waren, konnten Zytoplasmaströmungen und die Richtung des Vesikeltransports beobachtet werden. Durch Septierungsereignisse wird die zytoplasmatische Strömung beeinflusst und insbesondere kann der rückwärtsgerichtete Ausstrom von Zytoplasma verhindert werden. In der *A. gossypii* ∆*wal1* Mutante konnte in den Zeitraffer-Aufnahmen kein Vakuolentransport beobachtet werden. Hier konnten mit Hilfe des lipophilen Farbstoffes FM4-64 zwar große Vakuolen gezeigt werden, deren Bildung war aber verlangsamt. Die Bildung großer Vakuolen durch die Fusion kleiner Vesikel scheint daher wichtig für das polare Hyphenwachstum zu sein. Interessanterweise zeigte auch die *A. gossypii ∆cla4* Mutante Defekte in der Beweglichkeit von Vakuolen im Gegensatz zur *∆bem2* Mutante, bei der schnelle Vakuolenbewegungen festgestellt wurden (Walther und Wendland, 2004b).

Die große Zahl an phänotypischen Gemeinsamkeiten legt eine gemeinsame Rolle von Cla4p und Wal1p bei der Steuerung der Aktinassemblierung nahe. Die *∆cla4* Mutante zeigt ebenso wie die *∆wal1* Mutante in *A. gossypii* Defekte in der Bildung von chitinreichen Septen, deren ursächlicher Defekt bereits beim Fehlen der Bildung eines Aktinrings festzustellen ist. *CLA4* kodiert für eine Kinase, die durch Cdc42p aktiviert werden kann und in *S. cerevisiae* beispielsweise an der Phosphorylierung von Typ-I Myosinen beteiligt ist. Damit könnte eine Signalkaskade von Cdc42 über Cla4 zu Myo3 und Wal1 führen und Arp2/3-abhängige Aktinassemblierung, Endozytose und Morphogenese steuern (Abbildung 20).

Damit würde Wal1p in einen Cdc42-abhängigen Signalweg eingebunden, der sowohl sekretorische Prozesse als auch Endozytose reguliert. WASP-Homologe von Ascomyzeten zeichnen sich insbesondere durch das Fehlen von Proteindomänen aus, die eine direkte Interaktion mit Rho-Proteinen, z.B. Cdc42p, ermöglichen könnten. Deshalb wäre es von Interesse zu untersuchen, welche morphogenetischen Konsequenzen sich durch den Einbau einer solchen G-Protein Binde-Domäne (GBD) in Wal1p ergeben, z.B.

ob eine solche Wal1-GBD Chimäre eine Deletion der Typ-I Myosine oder von *CLA4* komplementieren könnte. Andererseits könnte die Aktivität von Wal1p durch Phosphorylierung reguliert werden, wie dies in anderen Systemen gezeigt werden konnte (Wu *et al*., 2004).

Wal1p besitzt eine zentrale Rolle bei der Lokalisierung der Aktinpatches in die Hyphenspitze. Die subapikale Konzentration von Aktinpatches in Δ*wal1* Hyphen ist ein Phänotyp, der in dieser Form noch nicht in filamentösen Pilzen beobachtet wurde. Dagegen wurden in der Hyphenspitze Aktinfilamente gefunden ohne gleichzeitige Anwesenheit von Aktinpatches in dieser Region. Das zeigt, dass Defekte in der polaren Lokalisierung von Aktinpatches die Positionierung von Aktinfilamenten nicht notwendigerweise beeinflusst. Die reduzierte polare Wachstumsgeschwindigkeit von Δ*wal1* Hyphen könnte daher durch die Formin-abhängige Assemblierung linearer Aktinfilamente in der Hyphenspitze aufrechterhalten werden. Unabhängig davon werden auch in der Δ*wal1* Mutante Aktinpatches immer noch generiert und ihre Lokalisierung in subapikale Hyphenregionen ist deutlich sichtbar. Offenbar kann die Aktin-Assemblierung auch durch andere Proteine wie Abp1p oder Pan1p realisiert werden, deren Homologe in *S. cerevisiae* eine Rolle für die Endozytose als Aktivatoren des Arp2/3-Komplexes spielen (Kaksonen *et al*., 2003). Jedoch ist der Mechanismus der Bildung von Aktinpatches bis heute nicht bekannt, deren Lokalisierung an die Hyphenspitze ist aber ein Wal1p-abhängiger Prozess, was durch diese Arbeit belegt werden konnte. Wal1p besitzt eine N-terminale WH1-Domäne (WH1 WASP-homology domain 1), welche für die Bindung an Lipide der Plasmamembran, speziell an Phosphatidylinositol-4,5-bisphosphate, verantwortlich ist (Rohatgi *et al*., 1999). Wal1p könnte also als Ankerprotein für die Positionierung kortikaler Aktinpatches fungieren, das die Signale der Rho-GTPasen zum Arp2/3-Komplex weiterleitet.

Neben der Fehllokalisierung der Aktinpatches wurden in Δ*wal1* Hyphen Defekte in der Vakuolenmorphologie, deren Positionierung und Beweglichkeit festgestellt. Endosomen der Δ*wal1* Hyphen lokalisieren in den gleichen subapikalen Regionen wie die Aktinpatches. Ein Defekt der Vakuolenmorphologie ist daher ein sekundärer Effekt einer *WAL1*-Deletion. Ein weiterer Defekt der Δ*wal1* Mutante war eine drastisch reduzierte Fähigkeit, Sporen zu bilden. Sporangien werden im Wildtyp aus durch Septenbildung hervorgegangenen Kompartimenten differenziert.

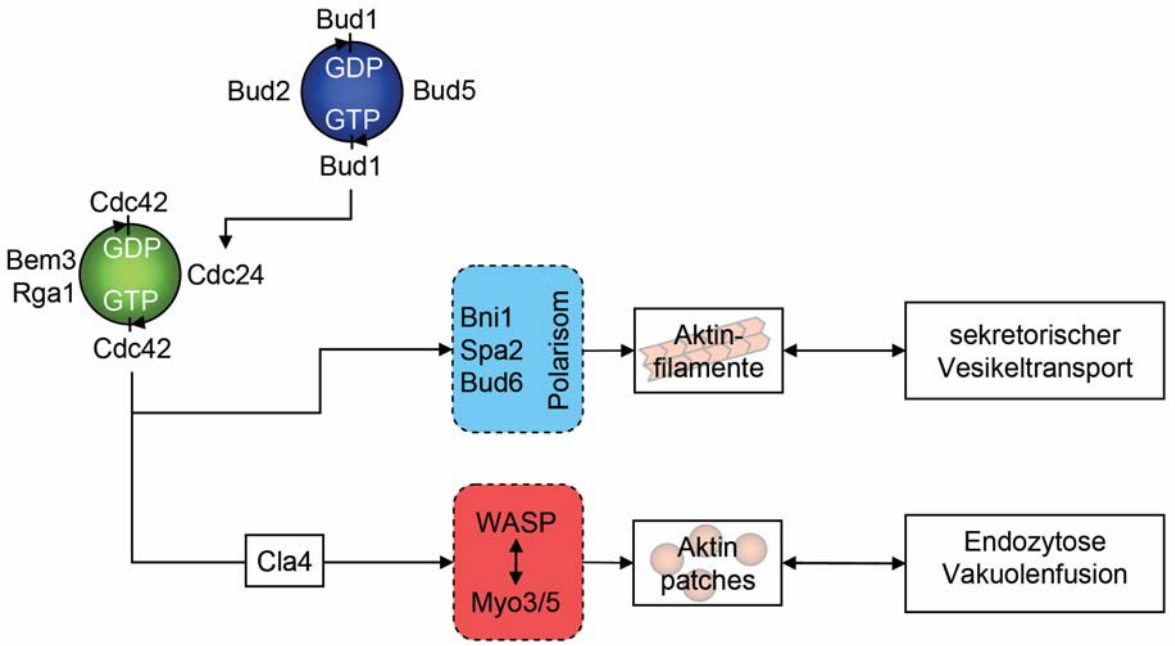

Abbildung 20 | Signalwege, die an der Endo- und Exozytose beteiligt sind.
An der Hyphenspitze sind verschiedene GTPase-Module an der Etablierung der Zellpolarität beteiligt. Cdc42p aktiviert das Polarisom. Besonders Bni1p ist in die Assemblierung linearer Aktinfilamente involviert. Aktinfilamente dienen als Gerüst für den sekretorischen Vesikeltransport. Cdc42p aktiviert auch die PAK-ähnliche Kinase Cla4p, die Typ I Myosine phosphorylieren kann. Typ I Myosine (Myo3,5p) und WASP-Homologe (Wal1p) aktivieren die Arp2/3-abhängige Aktinassemblierung, die für Endozytose und Vakuolenfusion gebraucht wird.

Da die *Δwal1* Mutante Defekte in der Bildung von chitinreichen Septen aufwies, können in *Δwal1* Hyphen keine Kompartimente gebildet werden. Damit ist ein wichtiger Schritt in der Sporenbildung inhibiert. Ähnliche Beobachtungen wurden auch in der septenlosen *A. gossypii* Δ*cyk1* Mutante gemacht. Cyk1p gehört zur Familie der IQGAP-Proteine und ist am Aufbau des Aktinrings an zukünftigen Stellen der Septierung in *A. gossypii* beteiligt. Die Deletion von *CYK1* lieferte Mutanten die keine Septen und ebenfalls keine Sporangien bilden (Wendland und Philippsen, 2002).

In jüngsten Studien wurde die Rolle der Rho-GTPasen für die Organisation des Aktinzytoskeletts auf molekularer Ebene charakterisiert (Wendland und Philippsen, 2001). Dabei wurde festgestellt, dass Cdc42p für die Etablierung der Zellpolarität, Rho1p für die Aufrechterhaltung der Zellwandintegrität und Rho3 für die Aufrechterhaltung polaren Wachstums verantwortlich ist. Durch die Fertigstellung des *Ashbya* Genom Projektes

konnte eine weitere Rho-GTPase, *RHOH*, gefunden werden, die als Tandem-Duplikation im Ashbya Genom neben *RHO1* auftritt. Damit besitzt *A. gossypii* zwei *RHO1*-Paraloge während in *S. cerevisiae* nur ein *RHO1*-Gen zu finden ist. Eine initiale Funktionsanalyse dieser neuen GTPase durch Deletion des Gens in *A. gossypii* ergab eine zumindest partiell überlappende Funktion von RhoHp und Rho1p bei der Aufrechterhaltung der Zellwandintegrität. Eine Δ*rhoH* Mutante zeigte Zell-Lyse an den Hyphenspitzen auf Festmedien. Anders als in der Δ*rho1* Mutante war die Keimung von Δ*rhoH* Sporen durch die Deletion nicht beeinträchtigt, aber bereits in jungen Myzelien konnten lysierte Hyphenspitzen beobachtet werden. Rho1p und RhoHp besitzen offenbar eine überlappende Funktion. Die Deletion von *RHO1* zeigte einen größeren Einfluss auf die Zellwandintegrität als die Deletion von *RHOH*. Die Deletion beider Gene *RHO1* und *RHOH* führte zu einem Letalphänotyp, bei dem transformierte Sporen überhaupt nicht in der Lage waren, auszukeimen und damit der Δ*rho1* Phänotyp noch verstärkt wurde. Eine ähnliche Anordnung dieser *RHO1*-Paraloge wurde im nahe verwandten Pilz *Holleya sinecauda* festgestellt.

Literatur

5. Literatur

1. **Alani E, Kleckner N.** A new type of fusion analysis applicable to many organisms: protein fusions to the URA3 gene of yeast. *Genetics*. 1987;117(1):5-12.
2. **Andrews DL, Egan JD, Mayorga ME, Gold SE.** The Ustilago maydis ubc4 and ubc5 genes encode members of a MAP kinase cascade required for filamentous growth. *Mol Plant Microbe Interact*. 2000;13(7):781-6.
3. **Atkinson HA, Daniels A, Read ND.** Live-cell imaging of endocytosis during conidial germination in the rice blast fungus, Magnaporthe grisea. *Fungal Genet Biol*. 2002;37(3):233-44.
4. **Ayad-Durieux Y, Knechtle P, Goff S, Dietrich F, Philippsen P.** A PAK-like protein kinase is required for maturation of young hyphae and septation in the filamentous ascomycete Ashbya gossypii. *J Cell Sci*. 2000;113 Pt 24:4563-75.
5. **Backen AC, Broadbent ID, Fetherston RW, Rosamond JD, Schnell NF, Stark MJ.** Evaluation of the CaMAL2 promoter for regulated expression of genes in Candida albicans. *Yeast*. 2000;16(12):1121-9.
6. **Bain JM, Stubberfield C, Gow NA.** Ura-status-dependent adhesion of Candida albicans mutants. *FEMS Microbiol Lett*. 2001;204(2):323-8.
7. **Barelle CJ, Bohula EA, Kron SJ, et al.** Asynchronous cell cycle and asymmetric vacuolar inheritance in true hyphae of Candida albicans. *Eukaryot Cell*. 2003;2(3):398-410.
8. **Bartie KL, Williams DW, Wilson MJ, Potts AJ, Lewis MA.** Differential invasion of Candida albicans isolates in an in vitro model of oral candidosis. *Oral Microbiol Immunol*. 2004;19(5):293-6.
9. **Bartnicki-Garcia S, Bartnicki DD, Gierz G, Lopez-Franco R, Bracker CE.** Evidence that Spitzenkorper behavior determines the shape of a fungal hypha: a test of the hyphoid model. *Exp Mycol*. 1995;19(2):153-9.
10. **Bassilana M, Blyth J, Arkowitz RA.** Cdc24, the GDP-GTP exchange factor for Cdc42, is required for invasive hyphal growth of Candida albicans. *Eukaryot Cell*. 2003;2(1):9-18.
11. **Bassilana M, Hopkins J, Arkowitz RA.** Regulation of the Cdc42/Cdc24 GTPase module during Candida albicans hyphal growth. *Eukaryot Cell*. 2005;4(3):588-603.
12. **Bauer Y, Knechtle P, Wendland J, Helfer H, Philippsen P.** A Ras-like GTPase is involved in hyphal growth guidance in the filamentous fungus Ashbya gossypii. *Mol Biol Cell*. 2004;15(10):4622-32.
13. **Berman J, Sudbery PE.** Candida albicans: a molecular revolution built on lessons from budding yeast. *Nat Rev Genet*. 2002;3(12):918-30.
14. **Boyce KJ, Hynes MJ, Andrianopoulos A.** Control of morphogenesis and actin localization by the Penicillium marneffei RAC homolog. *J Cell Sci*. 2003;116(Pt 7):1249-60.
15. **Boyce KJ, Hynes MJ, Andrianopoulos A.** The Ras and Rho GTPases genetically interact to co-ordinately regulate cell polarity during development in Penicillium marneffei. *Mol Microbiol*. 2005;55(5):1487-501.
16. **Brakhage AA, Langfelder K.** Menacing mold: the molecular biology of Aspergillus fumigatus. *Annu Rev Microbiol*. 2002;56:433-55.

17. **Brand A, MacCallum DM, Brown AJ, Gow NA, Odds FC.** Ectopic Expression of URA3 can influence the virulence phenotypes and proteome of Candida albicans but can be overcome by targeted reintegration of URA3 at the RPS10 locus. *Eukaryot Cell*. 2004;3(4):900-9.
18. **Cabib E, Drgonova J, Drgon T.** Role of small G proteins in yeast cell polarization and wall biosynthesis. *Annu Rev Biochem*. 1998;67:307-33.
19. **Care RS, Trevethick J, Binley KM, Sudbery PE.** The MET3 promoter: a new tool for Candida albicans molecular genetics. *Mol Microbiol*. 1999;34(4):792-8.
20. **Casadevall A, Pirofski L.** Host-pathogen interactions: the attributes of virulence. *J Infect Dis*. 2001;184(3):337-44.
21. **Chandra J, Kuhn DM, Mukherjee PK, Hoyer LL, McCormick T, Ghannoum MA.** Biofilm formation by the fungal pathogen Candida albicans: development, architecture, and drug resistance. *J Bacteriol*. 2001;183(18):5385-94.
22. **Cheng S, Nguyen MH, Zhang Z, Jia H, Handfield M, Clancy CJ.** Evaluation of the roles of four Candida albicans genes in virulence by using gene disruption strains that express URA3 from the native locus. *Infect Immun*. 2003;71(10):6101-3.
23. **Choi W, Dean RA.** The adenylate cyclase gene MAC1 of Magnaporthe grisea controls appressorium formation and other aspects of growth and development. *Plant Cell*. 1997;9(11):1973-83.
24. **Cole L, Orlovich DA, Ashford AE.** Structure, function, and motility of vacuoles in filamentous fungi. *Fungal Genet Biol*. 1998;24(1-2):86-100.
25. **Crampin H, Finley K, Gerami-Nejad M, et al.** Candida albicans hyphae have a Spitzenkorper that is distinct from the polarisome found in yeast and pseudohyphae. *J Cell Sci*. 2005;118(Pt 13):2935-47.
26. **Da Costa SR, Sou E, Xie J, et al.** Impairing actin filament or syndapin functions promotes accumulation of clathrin-coated vesicles at the apical plasma membrane of acinar epithelial cells. *Mol Biol Cell*. 2003;14(11):4397-413.
27. **Dieterich C, Schandar M, Noll M, et al.** In vitro reconstructed human epithelia reveal contributions of Candida albicans EFG1 and CPH1 to adhesion and invasion. *Microbiology*. 2002;148(Pt 2):497-506.
28. **Duncan MC, Cope MJ, Goode BL, Wendland B, Drubin DG.** Yeast Eps15-like endocytic protein, Pan1p, activates the Arp2/3 complex. *Nat Cell Biol*. 2001;3(7):687-90.
29. **Durrenberger F, Wong K, Kronstad JW.** Identification of a cAMP-dependent protein kinase catalytic subunit required for virulence and morphogenesis in Ustilago maydis. *Proc Natl Acad Sci U S A*. 1998;95(10):5684-9.
30. **Eissenberg LG, Goldman WE.** Histoplasma variation and adaptive strategies for parasitism: new perspectives on histoplasmosis. *Clin Microbiol Rev*. 1991;4(4):411-21.
31. **Engqvist-Goldstein AE, Drubin DG.** Actin assembly and endocytosis: from yeast to mammals. *Annu Rev Cell Dev Biol*. 2003;19:287-332.
32. **Evangelista M, Klebl BM, Tong AH, et al.** A role for myosin-I in actin assembly through interactions with Vrp1p, Bee1p, and the Arp2/3 complex. *J Cell Biol*. 2000;148(2):353-62.
33. **Evangelista M, Pruyne D, Amberg DC, Boone C, Bretscher A.** Formins direct Arp2/3-independent actin filament assembly to polarize cell growth in yeast. *Nat Cell Biol*. 2002;4(3):260-9.
34. **Evangelista M, Zigmond S, Boone C.** Formins: signaling effectors for assembly and polarization of actin filaments. *J Cell Sci*. 2003;116(Pt 13):2603-11.

35. **Felk A, Kretschmar M, Albrecht A, et al.** Candida albicans hyphal formation and the expression of the Efg1-regulated proteinases Sap4 to Sap6 are required for the invasion of parenchymal organs. *Infect Immun*. 2002;70(7):3689-700.
36. **Feng Q, Summers E, Guo B, Fink G.** Ras signaling is required for serum-induced hyphal differentiation in Candida albicans. *J Bacteriol*. 1999;181(20):6339-46.
37. **Fischer-Parton S, Parton RM, Hickey PC, Dijksterhuis J, Atkinson HA, Read ND.** Confocal microscopy of FM4-64 as a tool for analysing endocytosis and vesicle trafficking in living fungal hyphae. *J Microsc*. 2000;198 (Pt 3):246-59.
38. **Fonzi WA, Irwin MY.** Isogenic strain construction and gene mapping in Candida albicans. *Genetics*. 1993;134(3):717-28.
39. **Gantner BN, Simmons RM, Underhill DM.** Dectin-1 mediates macrophage recognition of Candida albicans yeast but not filaments. *Embo J*. 2005;24(6):1277-86.
40. **Gerami-Nejad M, Berman J, Gale CA.** Cassettes for PCR-mediated construction of green, yellow, and cyan fluorescent protein fusions in Candida albicans. *Yeast*. 2001;18(9):859-64.
41. **Gerami-Nejad M, Hausauer D, McClellan M, Berman J, Gale C.** Cassettes for the PCR-mediated construction of regulatable alleles in Candida albicans. *Yeast*. 2004;21(5):429-36.
42. **Gimeno CJ, Fink GR.** Induction of pseudohyphal growth by overexpression of PHD1, a Saccharomyces cerevisiae gene related to transcriptional regulators of fungal development. *Mol Cell Biol*. 1994;14(3):2100-12.
43. **Gimeno CJ, Ljungdahl PO, Styles CA, Fink GR.** Unipolar cell divisions in the yeast S. cerevisiae lead to filamentous growth: regulation by starvation and RAS. *Cell*. 1992;68(6):1077-90.
44. **Girbardt M.** Der Spitzenkörper von Polystictus versicolor. *Planta*. 1957;50:47-59.
45. **Gola S, Martin R, Walther A, Dunkler A, Wendland J.** New modules for PCR-based gene targeting in Candida albicans: rapid and efficient gene targeting using 100 bp of flanking homology region. *Yeast*. 2003;20(16):1339-47.
46. **Gold S, Duncan G, Barrett K, Kronstad J.** cAMP regulates morphogenesis in the fungal pathogen Ustilago maydis. *Genes Dev*. 1994;8(23):2805-16.
47. **Goldstein AL, Pan X, McCusker JH.** Heterologous URA3MX cassettes for gene replacement in Saccharomyces cerevisiae. *Yeast*. 1999;15(6):507-11.
48. **Goode BL, Rodal AA, Barnes G, Drubin DG.** Activation of the Arp2/3 complex by the actin filament binding protein Abp1p. *J Cell Biol*. 2001;153(3):627-34.
49. **Gouin E, Gantelet H, Egile C, et al.** A comparative study of the actin-based motilities of the pathogenic bacteria Listeria monocytogenes, Shigella flexneri and Rickettsia conorii. *J Cell Sci*. 1999;112 (Pt 11):1697-708.
50. **Hall A.** Rho GTPases and the actin cytoskeleton. *Science*. 1998;279(5350):509-14.
51. **Harris SD, Hamer L, Sharpless KE, Hamer JE.** The Aspergillus nidulans sepA gene encodes an FH1/2 protein involved in cytokinesis and the maintenance of cellular polarity. *Embo J*. 1997;16(12):3474-83.
52. **Harris SD, Read ND, Roberson RW, et al.** Polarisome meets spitzenkorper: microscopy, genetics, and genomics converge. *Eukaryot Cell*. 2005;4(2):225-9.
53. **Hazan I, Liu H.** Hyphal tip-associated localization of Cdc42 is F-actin dependent in Candida albicans. *Eukaryot Cell*. 2002;1(6):856-64.
54. **Hoepfner D, Brachat A, Philippsen P.** Time-lapse video microscopy analysis reveals astral microtubule detachment in the yeast spindle pole mutant cnm67. *Mol Biol Cell*. 2000;11(4):1197-211.
55. **Holley RA, Allan-Wojtas P, Phipps-Todd BE.** Nematospora sinecauda sp. nov., a yeast pathogen of mustard seeds. *Antonie Van Leeuwenhoek*. 1984;50(4):305-20.

56. **Hornby JM, Jensen EC, Lisec AD, et al.** Quorum sensing in the dimorphic fungus Candida albicans is mediated by farnesol. *Appl Environ Microbiol*. 2001;67(7):2982-92.
57. **Hoyer LL.** The ALS gene family of Candida albicans. *Trends Microbiol*. 2001;9(4):176-80.
58. **Hwang L, Hocking-Murray D, Bahrami AK, Andersson M, Rine J, Sil A.** Identifying phase-specific genes in the fungal pathogen Histoplasma capsulatum using a genomic shotgun microarray. *Mol Biol Cell*. 2003;14(6):2314-26.
59. **Imamura H, Tanaka K, Hihara T, et al.** Bni1p and Bnr1p: downstream targets of the Rho family small G-proteins which interact with profilin and regulate actin cytoskeleton in Saccharomyces cerevisiae. *Embo J*. 1997;16(10):2745-55.
60. **Irazoqui JE, Howell AS, Theesfeld CL, Lew DJ.** Opposing roles for actin in Cdc42p polarization. *Mol Biol Cell*. 2005;16(3):1296-304.
61. **Janatova I, Gourdon P, Meilhoc E, Klein RD, Masson JM.** ARS sequences in homologous and heterologous ADE2 loci are capable of promoting autonomous replication of plasmids in Schwanniomyces occidentalis. *Curr Genet*. 2000;37(5):298-303.
62. **Johnson DI, Pringle JR.** Molecular characterization of CDC42, a Saccharomyces cerevisiae gene involved in the development of cell polarity. *J Cell Biol*. 1990;111(1):143-52.
63. **Kaksonen M, Sun Y, Drubin DG.** A pathway for association of receptors, adaptors, and actin during endocytic internalization. *Cell*. 2003;115(4):475-87.
64. **Kamai Y, Kubota M, Kamai Y, Hosokawa T, Fukuoka T, Filler SG.** Contribution of Candida albicans ALS1 to the pathogenesis of experimental oropharyngeal candidiasis. *Infect Immun*. 2002;70(9):5256-8.
65. **Kim MK, Park HS, Kim CH, Park HM, Choi W.** Inhibitory effect of nikkomycin Z on chitin synthases in Candida albicans. *Yeast*. 2002;19(4):341-9.
66. **Kobielak A, Pasolli HA, Fuchs E.** Mammalian formin-1 participates in adherens junctions and polymerization of linear actin cables. *Nat Cell Biol*. 2004;6(1):21-30.
67. **Kruppa M, Krom BP, Chauhan N, Bambach AV, Cihlar RL, Calderone RA.** The two-component signal transduction protein Chk1p regulates quorum sensing in Candida albicans. *Eukaryot Cell*. 2004;3(4):1062-5.
68. **Leberer E, Harcus D, Dignard D, et al.** Ras links cellular morphogenesis to virulence by regulation of the MAP kinase and cAMP signalling pathways in the pathogenic fungus Candida albicans. *Mol Microbiol*. 2001;42(3):673-87.
69. **Lechler T, Shevchenko A, Li R.** Direct involvement of yeast type I myosins in Cdc42-dependent actin polymerization. *J Cell Biol*. 2000;148(2):363-73.
70. **Lee N, Kronstad JW.** ras2 Controls morphogenesis, pheromone response, and pathogenicity in the fungal pathogen Ustilago maydis. *Eukaryot Cell*. 2002;1(6):954-66.
71. **Lengeler KB, Davidson RC, D'Souza C, et al.** Signal transduction cascades regulating fungal development and virulence. *Microbiol Mol Biol Rev*. 2000;64(4):746-85.
72. **Lew DJ, Reed SI.** Morphogenesis in the yeast cell cycle: regulation by Cdc28 and cyclins. *J Cell Biol*. 1993;120(6):1305-20.
73. **Li R.** Bee1, a yeast protein with homology to Wiscott-Aldrich syndrome protein, is critical for the assembly of cortical actin cytoskeleton. *J Cell Biol*. 1997;136(3):649-58.
74. **Li YY, Yeh E, Hays T, Bloom K.** Disruption of mitotic spindle orientation in a yeast dynein mutant. *Proc Natl Acad Sci U S A*. 1993;90(21):10096-100.

75. **Lin X, Hull CM, Heitman J.** Sexual reproduction between partners of the same mating type in Cryptococcus neoformans. *Nature*. 2005;434(7036):1017-21.
76. **Liu H.** Transcriptional control of dimorphism in Candida albicans. *Curr Opin Microbiol*. 2001;4(6):728-35.
77. **Liu H, Kohler J, Fink GR.** Suppression of hyphal formation in Candida albicans by mutation of a STE12 homolog. *Science*. 1994;266(5191):1723-6.
78. **Lo HJ, Kohler JR, DiDomenico B, Loebenberg D, Cacciapuoti A, Fink GR.** Nonfilamentous C. albicans mutants are avirulent. *Cell*. 1997;90(5):939-49.
79. **Lorenz MC, Bender JA, Fink GR.** Transcriptional response of Candida albicans upon internalization by macrophages. *Eukaryot Cell*. 2004;3(5):1076-87.
80. **Lott TJ, Fundyga RE, Kuykendall RJ, Arnold J.** The human commensal yeast, Candida albicans, has an ancient origin. *Fungal Genet Biol*. 2005;42(5):444-51.
81. **Machesky LM.** The tails of two myosins. *J Cell Biol*. 2000;148(2):219-21.
82. **Madania A, Dumoulin P, Grava S, et al.** The Saccharomyces cerevisiae homologue of human Wiskott-Aldrich syndrome protein Las17p interacts with the Arp2/3 complex. *Mol Biol Cell*. 1999;10(10):3521-38.
83. **Marr KA.** Invasive Candida infections: the changing epidemiology. *Oncology (Williston Park)*. 2004;18(14 Suppl 13):9-14.
84. **Martin R, Walther A, Wendland J.** Deletion of the dynein heavy-chain gene DYN1 leads to aberrant nuclear positioning and defective hyphal development in Candida albicans. *Eukaryot Cell*. 2004;3(6):1574-88.
85. **Martin R, Walther A, Wendland J.** Ras1-induced hyphal development in Candida albicans requires the formin Bni1. *Eukaryot Cell*. 2005;in Revision.
86. **Mayorga ME, Gold SE.** A MAP kinase encoded by the ubc3 gene of Ustilago maydis is required for filamentous growth and full virulence. *Mol Microbiol*. 1999;34(3):485-97.
87. **McCollum D, Feoktistova A, Morphew M, Balasubramanian M, Gould KL.** The Schizosaccharomyces pombe actin-related protein, Arp3, is a component of the cortical actin cytoskeleton and interacts with profilin. *Embo J*. 1996;15(23):6438-46.
88. **McGoldrick CA, Gruver C, May GS.** myoA of Aspergillus nidulans encodes an essential myosin I required for secretion and polarized growth. *J Cell Biol*. 1995;128(4):577-87.
89. **Mitchell TK, Dean RA.** The cAMP-dependent protein kinase catalytic subunit is required for appressorium formation and pathogenesis by the rice blast pathogen Magnaporthe grisea. *Plant Cell*. 1995;7(11):1869-78.
90. **Moreau V, Galan JM, Devilliers G, Haguenauer-Tsapis R, Winsor B.** The yeast actin-related protein Arp2p is required for the internalization step of endocytosis. *Mol Biol Cell*. 1997;8(7):1361-75.
91. **Moreau V, Madania A, Martin RP, Winson B.** The Saccharomyces cerevisiae actin-related protein Arp2 is involved in the actin cytoskeleton. *J Cell Biol*. 1996;134(1):117-32.
92. **Moseley JB, Sagot I, Manning AL, et al.** A conserved mechanism for Bni1- and mDia1-induced actin assembly and dual regulation of Bni1 by Bud6 and profilin. *Mol Biol Cell*. 2004;15(2):896-907.
93. **Muller P, Katzenberger JD, Loubradou G, Kahmann R.** Guanyl nucleotide exchange factor Sql2 and Ras2 regulate filamentous growth in Ustilago maydis. *Eukaryot Cell*. 2003;2(3):609-17.
94. **Naglik JR, Challacombe SJ, Hube B.** Candida albicans secreted aspartyl proteinases in virulence and pathogenesis. *Microbiol Mol Biol Rev*. 2003;67(3):400-28, table of contents.

95. **Newman SL.** Interaction of Histoplasma capsulatum with human macrophages, dendritic cells, and neutrophils. *Methods Mol Med*. 2005;118:181-91.
96. **Noble SM, Johnson AD.** Strains and strategies for large-scale gene deletion studies of the diploid human fungal pathogen Candida albicans. *Eukaryot Cell*. 2005;4(2):298-309.
97. **Oberholzer U, Iouk TL, Thomas DY, Whiteway M.** Functional characterization of myosin I tail regions in Candida albicans. *Eukaryot Cell*. 2004;3(5):1272-86.
98. **Oberholzer U, Marcil A, Leberer E, Thomas DY, Whiteway M.** Myosin I is required for hypha formation in Candida albicans. *Eukaryot Cell*. 2002;1(2):213-28.
99. **O'Connor L, Lahiff S, Casey F, Glennon M, Cormican M, Maher M.** Quantification of ALS1 gene expression in Candida albicans biofilms by RT-PCR using hybridisation probes on the LightCycler. *Mol Cell Probes*. 2005;19(3):153-62.
100. **Odds FC.** Morphogenesis in Candida albicans. *Crit Rev Microbiol*. 1985;12(1):45-93.
101. **Odds FC.** Pathogenesis of Candida infections. *J Am Acad Dermatol*. 1994;31(3 Pt 2):S2-5.
102. **Odds FC, Gow NA, Brown AJ.** Fungal virulence studies come of age. *Genome Biol*. 2001;2(3):REVIEWS1009.
103. **Oh SH, Cheng G, Nuessen JA, et al.** Functional specificity of Candida albicans Als3p proteins and clade specificity of ALS3 alleles discriminated by the number of copies of the tandem repeat sequence in the central domain. *Microbiology*. 2005;151(Pt 3):673-81.
104. **Ohneda M, Arioka M, Nakajima H, Kitamoto K.** Visualization of vacuoles in Aspergillus oryzae by expression of CPY-EGFP. *Fungal Genet Biol*. 2002;37(1):29-38.
105. **Osherov N, Yamashita RA, Chung YS, May GS.** Structural requirements for *in vivo* myosin I function in Aspergillus nidulans. *J Biol Chem*. 1998;273(41):27017-25.
106. **Prillinger H, Schweigkofler W, Breitenbach M, et al.** Phytopathogenic filamentous (Ashbya, Eremothecium) and dimorphic fungi (Holleya, Nematospora) with needle-shaped ascospores as new members within the Saccharomycetaceae. *Yeast*. 1997;13(10):945-60.
107. **Pruyne D, Evangelista M, Yang C, et al.** Role of formins in actin assembly: nucleation and barbed-end association. *Science*. 2002;297(5581):612-5.
108. **Pruyne D, Gao L, Bi E, Bretscher A.** Stable and dynamic axes of polarity use distinct formin isoforms in budding yeast. *Mol Biol Cell*. 2004;15(11):4971-89.
109. **Read ND, Kalkman ER.** Does endocytosis occur in fungal hyphae? *Fungal Genet Biol*. 2003;39(3):199-203.
110. **Roberts RL, Fink GR.** Elements of a single MAP kinase cascade in Saccharomyces cerevisiae mediate two developmental programs in the same cell type: mating and invasive growth. *Genes Dev*. 1994;8(24):2974-85.
111. **Rohatgi R, Ma L, Miki H, et al.** The interaction between N-WASP and the Arp2/3 complex links Cdc42-dependent signals to actin assembly. *Cell*. 1999;97(2):221-31.
112. **Sagot I, Klee SK, Pellman D.** Yeast formins regulate cell polarity by controlling the assembly of actin cables. *Nat Cell Biol*. 2002;4(1):42-50.
113. **Sagot I, Rodal AA, Moseley J, Goode BL, Pellman D.** An actin nucleation mechanism mediated by Bni1 and profilin. *Nat Cell Biol*. 2002;4(8):626-31.
114. **Sanglard D, Hube B, Monod M, Odds FC, Gow NA.** A triple deletion of the secreted aspartyl proteinase genes SAP4, SAP5, and SAP6 of Candida albicans causes attenuated virulence. *Infect Immun*. 1997;65(9):3539-46.

115. **Schade D, Walther A, Wendland J.** The development of a transformation system for the dimorphic plant pathogen Holleya sinecauda based on Ashbya gossypii DNA elements. *Fungal Genet Biol*. 2003;40(1):65-71.
116. **Schaller M, Bein M, Korting HC, et al.** The secreted aspartyl proteinases Sap1 and Sap2 cause tissue damage in an in vitro model of vaginal candidiasis based on reconstituted human vaginal epithelium. *Infect Immun*. 2003;71(6):3227-34.
117. **Schaller M, Korting HC, Borelli C, Hamm G, Hube B.** Candida albicans-secreted aspartic proteinases modify the epithelial cytokine response in an in vitro model of vaginal candidiasis. *Infect Immun*. 2005;73(5):2758-65.
118. **Schaller M, Korting HC, Schafer W, Bastert J, Chen W, Hube B.** Secreted aspartic proteinase (Sap) activity contributes to tissue damage in a model of human oral candidosis. *Mol Microbiol*. 1999;34(1):169-80.
119. **Schaller M, Schackert C, Korting HC, Januschke E, Hube B.** Invasion of Candida albicans correlates with expression of secreted aspartic proteinases during experimental infection of human epidermis. *J Invest Dermatol*. 2000;114(4):712-7.
120. **Schmidt A, Hall MN.** Signaling to the actin cytoskeleton. *Annu Rev Cell Dev Biol*. 1998;14:305-38.
121. **Schmidt M.** Survival and cytokinesis of Saccharomyces cerevisiae in the absence of chitin. *Microbiology*. 2004;150(Pt 10):3253-60.
122. **Selmecki A, Bergmann S, Berman J.** Comparative genome hybridization reveals widespread aneuploidy in Candida albicans laboratory strains. *Mol Microbiol*. 2005;55(5):1553-65.
123. **Sharkey LL, Liao WL, Ghosh AK, Fonzi WA.** Flanking direct repeats of hisG alter URA3 marker expression at the HWP1 locus of Candida albicans. *Microbiology*. 2005;151(Pt 4):1061-71.
124. **Sharpless KE, Harris SD.** Functional characterization and localization of the Aspergillus nidulans formin SEPA. *Mol Biol Cell*. 2002;13(2):469-79.
125. **Sheu YJ, Santos B, Fortin N, Costigan C, Snyder M.** Spa2p interacts with cell polarity proteins and signaling components involved in yeast cell morphogenesis. *Mol Cell Biol*. 1998;18(7):4053-69.
126. **Stefan CJ, Padilla SM, Audhya A, Emr SD.** The phosphoinositide phosphatase Sjl2 is recruited to cortical actin patches in the control of vesicle formation and fission during endocytosis. *Mol Cell Biol*. 2005;25(8):2910-23.
127. **Stevens DA, Espiritu M, Parmar R.** Paradoxical effect of caspofungin: reduced activity against Candida albicans at high drug concentrations. *Antimicrob Agents Chemother*. 2004;48(9):3407-11.
128. **Stoldt VR, Sonneborn A, Leuker CE, Ernst JF.** Efg1p, an essential regulator of morphogenesis of the human pathogen Candida albicans, is a member of a conserved class of bHLH proteins regulating morphogenetic processes in fungi. *Embo J*. 1997;16(8):1982-91.
129. **Sudbery PE.** The germ tubes of Candida albicans hyphae and pseudohyphae show different patterns of septin ring localization. *Mol Microbiol*. 2001;41(1):19-31.
130. **Suzuki T, Mimuro H, Suetsugu S, Miki H, Takenawa T, Sasakawa C.** Neural Wiskott-Aldrich syndrome protein (N-WASP) is the specific ligand for Shigella VirG among the WASP family and determines the host cell type allowing actin-based spreading. *Cell Microbiol*. 2002;4(4):223-33.
131. **Torralba S, Heath IB.** Analysis of three separate probes suggests the absence of endocytosis in Neurospora crassa hyphae. *Fungal Genet Biol*. 2002;37(3):221-32.
132. **Ushinsky SC, Harcus D, Ash J, et al.** CDC42 is required for polarized growth in human pathogen Candida albicans. *Eukaryot Cell*. 2002;1(1):95-104.

133. **Vachova L, Palkova Z.** Physiological regulation of yeast cell death in multicellular colonies is triggered by ammonia. *J Cell Biol*. 2005;169(5):711-7.
134. **Veses V, Casanova M, Murgui A, Dominguez A, Gow NA, Martinez JP.** ABG1, a novel and essential Candida albicans gene encoding a vacuolar protein involved in cytokinesis and hyphal branching. *Eukaryot Cell*. 2005;4(6):1088-101.
135. **Wach A, Brachat A, Pohlmann R, Philippsen P.** New heterologous modules for classical or PCR-based gene disruptions in Saccharomyces cerevisiae. *Yeast*. 1994;10(13):1793-808.
136. **Walther A, Wendland J.** An improved transformation protocol for the human fungal pathogen Candida albicans. *Curr Genet*. 2003;42(6):339-43.
137. **Walther A, Wendland J.** Septation and cytokinesis in fungi. *Fungal Genet Biol*. 2003;40(3):187-96.
138. **Walther A, Wendland J.** Apical localization of actin patches and vacuolar dynamics in Ashbya gossypii depend on the WASP homolog Wal1p. *J Cell Sci*. 2004;117(Pt 21):4947-58.
139. **Walther A, Wendland J.** Polarized hyphal growth in Candida albicans requires the Wiskott-Aldrich Syndrome protein homolog Wal1p. *Eukaryot Cell*. 2004;3(2):471-82.
140. **Walther A, Wendland J.** RHOH shares functions in cell wall integrity with its paralog RHO1 in the filamentous ascomycete Ashbya gossypii. *Curr Genet*. 2005;in Revision.
141. **Wendland J.** Comparison of morphogenetic networks of filamentous fungi and yeast. *Fungal Genet Biol*. 2001;34(2):63-82.
142. **Wendland J, Ayad-Durieux Y, Knechtle P, Rebischung C, Philippsen P.** PCR-based gene targeting in the filamentous fungus Ashbya gossypii. *Gene*. 2000;242(1-2):381-91.
143. **Wendland J, Philippsen P.** Determination of cell polarity in germinated spores and hyphal tips of the filamentous ascomycete Ashbya gossypii requires a rhoGAP homolog. *J Cell Sci*. 2000;113 (Pt 9):1611-21.
144. **Wendland J, Philippsen P.** Cell polarity and hyphal morphogenesis are controlled by multiple rho-protein modules in the filamentous ascomycete Ashbya gossypii. *Genetics*. 2001;157(2):601-10.
145. **Wendland J, Philippsen P.** An IQGAP-related protein, encoded by AgCYK1, is required for septation in the filamentous fungus Ashbya gossypii. *Fungal Genet Biol*. 2002;37(1):81-8.
146. **Wendland J, Pohlmann R, Dietrich F, Steiner S, Mohr C, Philippsen P.** Compact organization of rRNA genes in the filamentous fungus Ashbya gossypii. *Curr Genet*. 1999;35(6):618-25.
147. **Wendland J, Walther A.** Ashbya gossypii: a model for fungal developmental biology. *Nat Rev Microbiol*. 2005;3(5):421-9.
148. **Wilson RB, Davis D, Enloe BM, Mitchell AP.** A recyclable Candida albicans URA3 cassette for PCR product-directed gene disruptions. *Yeast*. 2000;16(1):65-70.
149. **Wilson RB, Davis D, Mitchell AP.** Rapid hypothesis testing with Candida albicans through gene disruption with short homology regions. *J Bacteriol*. 1999;181(6):1868-74.
150. **Winter D, Lechler T, Li R.** Activation of the yeast Arp2/3 complex by Bee1p, a WASP-family protein. *Curr Biol*. 1999;9(9):501-4.
151. **Winter D, Podtelejnikov AV, Mann M, Li R.** The complex containing actin-related proteins Arp2 and Arp3 is required for the motility and integrity of yeast actin patches. *Curr Biol*. 1997;7(7):519-29.

152. **Woo M, Lee K, Song K.** MYO2 is not essential for viability, but is required for polarized growth and dimorphic switches in Candida albicans. *FEMS Microbiol Lett*. 2003;218(1):195-202.
153. **Wright MC, Philippsen P.** Replicative transformation of the filamentous fungus Ashbya gossypii with plasmids containing Saccharomyces cerevisiae ARS elements. *Gene*. 1991;109(1):99-105.
154. **Wu C, Lee SF, Furmaniak-Kazmierczak E, Cote GP, Thomas DY, Leberer E.** Activation of myosin-I by members of the Ste20p protein kinase family. *J Biol Chem*. 1996;271(50):31787-90.
155. **Wu C, Lytvyn V, Thomas DY, Leberer E.** The phosphorylation site for Ste20p-like protein kinases is essential for the function of myosin-I in yeast. *J Biol Chem*. 1997;272(49):30623-6.
156. **Wu X, Suetsugu S, Cooper LA, Takenawa T, Guan JL.** Focal adhesion kinase regulation of N-WASP subcellular localization and function. *J Biol Chem*. 2004;279(10):9565-76.
157. **Xu JR, Hamer JE.** MAP kinase and cAMP signaling regulate infection structure formation and pathogenic growth in the rice blast fungus Magnaporthe grisea. *Genes Dev*. 1996;10(21):2696-706.
158. **Xu JR, Urban M, Sweigard JA, Hamer JE.** The CPKA gene of Magnaporthe grisea is essential for appressorial penetration. *Mol Plant-Microbe Interact*. 1997;10(2):187-194.
159. **Yamashita RA, May GS.** Constitutive activation of endocytosis by mutation of myoA, the myosin I gene of Aspergillus nidulans. *J Biol Chem*. 1998;273(23):14644-8.
160. **Yamashita RA, Osherov N, May GS.** Localization of wild type and mutant class I myosin proteins in Aspergillus nidulans using GFP-fusion proteins. *Cell Motil Cytoskeleton*. 2000;45(2):163-72.
161. **Zhao X, Oh SH, Yeater KM, Hoyer LL.** Analysis of the Candida albicans Als2p and Als4p adhesins suggests the potential for compensatory function within the Als family. *Microbiology*. 2005;151(Pt 5):1619-30.

Thesen

6. Thesen

1. Das Aktinzytoskelett leistet einen wichtigen Beitrag zur Etablierung und Beibehaltung der Zellpolarität und Zellform eukaryoter Organismen.

2. Rho-Proteine als Organisatoren des Aktinzytoskeletts verarbeiten Signale und aktivieren Effektorproteine, die an der Aktinassemblierung beteiligt sind.

3. RhoHp in *Ashbya gossypii* ist ein Rho-Protein, das zusammen mit Rho1p an der Aufrechterhaltung der Zellwandintegrität beteiligt ist.

4. Pilze sind einfache eukaryotische Organismen, die wenige unterschiedliche Zellformen ausbilden. Dabei kann man hefeartiges Wachstum wie bei *Saccharomyces cerevisiae* von filamentösem Wachstum wie bei *A. gossypii* unterscheiden. Dimorphe Pilze wie der humanpathogene Pilz *Candida albicans* sind in der Lage, zwischen beiden Formen zu wechseln.

5. Die Organisation des Aktinzytoskeletts ist entscheidend für die Morphogenese von *C. albicans* und *A. gossypii* und insbesondere das Wiskott-Aldrich Syndrom Protein Homolog Wal1p ist essentiell für die Beibehaltung polaren Wachstums und die Myzelbildung.

6. Deletion der *WAL1* Gene von *C. albicans* und *A. gossypii* zeigte spezifische Defekte in der Organisation des kortikalen Aktinzytoskeletts.

7. *C. albicans und A. gossypii wal1* Mutanten zeigten daneben auch Defekte in der Endozytose und der Vakuolenmorphologie. Damit wurde gezeigt, dass Endozytose neben der Sekretion von Vesikeln ein Prozess ist, der einen wesentlichen Beitrag zu polarem Wachstum leistet.

8. Die Fähigkeit, Hyphen zu bilden wird als wesentlicher Virulenzfaktor bei *C. albicans* angesehen. Die *C. albicans wal1* Mutante zeigte eine verringerte Virulenz in einem Mausmodell für systemische Infektionen. Darüber hinaus konnte in einem Epithelmodell eine stark verringerte Adhäsionsfähigkeit von *wal1* Zellen festgestellt werden. Wildtyp-Hyphen dagegen zeigten starke Adhäsionsfähigkeit. Damit sind die Defekte in der Adhäsion und Hyphenbildung wesentliche Faktoren, die die Virulenz von *wal1* Zellen verringern.

9. Das Aktinzytoskelett liefert einen essentiellen Beitrag zur Hyphenbildung bei *C. albicans*. Auch konstitutive Aktivierung des Ras-Signalweges kann eine *wal1* Defekt nicht supprimieren.

10. Filamentöse Ascomyzeten zeigen unterschiedliche Wachstumsgeschwindigkeiten in juvenilen und maturierten Stadien, die durch *in vivo* Zeitraffer-Mikroskopie bestimmt werden können.

11. Zytoplasmatische Strömungen in *A. gossypii* Hyphen sind durch den Transport von Vakuolen leicht darstellbar. Die Strömungsrichtung innerhalb der Hyphen wird durch Septierungsereignisse beeinflusst. Kompartimentierung durch Septen verhindert den Ausstrom von Zytoplasma in andere Hyphenabschnitte. Die zytoplasmatische Strömung ist spitzenwärts gerichtet bei wachsenden Hyphen, kann aber auch umgekehrt werden, wenn das Spitzenwachstum sich verlangsamt oder zum Stillstand kommt.

12. Durch *in vivo* Zeitraffer Mikroskopie können Wachstumsprozesse und der Verlauf der zytoplasmatischen Strömung verfolgt werden und mutante Phänotypen charakterisiert werden. Die *in vivo* Fluoreszenz-Zeitraffer Mikroskopie ermöglicht zudem, mit GFP (grün-fluoreszierendes Protein) markierte Proteine in ihrer dynamischen subzellulären Lokalisierung zu verfolgen. Ebenso kann die Verteilung von Vakuolen und Mitochondrien untersucht werden. Dabei zeigen die *A. gossypii wal1* und *cla4* Mutanten eine verringerte Vakuolenmotilität.

13. In *A. gossypii* ist die Verteilung der Mitochondrien dagegen unabhängig von WASP.

14. Zur Erzeugung von Mutanten eignen sich in Ascomyzeten PCR-basierte Verfahren zur Herstellung genspezifischer Kassetten. Dabei ist die Länge der zu verwendenden flankierenden Homologieregion zum Ziellokus von entscheidender Bedeutung. In *C. albicans* können gute Effizienzien gerichteter Integrationsereignisse mit 100bp flankierender Homologieregion erreicht werden.

15. Durch die schnelle Erzeugung von Mutanten in *C. albicans* über die PCR-basierten Verfahren, die herkömmliche Klonierungsschritte bei der Herstellung von Disruptionskassetten ablösen, kann die Funktionsanalyse der *C. albicans* Gene nach der Fertigstellung der Genomsequenz deutlich beschleunigt werden.

7. Danksagung

An dieser Stelle möchte ich besonders Jürgen Wendland für die Überlassung dieses Thema und die immerwährende Unterstützung bei der Erstellung dieser Arbeit danken. Seine Förderung meiner wissenschaftlichen Arbeit hat mir in den letzten Jahren die Möglichkeit gegeben, an internationalen Konferenzen teilzunehmen und meine Ergebnisse zu präsentieren. Für die ständige Diskussionsbereitschaft und Hilfe vor allem aber für die freundschaftliche Atmosphäre im Labor bin ich ihm sehr dankbar.

Meinen Kollegen Yvonne, Ronny, Alex, Christian, Janine und Anja danke ich für all die hilfreichen Anregungen und lustigen Momente im Laboralltag. Ganz besonders möchte ich Yvonne danken, die mich durch ihre unermüdlich gute Laune und Hilfsbereitschaft bei der Arbeit im Labor und der Betreuung von Studenten überrascht hat.

Ferner gilt mein Dank Nir Osherov und Yona Shadkhan, die durch ihre Zusammenarbeit mit unserer Arbeitgruppe die Candida-Mausexperimente ermöglicht haben. Herrn Barth (Zeiss AG) danke ich für die schnelle Hilfe bei Problemen, die bei der Einrichtung des Mikroskops und der Anpassung des Heiztisches aufgetreten sind.

Bei allen Mitarbeiter des Instituts für Mikrobiologie, besonders aber bei Frau Prof. Dr. Kothe, will ich mich an dieser Stelle bedanken, die mich durch die Präsentation meiner Ergebnisse in Seminaren immer wieder auf neue Ideen gebracht hat. Allen Mitarbeitern des Hans-Knöll-Instituts danke ich für die freundliche Atmosphäre und Hilfsbereitschaft während der letzten Jahre. Desweiteren möchte ich Herrn Dr. Härtel und Dr. Sickinger für die Mithilfe bei der Durchführung des PIE-Assays danken.

Ich möchte auch den Gutachtern der Prüfungskommission Prof. Dr. Wöstemeyer und Prof. Dr. Ernst danken, die sich die Zeit nehmen, diese Arbeit zu lesen und zu begutachten.

All meinen Freunden danke ich für ihre Geduld, wenn ich mal wieder die Zeit im Labor vergessen habe und zu spät gekommen bin. Simone gilt dabei mein besonderer Dank für ihre langjährige Freundschaft und ihre immerwährende fröhliche Art.

Nicht zuletzt möchte ich meinen Eltern und Brüdern Matthias und Volkmar danken, die mir während der Erstellung dieser Arbeit eine große Hilfe waren und mich dabei unterstützt haben.

8. Selbständigkeitserklärung

Ich erkläre, dass ich die Dissertation «MOLEKULARE ANALYSEN ÜBER AKTINZYTOSKELETT UND POLARES WACHSTUM IN *ASHBYA GOSSYPII* UND *CANDIDA ALBICANS* MITTELS FLUORESZENZ-ZEITRAFFER MIKROSKOPIE» selbständig nur mit der darin angegebenen Hilfe verfasst und bei keiner anderen Fakultät oder Universität eingereicht habe.

_____

Andrea Walther

Jena

4. Oktober 2005

Andrea Walther
Liselotte-Herrmann-Stasse 38a
D-07747 Jena
+49 3641 365639

Curriculum vitae

Persönliche Informationen

Familienstand: ledig
Staatsangehörigkeit: deutsch
Alter: 26
Geburtsort: Frankenberg/Sachsen
Eltern: Dirk-Detlef Walther
Lieselotte Walther, geb. Thalheim

Schulbildung

Sept. 1985 - Aug. 1991 Wilhelm-Pieck-Schule Apolda
Sept. 1991 - Aug. 1997 Gymnasium „Bergschule“ Apolda
Aug. 1997 - Schulabschluss Abitur (Note: 1,3)

Studium

Okt. 1997 - Nov. 2002 Studium der Biologie, Friedrich-Schiller-Universität Jena; Hauptfach: Mikrobiologie, Nebenfächer: Genetik, Medizinische Mikrobiologie, Pharmakologie

Diplomarbeit

angefertigt im Zeitraum vom Dez. 2001bis Okt. 2002 am Institut für Mikrobiologie der Friedrich-Schiller-Universität Jena zum Thema: Funktionen von WASP-Homologen bei der Organisation des Aktinzytoskeletts in *Ashbya gossypii* und *Candida albicans*

Beschäftigungsverhältnisse

Dez. 2002 - Mai 2003 Wissenschaftliche Mitarbeiterin der Friedrich-Schiller-Universität, Jena
ab Juni 2003 - Wissenschaftliche Mitarbeiterin des Leibniz-Instituts für Naturstoff-Forschung und Infektionsbiologie – Hans-Knöll-Institut, Jena

Tagungsbeiträge

Joint Fungal Phytopathology Meeting, Siegmundsburg 30.-31. Aug. 2002
Titel: Funktionen von WASP Homologen bei der Organisation des Aktin-Cytoskeletts.

Joint Fungal Phytopathology Meeting, Siegmundsburg 12.-13. Sept. 2003
Titel: Mikroskopische Charakterisierung der mutanten Phänotypen in *C. albicans wal1*

DGHM-Tagung “Eukaryontische Krankheitserreger“, Jena, 25.-26 Feb.2005
Titel: *In vivo* fluorescence time lapse microscopy in *Candida albicans*.

10. Mitbetreuung von Lehrveranstaltungen

WS 2002 / 2003	Tutorium zur Vorlesung „Mikrobiologie für Ernährungswissenschaftler“ (2 SWS)
WS 2003 / 2004	Tutorium zur Vorlesung „Mikrobiologie für Ernährungswissenschaftler“ (2 SWS)
WS 2003 / 2004	Großpraktikum „Mikrobiologie“ für Hauptfach-Studenten (4 Wochen, 14:00-18:00 Uhr)
SS 2004	Praktikum „Mikrobiologie für Ernährungs-wissenschaftler“ (donnerstags 09:00-12:00 Uhr)
WS 2004 / 2005	Großpraktikum „Mikrobiologie“ für Hauptfach-Studenten (4 Wochen, 14:00-18:00 Uhr)
WS 2004 / 2005	Mitwirkung an der Ringvorlesung „Genetische Forschung in Jena“
WS 2004 / 2005	Vorbereitung der Vorlesung „Mikrobiologie für Ernährungswissenschaftler“ und Erstellung eines Skriptes
SS 2005	Vorbereitung des Praktikums „Mikrobiologie für Ernährungswissenschaftler“ und Erstellung eines Praktikumsskriptes

Publikationen der Dissertation

1

Jürgen Wendland

Andrea Walther

Ashbya gossypii: a model for fungal developmental biology.

Nat. Rev. Microbiol., 3: 421-429.

Ashbya ist ein filamentöser Pilz, der durch seine nahe Verwandtschaft zur einzelligen Hefe *S. cerevisiae* und die einfache genetische Manipulierbarkeit einen geeigneten Modellorganismus darstellt, um Mechanismen und regulatorische Protein-Netzwerke zu untersuchen, die filamentöses und einzelliges Wachstum unterscheiden.

ASHBYA GOSSYPII: A MODEL FOR FUNGAL DEVELOPMENTAL BIOLOGY

Jürgen Wendland and Andrea Walther

Abstract | *Ashbya gossypii* is a riboflavin-overproducing filamentous fungus that is closely related to unicellular yeasts such as *Saccharomyces cerevisiae*. With its close ties to yeast and the ease of genetic manipulation in this fungal species, *A. gossypii* is well suited as a model to elucidate the regulatory networks that govern the functional differences between filamentous growth and yeast growth, especially now that the *A. gossypii* genome sequence has been completed. Understanding these networks could be relevant to related dimorphic yeasts such as the human fungal pathogen *Candida albicans*, in which a switch in morphology from the yeast to the filamentous form in response to specific environmental stimuli is important for virulence.

STIGMATOMYCOSIS
A fungal infection resulting in wet, slimy kernels. It is transmitted by insect mouthparts that penetrate the kernel.

ISOTROPIC GROWTH PHASE
Non-polarized growth over the entire cell surface during spore germination.

Junior Research Group, Growth-control of Fungal Pathogens, Hans-Knöll Institute for Natural Products Research, Department of Microbiology, Friedrich-Schiller University, Hans-Knöll Strasse 2, D-07745 Jena, Germany. Correspondence to J.W. e-mail: juergen.wendland@uni-jena.de
doi:10.1038/nrmicro1148
Published online 8 April 2005

Ashbya gossypii was first described in 1926 by Ashby and Nowell[1] as a plant pathogen that causes STIGMATOMYCOSIS in fruit such as cotton (*Gossypium hirsutum*) or subtropical citrus fruits. *A. gossypii* does not develop specialized infection structures such as penetration hyphae. It relies on heteropterous insects, such as members of the genus *Leptoglossus,* for dispersal of spores or mycelial fragments. The spread of the disease is therefore readily controlled with insecticides, which might be one of the reasons why *A. gossypii* is not a devastating plant pathogen.

Ashbya gossypii was soon recognized for its ability to produce large quantities of riboflavin (vitamin B_2), which is responsible for its yellow colour[2–4] (FIG. 1). Riboflavin is a successful commercial product, and is used not only as a vitamin and food additive, but (as excess riboflavin is harmless in humans) also as a colourant (E101) in soft drinks and milk products. Analysis of riboflavin production dominated research in *A. gossypii* for more than half a century prior to the introduction of molecular genetic tools (TIMELINE).

A. gossypii: a filamentous yeast

Ashbya gossypii was first described as a 'filamentous yeast' in 1950 (REF. 5). This description was based in part on the habitat of *A. gossypii*, as it forms mycelia on fruit that are similar to the pseudomycelia that are formed by *Saccharomyces cerevisiae* on grapes. The uninucleate spores of *A. gossypii* have a haploid genome and are similar in cell wall carbohydrate and di-tyrosine composition to *S. cerevisiae* ascospores. This, together with other criteria such as rDNA phylogeny, led to a proposal to place *A. gossypii* in the *Saccharomycetaceae* family[6]. *A. gossypii* spores are needle-shaped and have filaments at one end that glue the spores together (FIG. 1). This distinguishes *A. gossypii* from one of its closest relatives, *Holleya sinecauda,* which produces spores of a similar shape but that are shorter and thicker and lack filaments (*sine cauda* means without tail).

Spores of *A. gossypii* germinate by initiating an ISOTROPIC GROWTH PHASE that results in the formation of a spherical germ cell. This growth phase can last up to 8 hours, and up to 3 rounds of nuclear divisions can occur before the switch to polarized growth leads to the emergence of a germ tube (FIG. 1). When a hyphal tip has formed, polarized growth can continue incessantly under favourable growth conditions. In common with the growth patterns of other filamentous ascomycetes such as *Aspergillus nidulans,* a septum is positioned at the neck, which divides the germ cell and the first hypha. A second germ tube then grows opposite to the first tube, which produces a bipolar

Timeline | **Key steps in *Ashbya gossypii* molecular biology**

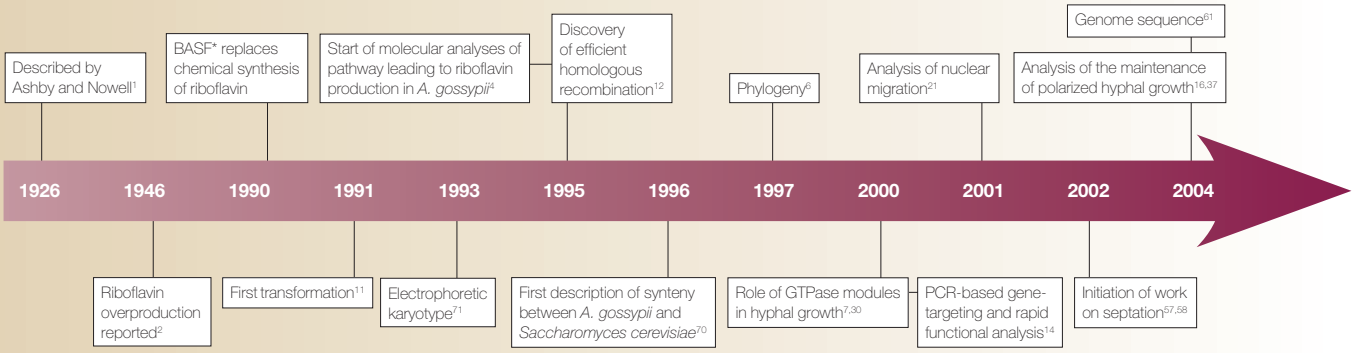

*Badische Anilin- und Soda-Fabrik AG

germination pattern. Hyphal tubes elongate and new hyphal tips are formed by lateral branching. This generates a juvenile mycelium. Following hyphal maturation, branches are preferentially formed at the hyphal tip in a dichotomous manner, producing Y-shaped hyphal filaments[7,8]. About 20–24 hours post-germination, a mature state of mycelial growth is reached and the edges of *A. gossypii* colonies only produce new tips using this growth pattern (FIG. 1). This distinguishes *A. gossypii* from most other filamentous ascomycetes. The life cycle ends when the mycelium has produced new spores. This occurs in the older parts of the mycelium and requires entry into a different developmental phase. Hyphal tubes fragment at septal sites and form single-celled SPORANGIA that contain the endospores. Preferred sites of sporulation are structures that are similar to SYNNEMATA. These are composed of several aerial hyphae that stick together to form macroscopically visible spikes. In *A. gossypii*, the secondary metabolite riboflavin is only produced when a culture is old and growth has ceased. Once growth has ceased, *A. gossypii* enters the sporulation phase, and a recent analysis reported that riboflavin protects spores against ultraviolet light[9]. In *A. nidulans*, a link between the production of a secondary metabolite (sterigmatocystin) and sporulation has also been observed[10].

Molecular tools for *A. gossypii*

Many of the molecular tools for *A. gossypii* were introduced by the Philippsen group in the 1990s. It became evident that *A. gossypii* is more similar, in terms of its molecular genetics, to yeast than to filamentous fungi.

Transformation of *A. gossypii* with plasmids that harbour the autonomously replicating sequence (ARS) elements of *S. cerevisiae*, as well as transformation by homologous recombination, were established using a G418/geneticin resistance marker gene[11,12]. Yeast ARS elements (but not yeast centromeres) function in *A. gossypii* but not in *H. sinecauda*. Conversely, an *A. gossypii* ARS element and the *A. gossypii* centromere of chromosome V function in *H. sinecauda* but not in *S. cerevisiae*[13]. Interestingly, *A. gossypii* integrates linear DNA with high efficiency at the homologous genomic locus (as does *S. cerevisiae*), in contrast to other filamentous fungi, in which ectopic integration at non-homologous positions frequently occurs. This led to the introduction of simple PCR-based gene targeting techniques in *A. gossypii* — the first time that this was achieved in a filamentous fungus[14,15].

Hyphal filaments of *A. gossypii* are multinucleate, so primary transformants will harbour two types of nuclei that contain either the mutant allele or the wild-type allele within a hyphal segment, and will therefore phenotypically be wild type. Such a mycelium will generate uninucleate spores that are a mixture of wild type and mutant. Selection of mutant spores allows the analysis of mutant phenotypes. Compared with other filamentous fungi, gene analysis in *A. gossypii* is therefore particularly convenient.

Other tools, including shuttle vectors, promoter and reporter constructs, as well as several selectable marker genes for dominant selection (antibiotic resistance) and strains auxotrophic for *LEU2* (leucine biosynthesis) and *THR4* (threonine biosynthesis) have been developed. The green fluorescent protein (GFP) used for protein localization studies is the yeast S65T-codon-modified version. Additionally, several fluorescent dyes can be used in *A. gossypii* to stain the actin cytoskeleton, vacuoles, and mitochondria[7,16].

Polarized hyphal growth in *A. gossypii*

Fungal growth occurs either as filamentous growth or as yeast-like growth. *S. cerevisiae* is the typical representative of a yeast, although on starvation for nitrogen or amino acids, which is common in natural habitats such as fruit surfaces, yeast cells switch to pseudohyphal growth[17,18]. *A. gossypii* grows in hyphal filaments for most of its life cycle, and only has single cell stages during spore germination and after fragmentation of the mycelium prior to sporulation. It is one of the most simple filamentous fungal species studied and does not form penetration structures to invade a host plant or elaborate fruiting bodies.

This simplicity should aid efforts to understand the molecular processes and networks that govern, for

SPORANGIUM
Cell or organ that produces or contains spores.

SYNNEMA/-TA
Erect hyphae that are grouped together. Conidia might be formed along the length of the synnema or just at its apex.

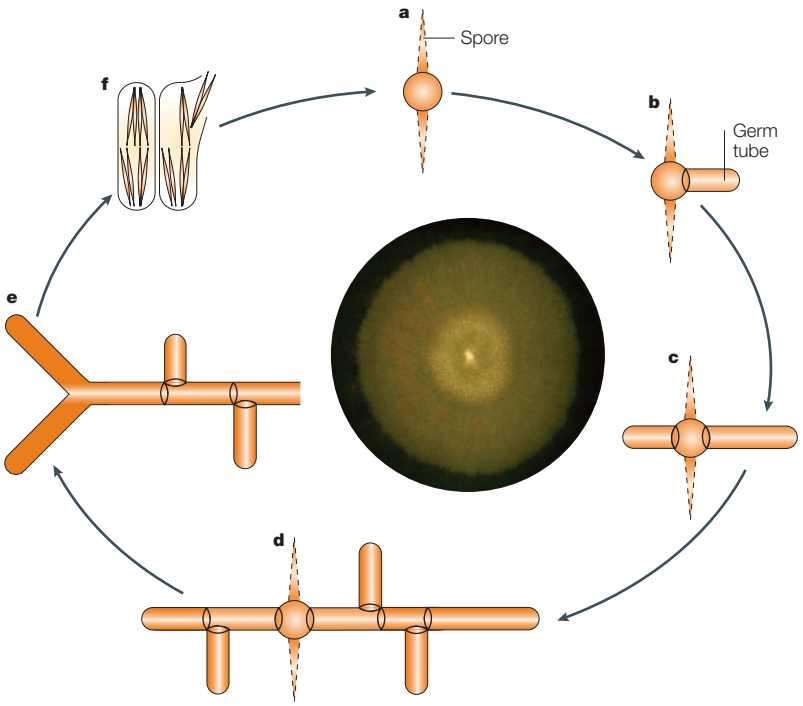

Figure 1 | **Life cycle of *Ashbya gossypii*.** In the centre, an *A. gossypii* colony is shown which was inoculated in the middle of the dish and grown for one week at 30°C. The yellow colour is caused by riboflavin production. The central part of the colony is the sporulation zone and is distinguished from non-sporulating mycelia by different colouration. In this area, 'spikes' are formed, which are aerial hyphae that adhere to each other and represent the main spore-producing tissue. Characteristic growth stages in *A. gossypii* development are (**a**) the isotropic growth phase during germination, (**b**) germ tube formation, (**c**) bipolar branching pattern, (**d**) juvenile mycelium, (**e**) dichotomous tip branching and (**f**) sporulation.

example, polarized hyphal growth in a filamentous fungus, and allow comparison of these processes with those in yeast. Understanding these processes might also offer new targets for antifungal drugs to curtail the growth of dimorphic fungal pathogens that can switch between yeast-like and filamentous forms in response to environmental stimuli. For example, in *C. albicans*, the dimorphic transition might facilitate adhesion to epithelial cells, penetration of host tissues and evasion of the cellular host immune response, and in the maize pathogen *Ustilago maydis*, the development of a filamentous dikaryon is required for virulence and entry into the BIOTROPHIC PHASE[19,20].

The fungal cytoskeleton

Fungal growth is supported by the actin and microtubule cytoskeletons. Long-range transport of vesicles to the growing tip and cycles of exocytosis of cell wall compounds, membrane and membrane proteins need to be coordinated to enable fast elongation rates. The microtubule cytoskeleton has a central role in nuclear distribution and nuclear migration. Deletion of the *A. gossypii DHC1* gene, which encodes the dynein heavy chain, resulted in clustering of nuclei at hyphal tips and drastically decreased growth rates[21]. By contrast, mutations in the *A. nidulans* dynein-heavy-chain homologue *nudA* (nuclear distribution) generated clusters of nuclei in germ cells, and therefore had the opposite effect on the phenotype[22]. In both mutants, however, the nuclear distribution defect could be ameliorated by the microtubule-destabilizing drug benomyl, which indicated that microtubule-based transport processes and specific motor proteins are involved[23]. The *Neurospora crassa* dynein-heavy-chain mutant *ro-1* (ropy) had distorted hyphal morphologies that resulted from misplacement of the SPITZENKÖRPER and a loss of growth directionality[24,25]. In *S. cerevisiae*, deletion of *DYN1* (dynein heavy chain) yields viable mutant strains that have defects in the alignment of the mitotic spindle in the mother–bud axis. Similar defects have been observed for *dyn1* mutants of *C. albicans*. In both yeasts, post-mitotic nuclear migration allowed correct distribution of nuclei between mother and daughter cells without serious growth defects[26,27]. However, *C. albicans dyn1* cells that were induced for filament formation could not transport nuclei into the hyphal tip, and could therefore not sustain filamentous growth[27]. Key questions still to be answered are the polarity of cytoplasmic microtubules in *A. gossypii,* the role of the hyphal tip in the coordination of nuclear distribution, and the mechanism of regulation of microtubule-dependent motor-protein activity to allow a balanced distribution of nuclei that promotes polarized hyphal growth.

In yeast, the actin cytoskeleton has an essential role in polarity establishment, whereas the involvement of the microtubule cytoskeleton in organelle and vesicle delivery is limited[28,29]. This led to the functional analysis of corresponding *A. gossypii* genes to determine their role in the organization of the actin cytoskeleton and hyphal growth[7,8,30]. The actin cytoskeleton comprises three different structures: cortical actin patches, actin cables and actin rings at septal sites (FIGS 2,3). During the isotropic phase of spore germination in *A. gossypii*, actin patches are randomly distributed in the germ cell. On generation of the first germ tube, patches are clustered at the incipient site of germ tube emergence, as occurs for bud emergence in *S. cerevisiae*. In yeast, polarized growth is initiated by the association of G1-cyclins (Cln1, Cln2 and Cln3) with the cyclin-dependent kinase Cdc28. Polarization is maintained only for a small period of the cell cycle, until activation of Cdc28 by the mitotic cyclins (Clb1 and Clb2) causes depolarization of the actin cytoskeleton and isotropic growth of the daughther cell[31]. The importance of cyclins for morphogenesis were recently demonstrated in *C. albicans*: two cyclins, Cln3 and Hgc1 (hyphal growth-specific G1 cyclin), are specifically expressed during yeast or filamentous growth, respectively[32,33]. The role of cyclins and cell cycle regulation for polarized hyphal growth have not yet been addressed in *A. gossypii*. In *A. nidulans*, apical growth and mitosis were shown to be independent, which indicates different regulatory networks in yeast-like and filamentous fungi[34].

In *A. gossypii* and all other filamentous fungi, polarization of the actin cytoskeleton is maintained and promotes hyphal elongation. Therefore, maintenance of polarized growth is one of the main features that distinguishes yeasts from filamentous fungi[35].

BIOTROPHIC PHASE
The pathogen invades host tissue without killing host cells and feeds on living cells.

SPITZENKÖRPER
A phase-dark, usually spherical body that is found in growing hyphal tips, and represents an accumulation of secretory vesicles — also known as the vesicle supply centre.

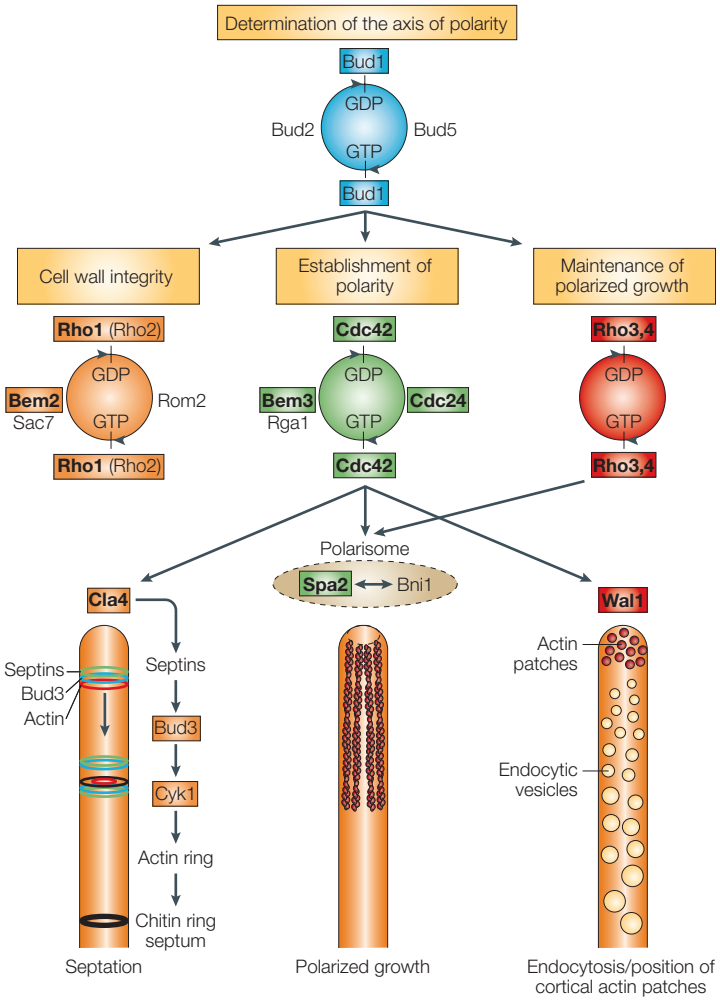

Figure 2 | **Potential signal cascades that regulate polarized hyphal growth and septation in *Ashbya gossypii*.** Several GTPase modules have been identified in *A. gossypii*, mainly based on homology to those in *Saccharomyces cerevisiae*. Proteins shown in bold type correspond to genes that have been analysed in *A. gossypii*. The modules were found to be involved specifically in one of the indicated processes, which are important steps leading to polarized hyphal growth. This is a schematic model of a protein network that controls septation, polarized growth and endocytosis.

In *S. cerevisiae*, the Bud1 GTPase module is required for bud-site selection, and loss of either the Ras-like Bud1 GTPase, its GEF (guanine nucleotide-exchange factor), Bud5, or its GAP (GTPase-activating protein), Bud2, results in random budding, without producing any important decrease in growth rate. This places Bud1 upstream of the cell-polarity-establishment machinery[36] (FIG. 2). In *A. gossypii*, the Bud1 homologue is required for maintenance of hyphal growth and determination of the site of polarized growth, and governs the localization of the POLARISOME component Spa2 (REF. 37) (FIG. 2). Hyphae of the *bud1* mutant frequently pause and resume growth. Hyphal growth required the localization of Spa2 at the hyphal tip, and growth was arrested once Spa2–GFP was no longer detected at the tip. Resumption of growth occurred at the tip, but in a manner that was not reliant on the previously established axis of polarity[37]. This indicates that the function of the Bud1 module is to activate the polarisome through the Cdc42 module. Whereas in *S. cerevisiae*, deletion of *BUD1* randomizes budding but does not reduce the ability of the cell-polarity-establishment Cdc42 module to initiate bud emergence, in *A. gossypii*, deletion of *BUD1* reduces the growth rate dramatically. Pausing and resumption of growth indicates that alternative routes of Cdc42 activation exist — possibly in a stochastic manner, as has been described in *S. cerevisiae*, which could explain the zig-zag phenotype of *bud1* hyphal growth[37,38]. Interestingly, *A. gossypii* Bud1does not seem to have a role in the early phases of germination and the generation of the bipolar germination pattern. At this stage, a Rho GAP protein, encoded by the *A. gossypii BEM2* (bud emergence) homologue, is important. Mutant *bem2* germ cells had a prolonged isotropic growth phase, generating enlarged germ cells that failed to produce the bipolar germination pattern. Hyphae were swollen and the distribution of cortical actin patches was delocalized. Interestingly, loss of polarity in the swollen hyphal tips of *bem2* mutants was overcome by establishing new cell polarities to form new hyphal tips at random positions[7] (FIG. 3b). This suggests that Bem2 regulates the activity of Cdc42. In *S. cerevisiae*, the function of Bem2 is controversial and includes either Rho1 or Cdc42 (FIG. 2). A multiple-budding phenotype (as seen in the multiple branch initiations of the *A. gossypii bem2* hyphae) has recently been described for certain *cdc42* alleles[39] in *S. cerevisiae*.

Polarity establishment and the switch from isotropic to polarized growth in *S. cerevisiae* and *A. gossypii* is dependent on the Rho protein Cdc42 and its GEF, Cdc24 (REF. 40). *S. cerevisiae* strains that harbour temperature-sensitive alleles of *cdc42* or *cdc24* fail to form buds at the restrictive temperature[41]. Mutant spores of heterokaryotic *A. gossypii CDC42/cdc42* or *CDC24/cdc24* strains germinate and produce enlarged germ cells in which the nuclear cycle is continued and many nuclei are generated. However, these germ cells fail to polarize the cortical actin patches and never form germ tubes[30]. This shows that the process of germination, as well as the nuclear cycle, does not require Cdc42 activity. Polarized growth in *S. cerevisiae* was shown to be governed by feedback loops, involving Bem1 and phosphorylation of Cdc24 by Cla4, controlling Cdc42 activity in either positive or negative ways[42,43]. This indicates that maintenance of polarized cell growth in filamentous fungi might depend on the specific and maintained activation of Cdc42 at the hyphal tip, either by constitutive positive feedback regulation or as a result of Ras activation.

Other GTP-binding proteins of the Rho family were also shown to affect hyphal morphogenesis in *A. gossypii* and *S. cerevisiae*. Mutant *Rho1* strains were non-viable, as hyphae lysed at the microcolony stage, similar to *S. cerevisiae rho1* mutants, in which cells lysed shortly after budding[30,44]. This indicates that functions of the cell-wall-integrity pathway for polarized growth are controlled by Rho1 in *A. gossypii*, as in *S. cerevisiae*[45].

POLARISOME
Protein complex that consists, in *S. cerevisiae*, of the formin Bni1, Spa2, Bud6 and Pea2, and is involved in organization of the actin cytoskeleton and required for polarized cell growth.

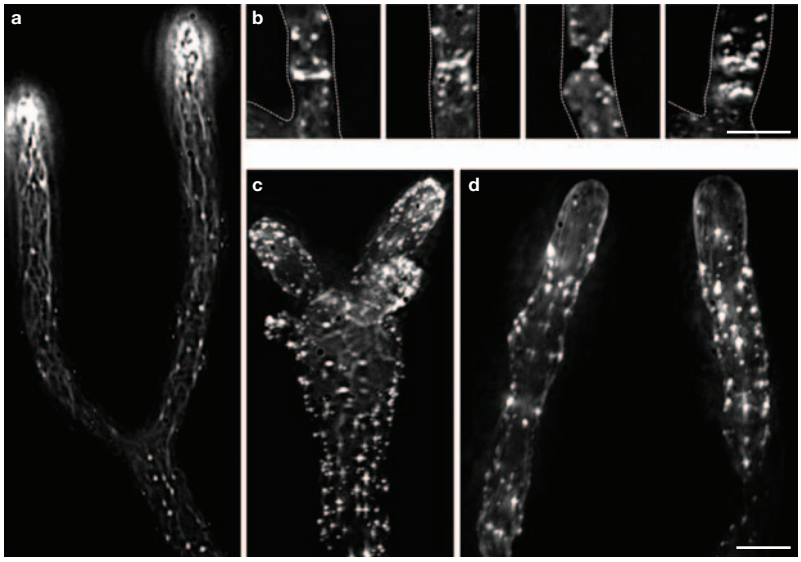

Figure 3 | **Actin cytoskeleton components in *Ashbya gossypii*.** Images of rhodamine–phalloidin stained hyphae. (**a**,**b**) Wild type, (**c**) *bem2* mutant and (**d**) *wal1* mutant. In wild-type and *bem2* hyphae, cortical actin patches are localized at the hyphal tip, whereas in the *wal1* mutant, patches cluster in subapical regions. Actin cables generate a meshwork of filaments in an apical direction inserting into (or emanating from) the hyphal tip, even in the absence of actin patches as seen in *wal1* (**a**,**c**,**d**). Loss of cell polarity in swollen *bem2* hyphae is overcome by newly formed branches (**c**). Actin rings at septal sites perform a dynamic constriction, which is required for the completion of septum formation (**b**). Hyphal cell walls are outlined in (**b**). Bars are 5 μm; the image series in **b** (derived from different hyphae aligned to show the order of events) is slightly enlarged.

In both *A. gossypii* and *S. cerevisiae*, defects in *RHO1* lead to cell death by lysis. In *S. cerevisiae*, there are temperature-sensitive mutations (such as *rho1-104*) which are viable at the permissive (lower) temperature but show the lysis phenotype at the non-permissive (higher) temperature.

RHO3 deletion mutants of *A. gossypii* showed defects in polarized morphogenesis that are not found in *S. cerevisiae*. First, during the hyphal growth phase, swellings occurred at the hyphal tips, which might indicate a defect in the targeted delivery of secretory vesicles, as was seen in certain *S. cerevisiae rho3* alleles[30,46] (FIG. 2). Isotropic growth at sites of swelling was overcome by reinitiating polarized growth similar to germ tube emergence after germination. Second, where recurrent polarized growth occurred, the direction of growth was maintained in the axis of previous cell polarity. Finally, during germination at elevated temperatures, deletion of *RHO3* resulted in lethality and lysis of the primary germ tube[30].

Polarisome

In *S. cerevisiae*, a protein complex named the polarisome was identified, which consists of the formin Bni1 that forms a complex with Spa2, Bud6 and Pea2 (REF. 47). The polarisome regulates the cortical actin cytoskeleton and thereby polarizes growth to a restricted surface area[48]. Deletion of any of the four polarisome-protein-encoding genes resulted in enlarged, swollen, round cells in *S. cerevisiae*[47]. The polarisome component Spa2 of *A. gossypii* was found to delimit the region of hyphal tip growth, therefore determining the diameter of the hyphae, which might be a similar function to that of Spa2 at the *S. cerevisiae* bud tips. Growth was slowed down in *A. gossypii spa2* mutant hyphae, but the organization of the actin cytoskeleton was not disturbed, which indicates that a *SPA2* deletion did not eliminate either polarisome or formin activity[49]. The polarisome can be activated through Rho-protein-dependent stimulation of Bni1 in *S. cerevisiae*[50,51] (FIG. 2). Other potential downstream targets of Rho-protein signalling that have been analysed in *A. gossypii* are the homologue of the Wiskott–Aldrich syndrome protein (WASP), Wal1, and a member of the p21 activated kinases, Cla4 (REFS 8,16) (FIG. 2). Deletion of the WASP homologue that is encoded by *LAS17/BEE1* in *S. cerevisiae* revealed defects in endocytosis and the assembly of the cortical actin cytoskeleton[52]. The apical positioning of cortical actin patches was lost in *wal1* hyphae (FIG. 3). Instead, a subapical accumulation of patches was observed. Insight into the function of Wal1 came from *in vivo* time-lapse analyses of endocytosis in wild-type and *wal1* strains. In the wild type, early endosomes are generated in the hyphal tip. Endosomes are fused and form large vacuoles in subapical regions of the hyphae (FIG. 2). Vivid motion of endosomes, as well as fusion and movement of large vacuoles, is readily observable in wild-type hyphae. In *wal1* hyphae, the tips lack both cortical actin patches and early endosomes. Furthermore, movement of endosomes and vacuoles is greatly reduced. As mitochondria were distributed in a wild-type-like manner in the *wal1* mutant, Wal1 functions to coordinate the positioning of cortical actin patches and endocytosis. This raises questions about how mitochondria are distributed in filamentous fungi, but excludes Wal1 from this process[16].

Our results revealed a more drastic mutant phenotype in the *wal1 A. gossypii* mutant compared with the *S. cerevisiae las17/bee1* mutant. Whereas the *C. albicans* WASP homologue was required for maintained polarized hyphal growth, disruption of *WAL1* in *A. gossypii* led to slow and bulbous growth of hyphae, which failed to produce septa[16,53]. This indicates that polarized hyphal growth depends on a firm regulation of secretion and endocytosis, which might not be required for yeast-like growth.

Septation in *A. gossypii*

The septation process of filamentous fungi is homologous to cytokinesis in yeast-like fungi[54]. Mechanistic differences exist in the positioning of septa and in septum construction, which can be defined by comparing closely related morphogenetic networks. Septation results in the compartmentalization of hyphae, in which the cell compartments are interconnected by septal pores (FIG. 4). This allows transport among compartments in filamentous fungi. Transport, or 'cytoplasmic streaming', can be observed as movement of vacuoles using *in vivo* timelapse recordings, and is tip-directed in *A. gossypii* as long as a hyphal tip promotes active growth. Once growth ceases, for example, due to contact

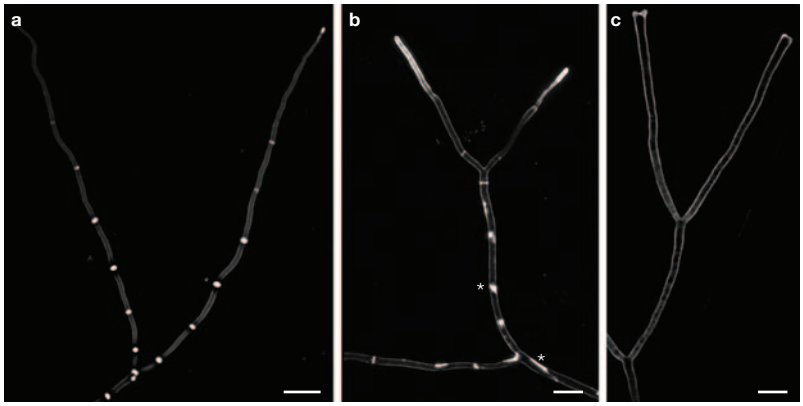

Figure 4 | **Septation and septation mutants in *Ashbya gossypii*.** Images of calcofluor-stained hyphae. (**a**) Wild type, (**b**) *bud3* mutant and (**c**) *cyk1* mutant. Hyphal segments with dichotomous branches are shown. In the wild type, regular septal intervals can be seen with a longer tip compartment (**a**). The *bud3* mutant shows aberrant and delocalized chitin depositioning but can also build regular septa (**b**). The *cyk1* mutant is aseptate (**c**). Cyk1p is essential for actin ring formation. Subsequently, no chitin can accumulate at presumptive septal sites, particularly at the base of dichotomous branches. Bar in **a** is 50 μm, bars in **b** and **c** are 20 μm.

inhibition which blocks apical extension, cytoplasmic streaming might be reversed backwards out of the tip, presumably to promote fast elongation of other hyphae[16]. Nuclei were shown to cross septal borders in *A. gossypii*[21]. Large vacuoles, however, do not cross septa. Therefore, through septation, cytoplasmic streaming can be redirected, and hyphal tips do not lose their cytoplasm[16].

In *S. cerevisiae*, Cdc42 triggers the assembly of a septin ring at the incipient bud site through its effector proteins Cla4 and Bni1 (REF. 55) (FIG. 2). Septins belong to a family of conserved proteins in animals and fungi that are required for cytokinesis as well as other processes[56].

The *cla4* mutation in *A. gossypii* showed defects in hyphal growth as well as defects in septation. This indicated a similar role for Cla4 in the assembly of early septal protein complexes in *A. gossypii*, whereas a participation of Cla4 in a feedback loop to control Cdc42 activity has yet to be analysed[8]. Also, Cla4 might be involved in a tip-based process of positioning septa at regular intervals along the hyphal tube. Further evidence of such a role for the hyphal tip came from *in vivo* timelapse recordings of juvenile *A. gossypii* mycelia[49]. It was found that lateral branching and septation events cause a decrease in the apical extension rate of a hyphal tip that belongs to the same cellular compartment. This might be the result of the diversion of part of the secretory apparatus away from the tip towards branches or septal sites. Importantly, during this transient decrease in tip growth, potential cortical landmarks might be positioned, as it was found that after resumption of growth these pausing sites were used for the generation of septa or branches[49]. The molecular nature of these putative landmarks is currently unknown, but a hypothesis is that a septin ring is formed at these positions, which generates an upstream signal for septum formation, although this needs to be experimentally confirmed.

CORTICAL CUES
Membrane-associated proteins that function as landmarks to direct protein complexes that are required for the establishment of cell polarity.

In *S. cerevisiae*, CORTICAL CUES are important in determining bud-site selection. Bud3 and Bud4, for example, are required for the axial budding pattern of haploid (**a** or α mating type) cells, whereas Bud8 and Bud9 are important for determining bud-site selection in diploid (**a**/α) cells[36,54]. The existence of *BUD* homologues in the *A. gossypii* genome was first discovered because of the conserved linkage of *BUD3* to the *LEU2* gene in both *S. cerevisiae* and *A. gossypii*[57]. In common with its homologue in *S. cerevisiae*, the *A. gossypii* Bud3 protein transiently localizes to septal sites. First, Bud3 localization occurs as a single ring, which is split into a double ring on chitin accumulation and septum formation. After a septum has formed, the Bud3 rings disassemble from this septal site. The localization of Bud3 (in the absence of septum formation) might be sufficient to serve as positional information for lateral branching. Interestingly, the C-terminal portion of the *A. gossypii* Bud3 (even though highly divergent in sequence to *S. cerevisiae* Bud3) localizes correctly to the bud neck in *S. cerevisiae* and also performs ring splitting. Deletion mutants of *bud3* showed defects in septum formation in *A. gossypii* (FIG. 4). This defect was only partial, however, as some septa seemed normal, whereas at malformed septal sites, aberrant deposition of chitin occurred. The actin cytoskeleton in *bud3* mutants was defective for actin-ring formation. Instead of actin rings at aberrantly formed septal sites, linear actin filaments were formed and were attached to the cell cortex. This phenotype was due to the partial mislocalization of Cyk1, which is the *A. gossypii* homologue of *S. cerevisiae* Iqg1 (IQ-containing-motif GTPase-activating protein 1)/Cyk1, and is essential for actin ring formation[57,58]. Linear actin rings in *A. gossypii* co-localized with linear Cyk1 filaments, which places Bud3 upstream of Cyk1. As septation in *bud3* mutants was not completely aberrant, other proteins might be involved in this process together with Bud3. One of the most interesting candidates is the *A. gossypii* Bud4 homologue, which, in *S. cerevisiae*, interacts with Iqg1/Cyk1 (REF. 59).

Once all the protein complexes required for septation have been assembled, a signal is required to initiate the dynamic events that lead to septum formation and chitin accumulation in *A. gossypii*. During septum formation in *S. cerevisiae*, the septin ring splits in two, as with the Bud3 ring. Therefore, ring splitting produces a corral that prevents diffusion of proteins out of the septal site[60]. Such a barrier might also be used to determine the size of the septum, as the space between the split rings is filled by the chitin-rich septum. Chitin accumulation occurs concomitantly with the constriction of the acto-myosin ring. The *A. gossypii* Cyk1 filaments also undergo ring constriction, which indicates that Cyk1 is not only required for the formation of the actin ring but also for the dynamic processes of the ring. In filamentous fungi, several future sites of septation, revealed by the positioning of uncontracted actin rings, might occur within the hyphal tip cell. In *A. gossypii*, activation of-actin-ring constriction, which leads to chitin accumulation, occurs from the basal end towards the tip by an unknown mechanism[57,58].

Table 1 | **Comparison of *A. gossypii* and *S. cerevisiae* genomes**

Feature	*Ashbya gossypii*	*Saccharomyces cerevisiae*
Genome size	8.8 Mb (+rDNA repeats)	12.1 Mb (+rDNA repeats)
Number of chromosomes	7	16
GC-content	52%	38%
Number of genes	4,718	5,570
Number of introns	221	~250
% of genes with homologues in *S. cerevisiae*	95%	100%
Protein-coding sequences	80%	~70%
Gene density	1.9 kb	2.1 kb

C, cytosine; G, guanine.

Genome organization

The *A. gossypii* genome sequence is now publicly available and is one of the best-annotated eukaryotic genome sequences, largely owing to the large degree of SYNTENY with the *S. cerevisiae* genome and to the relative compactness and simplicity of the *A. gossypii* genome[61] (TABLE 1). The *A. gossypii* genome sequence was used to reanalyse the genome annotation of *S. cerevisiae* and, as was concluded in a similar study using the genome sequence of *Kluyveromyces waltii,* provides strong evidence for an ancient genome duplication in the *Saccharomyces* lineage[61–63].

About 95% of all *A. gossypii* genes have a homologue in *S. cerevisiae,* which indicates that the basic cellular functions and morphogenetic machineries are well conserved between these species. Because of the genome duplication, the *S. cerevisiae* genome might contain two homologues of a single *A. gossypii* gene, which might be relevant for morphogenesis. Several genes belong to this group, for example, *A. gossypii* has only one homologue of the *S. cerevisiae BUD8/BUD9* genes which encode bipolar landmark proteins, one homologue of the *S. cerevisiae RAS1/RAS2* pair, one homologue of the *SPA2/SPH1* (Spa2 homologue) twins, and one homologue of the GTPase-activating proteins *RGA1/RGA2*. Bud8 and Bud9 proteins localize to the distal and proximal pole in diploid *S. cerevisiae* cells, respectively. Hyphae of a filamentous fungus have unipolar growth and might therefore have no need to mark distal regions. Furthermore, in *A. gossypii*, Bud3 might be part of the landmark that coordinates lateral branching with septal sites, as lateral branches are preferably positioned next to septa. On the other hand, *S. cerevisiae* genes that are absent from *A. gossypii* might be important for growth differences. One such gene is *CTS1,* which encodes a chitinase in yeast [64]. In *S. cerevisiae*, this protein is required for mother–daughter cell separation/cytokinesis. *CTS1* is expressed in a daughter-cell-specific manner. Cts1 dissolves part of the chitin ring that connects mother and daughter cells, producing the different intensities of bud scars and birth scars on the mother and daughter cell surface, respectively, on chitin staining[64]. Lack of such an activity in *A. gossypii* is consistent with its life cycle, as separation of septate compartments could abolish hyphal growth.

This is in accord with observations in *A. nidulans* that the chitinase encoded by *chiA* is developmentally expressed and upregulated during CONIDIOPHORE development, which requires a transition process to produce uninucleate metulae, phialides and conidia from multinucleate hyphal cells[65]. Another gene that is absent from *A. gossypii* is *SLA2*, which in *S. cerevisiae* has been shown to interact with Cla4 using a two-hybrid system, and has a role in cell polarization and endocytosis[66,67]. Loss of this gene might have occurred in *A. gossypii*, as other filamentous ascomycetes have *SLA2* homologues. Interestingly, *SLA2* in *A. gossypii* might have been lost during the evolution of a mating-type locus.

The *A. gossypii* genome harbours 3 loci on chromosomes 4, 5, and 6 that contain a homologue of the *S. cerevisiae MATA1* (mating-type locus gene A1) gene, and in all 3 cases these genes are linked to a homologue of the *S. cerevisiae* gene *SUI1*. Two of those loci, on chromosomes 4 and 5, are located at the ends of the chromosomes near telomeric repeats. This is reminiscent of the position of the silent mating-type cassettes *S. cerevisiae*, which are located at both ends of chromosome III close to the telomeres. Closer inspection of the annotated *A. gossypii* sequence indicates that, adjacent to the *A. gossypii MATA1* gene in all three loci, there is a divergently transcribed gene with similarity to the *Kluyveromyces lactis* a2 mating-type protein[61] (annotated as no homology in bakers' yeast: NOHBY670, NOHBY532, and NOHBY421). A comparison of the *MAT* locus of chromosome 6 of *A. gossypii* with the mating-type locus of *K. lactis*[68] revealed the conservation of adjacent genes on both flanks of the *MAT* loci (FIG. 5). The genes missing from the *A. gossypii MAT* locus compared with *K. lactis* (particularly *SLA2)* are not present elsewhere in the genome.

The identification of a mating-type locus in *A. gossypii* and the assignment of the wild type as a MAT**a** strain enables a more detailed analysis of whether *A. gossypii* spores are of sexual or asexual origin. The following possibilities need to be explored. First, is there an equivalent of an *A. gossypii* MATα strain in nature? Second, is the mating-type locus involved in sporulation observed of the wild-type strain or is this purely asexual reproduction? Finally, does the mating system allow both homothallic (self) and heterothallic (outcross) matings, as in *A. nidulans*[69]? To analyse this in detail, deletions in the pheromone-receptor homologues *STE2* and *STE3* will be required. Further analyses of the genome sequence revealed, for example, the presence of homologues of sporulation-specific *S. cerevisiae* genes such as the initiator of meiosis genes, *IME1* and *IME2*, which might also indicate the presence of a sexual cycle in *A. gossypii*.

SYNTENY
Evolutionary conservation of gene order (including their transcriptional orientation) between two loci.

CONIDIOPHORE
Structure that bears and generates the conidiospores.

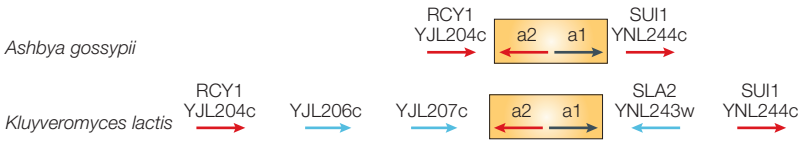

Figure 5 | **The mating-type *MATA* locus of *Ashbya gossypii*.** The *A. gossypii MAT* locus on chromosome 6 displays syntenic gene arrangements with the *Kluyveromyces lactis MAT* locus, including conservation of flanking genes on both sides of the *MAT* locus. In the *A. gossypii* genome, no homologues of YJL206c, YJL207c or YNL243w are present. MAT, mating type.

Conclusions

In the past decade, *A. gossypii,* a fungal species used for riboflavin/vitamin B_2 production, has become a model organism for the study of cell biology of multicellular filamentous fungi. With tools for easy genetic manipulation and the *A. gossypii* genome sequence now available, several new research avenues are now available. *A. gossypii* is a filamentous ascomycete that has similarities with yeasts and filamentous fungi, and provides a suitable model organism to study the cell biology and evolution of both these forms.

The set of conserved morphogenetic genes among *A. gossypii* and *S. cerevisiae* can now be analysed in detail. Specific problems in the biology of filamentous fungi that are linked to this type of growth, such as organelle transport and cytoplasmic streaming, as well as septation and the control of cell and nuclear cycles, can be analysed in *A. gossypii*. For the set of duplicated genes in *S. cerevisiae* (or for the few duplications that occurred in the *A. gossypii* lineage, for example of the *RHO1* and *BNR1* genes), ancient and evolved functions might be determined. In addition, with the use of transcriptional profiling, general responses to stresses such as heat shock, peroxide and starvation can be analysed and directly compared with *S. cerevisiae* with regard to potential evolutionary aspects. Comparison with pathogenic fungi, such as *C. albicans*, might also provide insights into new strategies of antifungal drug development.

1. Ashby, S. F. & Nowell, W. The fungi of stigmatomycosis. *Ann. Bot.* **40**, 69–84 (1926).
2. Wickerham, L. S., Flickinger, M. H. & Johnson, R. M. Production of riboflavin by *Ashbya gossypii*. *Arch. Biochem.* **9**, 95–98 (1946).
3. Demain, A. L. Riboflavin overproducers. *Annu. Rev. Microbiol.* **26**, 369–388 (1972).
4. Stahmann, K. P., Revuelta, J. L. & Seulberger, H. Three biotechnological processes using *Ashbya gossypii*, *Candida famata*, or *Bacillus subtilis* compete with chemical riboflavin production. *Appl. Microbiol. Biotechnol.* **53**, 509–516 (2000).
5. Mickelson, M. M. The metabolism of glucose by *Ashbya gossypii*. *J. Bacteriol.* **59**, 659–666 (1950).
6. Prillinger, H. *et al.* Phytopathogenic filamentous (*Ashbya*, *Eremothecium*) and dimorphic fungi (*Holleya*, *Nematospora*) with needle-shaped ascospores as new members within the *Saccharomycetaceae*. *Yeast* **13**, 945–960 (1997).
Phylogenetic analyses that demonstrate the close relationship of *Ashbya* spp. with the yeast family.
7. Wendland, J. & Philippsen, P. Determination of cell polarity in germinated spores and hyphal tips of the filamentous ascomycete *Ashbya gossypii* requires a rhoGAP homolog. *J. Cell Sci.* **113**, 1611–1621 (2000).
8. Ayad-Durieux, Y., Knechtle, P., Goff, S., Dietrich, F. & Philippsen, P. A PAK-like kinase is required for maturation of young hyphae and septation in the filamentous ascomycete *Ashbya gossypii*. *J. Cell Sci.* **113**, 4563–4575 (2000).
This study describes the role of *A. gossypii CLA4* in septation and growth promotion.
9. Stahmann, K. P. *et al.* Riboflavin, overproduced during sporulation of *Ashbya gossypii*, protects its hyaline spores against ultraviolet light. *Environ. Microbiol.* **3**, 545–550 (2001).
10. Hicks, J. K., Yu, J. H., Keller, N. P. & Adams, T. H. *Aspergillus* sporulation and mycotoxin production both require inactivation of the FadA Gα-protein-dependent signalling pathway. *EMBO J.* **16**, 4916–4923 (1997).
11. Wright, M. C. & Philippsen, P. Replicative transformation of the filamentous fungus *Ashbya gossypii* with plasmids containing *Saccharomyces cerevisiae* ARS elements. *Gene* **109**, 99–105 (1991).
12. Steiner, S., Wendland, J., Wright, M. C. & Philippsen, P. Homologous recombination as the main mechanism for DNA integration and cause of rearrangements in the filamentous ascomycete *Ashbya gossypii*. *Genetics* **140**, 973–987 (1995).
13. Schade, D., Walther, A. & Wendland, J. The development of a transformation system for the dimorphic plant pathogen *Holleya sinecauda* based on *Ashbya gossypii* DNA elements. *Fungal Genet. Biol.* **40**, 65–71 (2003).
14. Wendland, J., Ayad-Durieux, Y., Knechtle, P., Rebischung, C. & Philippsen, P. PCR-based gene targeting in the filamentous fungus *Ashbya gossypii*. *Gene* **242**, 381–391 (2000).
This was the first demonstration of PCR-based transformation in a filamentous fungus.
15. Wendland, J. PCR-based methods facilitate targeted gene manipulations and cloning procedures. *Curr. Genet.* **44**, 115–123 (2003).
16. Walther, A. & Wendland, J. Apical localization of actin patches and vacuolar dynamics in *Ashbya gossypii* depend on the WASP homolog Wal1p. *J. Cell Sci.* **117**, 4947–4758 (2004).
This study demonstrates the importance of actin patch positioning in polarized morphogenesis and endocytosis.
17. Gimeno, C. J., Ljungdahl, P. O., Styles, C. A. & Fink, G. R. Unipolar cell divisions in the yeast *S. cerevisiae* lead to filamentous growth: regulation by starvation and RAS. *Cell* **68**, 1077–1090 (1992).
18. Braus, G. H., Grundmann, O., Bruckner, S. & Mosch, H. U. Amino acid starvation and Gcn4p regulate adhesive growth and *FLO11* gene expression in *Saccharomyces cerevisiae*. *Mol. Biol. Cell.* **14**, 4272–4284 (2003).
19. Berman, J. & Sudbery, P. E. *Candida albicans*: a molecular revolution built on lessons from budding yeast. *Nature Rev. Genet.* **3**, 918–930 (2003).
20. Kahmann, R. & Kamper, J. *Ustilago maydis*: how its biology relates to pathogenic development. *New Phytol.* **164**, 31–42 (2004).
21. Alberti-Segui, C., Dietrich, F., Altmann-Johl, R., Hoepfner, D. & Philippsen, P. Cytoplasmic dynein is required to oppose the force that moves nuclei towards the hyphal tip in the filamentous ascomycete *Ashbya gossypii*. *J. Cell Sci.* **114**, 975–986 (2001).
This study revealed nuclear distribution defects in *dyn1* mutants that are strikingly different from similar mutations in *A. nidulans*.
22. Xiang, X., Beckwith, S. M. & Morris, N. R. Cytoplasmic dynein is involved in nuclear migration in *Aspergillus nidulans*. *Proc. Natl Acad. Sci. USA* **91**, 2100–2104 (1994).
23. Willins, D. A., Xiang, X. & Morris, N. R. An α-tubulin mutation suppresses nuclear migration mutations in *Aspergillus nidulans*. *Genetics* **141**, 1287–1298 (1995).
24. Plamann, M., Minke, P. F., Tinsley, J. H. & Bruno, K. S. Cytoplasmic dynein and actin-related protein Arp1 are required for normal nuclear distribution in filamentous fungi. *J. Cell Biol.* **127**, 139–149 (1994).
25. Riquelme, M., Gierz, G. & Bartnicki-Garcia, S. Dynein and dynactin deficiencies affect the formation and function of the Spitzenkörper and distort hyphal morphogenesis of *Neurospora crassa*. *Microbiology* **146**, 1743–1753 (2000).
26. Eshel, D. *et al.* Cytoplasmic dynein is required for normal nuclear segregation in yeast. *Proc. Natl Acad. Sci. USA* **90**, 11172–11176 (1993).
27. Martin, R., Walther, A. & Wendland, J. Deletion of the dynein heavy chain gene *DYN1* leads to aberrant nuclear positioning and defective hyphal development in *Candida albicans*. *Euk. Cell* **3**, 1574–1588 (2004).
28. Matsui, Y. Polarized distribution of intracellular components by class V myosins in *Saccharomyces cerevisiae*. *Int. Rev. Cytol.* **229**, 1–42 (2003).
29. Pruyne, D., Legesse-Miller, A., Gao, L., Dong, Y. & Bretscher, A. Mechanisms of polarized growth and organelle segregation in yeast. *Annu. Rev. Cell. Dev. Biol.* **20**, 229–591 (2004).
30. Wendland, J. & Philippsen, P. Cell polarity and hyphal morphogenesis are controlled by multiple rho-protein modules in the filamentous ascomycete *Ashbya gossypii*. *Genetics* **157**, 601–610 (2001).
This is the first description of the role of multiple Rho GTPases in different stages of hyphal morphogenesis
31. Lew, D. J. & Reed, S. I. Morphogenesis in the yeast cell cycle: regulation by Cdc28 and cyclins. *J. Cell Biol.* **120**, 1305–1320 (1993).
32. Zheng, X. & Wang, Y. Hgc1, a novel hypha-specific G1 cyclin-related protein regulates *Candida albicans* hyphal morphogenesis. *EMBO J.* **23**, 1845–1856 (2004).
33. Bachewich, C. & Whiteway, M. Cyclin Cln3p links G1 progression to hyphal and pseudohyphal development in *Candida albicans*. *Euk. Cell* **4**, 95–102 (2005).
34. Riquelme, M., Fischer, R. & Bartnicki-Garcia, S. Apical growth and mitosis are independent processes in *Aspergillus nidulans*. *Protoplasma* **222**, 211–215 (2003).
35. Wendland, J. Comparison of morphogenetic networks of filamentous fungi and yeast. *Fungal Genet. Biol.* **34**, 62–83 (2001).
36. Madden, K. & Snyder, M. Cell polarity and morphogenesis in budding yeast. *Annu. Rev. Microbiol.* **52**, 687–744 (1998).
37. Bauer, Y., Knechtle, P., Wendland, J., Helfer, H. & Philippsen, P. A Ras like GTPase is involved in hyphal growth guidance in the filamentous fungus *Ashbya gossypii*. *Mol. Biol. Cell* **15**, 4622–4632 (2004).
This study incorporates signalling components upstream and downstream of Rho GTPases in the morphogenetic network.
38. Wedlich-Soldner, R., Altschuler, S., Wu, L. & Li, R. Spontaneous cell polarization through actomyosin-based delivery of the Cdc42 GTPase. *Science* **299**, 1231–1235 (2003).
39. Caviston, J. P., Tcheperegine, S. E. & Bi, E. Singularity in budding: a role for the evolutionary conserved small GTPase Cdc42p. *Proc. Natl Acad. Sci. USA* **99**, 12185–12190 (2002).
40. Johnson, D. I. Cdc42: an essential Rho-type GTPase controlling eukaryotic cell polarity. *Microbiol. Mol. Biol. Rev.* **63**, 54–105 (1999).
41. Bender, A. & Pringle, J. R. Multicopy suppression of the *cdc24* budding defect in yeast by *CDC42* and three newly identified genes including the ras-related gene *RSR1*. *Proc. Natl Acad. Sci. USA* **86**, 9976–9980 (1989).
42. Gulli, M. P. *et al.* Phosphorylation of the Cdc42 exchange factor Cdc24 by the PAK-like kinase Cla4 may regulate polarized growth in yeast. *Mol. Cell* **6**, 1155–1167 (2000).

43. Bose, I. *et al.* Assembly of scaffold-mediated complexes containing Cdc42p, the exchange factor Cdc24p, and the effector Cla4p required for cell cycle-regulated phosphorylation of Cdc24p. *J. Biol. Chem.* **276**, 7176–7186 (2001).
44. Yamochi, W. *et al.* Growth site localization of Rho1 small GTP-binding protein and its involvement in bud formation in *Saccharomyces cerevisiae*. *J. Cell Biol.* **125**, 1077–1093 (1994).
45. Kamada, Y. *et al.* Activation of yeast protein kinase C by Rho1 GTPase. *J. Biol. Chem.* **271**, 9193–9196 (1996).
46. Adamo, J. E., Rossi, G. & Brennwald, P. The Rho GTPase Rho3 has a direct role in exocytosis that is distinct from its role in actin polarity. *Mol. Biol. Cell* **10**, 4121–4133 (1999).
47. Sheu, Y. J., Santos, B., Fortin, N., Costigan, C. & Snyder, M. Spa2p interacts with cell polarity proteins and signaling components involved in yeast cell morphogenesis. *Mol. Cell Biol.* **18**, 4053–4069 (1998).
48. Fujiwara T. *et al.* Rho1p–Bni1p–Spa2p interactions: implication in localization of Bni1p at the bud site and regulation of the actin cytoskeleton in *Saccharomyces cerevisiae*. *Mol. Biol. Cell* **9**, 1221–1233 (1998).
49. Knechtle, P., Dietrich, F. & Philippsen, P. Maximal polar growth depends on the polarisome component AgSpa2 in the filamentous fungus *A. gossypii*. *Mol. Biol. Cell* **14**, 4140–4154 (2004).
50. Sagot, I., Klee, S. K. & Pellman, D. Yeast formins regulate cell polarity by controlling the assembly of actin cables. *Nature Cell Biol.* **4**, 42–50 (2002).
51. Dong, Y., Pruyne, D. & Bretscher, A. Formin-dependent actin assembly is regulated by distinct modes of Rho signaling in yeast. *J. Cell Biol.* **161**, 1081–1092 (2003).
52. Li, R. Bee1, a yeast protein with homology to Wiscott–Aldrich syndrome protein, is critical for the assembly of cortical actin cytoskeleton. *J. Cell Biol.* **136**, 649–658 (1997).
53. Walther, A. & Wendland, J. Polarized hyphal growth in *Candida albicans* requires the Wiskott–Aldrich syndrome protein homolog Wal1p. *Euk. Cell* **3**, 471–482 (2004).
54. Walther, A. & Wendland, J. Septation and cytokinesis in fungi. *Fungal Genet. Biol.* **40**, 187–196 (2003).
55. Kadota, J., Yamamoto, T., Yoshiuchi, S., Bi, E. & Tanaka, K. Septin ring assembly requires concerted action of polarisome components, a PAK kinase Cla4p, and the actin cytoskeleton in *Saccharomyces cerevisiae*. *Mol. Biol. Cell* **15**, 5329–5345 (2004).
56. Longtine, M. S. *et al.* The septins: roles in cytokinesis and other processes. *Curr. Opin. Cell Biol.* **8**, 106–119 (1996).
57. Wendland, J. Analysis of the landmark protein Bud3 of *Ashbya gossypii* reveals a novel role in septum construction. *EMBO Rep.* **4**, 200–204 (2003).
This study demonstrates different roles for Bud3 homologues in *S. cerevisiae* and *A. gossypii*.
58. Wendland, J. & Philippsen, P. An IQGAP-related protein, encoded by *AgCYK1*, is required for septation in the filamentous fungus *Ashbya gossypii*. *Fungal Genet. Biol.* **37**, 81–88 (2002).
59. Osman, M. A., Konopka, J. B. & Cerione, R. A. Iqg1p links spatial and secretion landmarks to polarity and cytokinesis. *J. Cell Biol.* **159**, 601–611 (2002).
60. Dobbelaere, J. & Barral, Y. Spatial coordination of cytokinetic events by compartmentalization of the cell cortex. *Science* **305**, 393–396 (2004).
61. Dietrich, F.S. *et al.* The *Ashbya gossypii* genome as a tool for mapping the ancient *Saccharomyces cerevisiae* genome. *Science* **304**, 304–307 (2004).
62. Brachat, S. *et al.* Reinvestigation of the *Saccharomyces cerevisiae* genome annotation by comparison to the genome of a related fungus: *Ashbya gossypii*. *Genome Biol.* **4**, R45 (2003).
63. Kellis, M., Birren, B. W. & Landers, E. S. Proof and evolutionary analysis of ancient genome duplication in the yeast *Saccharomyces cerevisiae*. *Nature* **428**, 617–624 (2004).
64. Colman-Lerner, A., Chin, T. E. & Brent, R. Yeast Cbk1 and Mob2 activate daughter-specific genetic programs to induce asymmetric cell fates. *Cell* **107**, 739–750 (2001).
65. Takaya, N., Yamazaki, D., Horiuchi, H., Ohta, A. & Takagi, M. Cloning and characterization of a chitinase-encoding gene (chiA) from *Aspergillus nidulans*, disruption of which decreases germination frequency and hyphal growth. *Biosci. Biotechnol. Biochem.* **62**, 60–65 (1998).
66. Baggett, J. J., D'Aquino, K. E. & Wendland, B. The Sla2p talin domain plays a role in endocytosis in *Saccharomyces cerevisiae*. *Genetics* **165**, 1661–1674 (2003).
67. Gourlay, C. W. *et al.* An interaction between Sla1p and Sla2p plays a role in regulating actin dynamics and endocytosis in budding yeast. *J. Cell Sci.* **116**, 2551–2564 (2003).
68. Butler, G. *et al.* Evolution of the *MAT* locus and its Ho endonuclease in yeast species. *Proc. Natl Acad. Sci. USA* **101**, 1632–1637 (2004).
69. Seo, J. A., Han, K. H. & Yu, J. H. The gprA and gprB genes encode putative G protein-coupled receptors required for self-fertilization in *A. nidulans*. *Mol. Microbiol.* **53**, 1611–1623 (2004).
70. Altmann-Johl, R. & Philippsen, P. *AgTHR4*, a new selection marker for transformation of the filamentous fungus *Ashbya gossypii*, maps in a four-gene cluster that is conserved between *A. gossypii* and *Saccharomyces cerevisiae*. *Mol. Gen. Genet.* **250**, 69–80 (1996).
71. Wendland, J. *Eigenschaften linearer und zirkulärer DNA–Moleküle im filamentösen Pilz* Ashbya gossypii. Diploma thesis, Univ. Giessen, Germany (1993).

Acknowledgements

The authors would like to thank the members of the Wendland and Philippsen labs for stimulating discussions. Research on *A. gossypii* in J.W.'s laboratory is supported by the Deutsche Forschungsgemeinschaft.

Competing interests statement

The authors declare no competing financial interests.

Online links

FURTHER INFORMATION

Jürgen Wendland's laboratory: http://pinguin.biologie.uni-jena.de/phytopathologie/pathogenepilze/index.html
***A. gossypii* genome:** http://data.cgt.duke.edu/ashbya
***A. gossypii* Genome Database:** http://agd.unibas.ch
***Saccharomyces* Genome Database:** http://www.yeastgenome.org
Access to this interactive links box is free online.

2

Andrea Walther

Jürgen Wendland

Apical localization of actin patches and vacuolar dynamics in *Ashbya gossypii* depend on the WASP-homolog Wal1p.

J Cell Sci., 117: 4947-4958.

Durch die Analyse des *A. gossypii* Wal1p konnte dessen Funktion für die Aufrechterhaltung polaren Hyphenwachstums über die Koordinierung kortikaler Aktinpatches aufgezeigt werden. Die Deletion von *WAL1* führte zu Defekten in der Endozytose und der Verteilung von Endosomen entlang der Hyphe.

Apical localization of actin patches and vacuolar dynamics in *Ashbya gossypii* depend on the WASP homolog Wal1p

Andrea Walther and Jürgen Wendland*

Junior Research Group: Growth-control of Fungal Pathogens, Hans-Knöll Institute for Natural Products Research and Department of Microbiology, Friedrich-Schiller University, Hans-Knöll Strasse 2, 07745 Jena, Germany

*Author for correspondence (e-mail: juergen.wendland@uni-jena.de)

Accepted 24 June 2004
Journal of Cell Science 117, 4947-4958 Published by The Company of Biologists 2004
doi:10.1242/jcs.01377

Summary

Analysis of the *Ashbya gossypii* Wiskott-Aldrich syndrome-like gene *AgWAL1* indicates that it is required for the maintenance of polarized hyphal growth. Growth and organelle dynamics of the wild type and of *wal1* and other mutant strains were monitored by in vivo (fluorescence) time-lapse microscopy. Loss of *WAL1* led to slow growth and defects in polarized growth that produced swellings in subapical regions, whereas formation of hyphal tips and dichotomous tip branching occurred as in the wild-type. Few actin cables in *Agwal1* cells were found to insert into the hyphal tip, but specific clustering of cortical actin patches was observed in subapical regions of hyphal tips instead of at the hyphal apex. Distribution and movement of vacuoles was observed in vivo using FM4-64. In the wild type and in the slowly growing mutant strains *bem2* and *cla4*, which lack a Rho-GTPase-activating protein and a PAK kinase, respectively, early endosomes appeared in the hyphal tip, whereas very few early endosomes and small vacuoles were found in the *wal1* mutant hyphal tips, thus linking the cortical patch defect of *wal1* hyphae with the distribution of endosomes. Vivid movement of vacuoles seen in the wild type and in the *bem2* mutant in subapical regions was largely reduced in the *wal1* and *cla4* mutants. The tubular structure of mitochondria (as visualized by DIOC6 in vivo) was similar in the wild type and the *wal1* mutant, although *wal1* mitochondria appeared to be larger. Interestingly, mitochondria were found to insert into the hyphal tips in both strains. Our results indicate a function for Wal1p in filamentous fungi in coordinating actin patch distribution with polarized hyphal tip growth.

Supplementary material available online at http://jcs.biologists.org/cgi/content/full/117/21/4947/DC1

Key words: Wiscott-Aldrich syndrome Protein, Cytoskeleton, Morphogenesis, Polar growth, Endocytosis

Introduction

The dynamic reorganization of the actin cytoskeleton is essential for cell polarization, morphogenesis, the distribution of organelles and cytokinesis (Drubin and Nelson, 1996). Elaborate mechanisms ensure temporal and spatial control of these events and require a network of proteins that includes Rho-GTPase modules as central regulators of the actin cytoskeleton (Schmidt and Hall, 1998; Wendland, 2001; Etienne-Manneville and Hall, 2002). In the yeast *Saccharomyces cerevisiae* and the filamentous fungus *Ashbya gossypii*, homologs of the Rho-GTPase Cdc42p and its guanine-nucleotide exchange factor Cdc24 have been shown to be required for the establishment of a polarized cortical actin cytoskeleton that is a prerequisite for bud emergence in yeast and the formation of new hyphal tips in *A. gossypii* (Johnson, 1999; Wendland and Philippsen, 2001). Rho-GTPases relay spatial and temporal information to effector proteins and are thus able to integrate multiple signalling inputs with the state of actin cytoskeletal organization (Schmidt and Hall, 1998). Among these effectors are multidomain adaptor proteins, such as members of the Formin, PAK (p21-activated kinase) and WASP (Wiskott-Aldrich syndrome protein) families, that can act as scaffolds (Frazier and Field, 1997; Ramesh et al., 1999; Mullins, 2000; Pollard et al., 2001; Sharpless and Harris, 2002; Wild et al., 2004). The *S. cerevisiae* formin Bni1p, which is activated by Cdc42p, has recently been shown to play a central role in the nucleation of actin cables, which is achieved in an Arp2/3 independent manner (Evangelista et al., 2002; Pruyne et al., 2002; Sagot et al., 2002; Evangelista et al., 2003).

WASP family members are conserved from fungi to humans and are built in a modular fashion. They bind to components of the Arp2/3 complex and actin monomers via C-terminal WH2/C/A (WASP-homology-2/central/acidic) domains and activate actin nucleation (Machesky and Insall, 1998; Machesky et al., 1999; Madania et al., 1999; Rohatgi et al., 1999; Winter et al., 1999; Prehoda et al., 2000). Mammalian WASPs carry a GTPase-binding domain that allows direct interaction with Cdc42p. Such a domain is missing from members of the SCAR (suppressor of cAMP receptor) subgroup as well as from all known fungal WASP family members. In the N-terminal part, WASP family members share a WH1/pleckstrin-homology domain (lacking in SCAR proteins), which is involved in lipid binding, and a basic region (missing in Wsp1p of *Schizosaccharomyces pombe*) (Lee et al.,

2000). Similar to WASP, which can link lipid (i.e. phosphatidylinositol-4,5-bisphosphate) signalling with the actin cytoskeleton, the PAK Cla4p in yeast can link lipid (in this case, via phosphatidylinositol-4-phosphate) and Cdc42p signalling (Rohatgi et al., 1999; Wild et al., 2004). The PAK-like kinase Cla4p in *A. gossypii* was found to be required for hyphal development and septation, and loss of *CLA4* led to a partial disorganization of apical actin patch clusters (Ayad-Durieux et al., 2000).

Secretion in hyphal-tip cells of filamentous fungi is highly polarized and growth of the hyphae is restricted to the tip. Cortical actin patches are clustered at the hyphal tips during the hyphal growth phase (Wendland, 2001). In the ectomycorrhizal basidiomycete *Suillus bovinus* and the dimorphic fungus *Candida albicans* during hyphal growth stages Cdc42p was found to be localized to hyphal tips, indicating that Cdc42p is not only required for hyphal tip formation but might also play a role during polarized hyphal growth (Gorfer et al., 2001; Hazan and Liu, 2002).

Mutations of *S. cerevisiae* genes belonging to the Arp2/3 complex or deletion of the *S. cerevisiae* WASP *LAS17*/*BEE1* led to a loss of cortical actin patch organization (Winter et al., 1997; Li, 1997). The yeast Las17/Bee1 protein acts as an activator of the Arp2/3 complex and is involved in endosome/vacuole motility (Winter et al., 1999; Yarar et al., 1999; Chang et al., 2003). N-WASP was also shown to promote the actin-dependent movement of endosomes and lysosomes in *Xenopus* eggs (Taunton et al., 2000). Although substantial progress has been made in the analysis of individual WASP-family-member domains, the cellular function of WASP homologs for polarized hyphal growth in filamentous fungi has so far not been elucidated. Recently, we could show that the WASP homolog of the dimorphic fungal pathogen *C. albicans* was required for hyphal growth. Yeast cells of *C. albicans* induced to form hyphae by serum at 37°C responded with an initial polar growth phase but failed to maintain polarized growth, which resulted in the formation of pseudohyphae, with true hyphae not being formed (Walther and Wendland, 2004). The *C. albicans* WASP mutant showed similar defects in the yeast stage to those of the *S. cerevisiae* WASP mutant, including aberrant localization of cortical actin patches in the mother cell during bud growth, endocytosis and the number of vacuoles per cell. Thus, the growth defects of the *C. albicans* WASP mutant resembled those also observed in a *C. albicans myo5* (encoding a type I myosin) mutant strain (Oberholzer et al., 2002).

We could not study defects during hyphal growth stages in the WASP mutant of *C. albicans* and so we aimed to isolate a WASP homologue and to characterize its mutant phenotypes in a true filamentous fungus. Deletion of *AgWAL1* led to severely reduced polar hyphal growth rates, increased isotropic growth and defects in septation. Cortical actin patches that cluster in hyphal tips of the wild type were found to accumulate specifically in subapical regions in the *wal1* mutant, whereas few actin cables inserted into the hyphal apex. In the *A. gossypii* wild type, a redirection of cytoplasmic streaming and vacuolar movement occurred towards newly growing hyphal tips. Loss of *WAL1* led to severely decreased vacuolar movement in subapical hyphal sections, which was also observed in a *cla4* mutant. Furthermore, *wal1* hyphal tips not only showed an exclusion of cortical actin patches but we also observed a lack of endosomal vesicles in the hyphal tips, suggesting a functional link between endocytosis and vacuole formation mediated by Wal1p in *A. gossypii*. Because mitochondria were positioned in the hyphal tips of both the wild type and the *wal1* mutant, specific mechanisms must exist in filamentous fungi to transport mitochondria and vacuoles to support polarized hyphal growth.

Materials and Methods

Strains and media

The *A. gossypii* wild-type strain ATCC10895 and a derivative thereof (*A. gossypii leu2, thr4*) were used. The *A. gossypii bem2* and *cla4* deletion strains have been described previously (Ayad-Durieux et al., 2000; Wendland and Philippsen, 2000). The *S. cerevisiae las17/bee1* deletion strains RLY157 (MAT**a** *ura3*-52 *his3-Δ200 leu2-3,112 lys2-801D bee1::LEU2*; kindly provided by R. Li, Harvard Medical School, Boston, MA), YMW171K (MAT**a** *las17::kanMX4, ade2-101, his3-200, leu2-1, lys2-801, trp1-63, ura3-52*), YMW172K (MATα *las17::kanMX4, ade2-101, his3-200, leu2-1, lys2-801, trp1-63, ura3-52*), and RH4207 (MAT**a** *las17::kanMX4, bar1::LYS2, ade2-101, his3-200, leu2-1, trp1-63, ura3-52*; kindly provided by B. Winsor, Institut de Biologie Moléculaire et Cellulaire, Strasbourg, France) were used for heterologous complementation experiments. Media were prepared as described previously (Wendland and Philippsen, 2001). *A. gossypii* strains were transformed by electroporation as described (Wendland et al., 2000). G418/geneticin was added to rich media for selection of antibiotic-resistant transformants at a final concentration of 200 μg ml^{-1}. Yeast cells were transformed according to the lithium-acetate procedure (Gietz et al., 1995). Yeast media were prepared as described (Wendland and Philippsen, 2001). The *Escherichia coli* strain DH5α served as host for plasmids.

Isolation of *AgWAL1*

AgWAL1 was isolated in a multicopy suppressor screen using the temperature sensitivity of the *las17/bee1* mutant yeast strains. Different plasmid libraries based on yeast episomal plasmids were used containing either *A. gossypii* or *S. cerevisiae* genomic DNA inserts. Transformed cells were plated on minimal medium plates and incubated for four days at 37°C, which is the restrictive temperature for *bee1/las17* cells. Several yeast transformants could be isolated. Total DNA was extracted from these colonies and transformed into *E. coli*. Plasmids were recovered and retransformed into the yeast strain RLY157 to verify their ability to enable growth of RLY157 at elevated temperature. This resulted in the isolation of five independent plasmids from a CEN-ARS based *S. cerevisiae* plasmid library and one plasmid from a YEp352-based *A. gossypii* plasmid library (kindly provided by P. Stahmann, Fachhochschule Lausitz, Senftenberg, Germany), termed pST-WAL1. The complete double strand sequence of the *A. gossypii* DNA insert as well as the terminal sequences of the yeast DNA inserts were determined (MWG Biotech, Ebersberg, Germany). The GenBank accession number for *A. gossypii WAL1* gene is AY144115.

Construction of plasmids

A plasmid clone, pWAL1cc, containing the complete *AgWAL1* gene was constructed by ligating a 3.5 kb *Sac*I fragment of pST-WAL1 into the *Sac*I site of pRS415. Plasmid pWAL1-XL was constructed making use of the in vivo recombination machinery of *S. cerevisiae* (Wendland, 2003). To this end, a polymerase chain reaction (PCR) fragment containing the complete *AgWAL1* open reading frame (ORF) was amplified from pST-WAL1 using the primers XL1-WAL1, 5′-TCTTGCTAGGATACAGTTCTCACATCACATCCGAACATAA-ACAACCATGGGTCTTCTAACGGCGGAAGAC-3′, and XL2-WAL1, 5′-ATGACAAGTTCTTGAAAACAAGAATCTTTTTATT-

GTCAGTACTGATCACCAATCATCAGCATTGTCATCG-3′. This PCR fragment contains terminal homology regions to the *AgTEF1* promoter and terminator to direct homologous recombination. Plasmid pRS415-kanMX is a yeast CEN-ARS plasmid that carries the kanMX selectable marker, which consists of the kanamycin resistance ORF (*kan*) under control of the *AgTEF1* promoter and terminator sequences. pRS415-kanMX was linearized using *Nru*I, which cleaves a unique site within the *kan* ORF. This linearized plasmid cannot be propagated in yeast because *S. cerevisiae* cannot reseal blunt-end DNA breaks. Linearized plasmid and the *AgWAL1* PCR product were co-transformed into yeast. By means of homologous recombination between the linearized plasmid and the PCR product, a new plasmid was generated, pAgWAL1-XL, in which the *AgWAL1* ORF is fused to the *AgTEF1* promoter and terminator. Correct integration was verified by sequencing.

Gene disruption and complementation

Insertion and deletion of *AgWAL1* were performed via PCR-generated *GEN3* disruption cassettes as described previously (Wendland et al., 2000). The following primers were used for the generation of the disruption cassettes: S1-WAL1 (5′-TTAAGCGGGCAATTCCCA-AAGCATCGAACAAGATTATAGATGTTGGCTAGGGATAACAG-GGTAATACAG-3′) and S2-WAL1 (5′-CTCTTGCAGGAGGACCG-ATGGCTTGTCCAATTGAGACTTGTCAACCTAGGCATGCAAG-CTTAGATCT-3′). Disruption of *AgWAL1* was verified by PCR using primers G1-WAL1 (5′-CGCGGATCCGTGTATACGCATATTACCT-GACGCAC-3′), G2 (5′-GTTTAGTCTGACCATC-3′), G3 (5′-TCG-CAGACCGATACCA-3′) and G4-WAL1 (5′-CGCGGATCCGAGC-GTGGGAAAGATCTGGGCGTCG-3′). Primary transformants of *A. gossypii* are heterokaryotic (i.e. mycelia with multinucleate hyphal segments carry two kinds of nuclei with either wild-type or mutant alleles). Sporulation yielded homokaryotic null mutants, which allowed phenotypic analyses of the mutant strains. The *Agwal1* mutant phenotype was complemented by plasmids carrying *AgWAL1*.

Cytological techniques

Septa were stained using calcofluor (0.1 μg ml^{-1}), with cells either grown in liquid rich medium or on slides covered with thin layers of rich medium, as described previously (Wendland and Philippsen, 2000). Actin was stained from exponentially growing cultures. Cells were fixed in formaldehyde (3.7%) and PBS, and stained with rhodamine-phalloidin (Molecular Probes, Leiden, The Netherlands) as described elsewhere (Oberholzer et al., 2002). Endocytosis was visualized using the vital dye FM4-64 (Molecular Probes). Strains were grown to exponential phase in liquid full medium, harvested and incubated with 2 μM FM4-64. Mitochondria were stained using DIOC6 (Molecular Probes). Cells were mounted on deep-well microscopy slides and then either used directly for microscopy to allow the analysis of early endocytosis or incubated with the dye for up to 16 hours before microscopic observation. Fluorescence microscopy was done on a fully motorized Zeiss AxioplanII imaging microscope with the appropriate filter combinations for each dye (Chroma Technology, Rockingham, VT). Images were taken using a digital video imaging system (Princeton Instruments (Roper Scientific), Trenton, NJ, USA) as described previously (Wendland and Philippsen, 2002).

Time-lapse microscopy

Strains were grown in either complete or minimal medium. Microscopy slides were prepared as follows. Deep-well slides were used and filled with 100 μl of YPD agar medium each, containing FM4-64 when required. This medium was heavily vortexed to increase the oxygen content. The deep well was then covered with an extra slide to generate an even surface; once the agar had solidified, the cover was removed, cells were applied and the well sealed with a coverslip. Microscopy was carried out at 26°C. Images were acquired in a fully automated fashion (2.5 second or 60 second intervals for FM4-64 or DIOC6 time-lapse, and 180 seconds for differential interference contrast (DIC) or Nomarski time-lapse series), collected into stacks and processed as video clips with a frame rate of 10 images per second using Metamorph Software (Universal Imaging Corporation, Downingtown, PA, USA).

Results

Isolation and protein comparison of fungal WASP homologues

A multicopy suppressor screen was performed on *bee1/las17* mutant yeast strains based on their temperature sensitivity and growth arrest at 37°C with the aim of isolating either extragenic suppressors or the WASP homologue of a filamentous fungus. With an *S. cerevisiae* genomic library, five plasmids were isolated containing different but overlapping inserts bearing in common the *S. cerevisiae LAS17/BEE1* gene. No other isolate was obtained. Using an *A. gossypii* genomic 2μ-ARS plasmid library, a single plasmid was obtained several times. Sequencing of the insert revealed the presence of an *A. gossypii* WASP homologue, *AgWAL1* (Wiskott-Aldrich syndrome like protein) and adjacent genes. Comparison of the *A. gossypii WAL1* locus with *S. cerevisiae* showed syntenic arrangements to two *S. cerevisiae* loci on chromosomes XII and XV, which is an indication of ancient synteny potentially revealing the gene order in a common ancestor that was altered in yeast after its apparent genome duplication but retained in *A. gossypii*. Interestingly, homologues of two *S. cerevisiae* genes located on different chromosomes (XII and XV) that are positioned next to each other in *A. gossypii*, *WAL1* and the *A. gossypii* homologue of YLR287c, are also neighbours in *Candida albicans* (see Fig. S1 in supplementary material).

The *AgWAL1* locus represents the only WASP homologue of *A. gossypii* that could be determined by examination of the complete *A. gossypii* genome sequence. *AgWAL1* (AGR285w) encodes a protein of 732 amino acids and is located on chromosome VII (Dietrich et al., 2004). The highest degree of amino acids sequence identity is found with the *S. cerevisiae* Las17/Bee1 protein (43%). Comparison of the specific WASP domains of Wal1p with WASP homologues from ascomycete fungi revealed conserved N-terminal WH1 (>65% amino acids sequence identity) and C-terminal VCA (43% and 56% amino acid sequence identity between *A. gossypii* and *C. albicans* or *A. gossypii* and *S. cerevisiae*, respectively) domains with a variable central proline-rich region (for a protein alignment, see Fig. S2 in supplementary material). Other fungal species whose genomes have been sequenced (e.g. *Neurospora crassa*, *Aspergillus nidulans*, *Magnaporthe grisea* and *Ustilago maydis*) also contain a unique WASP homologue. Although the WASPs of the filamentous fungi *N. crassa*, *A. nidulans* and *M. grisea* group together in phylogenetic tree analyses, the *A. gossypii* WASP forms a group with the WASPs of *S. cerevisiae* and *C. albicans* (not shown).

Disruption of *AgWAL1* results in temperature-sensitive growth inhibition

Disruption of *AgWAL1* was achieved by PCR-based gene targeting. Deletion resulted in the removal of 87% of the

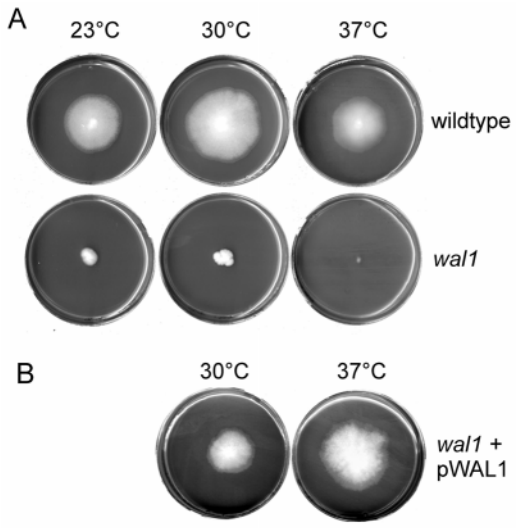

Fig. 1. Growth assay of wild-type and mutant strains. (A) Wild-type and *wal1* mutant were grown on YPD plates at the indicated temperatures for 5 days before photography. Optimal growth conditions are at 30°C. Loss of *WAL1* results in slow growth and temperature sensitivity (no growth) at elevated temperatures. (B) This temperature-sensitive phenotype can be complemented by introduction of a plasmid bearing the complete *WAL1* gene (pWAL1cc) at 37°C. Complementation with plasmid-borne *WAL1* at lower temperatures (30°C) results in increased growth of the mutant. However, owing to lack of selective pressure to maintain the plasmid growth rate is slower than in the wild type.

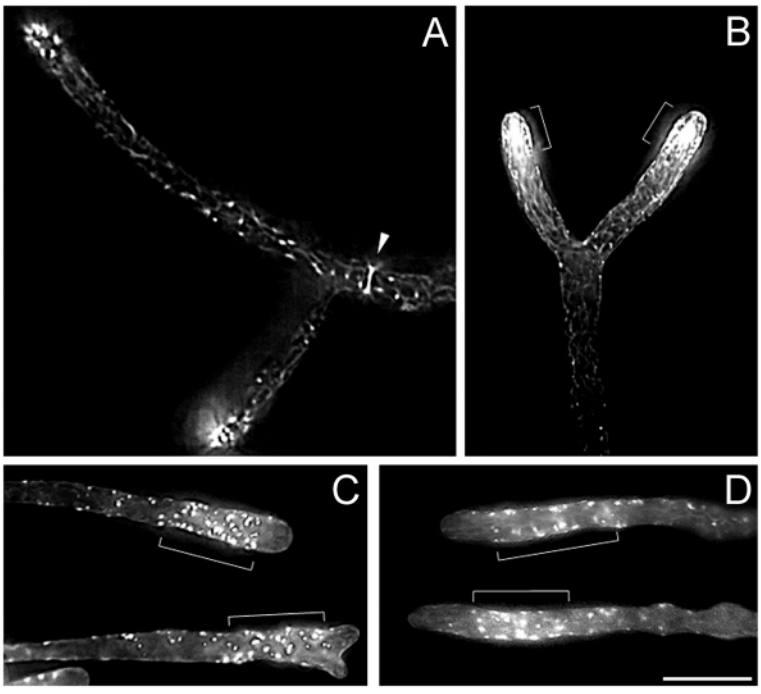

Fig. 2. Comparison of actin cytoskeletal organization in the wild type and in the *wal1* mutant. Representative fluorescent images are shown of hyphae stained with rhodamine-phalloidin of the wild type (A,B) and the *wal1* mutant (C,D). Small brackets mark the concentration of cortical actin patches in the hyphal tip of the wild type (A,B). Larger brackets point to the subapical region, where patches accumulate in *wal1* hyphae (C,D). Scale bar, 10 μm.

AgWAL1 ORF, thus generating a null allele (see Fig. S3 in supplementary material). Correct construction of the deletion was verified by PCR using standard verification primers. Primary transformants were wild-type-like in morphology owing to the heterokaryotic nature of the multinucleate hyphal compartments. Upon sporulation and clonal selection of mycelia containing only transformed *Agwal1* mutant nuclei, a slow-growth phenotype became evident. Furthermore, growth of *Agwal1* mutants at elevated temperature (above 35°C) was completely abolished (Fig. 1A). This temperature-sensitive growth inhibition could be rescued by reintroduction of plasmid-borne *AgWAL1* (Fig. 1B). Complementation with plasmid pWAL1cc, which contains only the *WAL1* gene, demonstrated that the mutant phenotype was due solely to the disruption of the genomic copy of *WAL1*. Heterologous complementation of the *S. cerevisiae bee1/las17* defect with *WAL1* was dependent on the high copy number of plasmid pST-WAL1 (containing a 2μ-ARS), because pWAL1cc (containing a yeast centromere and *ARSH4*) did not restore growth of the *bee1/las17* strain at elevated temperature.

Agwal1 mutant reveals defects in the organization of the actin cytoskeleton.

During the polarized hyphal growth phase in *A. gossypii* wild-type hyphae cortical actin patches are concentrated in the hyphal tips (Fig. 2A,B). Defects in the organization of the actin cytoskeleton can be observed as isotropic growth phases and swollen hyphal morphologies and result in slow growth phenotypes as was shown for *Agrho3* and *Agbem2* mutants (Wendland and Philippsen, 2000; Wendland and Philippsen, 2001). Therefore, we analysed the distribution of the cortical actin cytoskeleton in the *Agwal1* mutant (Fig. 2C,D). Localization of some of the cortical actin patches along the hyphae occurred in both wild-type and *wal1* hyphae. Clustering of cortical actin patches in the hyphal tips, as found in the wild type, did not occur in *wal1* hyphal tips (n=500 for each strain). Instead, cortical actin patches characteristically accumulated in subapical regions of *wal1* hyphal tips, which was never observed in the wild type (Fig. 2). In the wild type, actin cables formed an abundant meshwork of cables that was tip directed in the hyphal apex. In the *wal1* mutant, some actin cables were found to insert into the hyphal tip even when the tip did not contain any obvious cortical actin patches (Fig. 2C,D). Rhodamine-phalloidin staining also revealed the absence of actin rings at presumptive septal sites that can readily be found in wild-type hyphae. The presence and correct positioning of actin rings are, however, prerequisites for septation and chitin-ring formation in *A. gossypii* (Wendland and Philippsen, 2002). To explore this in more detail, we stained wild-type and mutant hyphae with calcofluor to analyse the distribution of chitin in the cell wall.

Agwal1 mutants show defects in septation

Wild-type hyphae are tube-like and form septa in regular intervals. Chitin is accumulated at these septal

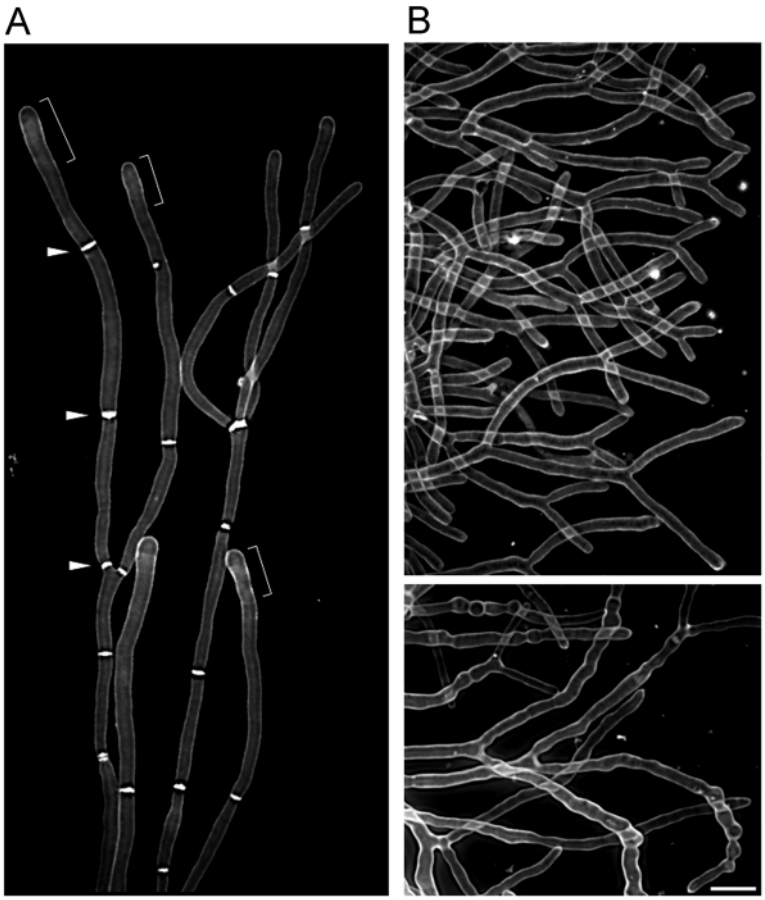

Fig. 3. Loss of *WAL1* leads to increased isotropic growth and defects in septation. (A) Wild-type hyphae showed accumulation of chitin at septal sites (arrowheads) and more intensely stained hyphal apices (brackets). (B,C) The *wal1* hyphae were stained uniformly and rarely displayed chitin-rich septa. Notice the swellings of *wal1* hyphae and the short distance between consecutive dichotomous tip branches. Staining was done using calcofluor. Scale bar, 20 μm.

sites and forms chitin rings. Furthermore, hyphal tips can be stained more brightly by calcofluor than subapical regions, indicating sites of active secretion (Fig. 3A). By contrast, hyphae of the *wal1* mutant are wider than wild-type hyphae, irregular in shape and periodically swollen. Mutant hyphal cell walls were stained uniformly by calcofluor, corresponding to delocalized cell surface growth and the bulbous hyphal shape. As was suggested by the absence of actin rings at presumptive septal sites, chitin rings were only rarely observed in the mutant hyphae (n=200), indicating a severe defect in septation (Fig. 3B). This corresponds to observations in the *Agcyk1* and *Agcla4* mutants, in which the failure to form actin rings at presumptive septal sites has been shown to be accompanied by lack of chitin accumulation (Ayad-Durieux et al., 2000; Wendland and Philippsen, 2002). Formation of sporangia depends on septation. Thus, lack of septa (as in the *Agcyk1* mutant) also resulted in the absence of sporulation in the *Agwal1* mutant (not shown).

Agwal1 mutants exhibit defects in the maintenance of polarized hyphal growth

To understand the growth defects of the *Agwal1* mutant more clearly, we compared growth of the mutant strain with the wild type using in vivo time-lapse microscopy. First, we characterized growth of the wild type. Juvenile mycelia, approximately 10 hours after inoculation of spores in complete medium, grew initially at a slow extension rate (Fig. 4A; see Movie 1 in supplementary material). Lateral branches were formed and strong vacuolarization of the hyphae was initiated about 6 hours later at the centre of the mycelium. At about this time, an increase in growth speed was observed and dichotomous tip branching occurred, which is a hallmark of colony maturation in *A. gossypii* (Wendland and Philippsen, 2000). Movie 1 also showed that some newly formed hyphal tips (n=7 in this movie) stopped hyphal elongation and became vacuolarized, and that cytoplasmic flow was redirected out of these hyphae to other growing ends (Fig. 4A, arrowheads). Additionally, growth was found to be terminated in some instances upon contact of a hyphal tip with other hyphae that blocked further elongation (n=4 in this movie), which also resulted in vacuolarization and redirection of cytoplasmic streaming (Fig. 4A, asterisks). Spore germination of the *Agwal1* mutant, in contrast to wild-type hyphae, was found not to result in the characteristic bipolar branching pattern (n=100), which, in the wild type, leads to the generation of two germ tubes at opposite ends of the germ cell (Fig. 4). Most often a second hyphal tube was produced directly adjacent to the first hypha. Growth of the mutant hyphae was very slow (Fig. 4B; see Movie 2 in supplementary material). Under time-lapse growth conditions mutant hyphae often stopped growing and hyphal cells lysed, which made it difficult to obtain time-lapse movies at this early stage of growth from the *wal1* mutant. Germination of heterokaryotic spores under selective conditions that favoured growth of only the *wal1* mutant in liquid culture revealed similar defects in the bipolar germination pattern (n=200).

In adult stages, hyphal growth rate of the wild type was accelerated (at least tenfold) upon hyphal maturation and reached on average 170 μm hour^{-1} (Fig. 5; see Movie 3 in supplementary material). The appearance of many vacuoles in adult wild-type hyphae occurred in subapical regions soon after hyphal tip growth. Using in vivo time-lapse microscopy, we were able to observe vacuolar movement (cytoplasmic streaming) in wild-type hyphae in the direction of the growing hyphal tip (Fig. 5; see Movies 1,3 in supplementary material). The speed of cytoplasmic streaming was dependent on the rate of tip growth. Interestingly, the direction of cytoplasmic streaming could also be influenced by septation. Once a septum had formed vacuoles could not pass across these sites (Fig. 5, asterisks; see Movie 3 in supplementary material). In the hypha shown, three consecutive septation events occurred. The first septum prevented backward flow of vacuoles. The second septum occurred at a dichotomous bifurcation and led to the direction of the vacuolar streaming into just the left branch. Finally, the third septum compartmentalized a hyphal segment

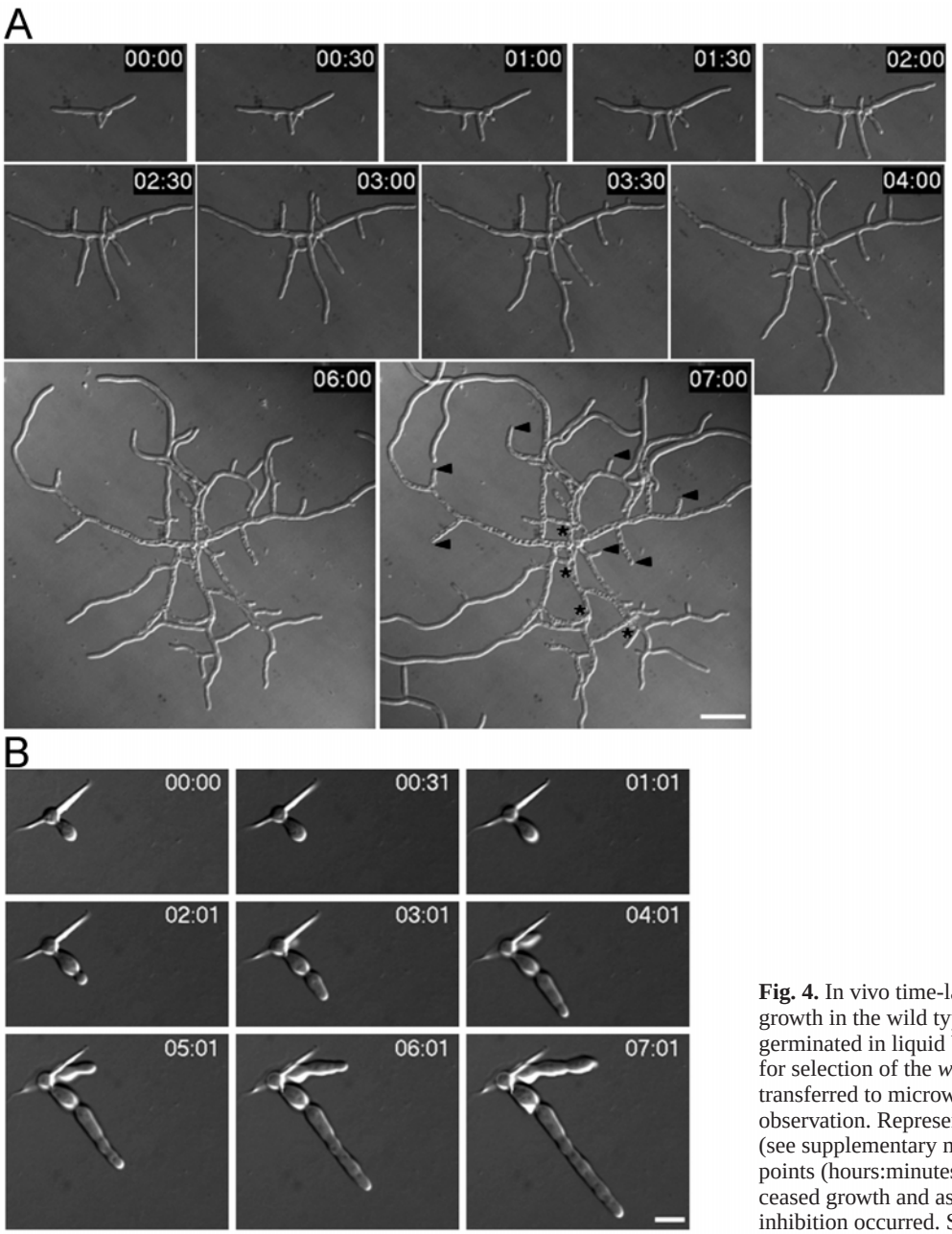

Fig. 4. In vivo time-lapse analysis of the early stages of growth in the wild type and the *wal1* mutant. Spores were germinated in liquid YPD or YPD supplemented with G418 for selection of the *wal1* mutant for 8 hours at 30°C and then transferred to microwell-containing slides for further observation. Representative frames from Movies 1 and 2 (see supplementary material) are shown at the indicated time points (hours:minutes). Arrowheads point to hyphal tips that ceased growth and asterisks mark positions where contact inhibition occurred. Scale bars, 40 μm (A), 20 μm (B).

and trapped the cytoplasm within. This also inhibited loss of cytoplasm out of this compartment. The septation event was soon followed by the formation of a new hyphal tip in this compartment (Fig. 5; see Movie 3 in supplementary material). Furthermore, retrograde flow was observed out of hyphae that stopped growing owing, for example, to contact inhibition (arrows indicate the direction of streaming in Fig. 5, whereas the arrowhead points to the relative positions of one of the large vacuoles).

In contrast to the wild type, mutant *Agwal1* hyphae reached radial growth rates of a maximum of only 15 μm hour^{-1} and were thus more than ten times slower than adult wild-type hyphae (Fig. 6; see Movie 4 in supplementary material). Nevertheless, growth direction was still highly polarized and dichotomous tip branching occurred in *Agwal1* hyphae. *Agwal1* mutant hyphae were filled with cytoplasm and only few vacuoles were visible that occurred very late during these in vivo observations (Fig. 7, bottom row). Cytoplasmic streaming can be seen in Movie 5 (see supplementary material) but streaming is not directed and vacuoles remain localized in the same hyphal segments in which they were formed, in contrast to the wild type. Interestingly, at several positions in subapical regions, swellings of hyphae occurred very rapidly (within 3 minutes; i.e. a single interval of image acquisition during the time-lapse analyses) (Fig. 6, boxes, left to right) and shown (top row to bottom row) as enlarged images in Fig. 7 (and see Movie 5 in supplementary material). The positions at which these swellings occurred might represent attempts of the hyphae to produce lateral branches.

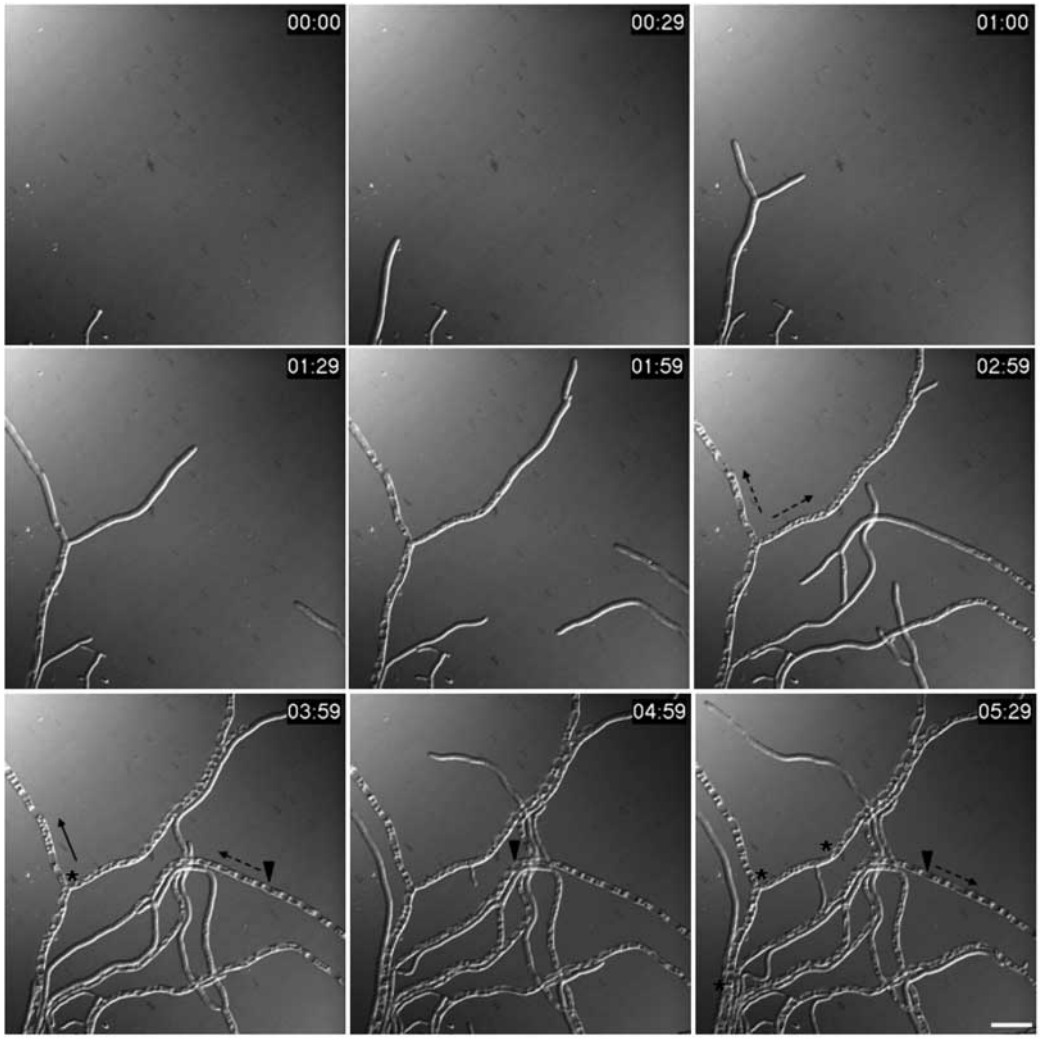

Fig. 5. In vivo time-lapse analysis of growth of adult stages of wild-type hyphae. Mycelium from exponentially grown liquid YPD cultures was transferred to slides and growth was monitored. Images represent frames from Movie 3 (see supplementary material) at the corresponding time points (hours:minutes). Septal sites are marked by asterisks. Cytoplasmic flow as visible by the movement of large vacuoles is indicated by arrows. Arrowheads mark the same vacuole at different time points. Septation alters the direction of flow and flow was also reversed in one hypha. Scale bar, 40 μm.

Organelle morphology and movement in *A. gossypii* wild-type and mutant strains

Wild-type hyphae showed rapid cytoplasmic streaming and vacuolar movement, in contrast to *wal1* hyphae, during our DIC observations. Because defects in polarized growth might be the result of defects in exo- or endocytosis, we examined and compared the vacuolar dynamics of different strains in vivo using the vital dye FM 4-64. In wild-type hyphal tips, fast-moving small vesicles (endosomes) were found. There were often tubular structures linking these vesicles with each other and resulting in fusion of vesicles (Fig. 8A; see Movie 6 in supplementary material). Staining of the wild-type endosomes was very efficient, resulting in bright fluorescent images. Staining of *wal1* hyphae was always more diffuse (Fig. 8B; see Movie 6 in supplementary material). Strikingly, whereas wild-type hyphae contained endosomes in the hyphal tips and, in subapical regions, had already fused these endosomes to smaller vacuoles, the *wal1* hyphal tips contained very few visible endosomal vesicles and thus appeared relatively empty (compare Fig. 8A,B; see Movie 6 in supplementary material). Other *A. gossypii* slow-growth mutants deficient in genes that are also involved in actin cytoskeleton dynamics had already been analysed (Ayad-Durieux et al., 2000; Wendland and Philippsen, 2000). We stained hyphae of these *cla4* and *bem2* mutants with FM4-64 to analyse whether early endosomes were present in the hyphal tips of these mutants. Both of these mutant strains contained endosomal vesicles in their hyphal tips that showed movement and tubular structures similar to the wild type (Fig. 8C,D; see Movies 8,9 in supplementary material). To compare the morphology of larger vacuoles of the different strains, we performed high resolution in vivo time-lapse analyses of older (non-growing) hyphal segments under the identical conditions, running for approximately 4:30 minutes with recordings every 2.5 seconds (Fig. 8E-H; see Movies 7-9 in supplementary material). In the wild type, large vacuoles showed rapid changes in shape, became elongated

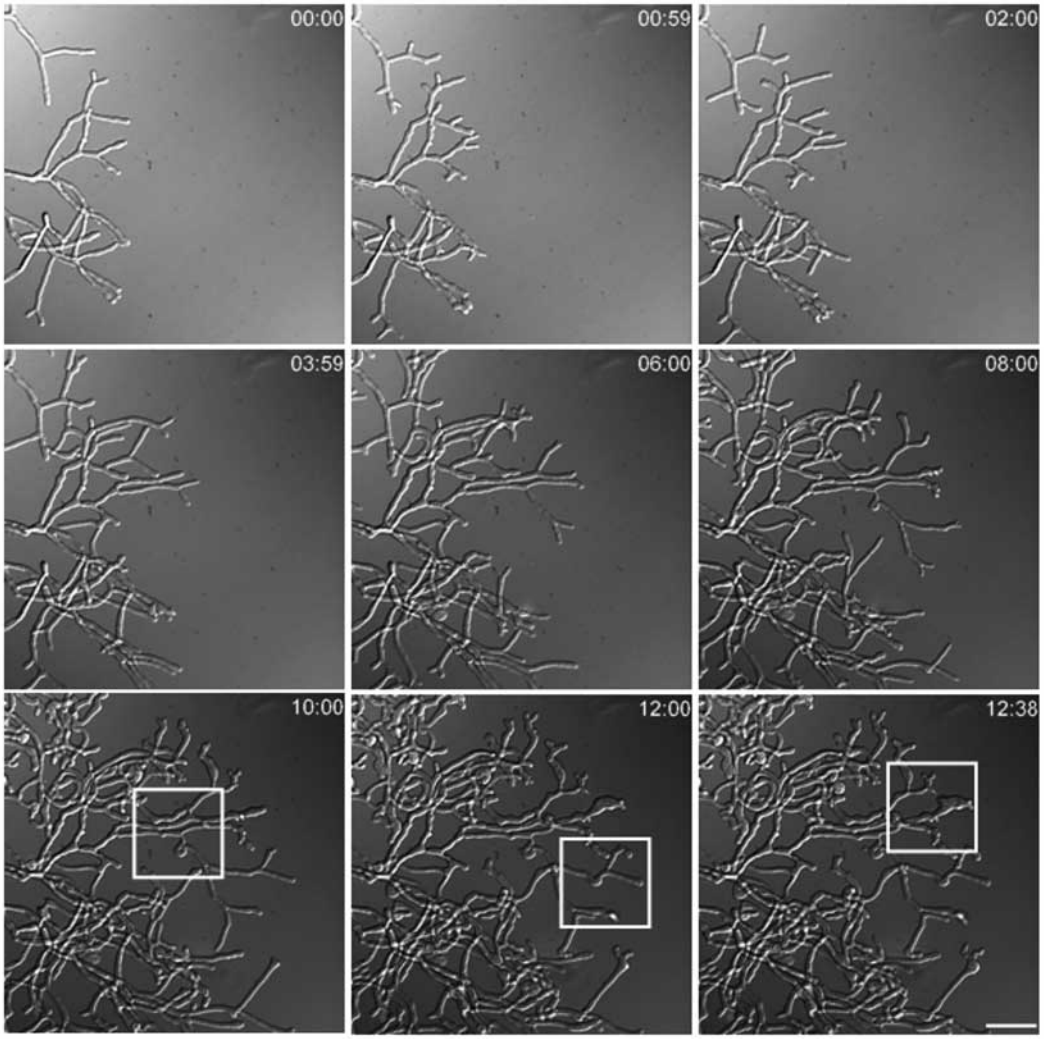

Fig. 6. In vivo time-lapse analysis of growth of adult stages of *wal1* hyphae. Mycelium from exponentially grown liquid YPD cultures was transferred to slides and growth was monitored. Images represent frames from Movie 4 (see supplementary material) at the corresponding time points (hours:minutes). Boxes indicate three regions processed for Fig. 7 and Movie 5 (see supplementary material). Scale bar, 40 μm.

and (in two instances) fusion events were observed. Interestingly, not all vacuoles seen in the wild-type panel of Movie 7 (see supplementary material) are in motion at the same time. In the middle of the movie, two vacuoles appeared to be moving at the same time, coming to a stop and thus appeared round in shape, and afterwards simultaneously initiated motion again. By contrast, the vacuoles on both sides (tipward and farther back) exhibit phases of motion and pausing independently of the vacuoles in the centre. In Movie 7 (see supplementary material), a *wal1* hypha is shown imaged under the same conditions as the wild type. Here, large vacuoles of the *wal1* hypha showed drastically reduced motion compared with the wild type. (Fig. 8E,F; see Movie 7 in supplementary material). Whereas large vacuoles in the *bem2* mutant readily changed shape, similar to the wild type, vacuoles of the *cla4* mutant were rounder and thus resembled more closely the vacuoles of *wal1* hyphae (Fig. 8G,H; see Movies 8,9 in supplementary material). Because these high-resolution recordings did not readily allow the analysis of vacuolar movement, we analysed wild-type and *wal1* hyphae in a time-lapse series over 3.0-4.5 hours with images taken at 1-minute intervals (see Movies 10,11 in supplementary material). In these movies, the generation and tipwards movement of large vacuoles was evident in the wild type. Hyphae of the *wal1* mutant grew much more slowly, did not contain endosomes in the hyphal tips, did not generate large vacuoles and displayed only oscillating, not tipwards, movement of vacuoles.

Because, in *S. cerevisiae*, several organelles are dependent on the actin cytoskeleton for movement, we also wanted to elucidate whether, like vacuolar movement, the motility of mitochondria was affected in the *wal1* mutant hyphae (Fig. 8I,J; see Movie 12 in supplementary material). To this end, we stained wild-type and *wal1* hyphae with the vital dye DIOC6 and recorded in vivo fluorescence time-lapse series. In the wild type, mitochondria showed tubular structures, localized to the hyphal tip and appeared to be very motile. Mitochondria in *wal1* hyphae appeared to be bigger than wild-type mitochondria. However, mitochondria in *wal1* hyphae showed a tubular structure and wild-type-like motility. Strikingly, in *wal1* hyphae mitochondria were localized along the hyphae

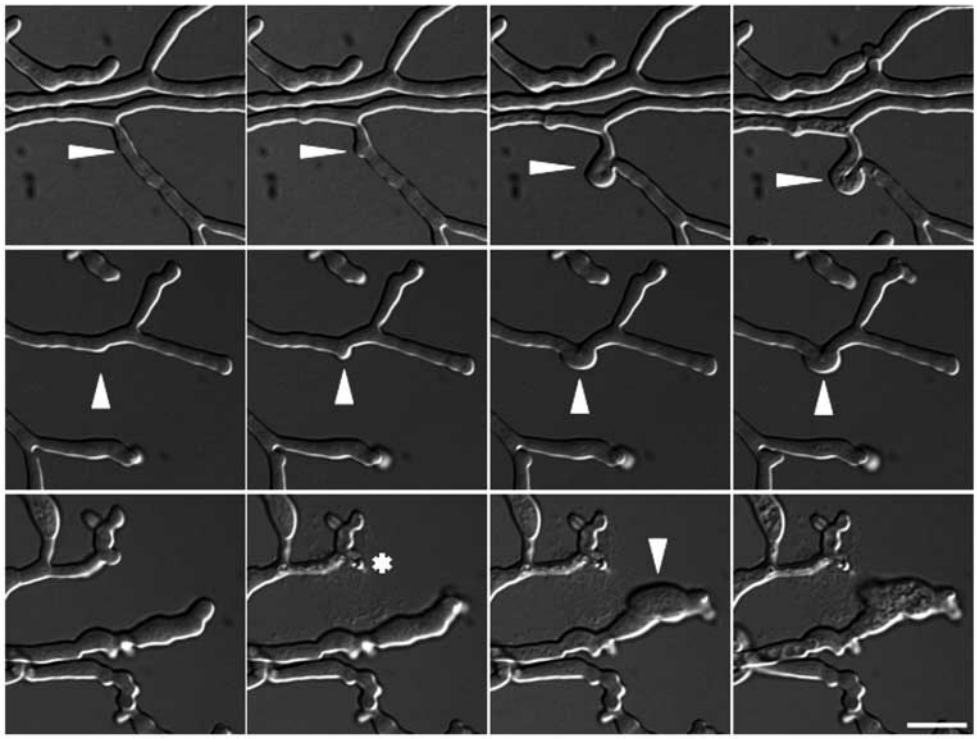

Fig. 7. Growth defect of subapical regions of *wal1* hyphae. Three rows represent boxed region in Fig. 6. Arrowheads point to subapical regions that result in aberrant swellings. The asterisk marks a hyphal tip that burst during the time-lapse imaging.

also including the hyphal tips. This finding is in sharp contrast to the distribution and movement of vacuoles in *wal1* hyphae.

Discussion

Members of the WASP family regulate a range of cellular processes that require dynamic reorganization of the actin cytoskeleton (Caron, 2002). The role of WASPs has been analysed in great detail in various organisms and a functional understanding has been gained towards the role of WASP in activating the Arp2/3 complex, resulting in the generation of branched actin filaments (Higgs and Pollard, 2001; Weaver et al., 2003). WASP is regulated by phosphorylation and autoinhibition by intramolecular contacts that can be relieved through binding to Cdc42p (Cory et al., 2003; Buck et al., 2004). Fungal WASPs are different from mammalian WASPs in this respect, because they lack a G-protein-binding domain. Consequently, the *S. cerevisiae* WASP Las17p/Bee1p was shown not to be autoinhibited but regulated by SH3-domain-containing proteins (Rodal et al., 2003).

Polarization of the actin cytoskeleton towards the hyphal tips is required for hyphal growth in filamentous fungi (Wendland, 2001). This results in the clustering of cortical actin patches at the hyphal tip and maintenance of polarized hyphal growth and tip-directed secretion in fungal hyphae (Momany, 2002). Previously, we have characterized the role of Rho-protein modules for polarized hyphal growth and the organization of the actin cytoskeleton in *A. gossypii* (Wendland and Philippsen, 2001). Because Rho-protein function is exerted via effector proteins, we are interested in elucidating the signalling route from Rho proteins to the actin cytoskeleton. In this effort, we recently analysed the *C. albicans* WASP homologue *WAL1* (Walther and Wendland, 2004). We observed similarities between the yeast stages of *C. albicans* and *S. cerevisiae* of WASP mutant strains that include a partially delocalized cortical actin cytoskeleton, defects in bud-site selection and endocytosis (Li, 1997; Walther and Wendland, 2004). Particularly, in the *C. albicans* WASP mutant, an increased number of vacuoles was found, suggesting a role in vacuole formation. *C. albicans* is a dimorphic fungus that can be induced to form true hyphae by, for example, the presence of serum at 37°C. The *C. albicans* WASP mutant, however, was not able to form hyphae under all laboratory conditions tested and thus we were not able to analyse hypha-specific defects in this organism. Therefore, we generated a WASP deletion mutant in the constitutively filamentous fungus *A. gossypii*.

Growth defects of the *A. gossypii wal1* mutant

The *Agwal1* mutant shows temperature-sensitive growth, which is completely abolished at elevated temperatures (e.g. 37°C). Polarized hyphal growth was drastically reduced in *wal1* hyphae, resembling growth rates of *bem2* and *cla4*. Cla4p was shown to be required for a process termed hyphal maturation (Ayad-Durieux et al., 2000). This describes the phenomenon that growth speed during mycelium formation is slow in juvenile mycelia and increases dramatically – in *A. gossypii* more then tenfold – in mature mycelia. The speed of polarized hyphal growth is dependent on the transport of secretory vesicles to the hyphal tip and the insertion of these vesicles into the membrane (Katz et al., 1972; Watters and Griffith, 2001). We found that fast polarized hyphal growth occurs at a time when large vacuoles are formed in subapical regions of hyphal filaments. With these vacuoles, transport processes in the direction of growing tips could be observed (see Movies 1,3 in supplementary material). Septation was found to block cytoplasmic streaming (corresponding to bulk tipwards organelle movement) resulting in a redirection of

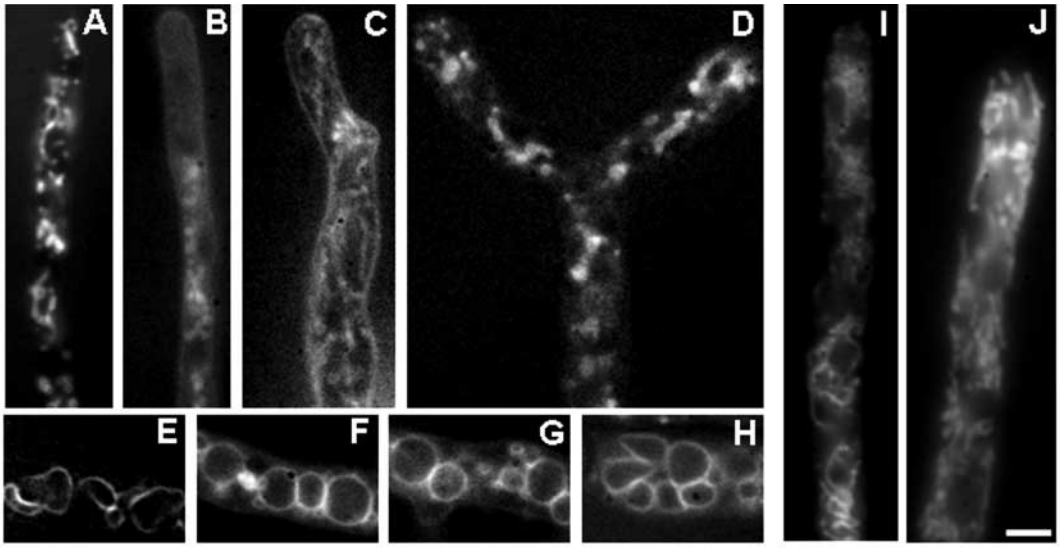

Fig. 8. Organelle distribution in *A. gossypii* wild-type and mutant strains. Vacuolar morphology of the wild type (A,E) and the *wal1* (B,F), *cla4* (C,G) and *bem2* (D,H) mutants was analysed at hyphal tip regions containing early endosomes (A-D) and in older hyphal segments that contained larger vacuoles (E-H) using the vacuolar dye FM4-64. Images are from Movies 6-9 (see supplementary material). Notice the tip localization and the presence of tubular structures of endosomes in the wild type and the *cla4* and *bem2* mutant strains, whereas *wal1* hyphal tips did not contain endocytic vesicles. Also, larger vacuoles of the wild type and the *bem2* mutant strain were highly motile over the imaged period, whereas *wal1* and *cla4* vacuoles appeared immobile. Mitochondria in wild-type (I) and *wal1* (J) hyphae were stained with DIOC6 (see Movie 12 in supplementary material).

transport (see Movie 3 in supplementary material). This was surprising given that nuclear migration through septal pores was frequently observed in *A. gossypii* (Alberti-Segui et al., 2000). Another surprising observation was retrograde flow of cytoplasm out of hyphae that stopped growing (e.g. owing to contact inhibition). This indicates that, in *A. gossypii*, polarized hyphal growth can serve as a sink for cellular components of subapical regions not compartmentalized by septation. In the *Agwal1* mutant, long-range transport of vacuoles was not evident in the time-lapse analyses. Large vacuoles were generated in *wal1* hyphae, although this process appeared to be delayed in comparison to the wild type. The process of vacuolar fusion might be of importance for polarized hyphal growth. In order to maintain rapid polarized growth, large amounts of cytoplasm need to be produced. This requirement could be lowered if rear parts of hyphal compartments were filled with large vacuoles. Therefore, defects in vacuolar fusion per se might affect polarized growth rates. *VAM4/YPT7* encodes a *S. cerevisiae* gene that is required for vacuole fusion (Wichmann et al., 1992). Deletion of the *VAM4/YPT7* homologue *avaA* in *A. nidulans*, however, was shown not to reduce the hyphal growth rate, although this mutant exhibited highly fragmented vacuoles (Ohsumi et al., 2002).

Septation defect of *Agwal1*

Deletion of *AgWAL1* resulted in a septation defect similar to that observed in *Agcla4* mutants: hyphae showed very few actin rings, and chitin accumulation at presumptive sites of septation was very rare. This is in contrast to the *S. cerevisiae bee1/las17* and the *C. albicans wal1* mutant strains, which did not show defects in cytokinesis and septum formation but rather showed increased rates of random budding (Madania et al., 1999; Walther and Wendland, 2004). The failure to form actin rings might be due to either the direct involvement of Wal1p in the polymerization of actin or the requirement for Wal1p in transport processes that are necessary to achieve polarized secretion to septal sites. Although many of the key players involved in septum formation in *S. cerevisiae* share homologues in filamentous fungi, our results indicate that there are mechanistic differences leading to septum formation between yeasts and filamentous fungi (Walther and Wendland, 2003). The *wal1* mutant strain was also found to be defective in sporulation. This corresponds to the sporulation defect of the aseptate *cyk1* strain (Wendland and Philippsen, 2002). In the wild-type strain, sporangia are formed by fragmentation of hyphae at septal sites. The failure to generate septa therefore results in the inability to produce sporangia and thus spores.

Wal1p plays a central role in the localization of cortical actin patches

Loss of *WAL1* resulted in the clustering of cortical actin patches in subapical parts of the hyphae, in contrast to the tipwards localization in the wild type. This represents a new actin cytoskeleton defect not previously observed in filamentous fungi. Delocalization of actin patches indicates that their presence in the hyphal tips is supporting polarized secretion and fast hyphal elongation that, in the *wal1* mutant, is now converted into more isotropic growth, resulting in widened diameters and swollen hyphae. Surprisingly, we found that a few actin cables were able to extend into hyphal tips even without the presence of actin patches (Fig. 2). This could be of mechanistic importance for the establishment and maintenance of polarized hyphal growth in filamentous fungi. In *S. cerevisiae*, Las17p/Bee1p is required for the activation of the

Arp2/3 complex and actin nucleation (Winter et al., 1999; Higgs and Pollard, 2001; Zalevsky et al., 2001). This activity might, however, be limited to the nucleation of branched filaments (Higgs and Pollard, 2001). By contrast, the formin family of proteins was shown to represent a class of actin nucleators that assemble straight filaments (Pruyne et al., 2002; Sagot et al., 2002). The *wal1* mutant phenotype displayed specific defects in the polarized localization of actin patches, whereas actin filaments were found to be tip localized in the absence of cortical patches in the tip. The reduced hyphal growth rate of *wal1* hyphae could therefore be the result of the basic activity provided by formin dependent assembly of actin filaments. This might occur in a Cdc42p-dependent manner, because *CDC42* was shown to be required for the establishment of cell polarity in *A. gossypii* (Wendland and Philippsen, 2001). In such a model, the polarity establishment machinery, involving the Cdc42p/Rho-protein module and formin effectors, is required for choosing a site of growth and polarizing the actin cable network to result in an initial growth phase. Subsequently, activation of WASP leads to the coordination of polarized secretion, the polarization of cortical actin patches, and long-range transport to the hyphal tip, which is a prerequisite of fast hyphal elongation. In *wal1* hyphae, slow growth might therefore be due to shortcomings in either the sufficient delivery of secretory vesicles to the tip or in defective exo- or endocytosis.

Nevertheless, in the *Agwal1* mutant, cortical actin patches were still generated and localization was clearly enriched in subapical parts of the hyphae. Other proteins that can activate actin assembly might be responsible for the generation of actin patches, such as *A. gossypii* homologues of the *S. cerevisiae ABP1* and *PAN1* genes. Currently, we do not know the mechanism for the accumulation of cortical actin patches at these specific subapical sites. However, localization of cortical actin patches to the hyphal tips requires Wal1p. Considering the protein domains of fungal WASPs, the N-terminal WH1/pleckstrin-homology domain can provide a link to plasma-membrane-associated lipids, specifically phosphatidylinositol-4,5-bisphosphate (Rohatgi et al., 1999). AgWal1p might act as a scaffold protein to coordinate the positioning of cortical actin patches with polarized morphogenesis by linking Rho-GTPase signalling with the ability to stimulate the Arp2/3 complex in combination with the use of lipids as positional information. Synergistic activation by lipid and Cdc42p signalling was shown for N-WASP and also the *S. cerevisiae* Cla4p, which thereby function as 'coincidence detectors' (Rohatgi et al., 1999; Wild et al., 2004).

Endocytosis and vacuolar fusion in *A. gossypii*

Loss of *WAL1* not only affected the localization of cortical actin patches but also resulted in defects in vacuolar morphology, positioning and movement. Strikingly, in *A. gossypii*, the tips of *wal1* hyphae were not only devoid of cortical actin patches but also lacking in endosomes. Both actin patches and endosomes formed in subapical parts of the hyphae. In *S. cerevisiae*, a tight association of actin clumps and endocytic vesicles was observed by inactivating Prk1p kinase using chemical genetics (Sekiya-Kawasaki et al., 2003). Transport of vacuoles in yeast is dependent on the actin cytoskeleton and type-V myosin motors (Weisman, 2003). Loss of *AgWAL1* might cripple the ability to generate actin filaments to provide tracks for vacuolar movement in the hyphae. A defect in vacuolar motility might therefore be a secondary consequence of the *wal1* mutation. In fact, the motility and directed movement of vacuoles in *wal1* hyphae was drastically reduced in comparison to the wild type. Whereas wild-type vacuoles displayed deformations and rapid shape changes, *wal1* vacuoles remained round and immobile, suggesting that relatively little motor-protein force influences these vacuoles. Our results further show that this phenotype of *wal1* hyphae is specific for vacuolar movement and distribution and does not affect the localization and movement of mitochondria.

We thank R. Li and B. Winsor for strains, and D. Schade for excellent technical assistance. This work was funded by grants of the Deutsche Forschungsgemeinschaft to JW (We2634/2-1) and by funds for the Research Group 'Fungal Pathogens' by the Friedrich-Schiller University and the Hans-Knöll Institute. GenBank accession number for *WAL1* is AY144115.

References

Alberti-Segui, C., Dietrich, F., Altmann-Johl, R., Hoepfner, D. and Philippsen, P. (2001). Cytoplasmic dynein is required to oppose the force that moves nuclei towards the hyphal tip in the filamentous ascomycete *Ashbya gossypii*. *J. Cell Sci.* **114**, 975-986.

Ayad-Durieux, Y., Knechtle, P., Goff, S., Dietrich, F. and Philippsen, P. (2000). A PAK-like protein kinase is required for maturation of young hyphae and septation in the filamentous ascomycete *Ashbya gossypii*. *J. Cell Sci.* **113**, 4563-4575.

Buck, M., Xu, W. and Rosen, M. K. (2004). A two-state allosteric model for autoinhibition rationalizes WASP signal integration and targeting. *J. Mol. Biol.* **338**, 271-285.

Caron, E. (2002). Regulation of Wiskott-Aldrich syndrome protein and related molecules. *Curr. Opin. Cell Biol.* **14**, 82-87.

Chang, F. S., Stefan, C. J. and Blumer, K. J. (2003). A WASP homolog powers actin polymerization-dependent motility of endosomes in vivo. *Curr. Biol.* **13**, 455-463.

Cory, G. O. C., Cramer, R., Blanchoin, L. and Ridley, A. J. (2003). Phosphorylation of the WASP-VCA domain increases its affinity for the Arp2/3 complex and enhances actin polymerization by WASP. *Mol. Cell* **11**, 1229-1239.

Dietrich, F. S., Voegeli, S., Brachat, S., Lerch, A., Gates, K., Steiner, S., Mohr, C., Poehlmann, R., Luedi, P., Choi, S. et al. (2004). The *Ashbya gossypii* genome as a tool for mapping the ancient *Saccharomyces cerevisiae* genome. *Science* **304**, 304-307.

Drubin, D. G. and Nelson, W. J. (1996). Origins of cell polarity. *Cell* **84**, 335-344.

Etienne-Manneville, S. and Hall, A. (2002). Rho GTPases in cell biology. *Nature* **420**, 629-635.

Evangelista, M., Pruyne, D., Amberg, D. C., Boone, C. and Bretscher, A. (2002). Formins direct Arp2/3-independent actin filament assembly to polarize cell growth in yeast. *Nat. Cell Biol.* **4**, 260-269.

Evangelista, M., Zigmond, S. and Boone, C. (2003). Formins: signaling effectors for assembly and polarization of actin filaments. *J. Cell Sci.* **116**, 2603-2611.

Frazier, J. A. and Field, C. M. (1997). Actin cytoskeleton: are FH proteins local organizers? *Curr. Biol.* **7**, R414-R417.

Gietz, R. D., Schiestl, R. H., Willems, A. R. and Woods, R. A. (1995). Studies on the transformation of intact yeast cells by the LiAc/SS-DNA/PEG procedure. *Yeast* **11**, 355-360.

Gorfer, M., Tarkka, M. T., Hanif, M., Pardo, A. G., Laitiainen, E. and Raudaskoski, M. (2001). Characterization of small GTPases Cdc42 and Rac and the relationship between Cdc42 and actin cytoskeleton in vegetative and ectomycorrhizal hyphae of *Suillus bovinus*. *Mol. Plant-Microbe Interact.* **14**, 135-144.

Hazan, I. and Liu, H. (2002). Hyphal tip-associated localization of Cdc42 is F-actin dependent in *Candida albicans*. *Eukaryotic Cell* **1**, 856-864.

Higgs, H. N. and Pollard, T. D. (2001). Regulation of actin filament network

formation through ARP2/3 complex: activation by a diverse array of proteins. *Annu. Rev. Biochem.* **70**, 649-676.

Johnson, D. I. (1999). Cdc42: an essential Rho-type GTPase controlling eukaryotic cell polarity. *Microbiol. Mol. Biol. Rev.* **63**, 54-105.

Katz, D., Goldstein, D. and Rosenberger, R. F. (1972). Model for branch initiation in *Aspergillus nidulans* based on measurements of growth parameters. *J. Bacteriol.* **109**, 1097-1100.

Lee, W. L., Bezanilla, M. and Pollard, T. D. (2000). Fission yeast myosin-I, Myo1p, stimulates actin assembly by Arp2/3 complex and shares functions with WASP. *J. Cell Biol.* **151**, 789-800.

Li, R. (1997). Bee1, a yeast protein with homology to Wiscott-Aldrich syndrome protein, is critical for the assembly of cortical actin cytoskeleton. *J. Cell Biol.* **136**, 649-658.

Machesky, L. M. and Insall, R. H. (1998). Scar1 and the related Wiskott-Aldrich syndrome protein, WASP, regulate the actin cytoskeleton through the Arp2/3 complex. *Curr. Biol.* **8**, 1347-1356.

Machesky, L. M., Mullins, R. D., Higgs, H. N., Kaiser, D. A., Blanchoin, L., May, R. C., Hall, M. E. and Pollard, T. D. (1999). Scar, a WASP-related protein, activates nucleation of actin filaments by the Arp2/3 complex. *Proc. Natl. Acad. Sci. USA* **96**, 3739-3744.

Madania, A., Dumoulin, P., Grava, S., Kitamoto, H., Scharer-Brodbeck, C., Soulard, A., Moreau, V. and Winsor, B. (1999). The *Saccharomyces cerevisiae* homologue of human Wiskott-Aldrich syndrome protein Las17p interacts with the Arp2/3 complex. *Mol. Biol. Cell* **10**, 3521-3538.

Momany, M. (2002). Polarity in filamentous fungi: establishment, maintenance and new axes. *Curr. Opin. Microbiol.* **5**, 580-585.

Mullins, R. D. (2000). How WASP-family proteins and the Arp2/3 complex convert intracellular signals into cytoskeletal structures. *Curr. Opin. Cell Biol.* **12**, 91-96.

Oberholzer, U., Marcil, A., Leberer, E., Thomas, D. Y. and Whiteway, M. (2002). Myosin I is required for hypha formation in *Candida albicans*. *Eukaryotic Cell* **1**, 213-228.

Ohsumi, K., Arioka, M., Nakajima, H. and Kitamoto, K. (2002). Cloning and characterization of a gene (*avaA*) from *Aspergillus nidulans* encoding a small GTPase involved in vacuolar biogenesis. *Gene* **291**, 77-84.

Pollard, T. D., Blanchoin, L. and Mullins, R. D. (2001). Actin dynamics. *J. Cell Sci.* **114**, 3-4.

Prehoda, K. E., Scott, J. A., Mullins, R. D. and Lim, W. A. (2000). Integration of multiple signals through cooperative regulation of the N-WASP-Arp2/3 complex. *Science* **290**, 801-806.

Pruyne, D., Evangelista, M., Yang, C., Bi, E., Zigmond, S., Bretscher, A. and Boone, C. (2002). Role of formins in actin assembly: nucleation and barbed-end association. *Science* **297**, 612-615.

Ramesh, N., Anton, I. M., Martinez-Quiles, N. and Geha, R. S. (1999). Waltzing with WASP. *Trends Cell Biol.* **9**, 15-19.

Rodal, A. A., Manning, A. L., Goode, B. L. and Drubin, D. G. (2003). Negative regulation of yeast WASP by two SH3 domain-containing proteins. *Curr. Biol.* **13**, 1000-1008.

Rohatgi, R., Ma, L., Miki, H., Lopez, M., Kirchhausen, T., Takenawa, T. and Kirschner, M. W. (1999). The interaction between N-WASP and the Arp2/3 complex links Cdc42-dependent signals to actin assembly. *Cell* **97**, 221-231.

Sagot, I., Rodal, A. A., Moseley, J., Goode, B. L. and Pellman, D. (2002). An actin nucleation mechanism mediated by Bni1 and profilin. *Nat. Cell Biol.* **4**, 626-631.

Schmidt, A. and Hall, M. N. (1998). Signaling to the actin cytoskeleton. *Annu. Rev. Cell Dev. Biol.* **14**, 305-338.

Sekiya-Kawasaki, M., Groen, A. C., Cope, M. J., Kaksonen, M., Watson, H. A., Zhang, C., Shokat, K. M., Wendland, B., McDonald, K. L., McCeffery, J. M. et al. (2003). Dynamic phosphorylation of the cortical actin cytoskeleton and endocytic machinery revealed by real-time chemical genetic analysis. *J. Cell Biol.* **162**, 765-772.

Sharpless, K. E. and Harris, S. D. (2002). Functional characterization and localization of the *Aspergillus nidulans* formin SEPA. *Mol. Biol. Cell* **13**, 469-479.

Taunton, J., Rowning, B. A., Coughlin, M. L., Wu, M., Moon, R. T., Mitchison, T. J. and Larabell, C. A. (2000). Actin-dependent propulsion of endosomes and lysosomes by recruitment of N-WASP. *J. Cell Biol.* **148**, 519-530.

Walther, A. and Wendland, J. (2003). Septation and cytokinesis in fungi. *Fungal Genet. Biol.* **40**, 187-196.

Walther, A. and Wendland, J. (2004). Polarized hyphal growth in *Candida albicans* requires the WASP homolog Wal1p. *Euk. Cell* **3**, 471-482.

Watters, M. K. and Griffiths, A. J. (2001). Tests of a cellular model for constant branch distribution in the filamentous fungus *Neurospora crassa*. *Appl. Environ. Microbiol.* **67**, 1788-1792.

Weaver, A. M., Young, M. E., Lee, W. L. and Cooper, J. A. (2003). Integration of signals to the Arp2/3 complex. *Curr. Opin. Cell Biol.* **15**, 23-30.

Weisman, L. S. (2003). Yeast vacuole inheritance and dynamics. *Annu. Rev. Genet.* **37**, 435-460.

Wendland, J. (2001). Comparison of morphogenetic networks of filamentous fungi and yeast. *Fungal Genet. Biol.* **34**, 63-82.

Wendland, J. (2003). PCR-based methods facilitate targeted gene manipulations and cloning procedures. *Curr. Genet.* **44**, 115-123.

Wendland, J. and Philippsen, P. (2000). Determination of cell polarity in germinated spores and hyphal tips of the filamentous ascomycete *Ashbya gossypii* requires a RhoGAP homolog. *J. Cell Sci.* **113**, 1611-1621.

Wendland, J. and Philippsen, P. (2001). Cell polarity and hyphal morphogenesis are controlled by multiple Rho-protein modules in the filamentous ascomycete *Ashbya gossypii*. *Genetics* **157**, 601-610.

Wendland, J. and Philippsen, P. (2002). An IQGAP-related protein, encoded by *AgCYK1*, is required for septation in the filamentous fungus *Ashbya gossypii*. *Fungal Genet. Biol.* **37**, 81-88.

Wendland, J., Ayad-Durieux, Y., Knechtle, P., Rebischung, C. and Philippsen, P. (2000). PCR-based gene targeting in the filamentous fungus *Ashbya gossypii*. *Gene* **242**, 381-391.

Wichmann, H., Hengst, L. and Gallwitz, D. (1992). Endocytosis in yeast: evidence for the involvement of a small GTP-binding protein (Ypt7p). *Cell* **71**, 1131-1142.

Wild, A. C., Jong, W. Y., Lemmon, M. A. and Blumer, K. J. (2004). The p21-activated protein kinase Cla4 is a coincidence detector of signaling by Cdc42 and phosphatidylinositol 4-phosphate. *J. Biol Chem.* **279**, 17101-17110.

Winter, D., Podtelejnikov, A. V., Mann, M. and Li, R. (1997). The complex containing actin-related proteins Arp2 and Arp3 is required for the motility and integrity of yeast actin patches. *Curr. Biol.* **7**, 519-529.

Winter, D. C., Choe, E. Y. and Li, R. (1999). Genetic dissection of the budding yeast Arp2/3 complex: a comparison of the in vivo and structural roles of individual subunits. *Proc. Natl. Acad. Sci. USA* **96**, 7288-7293.

Yarar, D., To, W., Abo, A. and Welch, M. D. (1999). The Wiskott-Aldrich syndrome protein directs actin-based motility by stimulating actin nucleation with the Arp2/3 complex. *Curr. Biol.* **9**, 555-558.

Zalevsky, J., Lempert, L., Kranitz, H. and Mullins, R. D. (2001). Different WASP family proteins stimulate different Arp2/3 complex-dependent actin-nucleating activities. *Curr. Biol.* **11**, 1903-1913.

3

Andrea Walther

Jürgen Wendland

RHOH shares functions in cell wall integrity with its paralog *RHO1* in the filamentous ascomycete *Ashbya gossypii*.

Curr. Genet. (in Revision, 23.06.05).

Rho-GTPasen haben wichtige Funktionen bei der Aktivierung von Effektorproteinen, die direkt oder in Proteinkomplexen an der Organisation des Aktinzytoskeletts beteiligt sind. Eine neuartige Rho-GTPase in *A. gossypii*, die ein Paralog von *RHO1* ist, wurde charakterisiert. Die Deletion von *RHOH* führte zu Zellwanddefekten und verstärkter Zell-Lyse an den Hyphenspitzen.

RESEARCH ARTICLE

Andrea Walther · Jürgen Wendland

RHOH shares functions in cell wall integrity with its paralog *RHO1* in the filamentous ascomycete *Ashbya gossypii*

Received: 2 June 2005

Abstract The organization of the actin cytoskeleton is of central importance in determining cell shape and morphogenesis. Rho-type GTP-binding proteins are known for their role to activate downstream effector proteins that act as scaffolds and direct the assembly of actin filaments. We have identified a novel Rho-type GTPase, *RHOH*, in the filamentous ascomycete *Ashbya gossypii* and also in one of its closest relatives, *Holleya sinecauda* both species belong to the genus *Eremothecium*. *RHOH* is a paralog of *AgRHO1* and was generated by tandem duplication in an evolutionary ancestor. Deletion of *RHOH* was carried out in both *A. gossypii* and *H. sinecauda* and showed that this gene is non-essential. However, a cell wall defect was observed that led to increased cell lysis at the hyphal tip and an increased sensitivity against the cell wall agent calcofluor and SDS in the *AgrhoH* strain. These results suggested overlapping functions between RhoH and Rho1. Deletion of both the *RHOH* and *RHO1* genes in *A. gossypii* exacerbated the mutant *rho1* phenotype and resulted in germination deficient spores indicating that Rho-type GTPases that regulate cell wall integrity are required for spore germination in contrast to Cdc42 which was previously shown to be dispensable for this process.

Keywords Rho-protein · GTPase · morphogenesis · polar growth · gene duplication

Communicated by: S. Hohmann

A.Walther · J. Wendland (✉)
Junior Research Group: Fungal Pathogens
Leibniz Institute for Natural Products Research and Infection Biology-Hans-Knöll Institute- and Dept. of Microbiology, Friedrich-Schiller University, Jena
Beutenbergstr. 11a
D-07745 Jena
E-mail: juergen.wendland@uni-jena.de
Tel.: +49-3641-656685
Fax: +49-3641-656620

Introduction

Cell polarity establishment and maintenance of polarized secretion are essential for morphogenesis and development (Drubin and Nelson, 1996). The actin and microtubule cytoskeleton play important roles in maintaining cell polarization and in providing cellular tracks for vesicle delivery. Complex processes of spatial and temporal coordination of protein localization and activation at sites of polarized growth need to be integrated (Pruyne and Bretscher, 2000). Rho-type GTPases, for example Cdc42, can activate downstream effector proteins such as members of the Wiskott-Aldrich Syndrome Protein- (WASP) and formin families (Schmidt and Hall, 1998). These effectors act as scaffolds that are able to initiate actin filament assembly and regulate processes of endocytosis and polarized delivery of secretory vesicles to sites of growth (Pruyne and Bretscher, 2000). Deletion of *CDC42* is lethal in *A. gossypii* but mutant spores derived from heterokaryotic primary transformants are able to germinate (Wendland and Philippsen, 2001). These germ cells show isotropic growth, are not able to polarize the actin cytoskeleton and thus cannot form germ tubes. Nuclear cycles continue generating multinucleate, round germ cells as terminal phenotype. This indicates that Cdc42 is not required for the initial steps breaking the dormancy of a spore (Wendland, 2001). On the other hand deletion of the *A. gossypii RHO1* gene resulted in reduced germination efficiency. Rho1 of *Saccharomyces cerevisiae* is an upstream regulator of the protein kinase C pathway that is involved in regulating cell wall and actin dynamics during budding and mating but also under stress responses to various cell wall integrity perturbing conditions (Zarzov et al., 1996, Heinisch et al., 1999; Reinoso-Martin et al., 2003). In *S. cerevisiae* mutants in the PKC-pathway particularly affecting the genes *BCK1*, *MKK1/MKK2*, and *SLT2,* encoding proteins of the MAP-kinase module downstream of Pkc1, show cell lysis defects that can be ameliorated by osmotic stabilization (Levin

and Bartlett-Heubusch, 1992). Osmotic stabilization during germination of *Agrho1* spores was found to increase germination efficiency about tenfold. However, the *Agrho1* colonies that were generated finally ceased growth and hyphal tips lysed resulting in a lethal phenotype (Wendland and Philippsen, 2001).

The *S. cerevisiae* genome contains several Rho-type GTPases, *CDC42* and *RHO1-5* which are distinct by several sequence features from other G-protein encoding genes (de Bettignies et al., 2001). Rho-proteins are regulatory molecules that switch between GTP- and GDP-bound stages controlled by specific guanine-nucleotide exchange factors (GEFs) and GTPase activating proteins (GAPs) (Hall, 1998). Since yeast-like growth of *S. cerevisiae* differs markedly form the filamentous growth of *A. gossypii* we wanted to analyze the function of the additional Rho-GTPase termed *RHOH* for Rho-homolog, in the *Ashbya* genome that was found during the genome sequencing project since we suspected that an additional Rho-type regulator could provide distinct morphologies not present in yeast.

Table 1. Strains used in this study

Strain[a]	Genotype	Reference
A. gossypii		
Agleu2	*leu2 (derivative of ATCC10895)*	Mohr and Philippsen, Biozentrum Basel
AWA3	*rhoH::GEN3/RHOH, leu2*	This study
AWA4	*rhoH::GEN3, leu2*	This study
AWA7	*rhoH-rho1::AgNATMX2, leu2*	This study
H. sinecauda		
Hsleu2	*leu2::DR*	Schade et al., 2003
HWA100	*rhoH::kanMX, leu2*	This study

Materials and methods

Strains and media

Strains used in this study are listed in Table 1. Media and growth conditions were used as described previously (Wendland and Philippsen, 2000; Schade et al., 2003). ClonNAT or G418 for the selection of nourseothricin or geneticin resistant transformants, respectively, was added to rich media at a concentration of 200µg/ml. For cell wall sensitivity assays calcofluor and SDS (sodium dodecylsulphate) was added in different concentrations to the solid media.

Isolation of gene sequences

The *A. gossypii* and *Kluyveromyces waltii RHOH-RHO1* sequences were obtained from the *Ashbya* genome sequence resources available at http://agd.unibas.ch/ and are entered with accession number AADM01000261 for *K. waltii*. The *H. sinecauda RHOH-RHO1* locus was amplified by PCR using degenerate primers containing restriction sites at the 5'-ends (#685 and #686; all primers are listed in Tab. 2). The PCR fragment was cloned and sequenced. Subsequently additional PCR-fragments containing *HsRHO1* were obtained (using primers #1010, #1011, and #1012) which generated overlapping sequences. The contig sequence of *HsRHOH* and *HsRHO1* (1258bp) has been entered in Genbank and will be rpovided with a accession number. Subsequently a 1,1kb fragment was amplified from *H. sinecauda* genomic DNA based on the contig information (using primers #1032 an d#1033) and this insert was cloned into pRS415. This plasmid was then transformed into *S. cerevisiae* to allow use of the yeast *in vivo* recombination machinery as described (Wendland, 2003). This resulted in the integration of the *kanMX* selectable marker within *HsRHOH* thus generating a *H. sinecauda* disruption cassette for *RHOH*. Excision of the cassette for transformation was done by *Bam*HI and *Xho*I. Correct targeting was verified by PCR (using primers #716 and #717).

Gene disruption

Transformation of *A. gossypii* and *H. sinecauda* was done by electroporation. Gene deletions in *A. gossypii* are done by using short flanking homology regions as described (Wendland et al., 2000). This allowed the generation of *RHOH* single or due to its tandem arrangement, *RHOH-RHO1* double deletions. Clonal selection of primary heterokaryotic transformants allowed the assessment of homokaryotic mutant phenotypes. Gene disruption in *H. sinecauda* was done using a *RHOH*-specific disruption cassette since, in our hands, short-flanking homology regions are not sufficient to result in correct gene targeting.

Standard procedures

For recombinant DNA methods, such as restriction analyses, standard methods were employed (Sambrook et al., 1989). PCR on mycelial fragments or cells was performed for verification of transformants using standard procedures (Walther and Wendland, 2003). Sequencing was performed by MWG-Biotech (Ebersberg, Germany). Oligonucleotides were obtained from Genaxxon Bioscience (Biberach, Germany). Microscopy was done on an Axiovert 40 CFL microscope (Zeiss, Jena) equipped with a digital camera (Canon G5).

Results

Identification of paralogous *RHOH* and *RHO1* genes in ascomycetes

During the *Ashbya* genome sequencing project a novel Rho-type GTPase was identified, termed *RHOH* (Rho-homolog), which is not present in *Saccharomyces cerevisiae* (Dietrich et al., 2004). Surprisingly this gene was found to be located just upstream of the previously characterized *RHO1* (Wendland and Philippsen, 2001).Comparison of the *RHO1*-loci of *A. gossypii* and *S. cerevisiae* revealed partial synteny (Fig. 1). However, *S. cerevisiae* lacks a *RHOH* ortholog. A comparison with the recently published genome sequence of *Kluyveromyces waltii* shows that the *RHO1* loci of *S. cerevisiae* and *K. waltii* are syntenic, only that in *K.waltii* a *RHOH* orthologue can be found (Kellis et al., 2004). Furhtermore, in the Ashbya genome a break of synteny is obvious starting at the position

Table 2. Oligonucleotide primers used in this study

Primer	Sequence[a]
#474 G3	TCGCAGACCGATACCA
#685 Rho1tandem-down	cgc**ggatcc**GCNYTNTGGGAYACNGCNGGNCARGARG
#686 Rho1tandem-up	cgg**gaattc**CANGTYTTNCCRCANGCNCCRTCNCC
#697 S1-AgRHOH	GAGACCGCGGGGGAGATCTCGCAGAAGAGCGCAGGTTCTGCTTATACTCGGACAATAACAGGCTGG GAAGTGACAGTTTCAGAAATgctagggataacagggtaatacag
#698 S2-AgRHOH	TGTGACTGCACGGAGAGACCGTGGATATGTATGTAATTGACCGATGACTATGGATGCGGCGGCCGC GTaggcatgcaagcttagatct
#699 G1-AgRHOH	CGGTGCAATAGGAAGCCCACGC
#715 HsS2-RHOH	GTTCGTAGTGCTTGTGCAGGTATTCGAGGACGCAAGGCGGCTGAGGCGGGGCAGAGCCCCAGCGTT GCGGAATGTGGGTCACGTGACTAGGGCTGCGGAAACTggatggcggcgttag
#716 G1-HsRHOH	ACCGCTATCTTACCCCGAC
#717 G4-HsRHOH	tgttacaaatgggctacggc
#872 G1-HsRHO1	GCCAAACCGGTTGGATTTACTAACAGC
#944 AgRHOH-3'	GTAGGATATGTAGGCGGAAGCG
#1010	GCNCKNGTNGCNGCnTCRAANACYTCNYKNACNCC
#1011	CNCCXXXNCCNGTYTTNGCNSWRCAYTC
#1012	GCTATACTTAGCATTGCCAAACCGGTTGG
#1032 HsRHO-P1	gttt**ggatcc**GTTTCTCGGTTGATATACCCG
#1033 HsRHO-P2	aacct**ctcgag**CCTGGGACTGAGACACTGG
#1034 HsRHO-V2	GTACTCCACAGCTCCAATTTGGTCC
#1035 S1-HsRHOH	CACGAGGAAGTCCCGCTCCTCCACCGCAGGCCGCCGCGCTGCCTCgatctgtttagcttgcctcg
#1114 G4-AgRHOH	GGCTTGGCCTGAACAGTATCGTG
#1202 N2	gcgtttccctgctcgcaggtc
#1213 G1a-AgRHOH	GCGTCGCGTCGCCTTCTCCG
#1214 ScTEFp-up1	gggtaatttgtcgcggtctggg
#1215 ScTEFp-down1	gcccatcagattgatgtcctcc
#1216 S1a-AgRhoH	GAGACCGCGGGGGAGATCTCGCAGAAGAGCGCAGGTTCTGCTTATACTCGGACAATAACAGGCTGG GAAGTGACAGTTTCAGAAATgaagcttcgtacgctgcaggtc
#1220 S2a-AgRHO1	GGACAGCAGCGGAGTACAGGGCTCCAGTCTAGCCTCACCCAGCGCCAGCAGCGCCCGCCCATCACC tctgatatcatcgatgaattcgag

[a] Uppercase sequences correspond to genomic DNA. Lowercase sequences correspond to 3'-terminal annealing regions for the amplification of transformation cassettes or to 5'-terminal sequences added to contain restriction sites (marked in bold) for suitable cloning. All sequences are written from 5' to 3'.

of the $tRNA^{Glu}$ gene (there is a $tRNA^{Ile}$ gene just downstream of YPR169w). Genes encoding tRNAs are the only repetitive DNA elements found in the *Ashbya* genome. It was, therefore, postulated that genome rearrangements in *Ashbya* may occur via recombination at these tRNA-loci (Dietrich et al., 2004). This genome rearrangement event is unique to the Ashbya lineage. The position of the *RHOH* gene suggests that it is paralogous to *RHO1* and thus has arisen by tandem gene duplication. A comparison of the *A. gossypii*, *S. cerevisiae*, and *K. waltii* genomes suggests that the *RHO1-RHOH* duplication event is ancient in the yeast lineage. To investigate this in more detail we deduced degenerate primers based on the conserved sequences of Rho-proteins such that they can only amplifiy fragments from genomic DNA if two RHO-genes were positioned in a tandem array (Fig. 2). In *A. gossypii* the fragment generated by these primers is 1,3 kb. These primers were used on genomic DNA of *Holleya sinecauda* which is one of the closest relatives of *A. gossypii*. We were able to generate a PCR fragment of 844bp which was cloned and sequenced and showed the presence of a *RHOH-RHO1* tandem array also in *H. sinecauda*. The observed size difference was solely due to a difference in the inter-ORF region including the terminator of *HsRHOH* and the promoter of *HsRHO1.* Using additional primers we amplified and cloned a 1,25 kb fragment of *HsRHOH* and *HsRHO1* which was used for the generation of a disruption cassette (see below).

Table 3. **Tandem duplications in *A. gossypii***

***Ashbya gossypii* genes**[a]							Seq. ident.[b]	*Yeast* genes[c]
AAL178w	**AAL179w**						35,0%	YKR013w/
618bp	**1083bp**							YJL079c
ABL188w	**ABL189w**						27,2%	YDL237w
1029bp	**1170bp**							
ABR025c	ABR026c	ABR027c	ABR028c	**ACR272c**	**ACR273w**	ADL398c	60%	YKL096w
618bp	480bp	3396bp	1161bp	**450bp**	**456bp**	465bp		*-CWP1*
ABR182w	**ABR183w**						62,8%	YPR165w
630bp	**624bp**							*-RHO1*
ABR246w	**ABR247w**	**ABR248w**	**ABR249w**	ACR171c			**87,3%**	YIR035c/
753bp	**753bp**	**786bp**	**753bp**	756bp				YIR036c
ACL200w	**ACL201w**	ACL202w	AFR530w				**94,6%**	YMR238w
1392bp	**1347bp**	1353bp	1380bp					*-DFG5*
ACR098c	**ACR099c**						35%	YOR213c/
663bp	**744bp**							YPL129w
ACR143w	**ACR144w**	ABL123c	**AGR407c**				41,5%	YPL154c
1182bp	**1227bp**	1485bp	**807bp**					*-PEP4*
ACR282c	**ACR283w**	ADL027w	**ADR122c**				29,7%	YAL018c
996bp	**681bp**	1011bp	**1128bp**					
ADL155c	**ADL156c**						55,2%	YOL119c
1461bp	**1452bp**							*-MCH4*
ADR081c	**ADR082c**						**89,2%**	YLR215c
1044bp	**1068bp**							-CDC123
ADR336c	**ADR337c**	AGL069c					54,5%	YNR055c
1707bp	**1713bp**	1785bp						*-HOL1*
ADR403c	ADR404c	**ADR405c**					26,7%	YAL051w
2913bp	2628bp	**2424bp**						YOR363c
AEL110w	**AEL111c**						51,4%	YKL164c
747bp	**1047bp**							YKL163w
AER452c	AER453c	**AER454c**	ABR159c	ACL114w			60,7%	YJR107w
969bp	831bp	**972bp**	1149bp	960bp				
AFR262c	**AFR263c**						**86,7%**	YGL246c
2328bp	**1131bp**							*-RAI1*
AGL325w	**AGL326w**	AEL132w					29,9%	YJL172w
1716bp	**1692bp**	1719bp						CPS1
AGL351w	**AGL352w**						47,9%	YMR307w
1668bp	**1602bp**							*-GAS1*
AGR038c	**AGR039c**						49,1%	YDR046c
1743bp	**1761bp**							YBR068c
AGR405c	**AGR406c**						62,0%	YCL057w
2154bp	**2052bp**							*-PRD1*

[a] *A. gossypii* genes correspond to the systematic nomenclature A (*Ashbya*), A-G (chromosome 1-7), L/R (left or right arm of the chromosome based on synteny to yeast) and three digits to indicate the ORF distance to the centromere. The ORF lengths are indicated for each gene to allow comparison.

[b] Sequence identity on the DNA level in percent. The highest percentage in pair-wise alignments is indicated and the given pair is printed in bold. Bold print of the percentage value indicates that the pair of sequences shared stretches of 100% sequence identity that are longer than 45bp and thus should be sufficient to allow homologous recombination between tandem repeats.

[C] Yeast genes are given by their systematic name or their standard name. In case a gene duplication/ twin ORF was also found in *S. cerevisiae* both genes were entered.

Analysis of tandem duplicated sequence in *Ashbya gossypii*

In a previous study integrative transformants were analysed that were generated with linearized plasmids. Several of these transformants had integrated multiple copies of the plasmid in tandem arrays that were gradually lost due to deletions upon recombination between the repetitive sequences (Steiner et al., 1995). This indicates that direct sequence repeats are unstable in *A. gossypii* due to the efficient homologous recombination machinery. This also allowed the introduction of PCR-based gene targeting methods in *A. gossypii* using 45bp of flanking target gene homology sufficient for the generation of gene

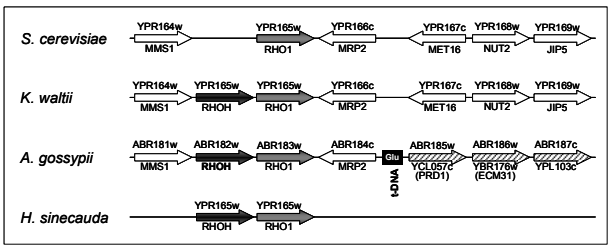

Fig. 1 Chromosomal map of *RHO1*-loci. Position and transcriptional orientation of genes in the *RHO1* loci of *Saccharomyces cerevisiae*, *Kluyveromyces waltii*, *Ashbya gossypii*, and *Holleya sinecauda* are shown. Systematic nomenclature corresponds to *S. cerevisiae* (e.g. YPR165w) or to *A. gossypii* (e.g. ABR183w). Loci between *S. cerevisiae* and *K. waltii* are syntenic with the exception of the presence of a *RHO1* paralogue in *K. waltii*. Gene order in *A. gossypii* is partially syntenic with *S. cerevisiae* suggesting a break point of synteny at the tRNA-encoding gene.

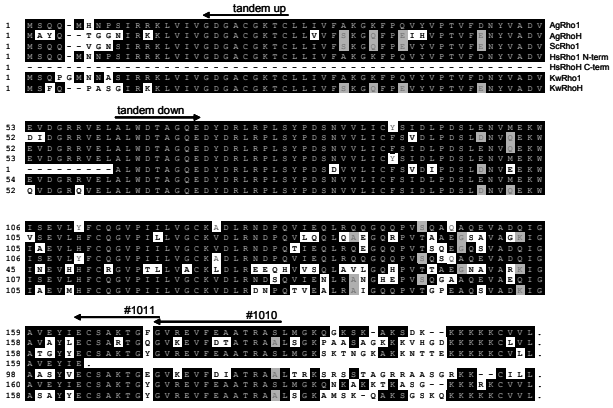

Fig. 2 Alignment of Rho-proteins. Rho1 and RhoH sequences of *A. gossypii* (Ag), *S. cerevisiae* (Sc), *H. sinecauda* (Hs), and *K. waltii* (Kw) are shown. Identical amino of the majority of sequences are shaded in black. Grey shades were assigned to a minority of identical amino acids. Arrows indicate amino acids that were taken to deduce degenerate primers used for the amplification of the *H. sinecauda RHOH-RHO1* fragment.

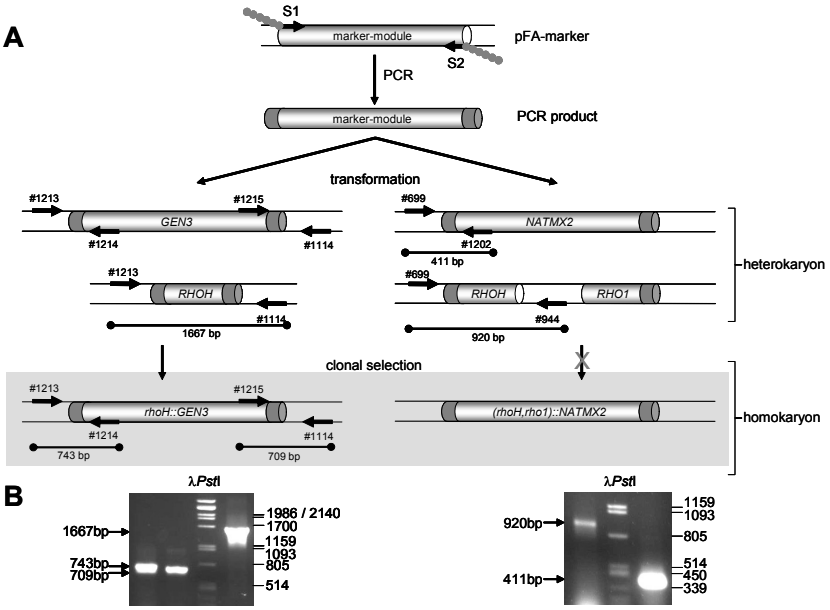

Fig. 3 Disruption of the *A. gossypii RHOH* and *RHO1* genes. (A) Schematic drawing showing the PCR-based gene disruption strategy. After amplification of selectable marker genes (either *GEN3* or *NATMX2*) and transformation into *A. gossypii* heterokaryotic primary transformants were selected. Clonal selection of uninucleate spores generated viable homokaryotic *AgrhoH* mutant strains while homokaryotic strains carrying the *rhoH-rho1* double deletion did not germinate indicating that this double deletion is lethal. Primer positions used for diagnostic PCR are indicated as well as the size of the expected PCR-fragments. (B) Verification of homologous integration. Both ends that were newly generated by insertion of the *GEN3* marker and disruption of the *RHOH* gene were obtained (left panel lanes a and b). The heterokaryon (lane c) shows the wild type band amplified with the outmost primers (the mutant band was not amplified due to its larger size). Upon clonal selection only the diagnostic bands (d, e) were obtained. Double deletion of *RHOH* and *RHO1* was verified by one diganostic band (lane f). In the heterokaryotic situation (lane f) a smaller band was obtained indicating the presence of the *RHOH* gene.

disruptions (Wendland et al., 2000). Therefore, tandem duplications should be rare in *Ashbya* or sequences of tandemly duplicated genes should be sufficiently divergent to escape recombination. An inspection of the *Ashbya* genome sequence indicated the presence of several tandem duplications besides the *RHOH-RHO1* case (Tab. 3). Further analysis showed that in most cases paralogues differ either in size or share a low degree of sequence identity which should eliminate the activation of the *Ashbya* recombination machinery. Only in four cases tandem gene pairs share a very high degree of sequence identity. This may either indicate a recent duplication event or the selective advantage of these genes in *Ashbya*. Based on the results with PCR-based gene targeting these sequence repeats could potentially be eliminated during a recombination event. The *A. gossypii RHOH* and *RHO1* gene pair exhibits only 62.8% identity on the DNA level (69.7% on the amino acids level) not generating sufficient overlap to allow recombination. AgRhoHp shares 75.2% identity with ScRho1p and AgRho1p shares 81.2% identity with ScRho1p indicating that the *Ashbya* proteins are similar to ScRho1 than to themselves (Fig. 2).

Deletion of the *A. gossypii RHOH-RHO1* paralogues

To establish a function of *AgRHOH* we went on to generate deletion mutant strains. To this end specific primers were designed for the amplification of deletion cassettes that result in either single deletion of *AgRHOH* or due to the tandem array in double deletion of both *RHOH* and *RHO1* (Fig. 3). After transformation heterokaryotic transformants were obtained that shared wild type phenotype and carried both nuclei with the wild type and nuclei with the mutant allele. Verification of correct gene targeting was done by PCR. Clonal selection generated a *rhoH::GEN3* mutant whereas we were not able to select a strain bearing a *rhoH, rho1* deletion indicating that such a deletion is lethal. Already the single deletion of *rho1* resulted in lethality at the mini-colony stage. A combined deletion of *rhoH* and *rho1* exacerbates this phenotype and mutant spores were entirely unable to germinate.

Phenotypic characterization of *rhoH* mutant hyphae did not reveal growth defects in the temperature range tested (20-37°C, not shown). Staining of the actin cytoskeleton also revealed no discernible defects in *rhoH* hyphae (not shown). Upon growth on solid media, however, hyphal tips at the colony edges of the *rhoH* strains were found to exhibit an increased tip-cell lysis phenotype not present in the wild type (Fig. 4).

This lysis phenotype was similar but much weaker than that observed in *rho1* mutants, which supports the observations showing that deletion of *RHOH* does not result in significant colonial growth delays. Since these results suggested that the function of RhoH contributes to cell wall integrity similar to that of Rho1 we went on to test if the cell wall disturbing agent calcofluor could inhibit colony growth of *rhoH* strains (Fig. 5). We found that concentrations of 100µg/ml resulted in 20% growth inhibition of *rhoH* colonies compared to the wild

type, whereas higher concentrations inhibited both mutant and wild type growth. Similar results were obtained by adding 0,001% SDS to the medium (not shown).

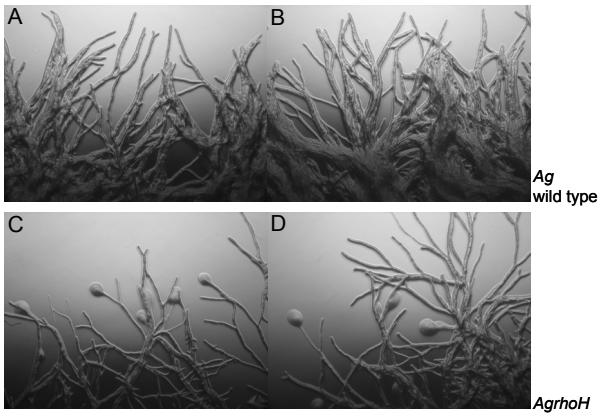

Fig. 4 Deletion of *RHOH* results in occasional lysis of hyphal tips. Images of *A. gossypii* colonies that were grown on solid full media plates at 30°C. The wild type (A,B) shows characteristic growth with dichotomous tip-branching. In the *rhoH* mutant strain (C, D) hyphal tip lysis occurred at some of the hyphal tips which can be observed only rarely in the wild type. Tip branching in the *rhoH* mutant was like in the wild type.

Deletion of *H. sinecauda* RHOH

For the functional analysis of *HsRHOH* we went on to generate a *HsrhoH* strain. To this end a disruption cassette was cloned based on the obtained sequence contig (see materials and methods). The use of long-flanking homology regions is required in *H. sinecauda* since we were not able to generate integrative transformants with short flanking homology regions. Using a cassette with 334bp flanking homology on the 5'-end and 774bp flanking homology on the 3'-end we were able to generate an insertion deletion at the very end of the *HsRHOH* ORF. This should result in a *rhoH* null phenotype since it eliminates the CAAX prenylation motif required for membrane insertion. Correct integration of the cassette was verified by colony PCR (Fig. 6). The *H. sinecauda rhoH* strain exhibited no growth defects and a cell lysis phenotype was not apparent even using a diluted spotting assay. This may be due to the fact that in the early growth stages *H. sinecauda* shows dimorphic growth and exhibits colonies consisting of filaments and yeast cells that did not allow the distinction of a subtle cell lysis defect.

Discussion

Ashbya gossypii has been introduced as a model for the study of fungal developmental biology (Wendland and Walther, 2005). In recent studies the role of Rho-proteins for the organization of the actin cytoskeleton has been analyzed on the molecular level (Wendland and Philippsen, 2001). This revealed conserved roles of the Cdc42-GTPase for the establishment of cell polarity, Rho1 for the maintenance of cell wall integrity, and Rho3 for the maintenance of polarized hyphal growth. Further studies on Rho-protein regulators showed that the Cdc42-module including the Cdc42 guanine nucleotide exchange factor Cdc24 is essential for polarized morphogenesis. The Rho-GTPase activating protein encoded by *AgBEM2* was found to determine cell polarity at all stages of development, but allowed germination and polarized cell growth but produced swollen hyphae with a severe retardation of polarized hyphal growth (Wendland and Philippsen, 2000, 2001). Since growth defects in these mutants were also related to defects in the organization of the actin cytoskeleton other genes that encode proteins directly involved in actin assembly were studied. The *A. gossypii* Wiskott-Aldrich Syndrome Protein-(WASP) homolog encoded by *WAL1* was shown to be required for actin patch positioning in the hyphal tip and *wal1* mutant strains also exhibited defects in endocytosis (Walther and Wendland, 2004).
With the completion of the *Ashbya* genome sequence the complete gene set of *A. gossypii* was analyzed and compared to yeast like and dimorphic fungi, particularly with the dimorphic human fungal pathogen *Candida albicans* to elucidate common molecular principles of polarized hyphal growth (Berman and Sudbery, 2002).

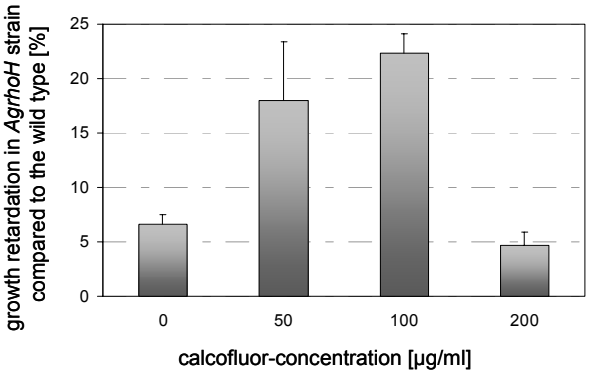

Fig. 5 Deletion of *RHOH* leads to increased sensitivity against calcofluor. Wild type and *rhoH* strains were incubated on solid media plates containing different amounts of calcofluor. Growth retardation of the *rhoH* strain compared to the wild type was monitored after four days of growth based on the colony diameter in three independent experiments.

The amount of redundancy in the *Ashbya* genome is surprisingly low and with just 9,2MB *Ashbya* encodes one of the smallest eukaryotic genomes. The compactness of the *Ashbya* genome is in part due to the small inter-ORF regions which, on average, is only about 340bp (Dietrich et al., 2004). Interestingly, in the case presented here,

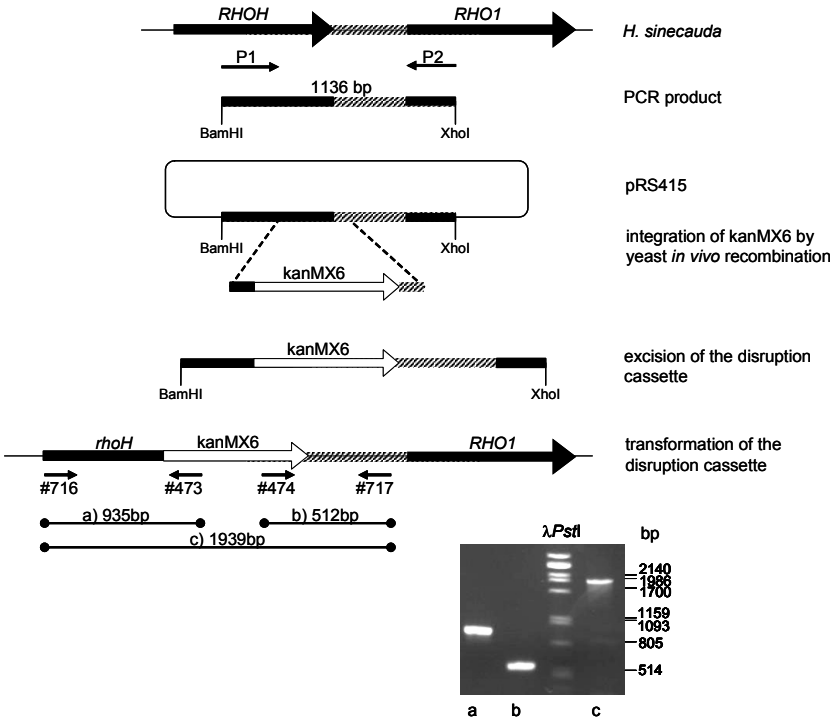

Fig. 6 Disruption of the *H. sinecauda RHOH* gene. Schematic representation of disruption cassette generation and transformation procedure to obtain a *HsrhoH* strain. Using sequence information obtained by amplification and sequencing of fragments from the *RHOH* locus with degenerate primers a new fragment was amplified with primers P1 and P2 and cloned into a yeast episomal plasmid. Integration of the *kanMX6* selectable marker gene and excision of the resulting fragment generated a *RHOH*-specific disruption cassette. Correct integration of this cassette was verified by PCR using the indicated primer combinations that yielded fragments of expected lengths (a-c in the image of the ethidium bromide stained agarose gel).

the inter-ORF region between the *RHOH* and *RHO1* paralogues of *Holleya sinecauda* (323bp) is drastically smaller than in *A. gossypii* (767bp). Smaller intergenic regions that were spanned by single-read end-sequencing of plasmid clones of a partial genomic *H. sinecauda* library, for example, corresponding to the homologous gene pairs the *A. gossypii* genes ABL185c-ABL186w, ACR031w-ACR032c, AFL097c-AFL098w, AFR179c-AFR180c, and AGL136c-AGL137w were found to be of equal size (a total of 518bp of intergenic region for these five *A. gossypii* gene pairs and 569bp in *H. sinecauda*) (Weber and Wendland, unpublished). A systematic comparison between *Ashbya* and *H. sinecauda* intergenic regions, however, requires a large set of sequence information.

The mammalian RhoA and RhoB GTPases which are 86% identical on the amino acids level but fulfil different functions (Adnane et al., 2002). The *RHO1* paralogues in *Ashbya* share only 62,8% identity on the protein level, but we present three lines of evidence indicating that the function of AgRhoH is overlapping with AgRho1 in maintaining cell wall integrity. First, deletion of *AgRHOH* resulted in a hyphal tip-cell lysis phenotype on solid media. This indicated a cell wall defect which became apparent as a growth delay on solid media containing the cell wall perturbing agent calcofluor. And finally, double deletion of *RHOH* and *RHO1* in *Ashbya* resulted in a spore lethal phenotype, which abolished germination of mutant spores, thus exacerbating the *rho1* phenotype (Wendland and Philippsen, 2001).

The occurrence of *RHO1* paralogues has been established in *A. gossypii*, *H. sinecauda*, and also in *K. waltii*, indicating an early duplication in the yeast lineage that is not present in the *S. cerevisiae* lineage. Since the *Ashbya* genome contains only a few tandem duplicated genes the frequency of duplication may be low or conversely the selection pressure on loss of duplications may be high. Further studies on the duplicated gene set in *Ashbya*, for example, on the CWP1 gene family encoding orthologs of the *S. cerevisiae* cell wall protein 1, may reveal other more specialized functions for *A. gossypii*.

Acknowledgement We thank Diana Schade for her excellent technical assistance in this project and Peter Philippsen for providing sequence data prior to publication. This research was supported by the Deutsche Forschungsgemeinschaft (grant We2634/2-1), the Friedrich-Schiller University, and the Hans-Knöll Institute.

References

Adnane J et al. (2002) RhoB, not RhoA, represses the transcription of the transforming growth factor beta type II receptor by a mechanism involving activator protein 1. J Biol Chem 277:8500-8507

Berman J, Sudbery PE (2002) Candida Albicans: a molecular revolution built on lessons from budding yeast. Nat Rev Genet 3:918-930

de Bettignies G, Thoraval D, Morel C, Peypouquet MF, Crouzet M (2001) Overactivation of the protein kinase C-signaling pathway suppresses the defects of cells lacking the Rho3/Rho4-GAP Rgd1p in Saccharomyces cerevisiae. Genetics 159:1435-1448

Dietrich FS et al. (2004) The Ashbya gossypii genome as a tool for mapping the ancient Saccharomyces cerevisiae genome. Science 304:304-307

Drubin DG, Nelson WJ (1996) Origins of cell polarity. Cell 84:335-344

Hall A (1998) Rho GTPases and the actin cytoskeleton. Science 279:509-514

Heinisch JJ, Lorberg A, Schmitz HP, Jacoby JJ (1999) The protein kinase C-mediated MAP kinase pathway involved in the maintenance of cellular integrity in Saccharomyces cerevisiae. Mol Microbiol 32:671-680

Kellis M, Birren BW, Lander ES (2004) Proof and evolutionary analysis of ancient genome duplication in the yeast Saccharomyces cerevisiae. Nature 428:617-624

Levin DE, Bartlett-Heubusch E (1992) Mutants in the S. cerevisiae PKC1 gene display a cell cycle-specific osmotic stability defect. J Cell Biol 116:1221-1229

Pruyne D, Bretscher A (2000) Polarization of cell growth in yeast. J Cell Sci 113 (Pt 4):571-585

Reinoso-Martin C, Schuller C, Schuetzer-Muehlbauer M, Kuchler K (2003) The yeast protein kinase C cell integrity pathway mediates tolerance to the antifungal drug caspofungin through activation of Slt2p mitogen-activated protein kinase signaling. Eukaryot Cell 2:1200-1210

Schmidt A, Hall MN (1998) Signaling to the actin cytoskeleton. Annu Rev Cell Dev Biol 14:305-338

Steiner S, Wendland J, Wright MC, Philippsen P (1995) Homologous recombination as the main mechanism for DNA integration and cause of rearrangements in the filamentous ascomycete Ashbya gossypii. Genetics 140:973-987

Walther A, Wendland J (2004) Apical localization of actin patches and vacuolar dynamics in Ashbya gossypii depend on the WASP homolog Wal1p. J Cell Sci Pt

Wendland J (2001) Comparison of morphogenetic networks of filamentous fungi and yeast. Fungal Genet Biol 34:63-82

Wendland J, Ayad-Durieux Y, Knechtle P, Rebischung C, Philippsen P (2000) PCR-based gene targeting in the filamentous fungus Ashbya gossypii. Gene 242:381-391

Wendland J, Philippsen P (2000) Determination of cell polarity in germinated spores and hyphal tips of the filamentous ascomycete Ashbya gossypii requires a rhoGAP homolog. J Cell Sci 113 (Pt 9):1611-1621

Wendland J, Philippsen P (2001) Cell polarity and hyphal morphogenesis are controlled by multiple rho-protein modules in the filamentous ascomycete Ashbya gossypii. Genetics 157:601-610

Wendland J, Walther A (2005) Ashbya gossypii: a model for fungal developmental biology. Nat Rev Microbiol 3:421-429

Zarzov P, Mazzoni C, Mann C (1996) The SLT2(MPK1) MAP kinase is activated during periods of polarized cell growth in yeast. Embo J 15:83-91

4

Diana Schade

Andrea Walther

Jürgen Wendland

Establishment of a transformation system for the plant pathogen *Holleya sinecauda* based on sequences of *Ashbya gossypii*.

Fungal Genet. Biol., 40(1): 65-71.

Um molekulare Unterschiede der Wachstumsformen von strikt filamentösen und dimorphen Pilzen zu untersuchen, wurde ein Transformationssystem für den phytopathogenen dimorphen Pilz *H. sinecauda* etabliert. Durch die Verwendung des dominanten Selektionsmarkers *kanMX* sowie eines Replikationsursprunges und einer Zentromer-Sequenz aus *A. gossypii* konnten frei-replizierende Plasmide transformiert und eine erste integrative Mutante erzeugt werden.

Available online at www.sciencedirect.com
SCIENCE DIRECT®
Fungal Genetics and Biology 40 (2003) 65–71
FUNGAL GENETICS AND BIOLOGY
www.elsevier.com/locate/yfgbi

The development of a transformation system for the dimorphic plant pathogen *Holleya sinecauda* based on *Ashbya gossypii* DNA elements☆

D. Schade, A. Walther, and J. Wendland*

Junior Research Group: Growth-control of Fungal Pathogens, Hans-Knöll Institut für Naturstoff-Forschung, Jena, Germany
Department of Microbiology, Friedrich-Schiller University, Winzerlaer Straße 10, Jena DE-07745, Germany

Received 23 December 2002; accepted 25 April 2003

Abstract

We have developed a transformation system for the dimorphic plant pathogenic fungus *Holleya sinecauda* based on an electroporation protocol used for the closely related filamentous fungus *Ashbya gossypii*. DNA-mediated transformation of the dominant selection marker *kanMX* generated *H. sinecauda* transformants that were resistant to the antibiotic drug G418/geneticin. Freely replicating plasmids could be established in *H. sinecauda* using an *A. gossypii* autonomously replicating sequence (ARS) element, whereas *Saccharomyces cerevisiae* ARS elements, which are functional in *A. gossypii*, were not functional in *H. sinecauda*. In addition, centromeric DNA of *A. gossypii* stabilized the maintenance of plasmids in *H. sinecauda* under non-selective conditions. We isolated a fragment of the *HsLEU2* gene and used this locus for targeted integration of *kanMX3*, consisting of the *kanMX* gene flanked by direct repeats. This allowed the construction of a *Hsleu2* strain which became G418 sensitive after direct repeat-induced marker excision. The *Hsleu2* strain can be complemented by the *ScLEU2* gene. Finally, we constructed high- and low-copy shuttle vectors for *H. sinecauda*.

Keywords: Transformation; Dimorphism; Freely replicating plasmid; Centromere; Gene disruption

1. Introduction

The morphological transition from yeast-like growth to hyphal growth can be found in a variety of fungal species. These include plant pathogenic fungi such as *Ustilago maydis* and human fungal pathogens such as *Candida albicans* (Brown and Gow, 1999; Mayorga and Gold, 1999). Most of our current knowledge on the dimorphic transition is derived from studies of invasive growth and the yeast to pseudohyphal switch in the baker's yeast *Saccharomyces cerevisiae*. However, *S. cerevisiae* is not a filamentous fungus, and may thus lack certain properties common in fungi that are able to promote hyphal growth. In order to analyze growth patterns in a strictly filamentous fungus on the molecular level, we have investigated regulatory components of hyphal growth in *Ashbya gossypii* which we chose as our model organism based on its close relationship to *S. cerevisiae*. We could show that Rho-module signaling via Cdc42p, Rho1p, Bem2p, or Rho3p was important for the regulation of polarized hyphal growth via the organization of the actin cytoskeleton (Wendland and Philippsen, 2000, 2001).

In this study we started the molecular investigation of the recently identified dimporphic fungus *Holleya sinecauda* which is a plant pathogen of mustard seeds (Holley et al., 1984). *H. sinecauda* is most closely related to *A. gossypii* based on rDNA comparisons (Prillinger et al., 1997; Wendland et al., 1999). We introduced the dominant selection system based on the *kanMX* marker gene which is composed of the open reading frame of the kanamycine resistance gene under control of the *A. gossypii TEF1* promoter and terminator as a tool for

☆ GenBank Accession Nos. are: AY148967, AY148968, and AY148969.

* Corresponding author. Fax: +49-3641-65-7633.
E-mail address: juergen.wendland@uni-jena.de (J. Wendland).

1087-1845/$ - see front matter © 2003 Elsevier Science (USA). All rights reserved.
doi:10.1016/S1087-1845(03)00064-1

transformation. Isolation of a fragment of the *HsLEU2* gene and the construction of a cloned disruption cassette lead to the generation of an auxotrophic *leu2* mutant strain via targeted gene disruption and represents the first gene deletion created in *H. sinecauda*. We further show heterologous complementation of the *H. sinecauda leu2* mutant by the *ScLEU2* gene. In addition, based on the heterologous function of *A. gossypii* centromeric DNA in *H. sinecauda* and the usage of an AgARS element replicative transformation could be established in *H. sinecauda* which allowed the construction of high-copy number and low-copy number *H. sinecauda–A. gossypii*-shuttle vectors that will be useful for testing the expression of genes in both species.

Based on the close relationship between *H. sinecauda* and *A. gossypii*, this species pair seems to be well suited for a developmental genetics approach to understand the evolution of different fungal growth forms.

2. Materials and methods

2.1. Strains and media

Holleya sinecauda strain, CBS8199, was obtained from the Fungal Stock Center (CBS, Baarn, NL). *H. sinecauda* grows in the same media as used for cultivation of *A. gossypii* and *S. cerevisiae* and grows optimally at 30 °C. As yeast strain RLY201 (MATa/α *URA3/ura3 HIS3/his3 trp1/trp1 leu2/leu2 lys2/lys2 CYK1/cyk1::LEU2*) was used. Complete media and media lacking leucine were prepared, as described previously (Wendland and Philippsen, 2001). G418/geneticin was added to rich media for selection of antibiotic-resistant transformants at a final concentration of 200 μg/ml. The *Escherichia coli* strain DH5α served as host for plasmids.

2.2. Construction of plasmids

Plasmids used in this study are listed in Table 1. Plasmid pRS415-kanMX was constructed by cutting pRS415 with *Sac*I and *Bam*HI and ligating a *kanMX* *Sac*I–*Bgl*II fragment (out of pFA-kanMX6) into these sites. Plasmid pRS426-*kanMX* was constructed by cutting pRS426 with *Stu*I and *Bam*HI and ligating an *Eco*RV–*Bam*HI *kanMX* fragment into these sites. Plasmid pRS426-*GEN3* was created by inserting a *Bam*HI fragment of *GEN3* (out of pGEN3) into the *Bam*HI site of pRS426. pFA-ARS-CEN5 and pFA-ARS plasmids are based on the pFA vector series and contain either a 2.8-kb *Eco*RI–*Spe*I fragment or a *Sph*I–*Hin*dII fragment of the *A. gossypii CEN5* locus derived from pAG1489 (a clone from an *A. gossypii* plasmid library; AF384989). Plasmid pHsLEU2 was generated by cloning of a *HsLEU2* PCR fragment into pSKBluescript using the restriction sites carried at the 5′-end of the degenerate oligonucleotide primers (see Table 2). The disruption cassette for *HsLEU2* deletion was constructed by inserting the *kanMX3* marker into the *Bgl*II site of the *HsLEU2* PCR fragment generating pHsleu2-kanMX3. The disruption cassette was excised prior to transformation by cleavage with *Bam*HI and *Kpn*I. The shuttle vector pLC-Shuttle was created by inserting a *Sma*I–*Pvu*II fragment carrying *kanMX* and the *A. gossypii CEN5*-ARS derived from pFA-AgCEN5-ARS into the unique *Sca*I site of pRS405, thus disrupting the amp-resistance gene. Similarly, pHC-Shuttle was generated by inserting a *Pvu*II–*Pme*I fragment carrying *kanMX* and the *A. gossypii* ARS derived from pFA-AgARS into the *Sca*I site of pRS405.

2.3. Plasmid stability assay

Plasmid transformants were selected on geneticin-containing media. They were then restreaked onto non-

Table 1
Plasmids used in this study

Plasmid	Relevant feature	Source
pRS405	*ScLEU2*	Sikorski and Hieter (1989)
pRS415	*ScLEU2*, ScCEN6-ARSH4	Sikorski and Hieter (1989)
pRS426	*ScURA3*, 2μARS	Christianson et al. (1992)
pFA-kanMX6	*AgTEF1p-kanR-AgTEF1t*	Wach et al. (1994)
pFA-lacZ-kanMX3	*DR-kanMX-DR*	Wach et al. (1994)
pFA-AgCEN5-ARS	*AgCEN5-ARS*, *kanMX6*	Wendland and Philippsen (2000, 2001)
pFA-AgARS	*AgARS*, *kanMX6*	Wendland and Philippsen (2000, 2001)
pRS415-kanMX	*ScLEU2*, *ScCEN6-ARSH4*, *kanMX6*	This study
pRS415-CEN5MX	*ScLEU2*, *AgCEN5-ARS*, *kanMX6*	This study
pRS426-kanMX	2μ-ARS,*kanMX6*	This study
pHsLEU2	PCR fragment of *HsLEU2* in pSK	This study
pHsleu2-kanMX	*Hsleu2::kanMX* disruption cassette	This study
pLC-Shuttle	ScLEU2, kanMX; AgCEN5-ARS	This study
pHC-Shuttle	ScLEU2, kanMX; Ag-ARS	This study

Table 2
Oligonucleotide primers used in this study

Primer number	Sequence of primer[a]
#565	cgc**ggatcc**GGNGCNGTNGGNGGNCCNA ARTGG
#566	ccc**aagctt**ATDATRTCNCCRAACATRTT
#567	ccc**aagctt**CCRTGRCANGGYTCRTANARNCC
#582	GTTCGCCCCGAACAGGGACTC
#583	GCCGAACATATTGCTAGTGAC

[a] Upper case sequences correspond to *H. sinecauda* genomic DNA or are derived from protein sequence alignments and correspond to the degenerate DNA sequence used for amplification of a *H. sinecauda LEU2* gene fragment. Lower case sequences correspond to 5′-terminal regions of primers containing restriction sites (in bold). All sequences are written from 5′ to 3′.

selective media and incubated for 2–3 days. After that cells of these colonies were transferred with a toothpick onto fresh selective plates and incubated for up to 4 days at 30 °C. Growth was readily visible and differences in colony morphology were also observed on the microscopic level.

2.4. Isolation of the HsLEU2 gene fragment

Based on protein sequence alignments degenerate oligonucleotides were designed to amplify an internal fragment of the *HsLEU2* (Table 2). PCR was carried out under standard conditions using genomic *H. sinecauda* DNA prepared as described (Hoffman and Winston, 1987). Sequence Accession Nos. are AY148967–AY148969.

2.5. Transformation

Transformation of *H. sinecauda* with plasmid DNA was conducted using three different protocols without additional modifications. Electroporation was used with protocols established either for *A. gossypii* or *S. cerevisiae* (Becker and Guarente, 1991; Wendland et al., 2000). The lithium-acetate procedure was used according to Gietz et al. (1995). Electroporation of *H. sinecauda* cells turned out to be more efficient than the lithium acetate procedure. A pretreatment with dithiothreitol (DTT) prior to the electric pulse as included in the *A. gossypii* electroporation protocol additionally increased the transformation efficiency twofold. Using the transformation protocol as established for *A. gossypii* 60 transformants/μg of DNA could be recovered whereas the other protocols were much less efficient.

For obtaining a G418 sensitive *leu2* strain the *H. sinecauda leu2::kanMX3* mutant strain was grown for several days in liquid medium until spores were formed. Treatment with zymolyase (10 μg/ml) produced spheroplasts of the remaining unsporulated cells that were lysed by detergent containing buffer (Spore buffer: 0,03% Triton X-100). Spores were obtained by centrifugation and washing steps with spore buffer. Spores were plated onto rich medium plates and grown for 4 days. Finally, replica plating of the colonies onto G418 containing media revealed colonies that had lost the *kanMX3* marker gene.

2.6. Microscopy

All images were taken on a motorized Zeiss Axioplan II imaging microscope. Metamorph 4.6 software was used to control image acquisition with a MicroMax1024 digital camera (Princeton Instruments). Staining procedures were conducted as described previously (Wendland and Philippsen, 2001).

3. Results

3.1. Morphological characterization of H. sinecauda

Colonial growth on solid full media shows elongated true hyphae at the colony edges whereas in comparison *S. cerevisiae* colonies do not form elongated cells (pseudohyphae) under theses conditions (Figs. 1A and B). Although filamentous growth is readily observable at the edges of *H. sinecauda* colonies, in the center of the colonies growth reverts to yeast-like and pseudohyphal growth. Filament formation of *H. sinecauda* occurs on solid media but is reduced in submerse culture which suggests that surface cues/adhesion provide one trigger for morphological switching (our unpublished results).

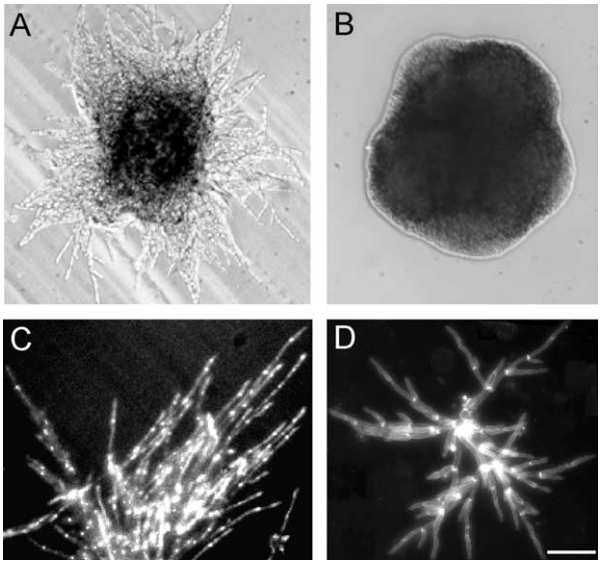

Fig. 1. Micrographs of 2-day-old *H. sinecauda* (A) and *S. cerevisiae* (B) colonies grown on microscopy slides covered with full medium at 30 °C. Images of *H. sinecauda* cells stained for nuclei (C) and septa (D). Bar, 25 μm for (A,B), 10 μm for (C,D).

Fluorescence microscopy showed that individual compartments contained only one nucleus both in the yeast phase (not shown) and during hyphal growth stages (Fig. 1C). Septa were found to be chitin rich and occurred at regular intervals. Lateral branches in *H. sinecauda* could be observed at sites of previous septation as has been described recently in *A. gossypii* (Wendland, 2003) (Fig. 1D).

3.2. Replicative transformation of H. sinecauda

Both *A. gossypii* and *S. cerevisiae* are sensitive to the antibiotic G418/geneticin. Dominant selectable marker genes, *kanMX* and *GEN3*, are available in which expression of the ORF of the kanamycin-resistance gene is controlled by either *AgTEF1* or *ScTEF2* promoter and terminator sequences, respectively. We found that *H. sinecauda* is sensitive to G418 at antibiotic concentrations >200 μg/ml and therefore decided to make use of this dominant selection system using the *kanMX* marker. Furthermore, both *A. gossypii* and *S. cerevisiae* can be transformed with freely replicating plasmids at high frequency. Thus, we tried to establish a transformation system for *H. sinecauda* based on plasmids. Since plasmid replication requires an ARS element for autonomous replication we chose to test three different plasmid constructs containing *kanMX*: (i) a yeast-shuttle vector pRS415 which carries a minimal centromere region of *ScCEN6* in combination with the *S. cerevisiae ARSH4* which is also functional in *A. gossypii*; (ii) a plasmid that was found to promote free replication in *A. gossypii* which contains a 2.8-kb region of *AgCEN5* including the complete and functional *AgCEN5* plus an adjacent ARS element, which, however, is not functional in *S. cerevisiae* (Wendland and Philippsen, unpublished); and (iii) a plasmid carrying this *AgARS* without the *AgCEN5* on a 1-kb fragment. *AgCEN5* resembles centromeric DNA of *S. cerevisiae* and also contains three centromeric DNA elements (CDEI, II, and III), only that CDEII is 160 bp in length instead of approximately 80 bp as in yeast (Wendland and Philippsen, unpublished results). After an incubation of 2–3 days, we observed transformant colonies of different sizes for each of the plasmid constructs used (Fig. 2A, top row). Cells transformed with pFA-AgCEN5-ARS formed large colonies, whereas cells transformed with pFA-AgARS were much smaller although they occurred with the same frequency. In contrast fewer transformants could be obtained with pRS415-kanMX (Fig. 2A, top row). To test whether this phenotype was still present after prolonged cultivation six transformants with each construct were restreaked onto new selective media. The difference in colony size between AgCEN5-ARS in comparison to AgARS plasmid transformants remained, whereas pRS415-kanMX transformants turned out to be abortive (Fig. 2A, bottom row). Additionally, we tested the *kanMX* marker on a yeast 2μ-ARS plasmid but were also unable to obtain stable transformants (not shown).

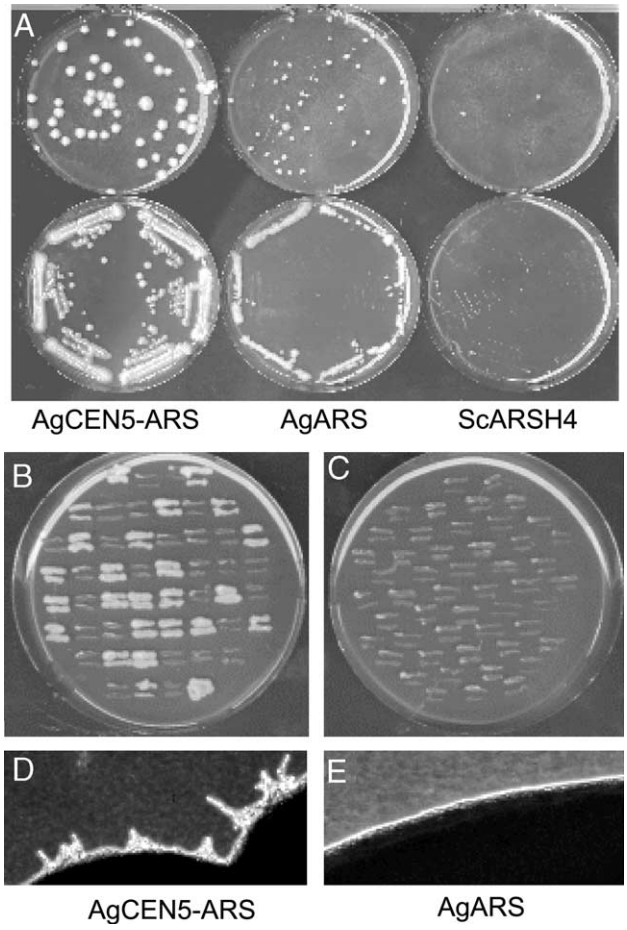

Fig. 2. Replicative transformation and heterologous centromere function in *H. sinecauda*. Transformation was performed with the indicated plasmids. Transformants were first plated on primary selective plates (A, top row). Six transformants from each of these plates were picked and restreaked on new selective plates (A, bottom row). Plasmid stability assays were performed with transformants carrying either AgCEN5-ARS (B,D) or AgARS (C,E) plasmids, respectively. After a non-selective growth period, 50 transformants each were restreaked on newly selective plates (B,C) and grown for 4 days at 30 °C. Transformants carrying the AgCEN5-ARS plasmid showed filaments at the colony edge (D), whereas AgARS transformants (as well as those AgCEN5-ARS transformants) that had lost their plasmids were abortive in growth and showed smooth colony edges (E). Plates were incubated for 4 days at 30 °C before photography.

3.3. Heterologous centromere function of AgCEN5 in H. sinecauda

We went on to examine whether the difference in colony size of the transformants could be due to either integration of the plasmid into the genome, a difference in ARS function or the heterologous function of *AgCEN5* circumventing a mother-bias in plasmid distribution and resulting in a 1:1 plasmid segregation. Two lines of evidence indicated that both plasmid constructs

were freely replicating in *H. sinecauda*: (i) upon prolonged incubation under non-selective conditions plasmid loss measured as the loss of G418 resistance was observed (see below) and (ii) isolation of genomic DNA of the transformants and retransformation into *E. coli* yielded kanamycine-resistant colonies. Isolation and restriction analyses confirmed the correct sizes of the plasmids used (data not shown). Additionally, both of the plasmids used are freely replicating in *A. gossypii*. Furthermore, the comparable transformation efficiency of both plasmids in *H. sinecauda* also suggests that ARS function was not impaired. Therefore, we tested whether *AgCEN5* could enhance plasmid stability of freely replicating plasmids in *H. sinecauda* under non-selective conditions (Figs. 2B–E). Our tests revealed that ARS plasmids are rapidly lost under non-selective conditions (Fig. 2C) in *H. sinecauda*, whereas AgCEN5-ARS plasmids are retained at high frequency such that approximately 50% of the colonies were able to regrow under the conditions used (Fig. 2B). On the microscopic level growth was evident as the ability to form filaments at the colony edges whereas abortive colonies showed smooth edges containing yeast cells only that had stopped to proliferate (Figs. 2D and E).

3.4. Isolation and disruption of HsLEU2

We isolated a fragment of the *HsLEU2* gene using degenerate PCR primers. In pairwise comparisons the fragment of the deduced HsLeu2p shared 70.6% amino acids sequence identity with AgLeu2p and 68.9% with the ScLeu2p. With the cloned 0.5 kb *LEU2* PCR fragment, we constructed a disruption cassette by inserting the *kanMX3* marker gene that bears terminal direct repeats into this fragment resulting in 5′ and 3′ flanking homology regions to the *HsLEU2* gene of 150 and 380 bp, respectively (Fig. 3A). This cassette was excised from the vector and used for transformation. Correct integration of the cassette into the *HsLEU2* locus was verified by analytical PCR (not shown). The constructed *HsLEU2* strain was resistant to the antibiotic drug G418. Spores that were initially grown on non-selective plates were replicated onto G418 containing plates which allowed the isolation of a *Hsleu2* strain that was sensitive to G418. Analytical PCR indicated that this strain was generated by marker excision at the *LEU2* locus that had left behind one copy of the direct repeat (Figs. 3B and C).

With a *H. sinecauda leu2* strain at hand, we were able to test for heterologous complementation of *Hsleu2* with a plasmid carrying *ScLEU2*. To this end, *Hsleu2* cells were transformed with the plasmid pRS415-CEN5MX. Transformants were able to grow on minimal media lacking leucine indicating the heterologous function of *ScLEU2* in *H. sinecauda* (Fig. 4).

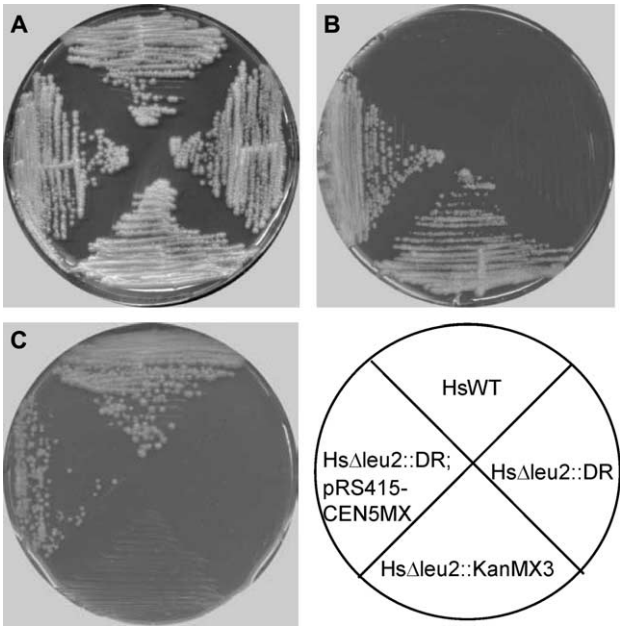

Fig. 4. Heterologous complementation and strain construction with *H. sinecauda*. Growth of the indicated strains on either rich medium (A), rich medium supplemented with 200 μg/ml G418 (B), and minimal medium lacking leucine (C) indicated the relevant properties of the strains.

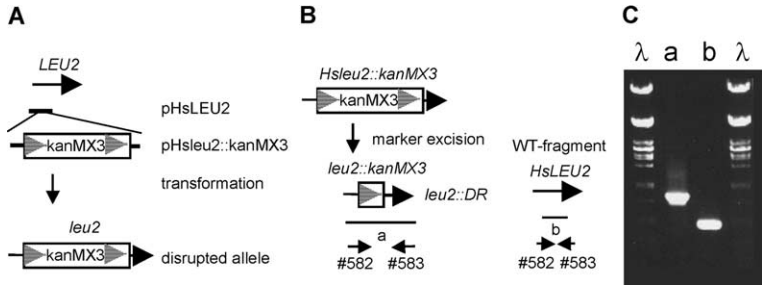

Fig. 3. Isolation and disruption of *HsLEU2*. (A) Schematic drawing showing the construction of a *HsLEU2* disruption cassette and integration into the *HsLEU2* gene. (B) Marker excision via homologous recombination leaving behind one direct repeat disrupting the *HsLEU2* gene as compared to the wild-type locus. (C) Image of an ethidium bromide-stained agarose gel showing products of PCR verification of the marker excision in comparison to wild-type using the indicated primers.

These results were incorporated in the construction of a new vectors that allow plasmid shuttling between *H. sinecauda* and *A. gossypii*. Both vectors are based on pRS405 which carries the *ScLEU2* and sequences for proliferation and blue–white colony selection in *E. coli*. Plasmid LC-Shuttle contains the AgCEN5-ARS designed to generate low-copy numbers whereas pHC-Shuttle only contains the AgARS to generate high-copy number *H. sinecauda* plasmid transformants.

4. Discussion

The morphological transition of dimorphic fungi from the yeast phase to the hyphal phase has been a focus of recent research because of (i) the expected simplicity to study eukaryotic cell differentiation and (ii) the role of hyphal growth in the virulence of *C. albicans*, for example, and the resulting potential for the development of new antifungal drugs (Sanchez-Martinez and Perez-Martin, 2001). Comparison of rDNA sequences indicated that the dimorphic fungus *H. sinecauda* is most closely related to *A. gossypii* which grows in a strictly filamentous form (Kurtzman, 1995; Prillinger et al., 1997; Wendland et al., 1999). On this basis a developmental genetic approach to analyze and compare morphological transitions seems to be very fruitful with the *H. sinecauda* and *A. gossypii* species pair. To be able to promote molecular genetic studies in *H. sinecauda*, we developed the essential tools for transformation of this fungus. In our efforts to establish replicative transformation, we found that ARS elements derived from *S. cerevisiae* (either ARSH4 or 2μ-ARS) were not able to promote efficient replication in *H. sinecauda* since only abortive transformants were obtained. This finding was surprising since these ARS elements allow the propagation of freely replicating plasmids in *A. gossypii* and also in other yeast species, e.g., *Schwanniomyces occidentalis* (Janatova et al., 2000; Wendland and Philippsen, 2000, 2001; Wright and Philippsen, 1991). The ARS element that proved to be functional in *H. sinecauda* was the ARS element associated with the *A. gossypii CEN5*. Heterologous AgARS and AgCEN5 function in *H. sinecauda* further support the close relationship between *H. sinecauda* and *A. gossypii* since these two *A. gossypii* DNA elements were found not to be functional in *S. cerevisiae* (Wendland and Philippsen, unpublished results). The only other example of heterologous centromere function described so far has been that of *S. uvarum* centromeric DNA in *S. cerevisiae* which also represent two very closely related species (Huberman et al., 1986). *H. sinecauda* plasmid transformants did not integrate the episomal DNA into the genome at detectable levels and plasmid loss could readily be observed. Therefore, replicative transformation in *H. sinecauda* may be very useful for the overexpression of genes or the increase in copy number of genes without requiring gene targeting into the genome. This opens the way to study the effects of overexpressed genes on the dimorphic switch.

Successful gene deletion was shown with the targeted integration at the *LEU2* locus. Additionally, direct repeat-induced marker excision was performed generating a strain that allows the use of two selectable markers which will be very useful for gene deletion and subsequent complementation experiments.

Acknowledgments

We are deeply indebted to the students of the Friedrich-Schiller University's Yeast Genetics Classes I, II, and III which participated in this work during their studies (http://pinguin.biologie.uni-jena.de/phytopathologie/pathogenepilze/index.html). We thank Rong Li for providing strains and Erika Kothe for discussions. Parts of this work were funded by the Friedrich-Schiller University and the Hans-Knöll Institute.

References

Becker, D.M., Guarente, L., 1991. High-efficiency transformation of yeast by electroporation. Methods Enzymol. 194, 182–187.

Brown, A.J., Gow, N.A., 1999. Regulatory networks controlling *Candida albicans* morphogenesis. Trends Microbiol. 7, 333–338.

Christianson, T.W., Sikorski, R.S., Dante, M., Shero, J.H., Hieter, P., 1992. Multifunctional yeast high-copy-number shuttle vectors. Gene 110, 119–122.

Gietz, R.D., Schiestl, R.H., Willems, A.R., Woods, R.A., 1995. Studies on the transformation of intact yeast cells by the LiAc/SS-DNA/PEG procedure. Yeast 11, 355–360.

Hoffman, C.S., Winston, F., 1987. A 10-min DNA preparation from yeast efficiently releases autonomous plasmids for transformation of *Escherichia coli*. Gene 57, 267–272.

Holley, R.A., Allan-Wojtas, P., Phipps-Todd, B.E., 1984. *Nematospora sinecauda* sp. nov., a yeast pathogen of mustard seeds. Antonie Van Leeuwenhoek 50, 305–320.

Huberman, J.A., Pridmore, R.D., Jäger, D., Zonneveld, B., Philippsen, P., 1986. Centromeric DNA from *Saccharomyces uvarum* is functional in *Saccharomyces cerevisiae*. Chromosoma 94, 162–168.

Janatova, I., Gourdon, P., Meilhoc, E., Klein, R.D., Masson, J.M., 2000. ARS sequences in homologous and heterologous *ADE2* loci are capable of promoting autonomous replication of plasmids in *Schwanniomyces occidentalis*. Curr. Genet. 37, 298–303.

Kurtzman, C.P., 1995. Relationships among the genera *Ashbya*, *Eremothecium*, *Holleya*, and *Nematospora* determined from rDNA sequence divergence. J. Ind. Microbiol. 14, 523–530.

Mayorga, M.E., Gold, S.E., 1999. A MAP kinase encoded by the *ubc3* gene of *Ustilago maydis* is required for filamentous growth and full virulence. Mol. Microbiol. 34, 485–497.

Prillinger, H., Schweigkofler, W., Breitenbach, M., Briza, P., Staudacher, E., Lopandic, K., Molnar, O., Weigang, F., Ibl, M., Ellinger, A., 1997. Phytopathogenic filamentous (*Ashbya*, *Eremothecium*) and dimorphic fungi (*Holleya*, *Nematospora*) with needle-shaped ascospores as new members within the *Saccharomycetaceae*. Yeast 13, 945–960.

Sanchez-Martinez, C., Perez-Martin, J., 2001. Dimorphism in fungal pathogens: *Candida albicans* and *Ustilago maydis*—similar inputs, different outputs. Curr. Opin. Microbiol. 4, 214–221.

Sikorski, R.S., Hieter, P., 1989. A system of shuttle vectors and yeast host strains designed for efficient manipulation of DNA in *Saccharomyces cerevisiae*. Genetics 122, 19–27.

Wach, A., Brachat, A., Pöhlmann, R., Philippsen, P., 1994. New heterologous modules for classical PCR-based gene disruptions in *Saccharomyces cerevisiae*. Yeast 10, 1793–1808.

Wendland, J., 2003. Analysis of the landmark protein Bud3p of *Ashyba gossypii* reveals a novel role in septum construction. EMBO Rep. 4, 200–204.

Wendland, J., Ayad-Durieux, Y., Knechtle, P., Rebischung, C., Philippsen, P., 2000. PCR-based gene targeting in the filamentous fungus *Ashbya gossypii*. Gene 242, 381–391.

Wendland, J., Philippsen, P., 2000. Determination of cell polarity in germinated spores and hyphal tips of the filamentous ascomycete *Ashbya gossypii* requires a rhoGAP homolog. J. Cell Sci. 113, 1611–1621.

Wendland, J., Philippsen, P., 2001. Cell polarity and hyphal morphogenesis are controlled by multiple rho-protein modules in the filamentous ascomycete *Ashbya gossypii*. Genetics 157, 601–610.

Wendland, J., Pöhlmann, R., Dietrich, F., Steiner, S., Mohr, C., Philippsen, P., 1999. Compact organization of rRNA genes in the filamentous fungus *Ashbya gossypii*. Curr. Genet. 35, 618–625.

Wright, M.C., Philippsen, P., 1991. Replicative transformation of the filamentous fungus *Ashbya gossypii* with plasmids containing *Saccharomyces cerevisiae* ARS elements. Gene 109, 99–105.

5

Andrea Walther

Jürgen Wendland

Polarized hyphal growth in *Candida albicans* requires the WASp homolog Wal1p.

Eukaryot. Cell., 3(2): 471-482.

Der morphologische Wechsel von der Hefe- in die Hyphenphase ist eine wichtige Eigenschaft des humanpathogenen Pilzes *C. albicans*. Dafür ist die Reorganisation des Aktinzytoskeletts erforderlich. Die Deletion von *WAL1* führte zu Defekten in der Organisation des Aktinzytoskeletts und dem Verlust der Zellen, Hyphen ausbilden zu können. Weiterhin zeigten *wal1* Zellen einen Defekt in der Endozytose und der Vakuolenmorphologie.

EUKARYOTIC CELL, Apr. 2004, p. 471–482 Vol. 3, No. 2
1535-9778/04/$08.00+0 DOI: 10.1128/EC.3.2.471–482.2004

Polarized Hyphal Growth in *Candida albicans* Requires the Wiskott-Aldrich Syndrome Protein Homolog Wal1p†

A. Walther and J. Wendland*

Junior Research Group: Growth Control of Fungal Pathogens, Hans-Knöll Institute for Natural Products Research and Department of Microbiology, Friedrich-Schiller University, Jena D-07745, Germany

Received 26 July 2003/Accepted 1 December 2003

The yeast-to-hypha transition is a key feature in the cell biology of the dimorphic human fungal pathogen *Candida albicans*. Reorganization of the actin cytoskeleton is required for this dimorphic switch in *Candida*. We show that *C. albicans WAL1* mutants with both copies of the Wiskott-Aldrich syndrome protein (WASP) homolog deleted do not form hyphae under all inducing conditions tested. Growth of the wild-type and *wal1* mutant strains was monitored by in vivo time-lapse microscopy both during yeast-like growth and under hypha-inducing conditions. Isotropic bud growth produced round *wal1* cells and unusual mother cell growth. Defects in the organization of the actin cytoskeleton resulted in the random localization of actin patches. Furthermore, *wal1* cells exhibited defects in the endocytosis of the lipophilic dye FM4-64, contained increased numbers of vacuoles compared to the wild type, and showed defects in bud site selection. Under hypha-inducing conditions *wal1* cells were able to initiate polarized morphogenesis, which, however, resulted in the formation of pseudohyphal cells. Green fluorescent protein (GFP)-tagged Wal1p showed patch-like localization in emerging daughter cells during the yeast growth phase and at the hyphal tips under hypha-inducing conditions. Wal1p-GFP localization largely overlapped with that of actin. Our results demonstrate that Wal1p is required for the organization of the actin cytoskeleton and hyphal morphogenesis in *C. albicans* as well as for endocytosis and vacuole morphology.

Polarized cell growth is a basic feature of the morphogenesis of a cell. Highly elongated cell growth can be found in specialized cells such as neurites, plant root hairs, and pollen tubes but is most prominent in fungal hyphae (10, 21, 45). Fungi grow either a in yeast-like or filamentous manner. Dimorphic fungi are able to switch between these two growth modes. A dimorphic transition occurs in a variety of pathogenic fungi such as the maize pathogen *Ustilago maydis* and the human pathogen *Candida albicans* (6, 32). In *C. albicans* the ability to initiate hyphal growth is associated with its virulence (27). Polarized growth in ascomycetous fungi is dependent on the actin cytoskeleton, whereas microtubules are not required to initiate hyphal extensions (19, 52). Rho protein modules are central regulators for the organization of the actin cytoskeleton (12). In fungal cells these modules determine the establishment of cell polarity and the maintenance of hyphal growth (12, 48). The actin cytoskeleton can be divided into two components: actin cables and cortical actin patches. Actin cables in *Saccharomyces cerevisiae* are positioned in a mother-daughter axis and serve as tracks for the transport of secretory vesicles delivering plasma membrane and cell wall compounds to sites of growth (37). The yeast formin Bni1p plays a key role in the Arp2/3-independent assembly of actin cables (14, 15, 38, 40). Cortical actin patches are positioned at sites of exo- and endocytosis. They localize to sites of polarized growth, for example, to the growing bud and to hyphal tips in *C. albicans* and to the hyphal tips in filamentous fungi (for reviews, see references 37 and 45). However, the role of cortical actin patches during polarized growth or hypha formation in both *S. cerevisiae* and *C. albicans* has been questioned (5, 36). In *S. cerevisiae* the Arp2/3 complex was shown to be required for endocytosis and the assembly of actin patches (30, 49). The Arp2/3 complex can be activated by the *S. cerevisiae* homolog of the human Wiskott-Aldrich Syndrome protein (WASP), encoded by the *LAS17/BEE1* gene (9, 50). In our efforts to understand signaling routes to the actin cytoskeleton, we identified the *C. albicans* WASP homolog and characterized its role for polarized morphogenesis and hyphal growth in *C. albicans*. Mutant *wal1* cells were not able to produce hyphae under all conditions tested. Surprisingly, even though *wal1* yeast cells grew isotropically, initiation of polarized morphogenesis occurred under hypha-inducing conditions and resulted in the formation of elongated, pseudohyphal cells. In addition to the defects in the organization of the actin cytoskeleton, *wal1* mutants showed defects in endocytosis and vacuolar morphology.

MATERIALS AND METHODS

Strains and media. The *C. albicans* and *S. cerevisiae* strains used in this study are listed in Table 1. Growth media and standard procedures were described previously (44). Maltose (2%) was supplied as the sole carbon source to induce expression from the *MAL2* promoter.

Construction of disruption cassettes. The *C. albicans* WASP homolog *WAL1* was identified in the genomic sequence (http://www-sequence.stanford.edu/group/candida) and contains an open reading frame (ORF) of 2,142 bp. Based on this sequence, two primers were designed (primer sequences are listed in Table 2), KpnI-WAL1 (no. 556) and XbaI-WAL1 (no. 557), to amplify a 1,551-bp fragment from genomic *C. albicans* DNA containing the 5′ end of the *WAL1* ORF. This fragment was cloned into pBluescript SK(+) using the terminally attached restriction sites, generating pSK-5′WAL1. The sequence of the

* Corresponding author. Mailing address: Department of Mikrobiology, Hans-Knoell Institute for Natural Products Research e.V. and Friedrich-Schiller-University, Hans-Knoell Str.2/Winzerlaer Str. 10, D-07745 Jena, Germany. Phone: 49-3641-65-7639. Fax: 49-3641-65-7633. E-mail: juergen.wendland@uni-jena.de.

† Supplemental material for this article may be found at http://ec.asm.org/.

TABLE 1. Strains used in this study

Strain	Genotype	Reference
C. albicans		
SC5314	Wild type	15a
BWP17	*ura3*::λ*imm34*/*ura3*::λ*imm34 his1*::*hisG*/*his1*::*hisG*/*arg4*::*hisG*/*arg4*::*hisG*	48a
CAT4	*WAL1*/*wal1*::*HIS1* in BWP17	This study
CAT5	*WAL1*/*wal1*::*URA3* in BWP17	This study
CAT6	*wal1*::*URA3*/*wal1*::*HIS1* in BWP17	This study
CAT10	*wal1*::*MAL2p-WAL1*:*HIS1*/*wal1*::*URA3* in BWP17	This study
CAT19	*WAL1-GFP*:*HIS1*/*WAL1* in BWP17	This study
CAT20	*WAL1-GFP*:*URA3*/*WAL1* in BWP17	This study
CAT21	*WAL1-GFP*:*HIS1*/*wal1*::*URA3* based on CAT19	This study
S. cerevisiae		
RLY157	*MAT***a** *ura3-52 his3-*Δ*200 leu2-3,112 lys2-801Dbee1*::*LEU2*	25
YMW171K	*MAT***a** *las17*::*kanMX4 ade2-101 his3-200 leu2-1 lys2-801 trp1-63 ura3-52*	28
RH4207	*MAT***a** *las17*::*kanMX4 bar1*::*LYS2 ade2-101 his3-200 leu2-1 trp1-63 ura3-52*	28

insert was verified (MWG-Biotech, Ebersberg, Germany). Cleavage of this plasmid by HincII and ClaI resulted in the removal of an internal 460-bp fragment of the insert, which was replaced by the selectable marker genes *URA3* and *HIS1*, respectively, which were excised from pFA-URA3 and pFA-HIS1 (16) with PvuII-ClaI and HincII-ClaI, respectively. In this way, plasmids pSK-Cawal1::URA3 and pSK-Cawal1::HIS1 were generated that carry disruption cassettes in which the selectable marker genes are flanked by 235 bp at the 5′ end and 821 bp at the 3′ end with regions from the *WAL1* target locus. Both disruption cassettes were released from the plasmid backbone prior to transformation by cleavage with XbaI and KpnI. With the development of the pFA vector series (16), further genetic manipulations were carried out using PCR-based approaches.

Construction of *MAL2* promoter-*WAL1* ORF fusion. To place *WAL1* under control of the regulatable *MAL2* promoter, a PCR-based approach was applied. To this end, a cassette was amplified from plasmid pFA-HIS1-MAL2p (16) with primers 676 and 677. With these primers, 100 bp of sequence with homology to two positions at the 5′ end of the *WAL1* gene was added to the cassette. This PCR fragment was used to transform a heterozygous *WAL1*/*wal1*::*URA3* strain, placing the only copy of *WAL1* under regulated expression.

Construction of the *WAL1-GFP* fusion. To generate a *WAL1-GFP* fusion, a similar PCR-based approach was applied. Transformation cassettes were amplified from pFA-GFP-URA3 and pFA-GFP-HIS1 using primers 956 and 957, which, again, added 100 bp of flanking homology region to the FA cassettes (the green fluorescent protein [GFP] variant used in these constructs was derived from plasmids described previously [8, 33]). The amplified PCR fragments were transformed into strain BWP17, generating strains CAT19 and CAT20, in which one allele of *WAL1* was tagged with GFP while the other allele remained wild type. Using CAT19 in another PCR-targeting experiment, the remaining wild-type copy of *WAL1* was deleted with a disruption cassette generated with primers 676 and 957 using pFA-URA3 as the template. The resulting strain, CAT21, carries only the GFP-tagged *WAL1* allele under its endogenous promoter, thus producing only Wal1 protein tagged with the GFP moiety. All three GFP-tagged strains revealed similar GFP signals. However, CAT21 produced brighter GFP signals than did the heterozygous strains.

Transformation of *C. albicans*. The lithium acetate procedure was used as described previously (44). Basic features of this protocol include an overnight incubation with lithium acetate and a subsequent heat shock for 15 min at 44°C. Correct gene targeting was verified by PCR analysis of the transformants. Locus- and marker-specific primers were as listed in Table 2.

Hyphal induction of *C. albicans*. Different protocols were used to induce hypha formation in *C. albicans* strains at 37°C. Hyphal induction occurred most vigorously in minimal medium containing 10 to 20% serum (calf serum; Sigma). Alternatively, hyphal induction was carried out in spider medium (26). Plates inoculated with different strains were incubated for 4 to 7 days before being photographed. Hyphal induction was also tested in liquid minimal media.

Time-lapse microscopy. Strains were pregrown in either complete or minimal medium, harvested, washed, and resuspended in sterile water. Small aliquots of cells were applied on deep-well slides prepared as described previously (20). It was of utmost importance to provide sufficient oxygen supply to the cells within the medium to support the growth of *C. albicans*. To achieve this, the medium was vigorously vortexed prior to the preparation of microscopy slides, using a FVL2400 Combi-Spin vortex (Peqlab, Erlangen, Germany). Minimal medium or full medium (supplemented with 10 to 20% serum for hyphal induction) was diluted 1:1 with water-agarose containing 3.4% agarose. Temperature control was achieved with a heat stage (built at the Biozentrum Basel and generously provided by P. Philippsen) which was mounted on the microscope table and heated with a water bath. All microscopy was done on a motorized Zeiss Axioplan II imaging microscope. Images were acquired using Metamorph 4.6 software (Universal Imaging Corp.) and a digital imaging system (MicroMax1024; Princeton Instruments). Images were collected into stacks. Stacks containing bright-field/differential interference contrast (DIC) images were processed separately from images displaying GFP or vacuolar fluorescence. The stacks were than combined by using overlay tools of the Metamorph software and processed as videoclips with a frame rate of 10 images/s.

Staining procedures. For actin staining, early-log-phase cells were fixed with 3.7% formaldehyde. Fixation and incubation with rhodamine-phalloidin were performed essentially as described previously (36). Chitin staining was done by directly adding calcofluor (1 μl of a 1-mg/ml stock) to 100 μl of cell suspension, incubating for 15 min, and washing. Vacuolar staining was done using the lipophilic dye FM4-64 (43). For the analysis of vacuolar morphology, overnight cultures grown in YPD were used. Cells were incubated with FM4-64 (0.2 μg/ml) for 30 min at 30°C and then photographed. For FM4-64 time-lapse microscopy, exponentially grown cells of the wild type and the *wal1* mutant strain were placed on precooled microscope slides containing medium made of equal amounts of YPD and 3.4% water-containing agarose. GFP-images were obtained from early-log-phase cells grown in 0.25 × YPD that were washed once with water and resuspended in water. For GFP and actin colabeling, cells were fixed and stained with rhodamine-phalloidin as described above; the GFP signal was obtained using a narrow-band GFP filter set which excludes the actin signal monitored by a tetramethylrhodamine-5-isothiocyanate (TRITC) filter set. Other images were acquired using the appropriate filter sets (Chroma Technology).

Heterologous complementation. The *C. albicans WAL1* ORF was amplified from a plasmid library (kindly provided by J. Ernst) by using primers 975 and 976. The resulting PCR product carried terminal flanking homology regions to the *Ashbya gossypii TEF1* promoter and *TEF1* terminator. This PCR product was cotransformed into an *S. cerevisiae bee1*/*las17* strain together with NruI-linearized plasmid pRS415-kanMX carrying the KanMX selection marker (as described in reference 46). Transformant colonies appeared after 2 days of growth at 30°C on selective plates lacking leucine. Digestion of pRS415-kanMX with NruI cleaves a unique restriction site within the *kan* ORF. The *S. cerevisiae* in vivo recombination machinery was used to recombine the plasmid and PCR fragment, thus generating a new plasmid, pXL-CaWAL1, in which the *WAL1* ORF is placed under control of the *A. gossypii TEF* promoter (this promoter is functional in *S. cerevisiae*). Transformant colonies were restreaked on new selective plates and incubated at 37°C, the restrictive temperature for *bee1*/*las17* strains. Transformants that continued to grow were selected, and plasmid DNA was isolated from these transformants and amplified in *Escherichia coli*. Correct fusion that generated pXL-CaWAL1 was verified by PCR, restriction, and sequence analyses. Retransformation of pXL-WAL1 into *S. cerevisiae bee1*/*las17* cells revealed that heterologous complementation by pXL-CaWAL1 was dependent on a period (6 h) of growth at 30°C prior to the shift to 37°C. This preincubation was not required when using a plasmid carrying the *BEE1*/*LAS17*

gene, suggesting that even on overexpression of *WAL1* with the *AgTEF1* promoter, Wal1p is not fully competent to take over the position of Bee1p/Las17p.

RESULTS

The unique gene *WAL1* encodes the *C. albicans* WASP homolog. The *C. albicans* genome database at Stanford University was searched for sequences homologous to the human WASP. A single ORF was found which corresponds to orf19.6598.prot. This gene was designated *WAL1* (for "Wiskott-Aldrich syndrome-like"). Its ORF is 2,139 bp and encodes a 713-amino-acid protein with an apparent molecular mass of 76.9 kDa. Wal1p shows the highest sequence identity at the amino acid level to *S. cerevisiae* Las17p/Bee1p (37.6%) and *Schizosaccharomyces pombe* Wsp1p (27.7%). WASP family members contain specific functional domains including an amino-terminal WH1 domain and the carboxy-terminal WH2-C-A domain. Within these domains, conservation is particularly high, reaching 75% for WH1 domains and 60% for the acidic C terminus (Fig. 1). In contrast, the internal proline-rich region is rather divergent. Sequence analysis of Wal1p and all other fungal WASPs identified so far indicated that they do not contain Cdc42/Rac interactive binding (CRIB) motifs. Furthermore, heterologous complementation of the *S. cerevisiae bee1*/*las17* temperature-sensitive mutant phenotype with *WAL1* indicated that *WAL1* encodes the functional homologue of Bee1p/Las17p (for details, see Materials and Methods).

***WAL1* is not essential for cell viability in *C. albicans*.** To be able to study the function of *WAL1* in *C. albicans*, homozygous mutant strains were generated from independent heterozygous strains. Strain BWP17 was chosen as the progenitor strain since its auxotrophies enabled the sequential disruption of both alleles with the *HIS1* and *URA3* marker genes (for details, see Materials and Methods).

wal1::*HIS1*/*wal1*::*URA3* mutant strains were phenotypically identical, indicating that correct gene targeting had occurred as verified by analytical PCR. Additionally, starting from a heterozygous mutant strain (*WAL1*/*wal1*::*URA3*), the remaining copy of *WAL1* was placed under the control of the regulatable *MAL2* promoter, which is repressed in a glucose-containing regimen but can be induced by growth on maltose (see Materials and Methods). This strain (*wal1*::*MAL2p-WAL1*::*HIS1*/*wal1*::*URA3*) behaved phenotypically like the wild-type strain when grown on maltose but showed the WASP mutant phenotypes described below when grown on glucose. Thus, the deletion of *WAL1* is solely responsible for the observed morphological phenotypes of the *wal1* strains. Strains bearing disruptions in the *WAL1* genes or strains in which the expression of *WAL1* is downregulated are viable, demonstrating that *C. albicans WAL1* is not an essential gene.

The *S. cerevisiae* WASP mutant *bee1*/*las17* is temperature sensitive and does not grow at temperatures above 34°C (25). In contrast, growth of the *C. albicans* WASP mutant either in liquid culture or on solid-medium plates was not inhibited in the temperature range tested (20 to 42°C) (data not shown).

Wal1p is required for polarized cell growth during the yeast growth phase. We used digital in vivo microscopy to monitor and compare growth of the wild type (Fig. 2A) with growth of a *wal1* strain (Fig. 2B) (see Movies S1 to S3 in the supplemental material, which also includes a movie of the heterozygous

TABLE 2. Oligonucleotide primers used in this study

Primer no.	Primer name	Sequence[a]
392	XFP-primer	*CATAACCTTCGGGCATGGCACTC*
397	TEF-term	**CTGGGCAGATGTCGAGGC**
511	TEF-prom	**AGGATTTGCCACTGAGGTTCTTC**
549	G4-CaWAL1	CATATCAACTTAAATTTGGG
555	G1-CaWAL1	CCTTATATTCTCATCCATCC
556	KpnI-WAL1	ttcc**ggtacc**GGATAATATGATGATCAACTGTAGTTG
557	XbaI-WAL1	ataa**tctaga**CCAATGAATCTATTTTTTACCACTC
577	G1-WAL1	CCAATGAATCTATTTTTTACCACTC
599	U3	GGAGTTGGATTAGATGATAAAGGTGATGG
600	U2	GTGTTACGAATCAATGGCACTACAGC
601	H2	CAACGAAATGGCCTCCCCTACCACAG
602	H3	GGACGAATTGAAGAAAGCTGGTGCAACCG
676	S1-CaWAL1	GAATAACTTTGAATCACTTTCAAATAATTTTTTCTTTTTTCTTTCTTCCTCCTCGCGGGAATACTGAGTGAGTGGATGGGTGAGTGAGTGA GTCGGgaagcttcgtacgctgcaggtc
677	S1-MAL2p-WAL1	ATATAATCGAGCCACCGTTGCATCGATTATTTTATTGTTGGCTTTTGGAATAGCCCGTTTAACTTTTTCTTTATCTTGAGTAGTTAATATCCCCATtg tagttgattattagttaaaccac
720	G1-CaWAL1-GFP	ccg**gaattc**GCTAATACTGGCGGAGGAATTTC
742	G4-MAL2-WAL1	CGTTGAGCAGTATTCACATCC
956	S1-CaWAL1-GFP	AGCCGATGCACCACCTGCTACTTTAGCCGATGCATTAGCTTCTGCTTTGAATAAGAGGAAAGAAAAAGTTGCTCAAAGTGATGATGAAGAAGAT GATGATTGGggtctggcgcaggtgcttc
957	S2-CaWAL1	GTTACTTCATCTTTATAATTTTTATCTTGATTGAATATCCGAAACATTCAAACATTTCAATCACTCGGCAACTATCCTTAATTTTCGTATTTTTTTATTG Gtctgatatcatcgatgaattcgag
975	XL1-CaWAL1	TCTTGCTAGGATACAGTTCTCACATCACATCCGAACATAAACAACCatgggatattaactactcagataaag
976	XL2-CaWAL1	ATGACAAGTTCTTGAAAACAAGAATCTTTTTATTGTCAGTACTGAttaccaatcatcatcttctcatcac

[a] Capital letters correspond to *C. albicans* genomic DNA. Bold capital letters correspond to the *A. gossypii TEF* promoter or *TEF* terminator. Italic capital letters correspond to GFP. Lowercase letters correspond to 5′- terminal regions of primers containing restriction sites (bold) or to 3′-terminal annealing regions for the amplification of transformation cassettes. All sequences are written from 5′ to 3′.

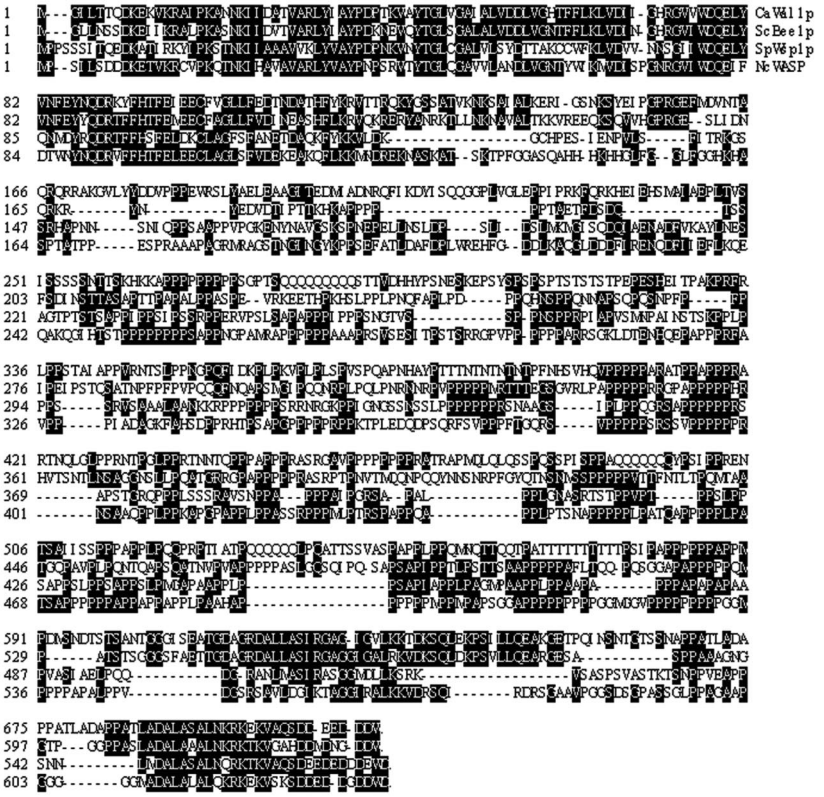

FIG. 1. Alignment of fungal WASP homologs. Amino acids corresponding to a majority of aligned sequences are shaded. Accession numbers: *C. albicans* Wal1p, orf19.6598.prot (http://www-sequence.stanford.edu/group/candida/index.html), *S. cerevisiae* Bee1p/Las17p, NP01482; *S. pombe* Wsp1p, NP594758; *Neurospora crassa* WASP, NCU07438.1 (http://www-genome.wi.mit.edu/annotation/fungi/neurospora/).

mutant strain). With our setup, we were able to monitor the growth of the strains over a period of approximately 10 h (sometimes up to 15 h). In contrast to similar studies with *S. cerevisiae* cells, it was essential to provide sufficient oxygen when growing *C. albicans* cells under these conditions (see Materials and Methods). We analyzed the *wal1* mutant strains, their BWP17 progenitor strain, and the wild-type strain (SC5314) for growth defects during the yeast stage. *WAL1*$^+$ cells were ellipsoidal. In contrast, *wal1* cells were found to be round and of heterogeneous size, with several cells clumping together. To quantify the cell morphology defect of *wal1* cells, we measured the lengths and widths of *WAL1* and *wal1* cells (Fig. 3A). Cell indices (length/width) of wild-type, BWP17, and heterozygous mutant strains were 1.3, corresponding to the ellipsoidal cell shape. This indicates that heterozygosity of *WAL1* did not result in morphological defects and that a single copy of *WAL1* is sufficient for wild-type-like growth. In contrast, the cell index of the *wal1* strain was 1.1, representing an almost spherical cell shape. The ability to form new buds was not affected in *wal1* cells. In the wild-type strain, bud emergence was followed by a period of polarized growth (Fig. 3B). *wal1* cells, however, quickly began to grow in an isotropic manner, which resulted in a decrease of the polarized-growth rate (Fig. 3B). Due to the extended duration of our time-lapse recordings, we were able to observe several consecutive cell divisions of wild-type and *wal1* cells. The time required for two consecutive bud emergence events of a single cell was used to calculate the average time of a cell cycle (Fig. 3C). Growth delays in the mutant strains were at least in part attributable to the remaining auxotrophies, since the heterozygous *WAL1*/*wal1*::*HIS1* strain grew more slowly than a heterozygous *WAL1*/*wal1*::*URA3* strain, which is a general feature that has been observed in other mutant strains as well (our unpublished results). In line with this observation, both of the heterozygous mutant strains required more time to complete a cell cycle than the homozygous mutant strain which carries only the *arg4* auxotrophy. The cell cycle times observed in the in vivo time-lapse recordings were found to be similar to the growth rates in liquid culture (data not shown). Cells of the *wal1* mutant appeared to be of heterogenous size. To analyze this in more detail, we monitored cell size changes of single cells over time (Fig. 3D). We found that wild-type mother cells only marginally increased in cell volume. In contrast, the volume of *wal1* mother cells increased more than 50% during the 6-h observation period, which corresponds to about four cell cycles. Another difference between the wild-type and *wal1* occurred during the detachment of mother and daugther cells, which in the wild-type resulted in a torsion of the daughter cell out of the mother-daughter cell axis whereas *wal1* mutant cells only rarely showed such an obvious displacement (Movies S1 and S3 in the supplemental material). Mutant *wal1* cells adhered and relocated as cell clumps, indicating a defect in cell separation. This led to the formation of cell heaps not observed in the wild type or in the heterozygous mutant strains, where all cells

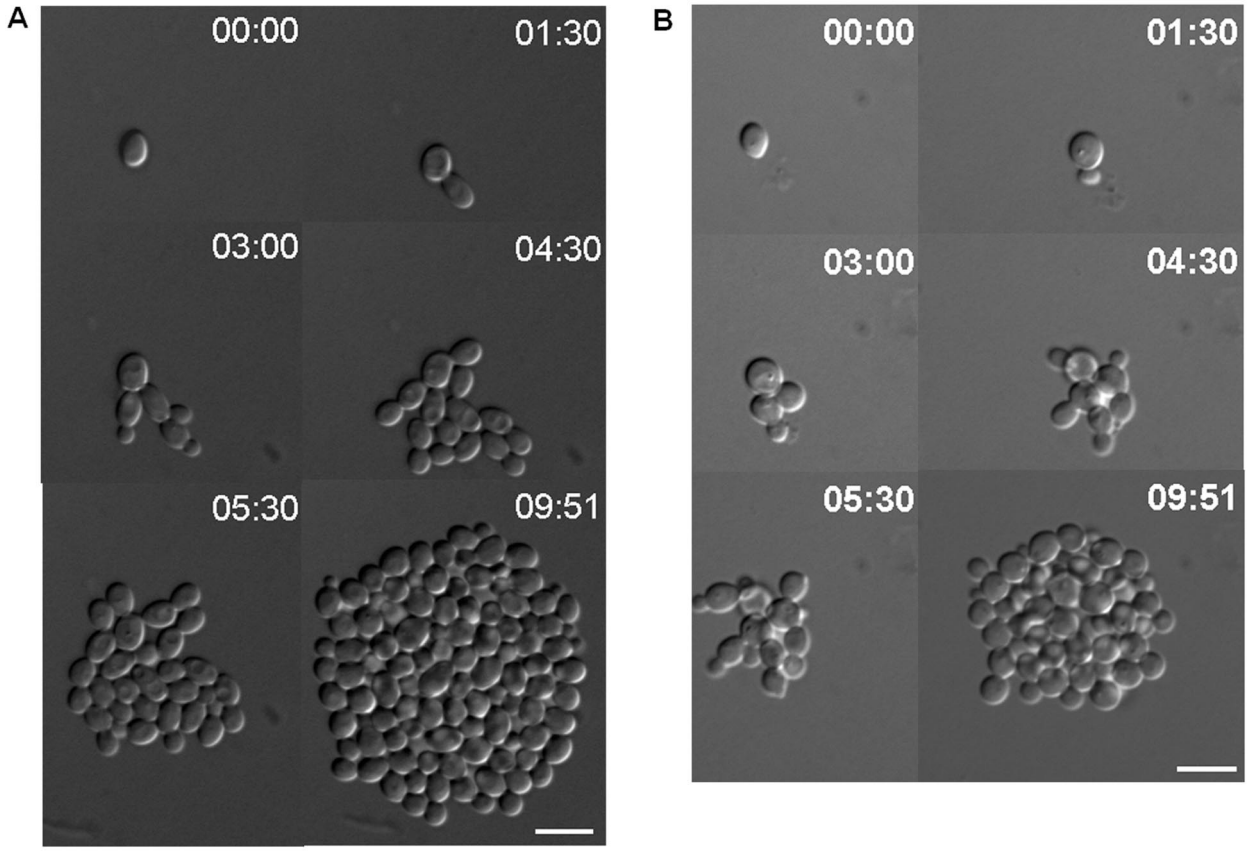

FIG. 2. In vivo time-lapse analysis of yeast cell growth of wild-type and *wal1* mutant strains. Representative frames of movies of the wild-type (A) and *wal1* (B) cells are shown at the same time points. Note the cell shape differences between wild-type (ellipsoidal) and *wal1* (round) cells. The small delay in cell cycle time of the *wal1* strain compared to the wild-type amounts adds up to one cell cycle interval after 10 h, resulting in different cell numbers. Bars, 10 μm. Time is given as hh:min.

remained in the focal plane during the time-lapse recordings, indicating that effective displacement had occurred. Cell clumps were also found when growing *wal1* in liquid culture. Cell aggregates could be resolved mechanically, indicating that cytokinesis and separation of mother and daughter cytoplasm had occurred.

Wal1p determines polarity development. In *S. cerevisiae*, the actin cytoskeleton is involved in establishing the bipolar budding pattern of diploid cells, and mutations in a number of genes including *BEE1*/*LAS17* affect the budding pattern (2, 25, 51). Therefore, we examined the distribution of bud scars in *wal1* and wild-type cells. Cells of the *wal1* strain with three or more bud scars showed a high degree of randomized bud-site selection whereas the wildtype displayed regular (bi)polar budding (Fig. 4; Table 3). Determination of a new bud site is an initial step that polarizes the actin cytoskeleton toward the incipient bud site in the wild type. We therefore examined the distribution and positioning of cortical actin patches in *wal1* in comparison to wild-type cells (Fig. 5). In wild-type cells, actin cortical patches localized within the bud at an early growth stage, then redistributed between mother and daughter cell during the isotropic growth phase of the bud, and finally localized to the bud neck to prepare for cytokinesis (Fig. 5A). In contrast, in *wal1* cells, cortical actin patches were randomly distibuted in mother and daughter cells throughout the cell cycle (Fig. 5B). Depolarization of cortical actin patches therefore accompanies isotropic growth, misplaced growth of mother cells, and defects in bud site selection of mutant cells.

Mutant *wal1* cells exhibit defects in endocytosis and in vacuolar morphology. Defects in vacuolar morphology resulting in fragmented vacuoles were observed in *S. cerevisiae* in a certain allele of *BEE1*/*LAS17*, *las17-16*, which contains a C-terminal deletion of 21 aa that inactivates the Arp2/3-complex activation domain (11). To determine defects in vacuolar morphology in the *wal1* strain, we stained *Candida* wild-type and *wal1* cells using the lipophilic dye FM4-64 (Table 4). Our results clearly show that in contrast to wild-type cells, which contain one or two large vacuoles, *wal1* strains contain a large number of cells with multiple vacuoles and only few cells with just one large vacuole (Table 4).

Furthermore, in *S. cerevisiae* the cortical actin cytoskeleton and Bee1p/Las17p are involved in endocytosis (28). Therefore, we examined endocytosis in *Candida* wild-type and *wal1* cells by monitoring the uptake of FM4-64 in vivo using time-lapse microscopy (Fig. 6; Movie S4 in the supplemental material). Wild-type cells rapidly incorporated the dye, which resulted in staining of endosomes that moved around in the cytoplasm after 4 min (Fig. 6). Later (beginning after approximately 30 min in the time-lapse sequence), vacuoles of the wild type were stained, indicating efficient transport of the dye to the vacuole

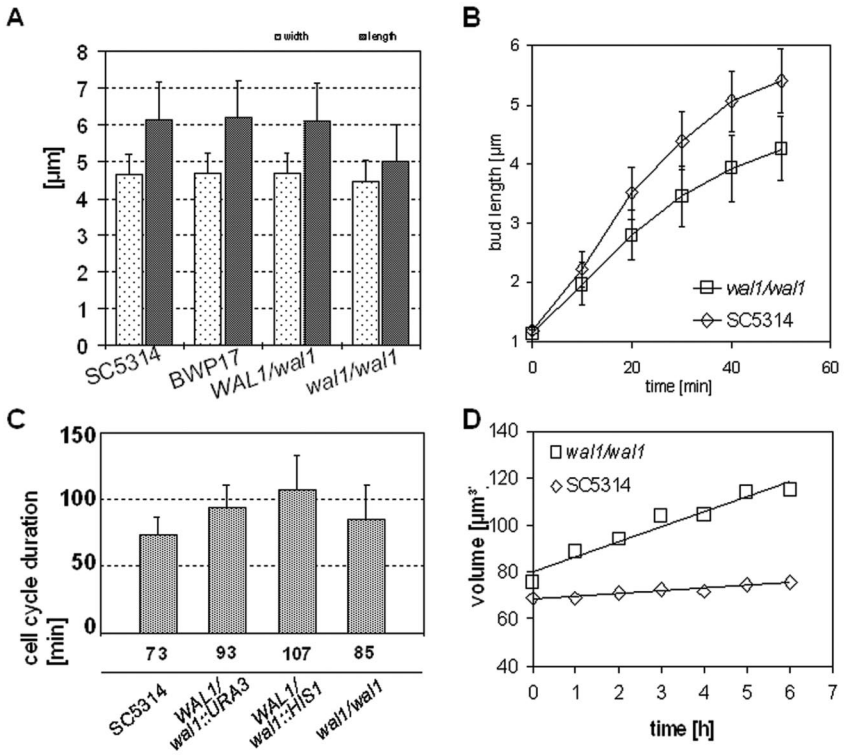

FIG. 3. Analysis of yeast cell morphology of the *wal1* mutant. (A) Cell sizes (length and width) of yeast cells of the indicated strains that were grown to early log phase in YPD were determined. The average of 500 cells per strain (measured using Metamorph 4.6. software) is displayed. (B) Comparison of bud growth of wild-type and *wal1* daughter cells. Using time-lapse microscopy, bud extension was measured for 60 min starting once a bud reached a size of >1 μm. For each strain, 18 cells were measured. The calculated growth rates for the wild type and the *wal1* strain were 5.8 and 4.2 μm/h, respectively. (C) Cell cycle duration was measured by analysis of time-lapse data. One cell cycle was measured as the time required from one bud emergence of a cell to its next budding event. For each strain, 24 to 40 cells were analyzed. Note the different effect on cell cycle duration in heterozygous strains carrying either *ura3* or *his1* auxotrophies. (D) Analysis of mother cell growth of the wild type and the *wal1* mutant. Time-lapse recordings of wild-type and *wal1* strains grown at 26°C were analyzed. At hourly intervals, cell sizes (length and width) of wild-type mother cells ($n = 7$) and *wal1* cells ($n = 7$) were measured. Based on these measurements, volumes of cells were calculated. For *wal1* cells, a spherical form was assumed based on the cell indices (Fig. 3A) and volume was calculated from $V = 1/6 \times \pi \times d^3$. Wild-type cells have an approximately ellipsoidal shape. Their volume was calculated as $V = \pi \times b^2 \times 4/3 \times a$, where a is half the length of the cell and b is half the width of the cell.

(Fig. 6). Cells of the *wal1* mutant, in contrast, required a prolonged time to internalize the dye (Fig. 6). Staining of endosomes was not observed in *wal1* cells. Vacuolar staining appeared with a long delay compared to the wild type and was found to be much weaker than in the wild type (Fig. 6).

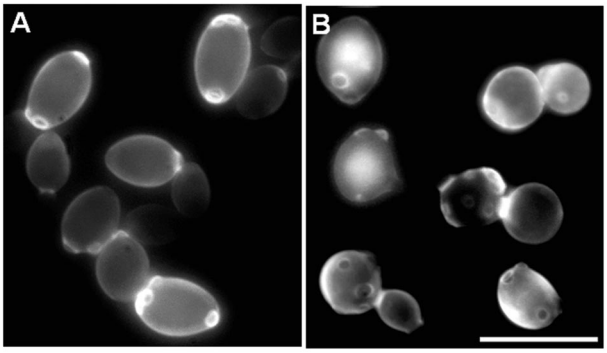

FIG. 4. Bud-site selection defects in *wal1* cells. The wild-type (A) and *wal1* mutant (B) strains were grown overnight in YPD at 30°C. The cells were stained with Calcofluor white, washed, and observed using fluorescence microscopy. Bar, 10 μm.

Wal1p is required for polarized hyphal growth in *C. albicans*. In contrast to *S. cerevisiae*, *C. albicans* is a dimorphic fungus that is capable of forming true hyphae. *WAL1*$^+$ and *wal1*$^-$ cells were induced to form hyphae under different inducing conditions (see Materials and Methods). Cells of the wild-type and heterozygous *WAL1/wal1* strains initiated the formation of hyphae when grown on spider medium or on medium supplemented with serum. In contrast, hyphal growth was abolished in the *wal1* mutant strain under these conditions (Fig. 7A). Hyphal growth resulted in wrinkled colonies (indicative of colonies containing hyphae and yeast cells), whereas yeast-like growth gave rise to shiny and smooth colonies. Hyphal growth was induced in the heterozygous mutant strain, in which the remaining copy of *WAL1* was placed under the control of the regulatable *MAL2* promoter when grown on serum-containing medium supplemented with maltose as the sole carbon source (Fig. 7B). These results demonstrate that Wal1p is required for hyphal growth in *C. albicans*. Microscopic examination indicated, however, that cell shape changes occurred in *wal1* cells induced for hypha formation. Therefore, time-lapse analyses were used to monitor the growth of the wild-type and *wal1* mutant strains under serum-inducing con-

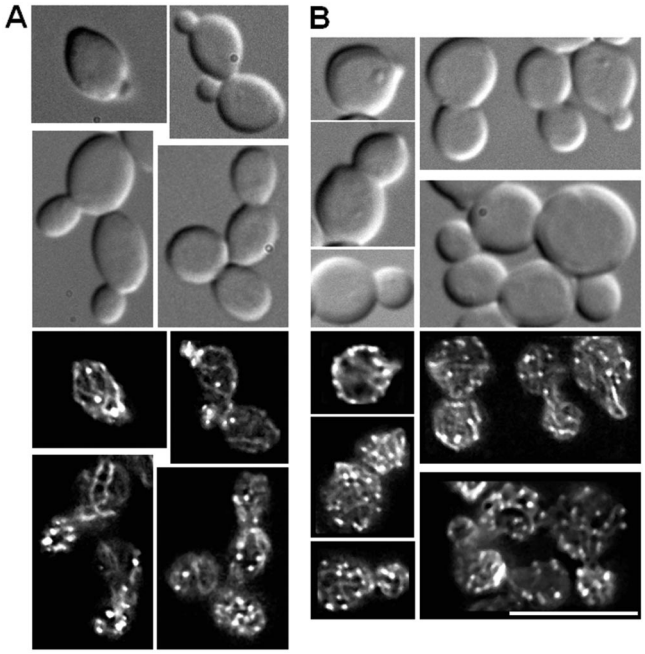

FIG. 5. Distribution of cortical actin patches in wild-type and *wal1* yeast cells. Logarithmically growing cells of the wild-type (A) and *wal1* mutant (B) strains were fixed twice for 1 h, washed, and stained overnight in rhodamine-phalloidin. Cells were imaged using DIC and fluoresence microscopy settings. Representative images of different cell cycle phases are shown, indicating the polarized distribution of cortical actin patches in the wild type and random localization of patches in the mutant. Bar, 10 μm.

TABLE 3. Analysis of bud site selection patterns

Pattern	% of SC5314 cells	Appearance	% of *Cawal1/wal1* cells	Appearance
Bipolar	52.8	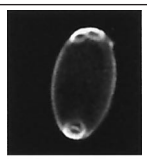	29.5	
Unipolar	44.0	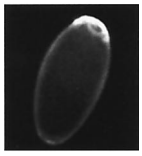	25.0	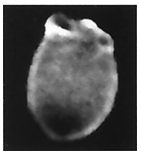
Random	3.1	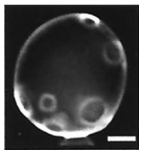	45.5	
No. of cells counted	159		852	

ditions (Fig. 8A and B; Movies S5 and S6 in the supplemental material). In the wild type, hyphal formation occurred almost immediately on induction. Hyphae grew out with an extension rate of approximately 20 μm/h. These hyphae maintained hyphal growth and formed lateral branches. Interestingly, in the center of the mycelium, yeast cells were produced after 5 to 6 h under inducing conditions (Fig. 8A; Movie S5 in the supplemental material). In contrast, *wal1* yeast cells initially responded to hyphal induction with polarized morphogenesis (Table 5). Polarized growth occurred with an extension rate of approximately 15 μm/h (Fig. 8B; Movie S6 in the supplemental material). Clear differences between hyphal and pseudohyphal cells can be seen at sites of septation. Whereas true hyphae formed septa that appeared as cross-walls not changing the diameter of the hyphal tube, pseudohyphal cells showed constrictions at septal sites (Fig. 8C and D; arrows). Thus, the septum position in the *wal1* mutant strain indicates that pseudohyphal cells were formed. In our experiments, 69% of wild-type cells responded to hypha-inducing conditions (10% serum) with germ tube formation, a few cells developed pseudohyphae, and a minor fraction did not respond and stayed in the yeast phase. In the same experiment, *wal1* cells did not form hyphae, the majority of cells (66%) formed pseudohyphae, and one-third of the cells did not respond to the induction (Table 5).

Wal1p exhibits a patch-like localization to sites of polarized secretion. To determine the intracellular localization of Wal1p, we fused GFP to the 3′ end of *WAL1* by using PCR-amplified cassettes with a 100-bp homology region to the target locus. We constructed two independent strains carrying heterozygous *WAL1/WAL1-GFP* alleles. From one of these strains, CAT19, a strain was constructed that produces only GFP-tagged Wal1p (*WAL1-GFP:HIS1/wal1::URA3*) under the control of its endogenous promoter. This strain, CAT21, showed wild-type morphology, indicating that the *WAL1-GFP* construct is fully functional and suggesting that the GFP signals that were obtained reflect the correct localization pattern of Wal1p. GFP signals were similar in all strains, but the brightest signal could be obtained from CAT21, which was therefore used for localization studies presented here. We analyzed the distribution of Wal1p-GFP in both yeast cells and in hyphal cells (Fig. 9). Wal1p-GFP localized in a patch-like structure to sites of growth; it accumulated in emerging buds and at the tips of hyphae (Fig. 9). This, in part, resembles the localization of cortical actin patches, which also cluster in daughter cells and at hyphal tips (Fig. 5). In *S. cerevisiae*, localization of myc-tagged Bee1p revealed that the majority of Bee1p patches colocalize with actin patches (25). Colocalization with actin patches was also observed for other proteins, for example, for the *C. albicans* Myo5p, representing the only myosin I (36). To determine the colocalization of Wal1p with actin patches, we used double-label experiments. To this end, the actin cytoskeleton of strain CAT21 (*WAL1-GFP*) that was induced for hyphal formation was stained with rhodamine-phalloidin. Overlay of the two signals revealed that Wal1p-GFP found as patches colocalized with actin patches (Fig. 9B). Additionally, other, more disperse Wal1p-GFP signals appeared not to colocalize with actin patches.

DISCUSSION

We chose to work on the dimorphic human fungal pathogen *C. albicans* in order to study polarized morphogenesis because

TABLE 4. Analysis of vacuolar morphology

No. of vacuoles	% of SC5314 cells	Appearance	% of *Cawal1/wal1* cells
1	54.9	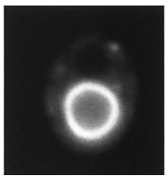	12.3
2 or 3	42.0	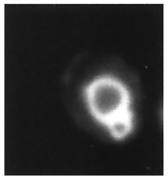	36.5
4 or more	3.1	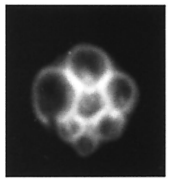	51.2
No. of cells counted	257		293

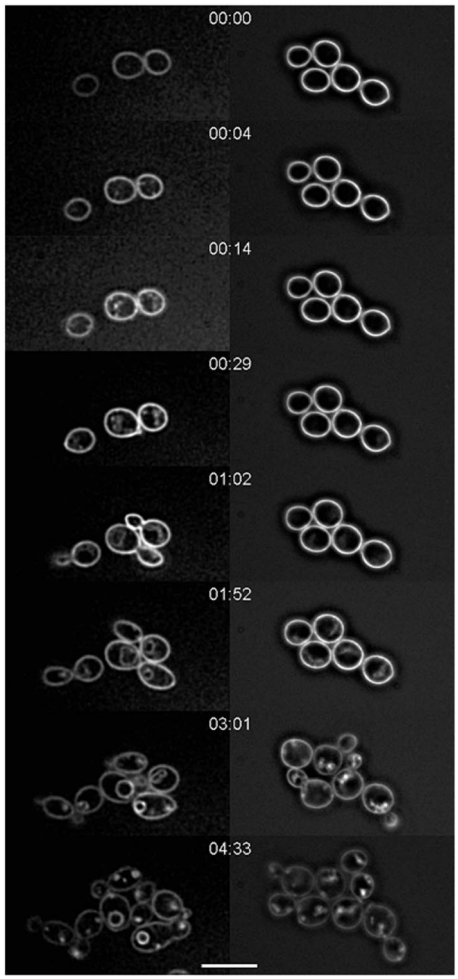

FIG. 6. In vivo time-lapse analysis of endocytosis of the lipophilic dye FM4-64. Uptake was monitored in the wild-type strain SC5314 (left column) and the *wal1* mutant strain (right column). Growth of cells and setup of the microscopy slides were as described in Materials and Methods. Representative frames of both movies are shown at the same time points (hh:min). Bar, 10 μm.

this organism is able to switch between yeast-like and hyphal growth modes under defined regimens. This dimorphism plays an important role during several stages of infection, for example, during invasion of host tissues, evasion of the cellular host immune response, and colonization of internal organs (22, 31). We have shown previously that in the filamentous fungus *A. gossypii*, Rho protein modules play a key role in the establishment of cell polarity via the Cdc42 module and during hyphal growth via the Rho3 module by regulating the organization of the actin cytoskeleton (47, 48). The regulatory role of the Cdc42 module on the architecture of the actin cytoskeleton during yeast and hyphal stages has recently been analyzed in detail in *C. albicans* (4, 17, 42). Other components that are involved in this process were found to be required for hyphal growth in *C. albicans*, such as the *SLA2* and *MYO5* (encoding a type I myosin) genes (3, 36). Signaling from Rho protein modules is transduced to the actin cytoskeleton by effector proteins (12, 45). Effectors that can regulate actin filament assembly either directly or via other protein-protein interactions are therefore of central importance for morphogenesis in *C. albicans* and may also serve as antifungal drug targets. Fungal WASPs are different from mammalian WASP in that they lack a CRIB motif. Thus, they cannot bind directly to GTP-loaded Cdc42p. Recently, it was suggested that activation of the *S. cerevisiae* WASP Bee1p/Las17p is mediated by a complex including the G-protein Rho3p, Exo70p, and Rvs167p (1, 39).

Functions of Wal1p. Disruption of *WAL1* caused major defects in yeast cell morphology, the organization of the cortical actin cytoskeleton, polarized growth under hypha-inducing conditions, early endocytosis, vacuolar morphology, and bud site selection. Defects of *wal1* cells during yeast-like growth were similar to those observed in *S. cerevisiae bee1/las17* mutants (25). *S. pombe wsp1* mutants also exhibit defects in cell morphology, which, however, did not result in isotropic growth phases and round cells (24). In wild-type *C. albicans* yeast cells, localization of cortical actin patches follows similar polarization-depolarization events to those in *S. cerevisiae*, whereas during hyphal stages the localization of patches resembles that of true filamentous fungi (36, 45, 52). In *wal1* cells, cortical actin patches were randomly positioned in mother and daughter cells during all stages of growth. This included the absence of clustered actin patches during bud emergence, suggesting that at this stage of the cell cycle, actin patches are dispensable. In contrast, the assembly of actin cables in *wal1* cells appeared to be as in the wild type. At least, actin cables were found in emerging buds and appeared to localize in a mother bud axis (see, for example, the cell at the bottom right corner of Fig. 5B). Actin nucleation to form cables has recently been shown to be dependent on the formin Bni1p in *S. cerevisiae* (14, 15, 38,

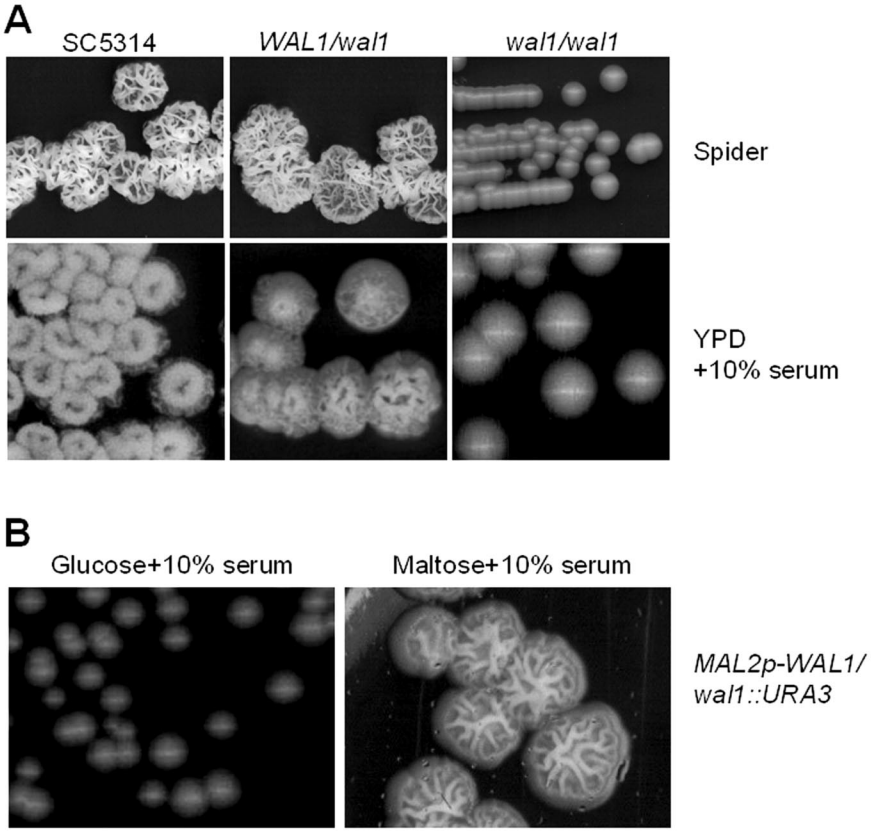

FIG. 7. Induction of hyphal growth in wild-type and mutant strains. (A) Hypha formation on solid media. Hypha formation was determined by plating the indicated strains as single cells on either Spider medium or YPD containing 10% serum. (B) Hyphal induction of strain CAT10 in which one allele of *WAL1* was deleted and the remaining copy was placed under control of the *MAL2* promoter. Plates contained 10% serum and complete medium with either glucose or maltose as the carbon source, resulting in either repressed or induced expression of *MAL2p-CaWAL1*, respectively. All plates were incubated for 4 days at 37°C prior to photography.

40). This supports a model in which bud emergence may be initiated via a pathway including Cdc42p and Bni1p whereas polarized morphogenesis is maintained by correct positioning of cortical actin patches and localized secretion, which requires a WASP homolog. In *C. albicans*, two formin homolgs were identified, corresponding to the *S. cerevisiae BNI1* and *BNR1* genes. Their function, particularly during early growth phases in *C. albicans*, is currently under investigation.

Contribution of Wal1p to polarized morphogenesis. Muntant *wal1* cells were unable to form hyphal filaments under all conditions tested, although these cells were able to initiate polarized morphogenesis to a limited degree on induction. Growth resulted in the formation of elongated pseudohyphal cells. In our time-lapse analyses under hypha-inducing conditions, we observed initial polarized morphogenesis in *wal1* cells that had kinetics comparable to that of the wild type. The *wal1* defect resulted in a failure to maintain polarized growth at the hyphal tip. Another hall mark of hyphal induction also failed to develop. Septation in hyphal filaments occurs as cross-walls compartmentalizing the hyphae without changing the hyphal diameter. In pseudohyphae, constrictions occur at septal sites which were also observed in *wal1* mutants. In *S. pombe* and *S. cerevisiae*, synthetic defects were observed in myosin I- and WASP-deficient strains (13, 24). This suggests a joint activity in a larger complex since WASP provides binding sites for myosin I binding through its proline-rich region (29). Indeed, in *S. cerevisiae*, Myo3p and Myo5p were found to interact via SH3 domains with the proline-rich region of Las17p/Bee1p (13). Additionally, fungal WASPs and type I myosins share a C-terminal acidic motif for activation of the Arp2/3 complex (23, 28). This is in line with observations in *C. albicans* myosin I mutants that exhibit morphological defects similar to those described in this study for *wal1*. Cells of the *myo5* mutant (carrying deletions in the only myosin I gene) were shown to be round during yeast stages and were unable to induce hyphal growth (36). A *myo5* S366D mutation, which mimics the phosphorylation of a serine residue at the TEDS-rule site and thus activates the protein, allowed hypha formation even in the absence of an accumulation of polarized actin patches (36).

Contribution of Wal1p to endocytosis and vacuolar morphology. In the *S. cerevisiae bee1/las17* mutants, defects in endocytosis were observed and Las17p/Bee1p was found to be required for endosome and vacuole movement (7, 28, 35). Here we provide in vivo time-lapse data that clearly show similar defects in the endocytosis of the dye FM4-64 into early endosomes (Fig. 6). In addition to uptake defects, vacuolar morphology in *wal1* cells was different from that in the wild type since cells were frequently found with perturbations in the

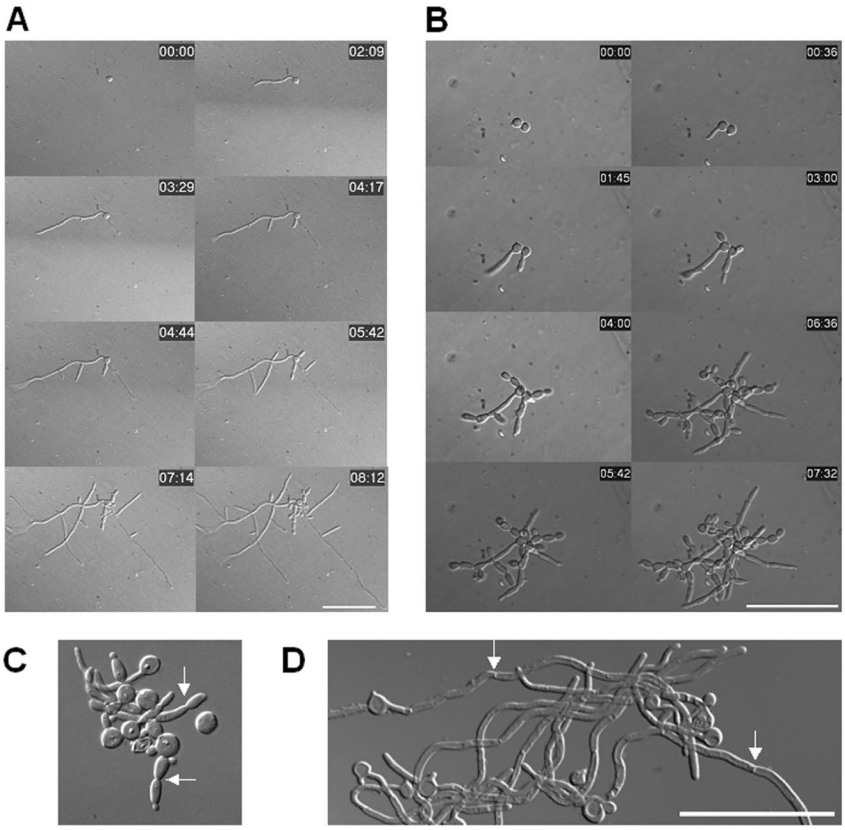

FIG. 8. In vivo time-lapse analysis of the growth of wild-type and *wal1* mutant strains under hypha-inducing conditions (A and B). Representative frames of movies of wild-type (A) and *wal1* (B) cells are shown at the indicated timepoints (hh:min). Cells were preincubated overnight in sterile water. Single cells were mounted on inducing solid media at 37°C. (C and D) Hyphal induction of strain CAT10 (*Mal2p-WAL1*/*wal1*) in liquid medium with glucose (C) or maltose (D) as the sole carbon source. Cells were pretreated as in panel A and incubated for 6 h prior to microscopic observation and photography. Inducing media were complete synthetic medium with 2% glucose (A to C) and 20% serum (A and B) and complete synthetic medium with 2% maltose (D) and 10% serum (C and D). Cells were incubated at 37°C. Bars, 50 μm.

number of vacuoles (Table 4). In *S. cerevisiae*, a signal cascade starting from the Rho-type GTPase Cdc42p is required for vacuole fusion (11, 34). A genomic analysis of all viable *S. cerevisiae* mutants for mutations of homotypic vacuole fusion revealed almost 100 genes with defective vacuolar morphology (41). Among these were a number of genes required for remodeling of the actin cytoskeleton, such as *CLA4* or *BEM2* (41). The same group, showed that the *las17-16* allele produced "fragmented" vacuoles, resulting in a multivacuolar phenotype (11). These and our results suggest that fungal WASP homologues may also be involved in homotypic vacuolar fusion.

Our characterization of *WAL1* and previous results with *MYO5* suggest that both gene products are required for transport processes during endocytosis and polarized morphogenesis. These processes are essential during hyphal growth in *C. albicans* and presumably in other filamentous fungi as well. Our time-lapse analyses indicated that hyphal morphogenesis on induction of starved cells is a very fast process. Recently, it was shown that hyphal elongation occurs independently of the cell cycle in *C. albicans*. Even cells that had initiated a budding cycle were able to respond to induction cues and switched growth mode to form filaments (18). This allows us to ask new questions about hyphal growth in *Candida*, specifically whether

TABLE 5. Analysis of polarized morphogenesis

Growth form	% of SC5314 cells	Appearance	% of *Cawal1*/*wal1* cells
Hyphae	69.1	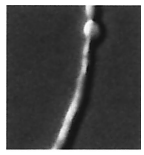	0.0
Pseudohyphae	13.4		66.6
Yeast	17.6	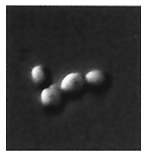	33.4
No. of cells counted	404		410

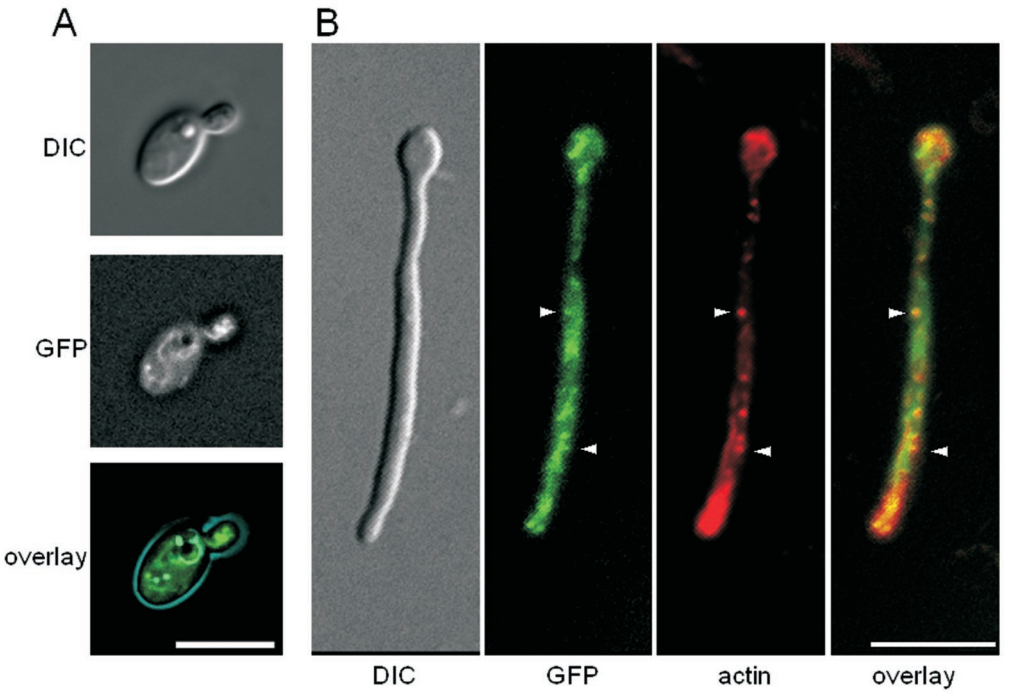

FIG. 9. Localization of Wal1p-GFP in yeast an hyphal cells. Cells of *C. albicans* strain CAT21 were used. (A) GFP fluorescence of yeast cells growing exponentially. (B) Colocalization of Wal1p-GFP and actin during the hyphal growth phase. Hyphal growth was induced by serum. Cells were fixed and stained with rhodamine-phalloidin. GFP and actin fluorescence was imaged using appropriate filter sets. Colocalization of Wal1p-GFP patches with actin patches is indicated by arrowheads. In the overlay, colocalization of GFP (green) and actin (red) results in yellow signals. Representative images of both growth phases are displayed. Bar, 10 μm.

the induction of hyphal-phase-specific genes is required to trigger hyphal formation or, rather, if hyphal induction is such a fast process that may be initiated, for example, by posttranslational modifications. Accordingly, a recent report demonstrated that phosphorylation of WASP in the acidic domain resulted in an increased affinity for the Arp2/3 complex, which was thus proposed to be required for WASP function (9). Understanding the signaling pathways in *C. albicans* that relay environmental signals to the actin cytoskeleton and result in the activation of key target proteins involved in the process of hyphal induction is thus one of the key fields of future research.

ACKNOWLEDGMENTS

We thank Joachim Ernst for providing plasmid libraries, Rong Li and Barbara Winsor for providing yeast strains, Ursula Oberholzer for discussions, Peter Philippsen for providing the heat stage, Manfred Barth (Zeiss, Jena) for his assistance in setting up the microscope, and Diana Schade for her excellent technical assistance.

J.W. is supported by the Deutsche Forschungsgemeinschaft, the Hans-Knöll Institut, and the Friedrich-Schiller University, Jena. Sequence data for *C. albicans* were obtained from the Stanford Genome Technology Center website at http://www-sequence.stanford.edu/group/candida. Sequencing of *C. albicans* was accomplished with the support of the NIDR and the Burroughs Wellcome Fund.

REFERENCES

1. **Adamo, J. E., G. Rossi, and P. Brennwald.** 1999. The Rho GTPase Rho3 has a direct role in exocytosis that is distinct from its role in actin polarity. Mol. Biol. Cell **10:**4121–4133.
2. **Amberg, D. C., J. E. Zahner, J. W. Mulholland, J. R. Pringle, and D. Botstein.** 1997. Aip3p/Bud6p, a yeast actin-interacting protein that is involved in morphogenesis and the selection of bipolar budding sites. Mol. Biol. Cell **8:**729–753.
3. **Asleson, C. M., E. S. Bensen, C. A. Gale, A. S. Melms, C. Kurischko, and J. Berman.** 2001. *Candida albicans INT1*-induced filamentation in *Saccharomyces cerevisiae* depends on Sla2p. Mol. Cell. Biol. **21:**1272–1284.
4. **Bassilana, M., J. Blyth, and R. A. Arkowitz.** 2003. Cdc24, the GDP-GTP exchange factor for Cdc42, is required for invasive hyphal growth of *Candida albicans*. Eukaryot. Cell **2:**9–18.
5. **Bretscher, A.** 2003. Polarized growth and organelle segregation in yeast: the tracks, motors, and receptors. J. Cell Biol. **160:**811–816.
6. **Brown, A. J., and N. A. Gow.** 1999. Regulatory networks controlling *Candida albicans* morphogenesis. Trends Microbiol. **7:**333–338.
7. **Chang, F. S., C. J. Stefan, and K. J. Blumer.** 2003. A WASp homolog powers actin polymerization-dependent motility of endosomes in vivo. Curr. Biol. **13:**455–463.
8. **Cormack, B. P., R. H. Valdivia, and S. Falkow.** 1996. FACS-optimized mutants of the green fluorescent protein GFP. Gene **173:**33–38.
9. **Cory, G. O., R. Cramer, L. Blanchoin, and A. Ridley.** 2003. Phosphorylation of the WASP-VCA domain increases its affinity for the Arp2/3 complex and enhances actin polymerization by WASP. Mol. Cell **11:**1229–1239.
10. **EauClaire, S., and W. Guo.** 2003. Conservation and specialization. The role of the exocyst in neuronal exocytosis. Neuron **37:**369–370.
11. **Eitzen, G., L. Wang, N. Thorngren, and W. Wickner.** 2002. Remodeling of organelle-bound actin is required for yeast vacuole fusion. J. Cell Biol. **158:**669–679.
12. **Etienne-Manneville, S., and A. Hall.** 2002. Rho GTPases in cell biology. Nature **420:**629–635.
13. **Evangelista, M., B. M. Klebl, A. H. Tong, B. A. Webb, T. Leeuw, E. Leberer, M. Whiteway, D. Y. Thomas, and C. Boone.** 2000. A role for myosin-I in actin assembly through interactions with Vrp1p, Bee1p, and the Arp2/3 complex. J. Cell Biol. **148:**353–362.
14. **Evangelista, M., D. Pruyne, D. C. Amberg, C. Boone, and A. Bretscher.** 2002. Formins direct Arp2/3-independent actin filament assembly to polarize cell growth in yeast. Nat. Cell Biol. **4:**260–269.
15. **Evangelista, M., S. Zigmond, and C. Boone.** 2003. Formins: signaling effectors for assembly and polarization of actin filaments. J. Cell Sci. **116:**2603–2611.

15a. **Fonzi, W. A., and M. Y. Irwin.** 1993. Isogenic strain construction and gene mapping in *Candida albicans*. Genetics **134:**717–728.

16. **Gola, S., R. Martin, A. Walther, A. Dünkler, and J. Wendland.** 2003. New modules for PCR-based gene targeting in *Candida albicans*: rapid and effi-

cient gene targeting using 100bp of flanking homology region. Yeast **20:** 1339–1347.
17. **Hazan, I., and H. Liu.** 2002. Hyphal tip-associated localization of Cdc42 is F-actin dependent in *Candida albicans*. Eukaryot. Cell **1:**856–864.
18. **Hazan, I., M. Sepulveda-Becerra, and H. Liu.** 2002. Hyphal elongation is regulated independently of cell cycle in *Candida albicans*. Mol. Biol. Cell **13:**134–145.
19. **Heath, I. B., G. Gupta, and S. Bai.** 2000. Plasma membrane-adjacent actin filaments, but not microtubules, are essential for both polarization and hyphal tip morphogenesis in *Saprolegnia ferax* and *Neurospora crassa*. Fungal Genet. Biol. **30:**45–62.
20. **Hoepfner, D., A. Brachat, and P. Phillppsen.** 2000. Time-lapse video microscopy analysis reveals astral microtubule detachment in the yeast spindle pole mutant *cnm67*. Mol. Biol. Cell **11:**1197–1211.
21. **Kost, B., E. Lemichez, P. Spielhofer, Y. Hong, K. Tolias, C. Carpenter, and N. H. Chua.** 1999. Rac homologues and compartmentalized phosphatidylinositol 4,5-bisphosphate act in a common pathway to regulate polar pollen tube growth. J. Cell Biol. **145:**317–330.
22. **Leberer, E., D. Harcus, D. Dignard, L. Johnson, S. Ushinsky, D. Y. Thomas, and K. Schroppel.** 2001. Ras links cellular morphogenesis to virulence by regulation of the MAP kinase and cAMP signalling pathways in the pathogenic fungus *Candida albicans*. Mol. Microbiol. **42:**673–687.
23. **Lechler, T., A. Shevchenko, and R. Li.** 2000. Direct involvement of yeast type I myosins in Cdc42-dependent actin polymerization. J. Cell Biol. **148:**363–373.
24. **Lee, W. L., M. Bezanilla, and T. D. Pollard.** 2000. Fission yeast myosin-I, Myo1p, stimulates actin assembly by Arp2/3 complex and shares functions with WASp. J. Cell Biol. **151:**789–800.
25. **Li, R.** 1997. Bee1, a yeast protein with homology to Wiscott-Aldrich syndrome protein, is critical for the assembly of cortical actin cytoskeleton. J. Cell Biol. **136:**649–658.
26. **Liu, H., J. Kohler, and G. R. Fink.** 1994. Suppression of hyphal formation in *Candida albicans* by mutation of a *STE12* homolog. Science **266:**1723–1726.
27. **Lo, H. J., J. Kohler, B. DiDomenico, D. Loebenberg, A. Cacciapuoti, and G. R. Fink.** 1997. Nonfilamentous *C. albicans* mutants are avirulent. Cell **90:**939–949.
28. **Madania, A., P. Dumoulin, S. Grava, H. Kitamoto, C. Scharer-Brodbeck, A. Soulard, V. Moreau, and B. Winsor.** 1999. The *Saccharomyces cerevisiae* homologue of human Wiskott-Aldrich syndrome protein Las17p interacts with the Arp2/3 complex. Mol. Biol. Cell **10:**3521–3538.
29. **Machesky, L.** 2000. The tails of two myosins. J. Cell Biol. **148:**219–221.
30. **Machesky, L., and K. L. Gould.** 1999 The Arp2/3 complex: a multifunctional actin organizer. Curr. Opin. Cell Biol. **11:**117–121.
31. **Marcil, A., D. Harcus, D. Y. Thomas, and M. Whiteway.** 2002. *Candida albicans* killing by RAW 264.7 mouse macrophage cells: effects of *Candida* genotype, infection ratios, and gamma interferon treatment. Infect. Immun. **70:**6319–6329.
32. **Mayorga, M. E., and S. E. Gold.** 1999. A MAP kinase encoded by the *ubc3* gene of *Ustilago maydis* is required for filamentous growth and full virulence. Mol. Microbiol. **34:**485–497.
33. **Morschhäuser, J., S. Michael, and J. Hacker.** 1998. Expression of a chromosomally integrated, single-copy GFP gene in *Candida albicans*, and its use as a reporter of gene regulation. Mol. Gen. Genet. **257:**412–420.
34. **Müller, O., D. I. Johnson, and A. Mayer.** 2001. Cdc42p functions at the docking stage of yeast vacuole membrane fusion. EMBO J. **20:**5657–5665.
35. **Naqvi, S. N., R. Zahn, D. A. Mitchell, B. J. Stevenson, and A. L. Munn.** 1998. The WASp homologue Las17p functions with the WIP homologue End5p/verprolin and is essential for endocytosis in yeast. Curr. Biol. **8:**959–962.
36. **Oberholzer, U., A. Marcil, E. Leberer, D. Y. Thomas, and M. Whiteway.** 2002. Myosin I is required for hypha formation in *Candida albicans*. Eukaryot. Cell **1:**213–228.
37. **Pruyne, D., and A. Bretscher.** 2000. Polarization of cell growth in yeast. J. Cell Sci. **113:**571–585.
38. **Pruyne, D., M. Evangelista, C. Yang, E. Bi, S. Zigmond, A. Bretscher, and C. Boone.** 2002. Role of formins in actin assembly: nucleation and barbed-end association. Science **297:**612–615.
39. **Roumanie, O., M. F. Peypouquet, D. Thoraval, F. Doignon, and M. Crouzet.** 2002. Functional interactions between the *VRP1-LAS17* and *RHO3-RHO4* genes involved in actin cytoskeleton organization in *Saccharomyces cerevisiae*. Curr. Genet. **40:**317–325.
40. **Sagot, I., A. A. Rodal, J. Moseley, B. L. Goode, and D. Pellman.** 2002. An actin nucleation mechanism mediated by Bni1 and profilin. Nat. Cell Biol. **4:**626–631.
41. **Seeley, E. S., M. Kato, N. Margolis, W. Wickner, and G. Eitzen.** 2002. Genomic analysis of homotypic vacuole fusion. Mol. Biol. Cell **13:**782–794.
42. **Ushinsky, S. C., D. Harcus, J. Ash, D. Dignard, A. Marcil, J. Morschhäuser, D. Y. Thomas, M. Whiteway, and E. Leberer.** 2002. *CDC42* is required for polarized growth in human pathogen *Candida albicans*. Eukaryot. Cell **1:**95–104.
43. **Vida, T. A., and S. D. Emr.** 1995. A new vital stain for visualizing vacuolar membrane dynamics and endocytosis in yeast. J. Cell Biol. **128:**779–792.
44. **Walther, A., and J. Wendland.** 2003. An improved transformation protocol for the human fungal pathogen *Candida albicans*. Curr. Genet. **42:**339–343.
45. **Wendland, J.** 2001. Comparison of morphogenetic networks of filamentous fungi and yeast. Fungal Genet. Biol. **34:**63–82.
46. **Wendland, J.** 2003. PCR-based methods facilitate gene manipulations and cloning procedures. Curr. Genet. **44:**115–123.
47. **Wendland, J., and P. Philippsen.** 2000. Determination of cell polarity in germinated spores and hyphal tips of the filamentous ascomycete *Ashbya gossypii* requires a rhoGAP homolog. J. Cell Sci. **113:**1611–1621.
48. **Wendland, J. and P. Philippsen.** 2001. Cell polarity and hyphal morphogenesis are controlled by multiple rho-protein modules in the filamentous ascomycete *Ashbya gossypii*. Genetics **157:**601–610.
48a. **Wilson, R. B., D. Davis, and A. P. Mitchell.** 1999. Rapid hypothesis testing with *Candida albicans* through gene disruption with short homology regions. J. Bacteriol. **181:**1868–1874.
49. **Winter, D., A. V. Podtelejnikov, M. Mann, and R. Li.** 1997. The complex containing actin-related proteins Arp2 and Arp3 is required for the motility and integrity of yeast actin patches. Curr. Biol. **7:**519–529.
50. **Winter, D. C., E. Y. Choe, and R. Li.** 1999. Genetic dissection of the budding yeast Arp2/3 complex: a comparison of the in vivo and structural roles of individual subunits. Proc. Natl. Acad. Sci. USA **96:**7288–7293.
51. **Yang, S., K. R. Ayscough, and D. G. Drubin.** 1997. A role for the actin cytoskeleton of *Saccharomyces cerevisiae* in bipolar bud-site selection. J. Cell Biol. **136:**111–123.
52. **Yokoyama, K., H. Kaji, K. Nishimura, and M. Miyaji.** 1990. The role of microfilaments and microtubules in apical growth and dimorphism of *Candida albicans*. J. Gen. Microbiol. **136:**1067–1075.

6

Ronny Martin
Andrea Walther
Jürgen Wendland

Deletion of the dynein heavy chain gene *DYN1* leads to aberrant nuclear positioning and defective hyphal development in *Candida albicans*.

Eukaryot. Cell., 3(6): 1574-88.

Zytoplasmatisches Dynein ist ein mikrotubuli-assoziiertes Motorprotein. *CaDYN1* codiert für die schwere Kette des Dyneins in *C. albicans*. Die Deletion von *DYN1* resultierte in langsam wachsenden Zellen, die Defekte in der Spindelorientierung und Kernverteilung aufwiesen. Unter hypheninduzierenden Bedingungen konnte ein Wachstumsstillstand der Hyphen beobachtet werden, was auf den fehlenden Transport der Zellkerne in die Hyphenspitze zurückgeführt werden konnte.

EUKARYOTIC CELL, Dec. 2004, p. 1574–1588 Vol. 3, No. 6
1535-9778/04/$08.00+0 DOI: 10.1128/EC.3.6.1574–1588.2004

Deletion of the Dynein Heavy-Chain Gene *DYN1* Leads to Aberrant Nuclear Positioning and Defective Hyphal Development in *Candida albicans*

R. Martin, A. Walther, and J. Wendland*

Junior Research Group, Growth-Control of Fungal Pathogens, Hans-Knöll Institute for Natural Products Research and Department of Microbiology, Friedrich-Schiller University, Hans-Knoell, Germany

Received 10 March 2004/Accepted 30 August 2004

Cytoplasmic dynein is a microtubule-associated minus-end-directed motor protein. *CaDYN1* encodes the single dynein heavy-chain gene of *Candida albicans*. The open reading frames of both alleles of *CaDYN1* were completely deleted via a PCR-based approach. *Cadyn1* mutants are viable but grow more slowly than the wild type. In vivo time-lapse microscopy was used to compare growth of wild-type (SC5314) and *dyn1* mutant strains during yeast growth and after hyphal induction. During yeast-like growth, *Cadyn1* strains formed chains of cells. Chromosomal *TUB1-GFP* and *HHF1-GFP* alleles were used both in wild-type and mutant strains to monitor the orientation of mitotic spindles and nuclear positioning in *C. albicans*. In vivo fluorescence time-lapse analyses with *HHF1-GFP* over several generations indicated defects in *dyn1* cells in the realignment of spindles with the mother-daughter axis of yeast cells compared to that of the wild type. Mitosis in the *dyn1* mutant, in contrast to that of wild-type yeast cells, was very frequently completed in the mother cells. Nevertheless, daughter nuclei were faithfully transported into the daughter cells, resulting in only a small number of multinucleate cells. *Cadyn1* mutant strains responded to hypha-inducing media containing L-proline or serum with initial germ tube formation. Elongation of the hyphal tubes eventually came to a halt, and these tubes showed a defect in the tipward localization of nuclei. Using a heterozygous *DYN1*/*dyn1* strain in which the remaining copy was controlled by the regulatable *MAL2* promoter, we could switch between wild-type and mutant phenotypes depending on the carbon source, indicating that the observed mutant phenotypes were solely due to deletion of *DYN1*.

Faithful segregation of nuclei is essential for the proliferation of the eukaryotic cell. Dynamic behavior of nuclei is required at several stages during the cell cycle for correct nuclear positioning, orientation of the mitotic spindle, and distribution of nuclei in the cytoplasm, particularly in filamentous fungi (18). Nuclear distribution has been studied in detail in the yeasts *Saccharomyces cerevisiae* and *Schizosaccharomyces pombe*, as well as in the filamentous fungi *Aspergillus nidulans* and *Neurospora crassa* (30, 31, 32). The spindle pole body (SPB) plays a central role in nuclear dynamics, as it is the organizing center of cytoplasmic microtubules (MTs) that emanate from the SPB outer plaque (4, 5). These cytoplasmic MTs interact with the cell cortex in *S. cerevisiae* via a search-and-capture mechanism that results in the orientation of the mitotic spindle in the mother-bud axis, in the positioning of the nucleus at the bud neck, and in the translocation of the daughter nucleus into the bud. A set of proteins are involved in this process, including Kar9p, Bim1p, Bud6p, the formin Bni1p, and Myo2p (3, 8, 12, 17, 33, 34). During anaphase, nuclear movement depends on the minus-end-directed microtubule motor protein Dyn1p (the *S. cerevisiae* dynein heavy-chain homolog), which provides the pulling force (1). Deletion of *DYN1* in *S. cerevisiae* or mutations in the conserved AAA domains of dynein involved in nucleotide binding and hydrolysis resulted in slower growing but viable mutant strains which displayed disruption of normal nuclear movement (13, 20). *S. cerevisiae* dynein mutants were shown not to be defective in mating and karyogamy (13). In contrast to short-range nuclear migration which delivers the nucleus into the mating projection of *S. cerevisiae*, in the hyphae of filamentous fungi long-range transport of nuclei and organelles into the hyphal tip is required and a uniform distribution of nuclei is achieved to support growth and development of a mycelium. Dynein heavy-chain mutants in *A. nidulans* (*nudA*) and *N. crassa* (*ro-1*) revealed severe defects in nuclear distribution (19, 29). Whereas during germination (the process in which a germ tube is formed from a round-shaped germ cell) in *A. nidulans nudA* mutant nuclei are not transported into the hyphal tube, the dynein heavy-chain mutants, such as *dhc1*, in the filamentous fungus *Ashbya gossypii* show a clustering of nuclei in the hyphal tips (2). In the *N. crassa ropy* class of mutants, with several genes of the dynein/dynactin complex, defects in nuclear positioning were also accompanied by morphological alterations (6, 19, 25, 26). In contrast to the hyphal morphology of the wild type, *ropy* mutants show distorted morphologies indicative of a loss-of-growth directionality and an out-of-tip-focus Spitzenkörper (21). Cytoplasmic dynein in dimorphic fungi has so far only been studied in the plant pathogenic fungus *Ustilago maydis*, in which it is encoded by two genes, *dyn1* and *dyn2* (23). Dynein is essential in *U. maydis*, in contrast to the cases of *S.*

* Corresponding author. Mailing address: Hans-Knoell Institute for Natural Products Research e.V. and Friedrich-Schiller-University Department of Microbiology, Hans-Knoell Str.2, D-07745 Jena, Germany. Phone: 49-3641-65-7639. Fax: 49-3641-65-6620. E-mail: juergen.wendland@uni-jena.de.

TABLE 1. Strains used in this study

Strain[a]	Genotype	Reference
SC5314	*Candida albicans* wild type	5a
BWP17	*ura3*::λ*imm34*/*ura3*::λ*imm34 his1*::*hisG*/*his1*::*hisG arg4*::*hisG*/*arg4*::*hisG*	28a
GC1	*DYN1*/*dyn1*::*URA3*	This study
GC2	*DYN1*/*dyn1*::*HIS1*	This study
GC3	*dyn1*::*URA3*/*dyn1*::*HIS1*	This study
GC4	*dyn1*::*HIS1*/*dyn1*::*URA3*	This study
GC6	*TUB1*/*TUB1-GFP*::*URA3*	This study
GC8	*dyn1*::*URA3*/*dyn1*::*HIS1 TUB1*/*TUB1-GFP*::*ARG4*	This study
GC12	*HHF1*/*HHF1-GFP*::*URA3*	This study
GC17	*dyn1*::*URA3*/*dyn1*::*HIS1 HHF1*/*HHF1-GFP*::*ARG4*	This study
CAT23	*dyn1*::*URA3*/*MAL2p-DYN1*:*HIS1*	This study

[a] All GC strains are derivates of BWP17 with the indicated genotypic alterations.

cerevisiae, and, as we show here, *Candida albicans*. In this report we present mutational analysis of the *DYN1* gene of *C. albicans* and, by using in vivo time-lapse microscopy, show its involvement in nuclear positioning and spindle movement during yeast-like growth. Slight growth defects in the yeast phase yielded elongated cells, whereas under regimens inducing hyphal growth in *C. albicans dyn1* mutants exhibited defects in hyphal formation and in the maintenance of hyphal growth that can be explained by defects in nuclear distribution within the hyphae.

MATERIALS AND METHODS

Strains and media. *C. albicans* strains used in this study are listed in Table 1. Cells were grown in YPD (1% yeast extract, 2% peptone, 2% glucose) or complete supplement medium (CSM) at 30°C. For hyphal induction in liquid minimal media, 10% serum (calf serum; Sigma) was added to CSM and then was incubated at 37°C. For hyphal induction on plates, CSM with 10 to 20% serum or Spider medium (14) was used. *MAL2p-DYN1* cultures were grown on minimal medium containing 2% maltose as the sole carbon source to induce expression. Plates were incubated 4 to 7 days at 37°C prior to photography.

Disruption of *CaDYN1*. The *C. albicans* homolog of the dynein heavy-chain gene *DYN1* was identified in the genomic sequence (http://www-sequence.stanford.edu/group/candida). Deletions of the complete open reading frames of both alleles of *CaDYN1* were performed by PCR-generated *FA-URA3* and *FA-HIS1* disruption cassettes (using primers #678 and #679) as described previously (7). Primers used for construction of the cassettes and verification of the deletions are listed in Table 2. Independent transformants were produced, and the disruptions were verified by PCR on whole yeast cells as described previously (27). Identical phenotypes of the independent homozygous transformants were used to indicate that the correct mutant strains were constructed. To place *DYN1* under control of the regulatable *MAL2* promoter, we used the heterozygous *DYN1*/*dyn1*::*URA3* (GC1) strain and transformed it with PCR fragments amplified from pFA-HIS1-MAL2p with primers #678 and #1122. Promoter shutdown experiments further verified the correct construction of mutant strains, which therefore were not further analyzed by DNA-hybridization techniques.

GFP tagging of *HHF1* and *TUB1*. In order to fuse the genes encoding either histone H4 or α-tubulin with green fluorescent protein (GFP), a PCR-based approach was applied. To this end, transformation cassettes were amplified from plasmids pFA-GFP-URA3 (for use in BWP17) or pFA-GFP-ARG4 (for use in GC3) with primers #692 and #693 for *HHF1* and primers #694 and #695 for *TUB1*. With these primers, 100 bp of homology to two positions at the 3′ ends of the target genes were added to PCR-amplified cassettes as described previously (7). The PCR fragments were then used to transform either BWP17 or the homozygous *dyn1*/*dyn1* mutant strain GC3 to generate strains that contain heterozygous *HHF1*/*HHF1-GFP* or *TUB1*/*TUB1-GFP* alleles.

TABLE 2. Oligonucleotide primers used in this study

Primer	Sequence[a]
#599 U3	GGAGTTGGATTAGATGATAAAGGTGATGG
#600 U2	GTGTTACGAATCAATGGCACTACAGC
#601 H2	CAACGAAATGGCCTCCCCTACCACAG
#602 H3	GGACGAATTGAAGAAAGCTGGTGCAACCGGCTAACCAGCTGCAATCAAGTTTAATGGGATCAATTAAC
#678 S1-*DYN1*	TATAGTGTTGTCTGATACACGTCTAATTGTGCAAAAGTACACACACAAACCAAAAGTGTGAGgaagcttcgtacgctgcaggtcAATCTTCAGATAGATCAAGTACAGATTCCACGATTTCTA
#679 S2-*DYN1*	ATCCAAGTTGTTTTTTCACTAACAGATTGGCATCATCAGACAAGTAAATCCAAGATAATGGtctgatatcatcgatgaattcgag
#680 G1-*DYN1*	GTGTGACTTCAACCCTTCTTTG
#681 G4-*DYN1*	GATGCTTCCGGTTCTATCAACAG
#692 S1-*HHF1*-GFP	CTGTTACTTACACTGAACATGCTAAAAGAAAACCGTCACTTCATTGGATGTTGTTTACGCTTTGAAGAGACAAGGTAGAACCTTGTATGGTTTCGGTGGTggtgctggcgcaggtgcttc
#693 S2-*HHF1*-GFP	GATAATGAACTTCAATGAATGACCATTTTATCTGACCAATAAAATCAAAATAGTAAAAAATTGGTGGAAATAAGATACCGAAAATAATTTGCTTGCCTTGtctgatattcatcgaatgaattcgag
#694 S1-*TUB1*-GFP	AGAAGGTGAATTCACTGAAGCTAGAGAAGACTTGGCTGCTTTAGAGAGAGATTATATTGAAGTTGGTACTGATTCTTTCCCTGAAGAAGAAGAAGAATATggtgctggcgcaggtgcttc
#695 S2-*TUB1*-GFP	CCCTCCTCTTAACCATTTGACACACCAAGAGAGTCAATTCCAAAAGTAAAAATTAAAAATCGGGCTTGGGAGTTCGGGTATATATGGTATATATATATAAGtctgatatcatcgatgaattcgag
#1121 G4-*DYN1-MAL2*p	GCGGTATATCATTCCTAAGTTCACC
#1122 S2-*DYN1-MAL2*p	CACACTGTGTAAATTTCGGCACATTTTCATTAAAAGGTAGAAAGCCTATTATACAGTCATATAATTGATTGACTGATAATAAGGGTGTGACCAGTTCTTCCcattgtagttgattattagttaaaccac

[a] Uppercase sequences correspond to *Candida albicans* genomic DNA. Lowercase sequences correspond to 3′-terminal annealing regions for the amplification of transformation cassettes. All sequences are written from 5′ to 3′.

A

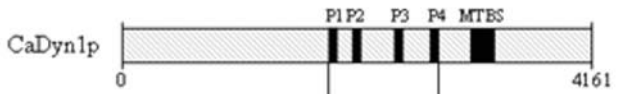

	P-Loop 1	P-Loop 2	P-Loop 3	P-Loop 4
CaDyn1p	GPAGTGKT	GESGSGKS	GPPGSGKT	GPSGSGKS
ScDyn1p	GPAGTGKT	GKAGCGKT	GPPGSGKT	GASRTGKT
AgDhc1p	GPAGTGKT	GDAGTGKT	GPPGSGKT	GPNYSGKT
DmDyhc1p	GPAGTGKT	GPSGSGKS	GPPGSGKT	GVSGAGKT
HsDyhc1p	GPAGTGKT	GPSGSGKS	GPPGSGKT	GVSGAGKT

B

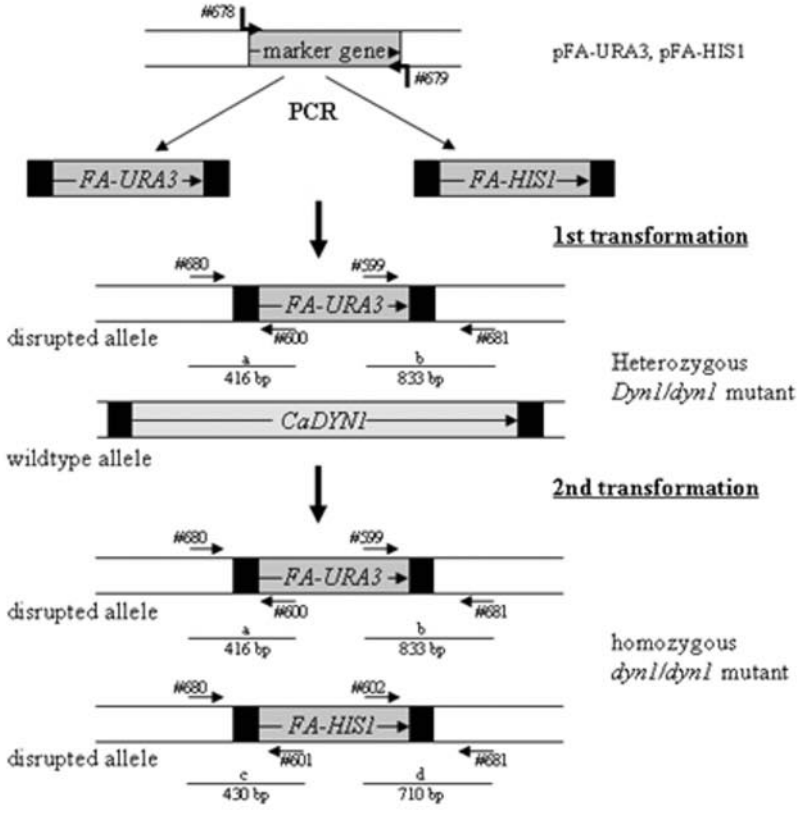

C

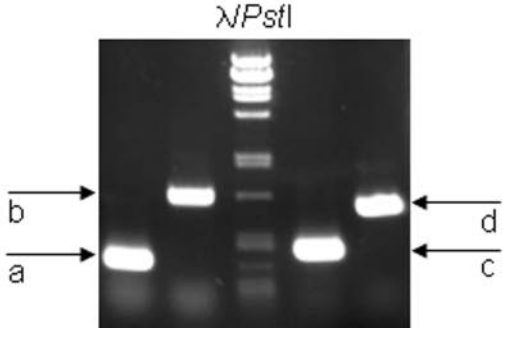

Transformation of *C. albicans*. The lithium-acetate procedure was used to transform *C. albicans* as described previously (27). Basic features of this protocol include an overnight incubation with lithium-acetate followed by heat shock for 15 min at 44°C.

Staining procedures. For examination of nuclear positioning in the heterozygote mutants GC1 and GC2 and the *TUB1-GFP*-labeled strains, cells were stained with 4,6-diamino-2-phenylindol (DAPI; 1 mg/ml; Molecular Probes). For this staining, 200 μl of a cell suspension was fixed with 500 μl of 70% ethanol, and 1 μl of DAPI was added. After incubation for 2 min at room temperature, cells were analyzed by fluorescence microscopy. Chitin staining was done by directly adding 1 μl of calcofluor (1 mg/ml) to a 100-μl cell suspension followed by an incubation of 15 min at room temperature and a subsequent washing step. The positioning of septa is a valuable criterion to distinguish between true hyphae and pseudohyphae and was used to score the cell morphological defects of *dyn1* strains (24). Additionally, septation in hyphae occurs without producing constrictions at the septal site, whereas in pseudohyphal cells invaginations at the sites of septation are found.

Time-lapse microscopy. Strains were grown to exponential phase either in complete or minimal medium, harvested, washed, and resuspended in sterile water. Small aliquots of cells (1.5 μl) were applied on microscopy slides with deep wells. Enrichment of media with oxygen and preparation of the media for microscopy were done as described previously (28). Temperature control was achieved via a heat stage mounted on the microscope table. Microscopy was done on a fully automated motorized Zeiss Axioplan II imaging microscope. Images were acquired by using Metamorph 4.6 software (Universal Imaging Corporation) and a digital imaging system (MicroMax1024; Princeton Instruments). For Hhf1-GFP, acquisition of images was done in 90-s intervals using 0.7-s exposure times and illumination transmission that was reduced to 5% by using appropriate neutral-density filters (Chroma Technology). Image acquisition into stacks was done via custom-designed software journals. Stacks containing brightfield/DIC (differential interference contrast) images were processed separately from images displaying GFP fluorescence. By using these conditions, nuclear dynamics of individual cells could be tracked for more than 10 h. A red look-up table was assigned to the phase-contrast images, and a green look-up table was assigned for the fluorescent images. Stacks were then combined by using overlay tools of the Metamorph software, converted to 8-bit format and processed as video clips with frame rates of 10 images/s.

RESULTS

The unique gene *DYN1* encodes the *C. albicans* dynein heavy chain. A search of the *C. albicans* genome database at Stanford University was performed to identify a sequence homologous to that of the dynein heavy-chain gene *DYN1* of *S. cerevisiae* and *DHC1* of *A. gossypii*. One open reading frame, corresponding to orf19.5999, was found to encode the single dynein heavy-chain gene, designated *DYN1* in *C. albicans*. *DYN1* (located on chromosome 3 based on the Stanford data) encodes a protein of 4,161 amino acids, with strong conservation relative to other fungal as well as mammalian dynein homologs, which range from 35% identity to 57% similarity on the protein level. Particularly well conserved are the microtubule-binding domain and the four P loops involved in ATP binding (Fig. 1A).

TABLE 3. Comparison of wild-type and *dyn1* yeast cells

Parameter	Wild type	GC1 (*DYN1*/*dyn1*)	GC3 (*dyn1*/*dyn1*)
Cell cycle duration (min)	71 ± 5	83 ± 3	114 ± 6
Cell length (n = 500) (μm)	5.9 ± 0.3	7.0 ± 0.4	11.4 ± 0.6
Cell width (n = 500) (μm)	4.5 ± 0.2	4.0 ± 0.2	5.0 ± 0.3
Single (or budded) cells versus cell aggregates (n = 500) (%)	87 versus 13	81 versus 19	28 versus 72

***DYN1* is not essential for cell viability in *C. albicans*.** To be able to study the role of dynein on nuclear migration during the different growth stages of *C. albicans*, we generated homozygous deletion strains via PCR-based gene targeting, starting with independent heterozygous strains (Fig. 1B). Strain BWP17 was chosen as a progenitor strain, because its auxotrophies enabled the sequential disruption of both alleles with the *FA-HIS1* and *FA-URA3* marker genes according to Gola et al. (7). Independent homozygous *dyn1*::*HIS1*/*dyn1*::*URA3* mutant strains were identical in their phenotypes (see below), indicating that correct gene targeting had occurred, as was verified by analytical PCR (Fig. 1B and C). Strains bearing complete open reading frame deletions in the *DYN1* genes are viable, demonstrating that *C. albicans DYN1* is not an essential gene.

Defects of *dyn1* mutant strains during yeast growth phase. By using in vivo time-lapse microscopy, we monitored growth of the wild-type and *dyn1* mutant strains over several generations (Fig. 2). Defects of the *dyn1* strain were quantified by using movie data, and additional measurements were taken from yeast cells grown in complete medium (Table 3). One of the major defects is the prolonged cell cycle time of *dyn1* mutants compared to that of the wild type, which increased by about 40 min. Cells of the wild type are ellipsoidal in shape, roughly 6 μm in length, and 4.5 μm in width. Cells of the heterozygous *DYN1*/*dyn1* mutant are slightly elongated, whereas the *dyn1* mutant cells are considerably longer than wild-type cells (Table 3). In addition, cell aggregates were formed in the homozygous *dyn1* mutant strains, indicating cell separation defects. Because dynein is involved in nuclear distribution, we aimed at the visualization of nuclear movement in *C. albicans* in vivo. To this end we used strain BWP17 and generated a fusion of the histone H4 gene with GFP (see Materials and Methods). As expected, Hhf1p-GFP-derived fluorescence marked the nucleus (Fig. 3). With the strong

FIG. 1. The *C. albicans* dynein heavy chain. (A) Schematic representation of the Dyn1 protein. The positions of the four ATP-binding sites (P-loops; P1, amino acids 1824 to 1832; P2, 2112 to 2119; P3, 2467 to 2474; and P4, 2809 to 2816) and the microtubule binding site (MTBS; amino acids 3151 to 3276) are indicated. Sequence alignment of the four P loops indicates identical P loops in P1 and P3 in the analyzed species, with greater divergence of P loops P2 and P4. Accession numbers of the protein sequences are the following: *C. albicans* CaDyn1p, orf19.5999.prot; *S. cerevisiae* ScDyn1p, NP_012980; *A. gossypii* AgDhc1p, AAK20175; *Drosophila melanogaster* DmDyhc1p, P37276; human HsDyhc1p, Q14204. (B) Deletion of *DYN1* via PCR-based gene targeting. Successive transformation of *C. albicans* strain BWP17 with PCR-amplified marker genes (*FA-URA3* and *FA-HIS1*) that provide 100 bp of terminal target homology regions. In a first transformation independent, heterozygous *DYN1*/*dyn1* strains were generated. From these strains independent homozygous *dyn1*/*dyn1* mutant strains were derived in a second transformation event. Primer numbers (see Table 2) correspond to specific primers used for cassette amplification or PCR verification as indicated. (C) Ethidium-bromide-stained agarose gel image showing the result of diagnostic PCR that was used to verify the correct insertion of the marker genes at the target locus as described (7). The expected fragment lengths for fragments a to d were as shown in panel B.

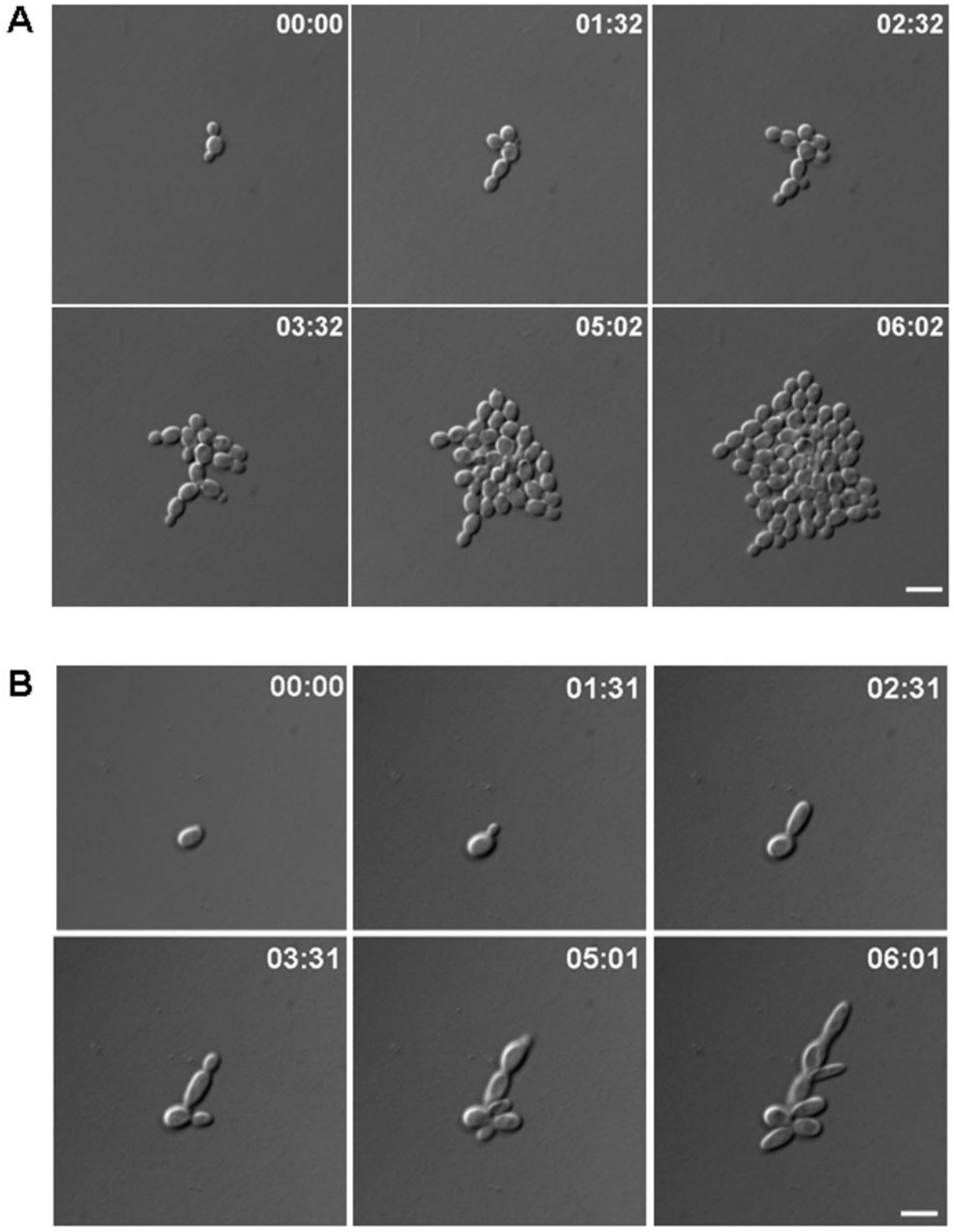

FIG. 2. In vivo time-lapse analyses of yeast phase growth of the wild-type (SC5314) and *dyn1* (GC3) strains. Representative frames of movies of the wild-type (A) and *dyn1* cells (B) are shown over a growth period of 6 h. Cell cycle times in the *dyn1* mutant are longer than in the wild type, resulting in slower growth. Also, cell morphology of *dyn1* yeast cells is more elongated than that in the wild type (see Table 3). Time is in hours:minutes. Bars, 10 μm. Movies are available at http://pinguin.biologie.uni-jena.de/phytopathologie/pathogenepilze/index.html.

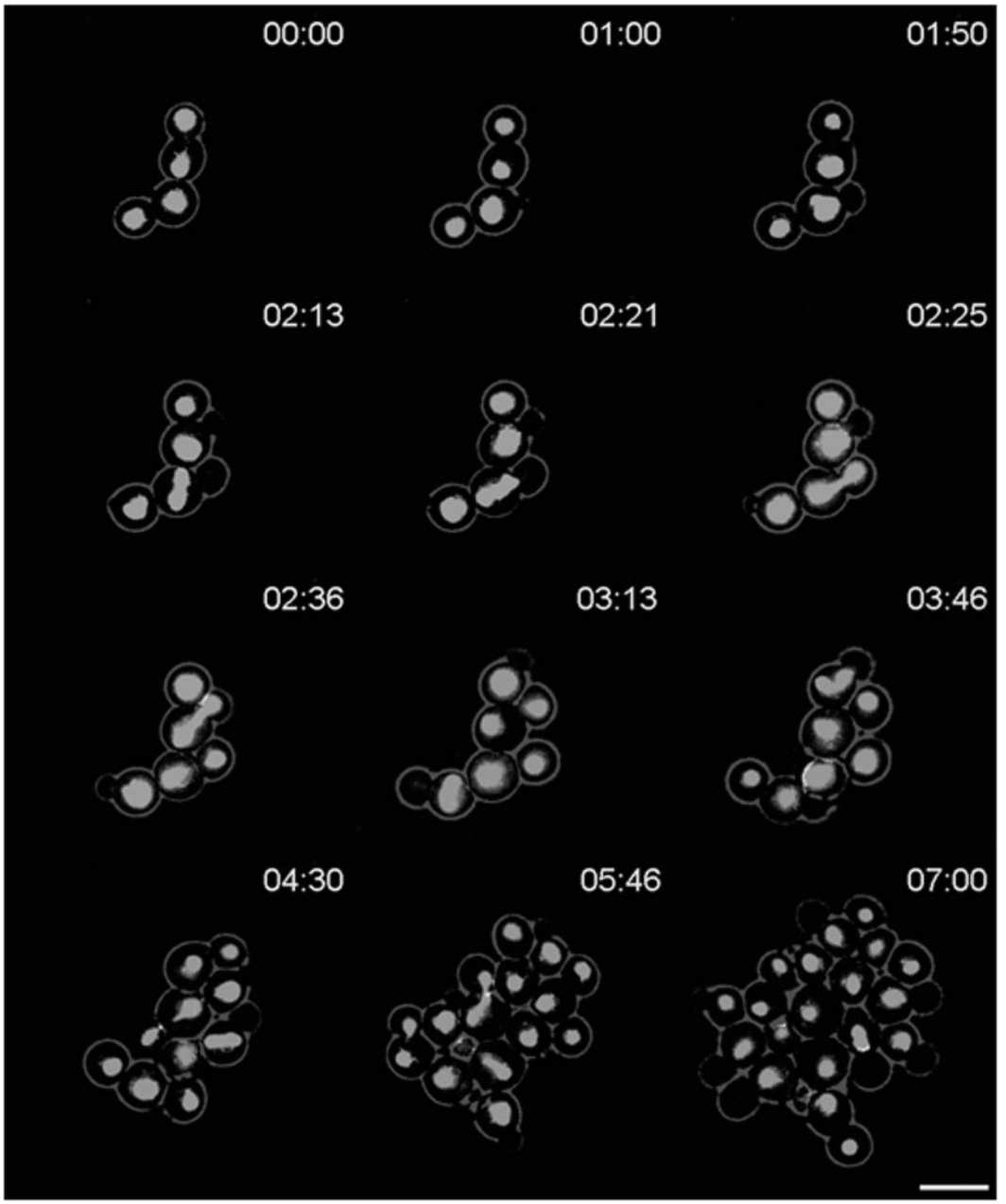

FIG. 3. In vivo fluorescence time-lapse analysis of Hhf1p-GFP in wild-type *C. albicans*. Representative frames of a movie with strain GC12. Cells were pregrown to exponential phase and were mounted on microscopy slides. Note the realignment of the elongated spindle in the interval between 2 h 13 min and 2 h 21 min, as indicated by arrows. Time is in hours:minutes. Bar, 10 μm. The movie is available at http://pinguin.biologie.uni-jena.de/phytopathologie/pathogenepilze/index.html.

signal intensity of the GFP label we were able to record time-lapse series to monitor nuclear movement in the progenitor strain (i.e., corresponding to the wild type) (Fig. 3).

Nuclear positioning in the *C. albicans* wild type. Different phases of nuclear movement were described for *S. cerevisiae*. They include nuclear positioning in the bud-neck region, elongation of the spindle along the mother-bud axis during anaphase, accompanied by the insertion of the anaphase nucleus into the bud-neck region, and nuclear division (10, 32). Our time-lapse data revealed differences between nuclear position-

TABLE 4. Nuclear migration in *C. albicans*[a]

Step	GC12 (%)	GC17 (%)
Nuclear movement to bud site	28.6	12.2
Spindle elongation in mother-daughter axis	28.6	12.2
Spindle realignment after elongation	71.4	0
Completion of mitosis on mother cell	0	87.8
No. of binucleate cells	0	4.3

[a] Data was acquired from time-lapse microscopy of HHF1-GFP-tagged strains ($n > 100$).

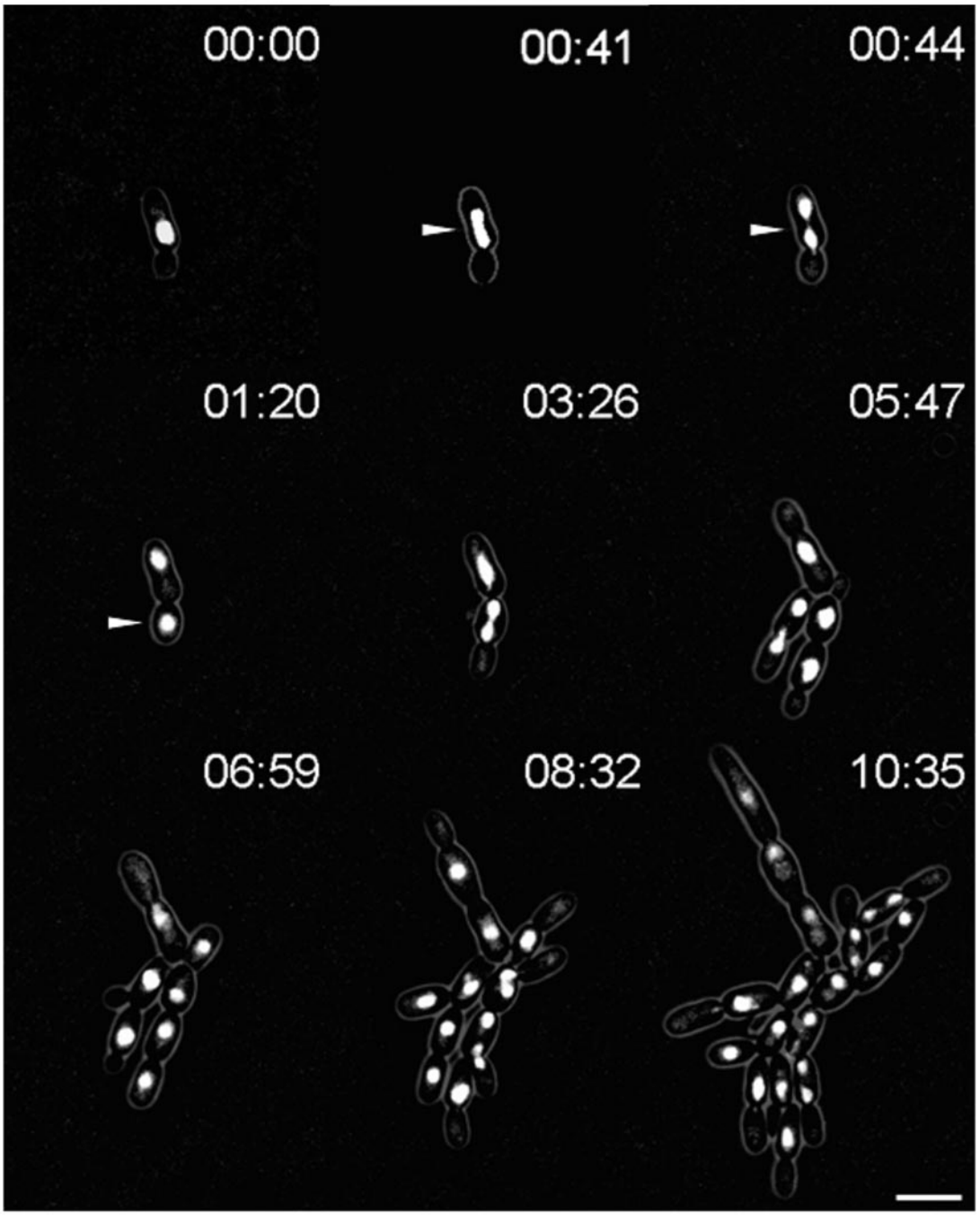

FIG. 4. In vivo fluorescence time-lapse analysis of Hhf1p-GFP in *C. albicans dyn1*. Representative frames of a movie with strain GC17. Cells were pregrown to exponential phase and were mounted on microscopy slides using the same conditions as those used for the time-lapse movie with strain GC12 (Fig. 3). Note the completion of mitosis in a mother cell and postmitotic nuclear migration between 41 and 44 min, as marked by the arrowheads. Time is in hours:minutes. Bar, 10 μm. The movie is available at http://pinguin.biologie.uni-jena.de/phytopathologie/pathogenepilze/index.html.

ing in *C. albicans* and that in *S. cerevisiae*. These changes are particularly obvious in premitotic nuclei. Here, only a quarter of the observed *C. albicans* nuclei were positioned directly at the mother-bud neck. Lack of early attachment to the mother-bud neck resulted in about 70% of the observed cases in anaphase spindle elongation that were not coordinated with the mother-bud axis. In the wild type, this lack of coordination was compensated for by the realignment of anaphase spindles, with the mother-bud neck requiring rotational movement of the spindle. Spindle alignment was accomplished prior to nuclear division, which was then followed by nuclear migration of the daughter nucleus into the bud (Table 4). To rule out the chance that the observed nuclear migration phenotypes in *C. albicans* were due to the strain background or the GFP label employed, we used DAPI staining of fixed cells of the *C. albicans* wild-type strain SC5314 as well as the CAI-4 and BWP17 strains. Data acquired indicated that 30% of the observed anaphase spindles ($n > 200$ for each strain) were not aligned in the mother-bud axis in these strains (data not shown). Because the data were derived from fixed cells, those spindles that already were realigned with the mother-bud axis could not be scored. Furthermore, in the *C. albicans* wild-type strain SC5314 as well as in the HHF1-GFP strain, misalignment of anaphase spindles with respect to the mother-bud axis did not result in the formation of binucleate cells. We conclude that in *C. albicans*, in contrast to *S. cerevisiae*, movement of the anaphase spindle to position the spindle in the mother-bud axis is a regular cell cycle event.

Nuclear positioning in the *C. albicans dyn1* strain. Based on the homozygous *dyn1* mutant strain (GC3), we constructed an *HHF1-GFP* fusion in this background by using the same PCR-based approach described above. This strain appeared, based on morphological criteria, phenotypically unaltered from the GC3 strain and was used for time-lapse analysis to monitor nuclear distribution (Fig. 4). Some striking differences were observed that distinguish nuclear dynamics in the *dyn1* mutant from those in the wild type. Movement of preanaphase nuclei towards the bud-neck region occurred less efficiently in the mutant than in the wild type. Spindle elongation of anaphase nuclei was less pronounced in the *dyn1* mutant, resulting in spindles shorter (maximum nuclear elongation, 6.2 μm; $n = 13$) than those of the wild type (maximum nuclear elongation, 8.7 μm; $n = 13$). Spindle realignment was not observed at all in the *dyn1* mutant, which, most notably, resulted in preferential completion of mitosis in the mother cell in the *dyn1* mutant strain (87.8% in the *dyn1* strain compared to only 7.1% in the wild type) (Table 4). Strikingly, however, even though the majority of mitotic events were completed in *dyn1* mother cells, postmitotic nuclear migration ensured the correct segregation of nuclei in the *dyn1* mutant, resulting in only a very small number of bi- or multinucleate cells.

Analysis of spindle positioning by Tub1-GFP fluorescence. Because the data acquired by monitoring Hhf1-Gfp fluorescence only indirectly revealed spindle positioning, we went on to construct *C. albicans* strains that carry *TUB1-GFP* fusions both in the wild-type and *dyn1* mutant background (see Materials and Methods). The Tub1p-GFP signal was found to correctly label the microtubules but was too weak to be used for in vivo fluorescent time-lapse recordings. Therefore, we used single time point images to quantify spindle positioning (Fig. 5). These data indicated that in the wild-type background, about 80% of the spindles were found to be in the mother-bud axis (corresponding to DAPI staining of fixed cells; see above), whereas in the *dyn1* mutant only 30% of the spindles were correctly positioned. The difference between the in vivo time-lapse data set with the Tub1p-GFP fluorescence data set in the wild type may be due to the fact that spindle realignment is a very fast process (requiring only 6 min). Thus, many spindles that were found to be positioned in the mother-bud axis may in fact have been realigned prior to their observation.

Loss of *DYN1* results in aberrant hyphal growth in *C. albicans*. Defects in the dynein/dynactin complex in filamentous fungi have been shown to severely cripple hyphal growth (2, 19, 29). In contrast to the yeast *S. cerevisiae*, *C. albicans* is a dimorphic fungus that can be induced to form true hyphae. We used the addition of serum to the medium as well as Spider medium to induce hyphal growth in the *dyn1* mutant strains (Fig. 6). While the wild type and the heterozygous *DYN1*/*dyn1* mutant readily responded to hypha-inducing conditions, the homozygous *dyn1* mutant showed defects in hypha formation. On these plates, *dyn1* colonies showed a less wrinkled appearance, and defects in hyphal growth were particularly evident by the lack of filaments at the colony edges (Fig. 6). To analyze this phenotype in more detail, we applied in vivo time-lapse microscopy to follow growth of the wild-type and *dyn1* mutant strains upon hyphal induction (Fig. 7A and B). As described previously (28), the wild type almost immediately responded to the external stimuli (37°C in the presence of serum) with hyphal induction. Hyphal growth was maintained for the 15-h duration of the time-lapse, lateral branches were formed, and a mycelium was generated (Fig. 7A). Hyphal induction of the *dyn1* strain resulted in the formation of germ tubes, although the polar growth rate was much slower than that in the wild type (Fig. 7B). However, growth of the filaments came to a halt after a short time, and once stopped it was not resumed at later stages. New filaments were formed from the initial yeast cell and lateral branching was also induced, but mycelium formation was inhibited in *dyn1* mutants, corresponding to the results of the plate assays. To quantify these time-lapse data, hyphal induction was done in liquid media, and germ tube and filament formation was monitored after 3 and 6 h (Table 5). These data indicated that initiation of germ tube formation occurs in the *dyn1* mutant with frequencies similar to those of the wild type. The appearance of septum formation within germ tubes is a hallmark of hyphal induction (24). We therefore compared septum positioning between the wild type and *dyn1* mutant 3 h after hyphal induction (Table 6). At this stage of hyphal induction, the differences between the wild type and *dyn1* mutant indicated a higher percentage of germ tubes of the *dyn1* mutant that had not formed septa (19%), presumably due to nuclear migration defects. The percentage of septa close to the bud neck in the wild type and *dyn1* mutant was found to correspond to the number of pseudohyphae that were formed.

To demonstrate that the described phenotypes of the *dyn1* mutant strain were due to the deletion of both alleles of *DYN1*, we used the heterozygous *DYN1*/*dyn1*::*URA3* strain (GC1) and fused the remaining copy of *DYN1* with the regulatable *MAL2* promoter, again using a PCR-based approach. To determine nuclear positioning in germ tubes and hyphae of the wild type, the *dyn1* mutant, and the strain expressing *DYN1* from the

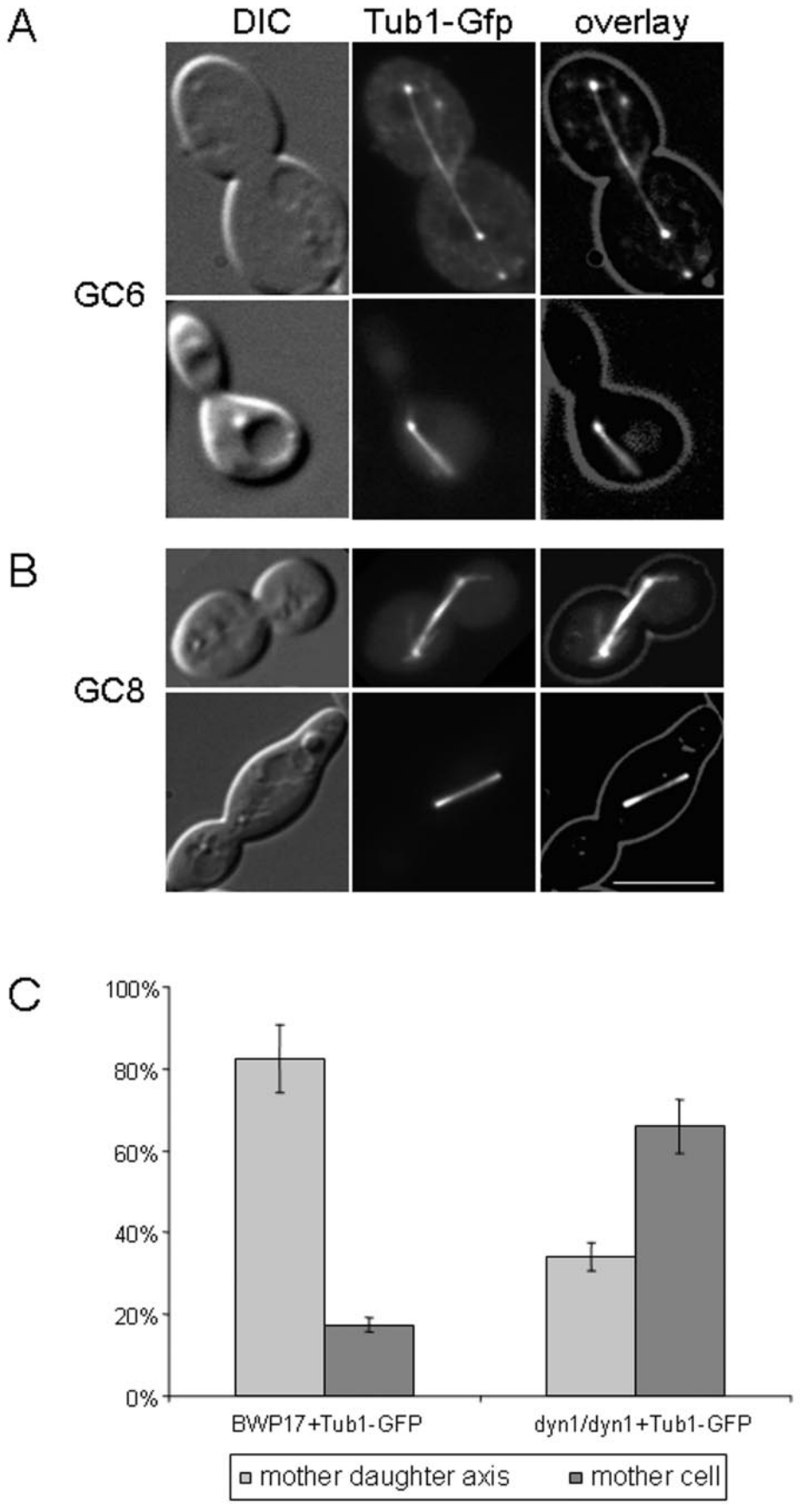
A
DIC
Tub1-Gfp
overlay
GC6
B
GC8
C
100%
80%
60%
40%
20%
0%
BWP17+Tub1-GFP
dyn1/dyn1+Tub1-GFP
mother daughter axis
mother cell

inducible maltose promoter (CAT23), we used DAPI staining of fixed cells. Hyphal growth in the wild type resulted in nuclear migration that moved one nucleus into the hyphal tip and produced regular intervals of nuclear spacing within the hyphae. In the *dyn1* mutant, few germ tubes were invaded by nuclei, so tips of germ tubes were found to be devoid of nuclei. The lack of sustained hyphal morphogenesis in the *dyn1* mutant was therefore found to be accompanied by the failure of delivery of nuclei into the apical parts of germ tubes (Fig. 8). In the strain carrying the *MAL2p-DYN1* construct, correct nuclear migration and positioning in germ tubes and hyphae was observed only during growth in maltose, whereas the mutant *dyn1* phenotype occurred under repressible conditions during growth in glucose, indicating that Dyn1p is essential for nuclear migration and positioning in *C. albicans* hyphae. This also indicates that the defects in nuclear positioning and nuclear movement described in this report are, in fact, solely due to the deletion of *DYN1* in *C. albicans*.

DISCUSSION

Cytoplasmic dynein is a minus-end-directed motor protein that is involved in transport processes of various organelles. In fungi, dynein is required for nuclear migration and nuclear positioning (30). Functional analyses of dynein have been performed with a variety of unicellular and filamentous fungal organisms, including *S. cerevisiae*, *U. maydis*, *A. nidulans*, *N. crassa*, and *A. gossypii* (2, 19, 23, 29). In the dimorphic plant pathogen *U. maydis*, the dynein heavy chain is encoded by two genes, *dyn1* and *dyn2* (23). However, in *U. maydis* nuclear migration differs from that in ascomycetous yeasts. During yeast-like growth, premitotic movement of the nucleus into the bud occurs, followed by mitosis and migration of one nucleus back into the mother cell. Upon loss of dynein function this nuclear migration is eliminated, resulting in mitotic division in the mother cell. This defect, in contrast to similar defects in *S. cerevisiae* and as we describe here for *C. albicans*, is lethal in *U. maydis* (23). *C. albicans* is one of the most important human fungal pathogens, and its ability to change from yeast to hyphal stages has been shown to contribute significantly to the virulence of this organism (15). We were, therefore, interested in elucidating the role of *C. albicans* dynein in nuclear migration and correct positioning as well as its relation to polarized hyphal growth. An influence on morphogenesis was revealed for the dynein/dynactin complex in *N. crassa*. *Neurospora ropy* mutants show distorted hyphal morphologies resulting in spiralized hyphal growth. This indicated a role of dynein in the positioning of the Spitzenkörper, which acts as a vesicle supply center that directs the trajectory of hyphal growth (21).

Functional analysis of *CaDYN1*: morphological defects. Rapid and efficient strain constructions were achieved by PCR-based gene targeting using 100 bp of target homology regions. *C. albicans dyn1* mutant strains showed prolonged cell cycle times and a more elongated yeast cell shape than those of the wild type. The latter phenotype was accompanied by the generation of cell aggregates in the *dyn1* strain that did not occur in the wild type; this activity was monitored by in vivo time-lapse microscopy. Under hypha-inducing conditions, vigorous filamentation occurred in the wild type, resulting in the formation of branched mycelia. *C. albicans dyn1* strains failed to support hyphal growth both on solid and in liquid media. Germ tube formation was initiated in the dynein mutant with wild-type frequencies, but hyphal growth after application of inducing extracellular stimuli came to a halt and swollen cells were generated that failed to produce elongated hyphal filaments. The germ tubes appeared to be in the hyphal state, because septa were frequently placed within the germ tubes of the *dyn1* mutant. Severe growth defects were also observed in dynein mutants of *A. nidulans* and *A. gossypii*. These were based either on a lack of nuclear migration into the hyphal tip in *A. nidulans* or on the trapping of nuclei in apical parts of hyphae in *A. gossypii* (2, 29).

Nuclear migration in the *C. albicans* wild type. We used GFP-tagged histone H4 and α-tubulin to monitor nuclear migration in *C. albicans*. The Hhf1p-GFP label proved to be strong enough for in vivo time-lapse microscopy, whereas Tub1p-GFP was too weak and did not sustain cell viability after prolonged UV exposure to capture fluorescent images. Our Hhf1p-GFP in vivo time-lapse recordings were efficiently run over several hours, enabling us to follow several cell cycles. Compared to the nuclear migration phases that were discerned in *S. cerevisiae*, in *C. albicans* several key differences were evident: (i) nuclear movement to the bud site, as shown for *S. cerevisiae* (10, 32), was not that pronounced in *C. albicans*; (ii) oscillatory movements of elongated spindles upon insertion into the bud neck could not be observed in *C. albicans*; (iii) as a consequence of the low frequency of nuclear migration to the bud neck, we observed spindle elongation in a manner not coordinated with the mother bud axis, which then required realignment of elongated spindles with the mother-bud axis in the *C. albicans* wild type. This realignment of the spindle ensured that mitoses resulted in correct nuclear distribution between mother and daughter cells, as there were very few instances in the wild type in which mitosis was completed in a mother cell. Such a realignment of elongated spindles is a very infrequent event in *S. cerevisiae* (10). In baker's yeast, the nucleus is moved close to the bud neck early in G_1/S phase via a Bim1p- and Kar9p-dependent search-and-capture mechanism that already ensures correct positioning of the spindle pole body with respect to the mother-daughter axis (11, 12, 17, 22, 30). Within the *Candida* genome sequence, open reading

FIG. 5. Orientation of mitotic spindles in *C. albicans*. Spindle positions in strains GC6 (*DYN1*/*DYN1 TUB1*/*TUB1-GFP*) and GC8 (*dyn1*/*dyn1 TUB1*/*TUB1-GFP*) were analyzed by fluorescence microscopy. (A) Representative images of wild-type spindle positions in which the spindle is either aligned in the mother daughter axis and extends into the daughter (top row) or is elongated in the mother cell (bottom row). (B) Images of the spindle positions in *dyn1* cells in which the spindle is either aligned in the mother daughter axis or is misaligned and elongated only in the mother cell. DIC images of cells were merged into an overlay with the images showing the GFP fluorescence. Bar, 10 μm. (C) Quantification (bars indicate the standard deviation of the mean) of spindle positioning in GC6 and GC8 (n = 130 for each strain) corresponding to the observed spindle positions in panels A and B.

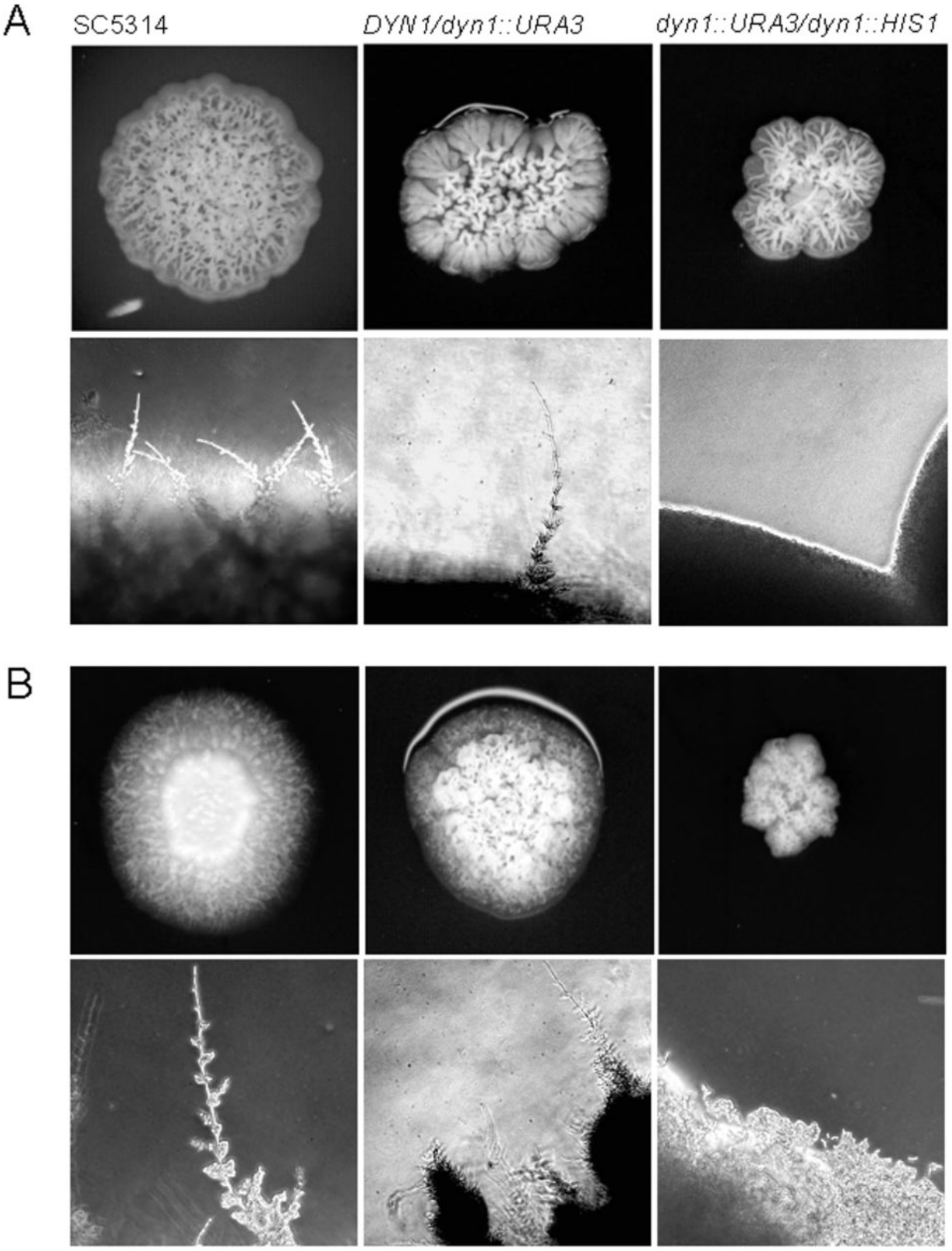

FIG. 6. Induction of hyphal growth in wild-type and mutant strains. Hypha formation on solid media was determined by plating the indicated strains on either (A) complete synthetic medium (CSM) containing 10% serum or (B) on Spider medium. All plates were incubated for 4 days at 37°C prior to photography. Note the abundant filamentation at the colony edges of both the wild type (SC5314) and heterozygous *DYN1*/*dyn1* on both media; this filamentation is completely absent in the homozygous *dyn1dyn1* mutant. Images representing magnifications of the colony edges were acquired via digital microscopy of the corresponding colonies.

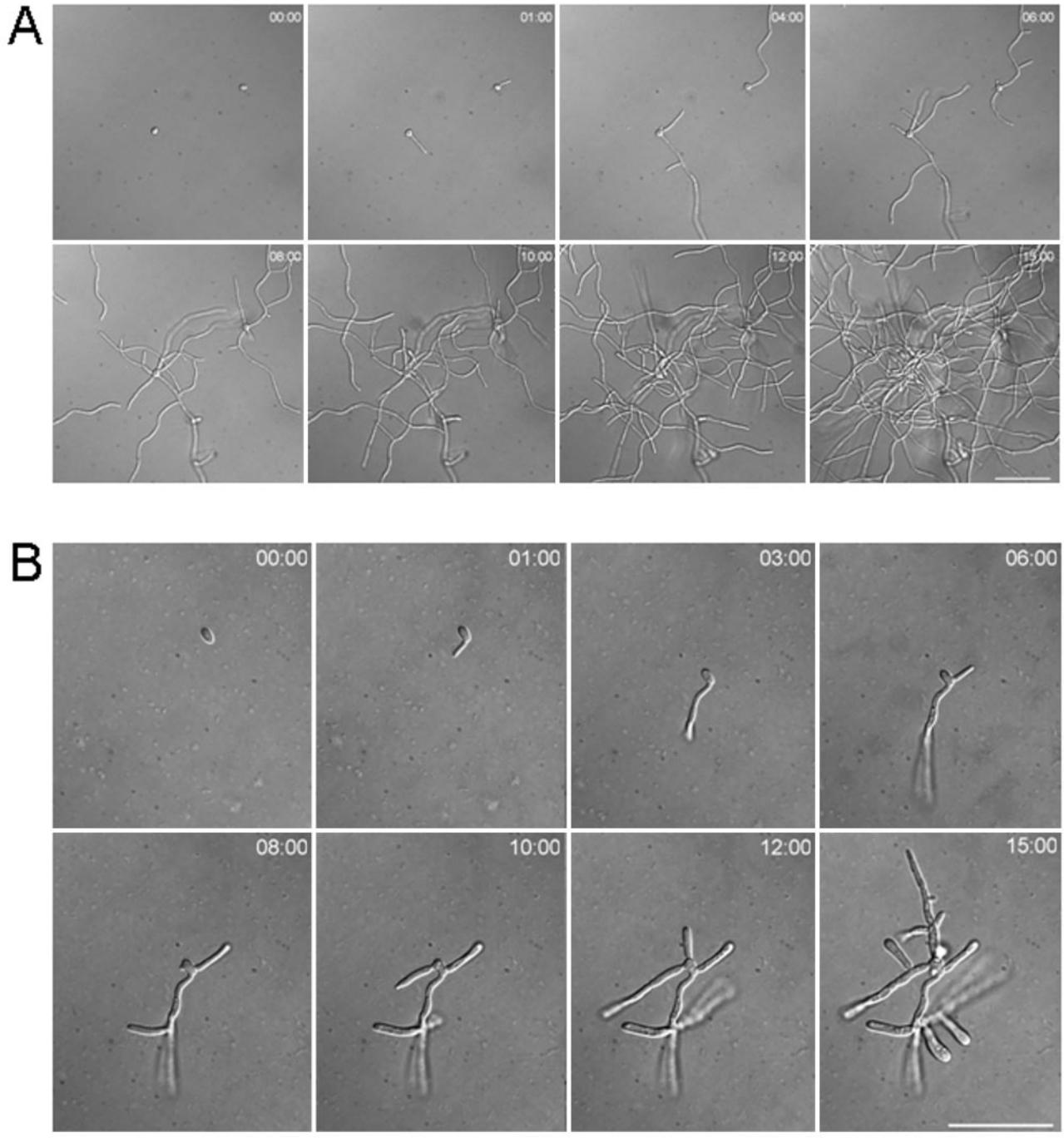

FIG. 7. In vivo time-lapse analyses of growth of wild-type and *dyn1* mutant strains under hypha-inducing conditions. Representative frames of movies of wild-type (A) and *Cadyn1* cells (B) are shown at the indicated time points. Cells were preincubated overnight in sterile water. Single cells were mounted on inducing solid CSM containing serum at 37°C. Time is in hours:minutes. Bars, 50 μm each. Movies are available at http://pinguin.biologie.uni-jena.de/phytopathologie/pathogenepilze/index.html.

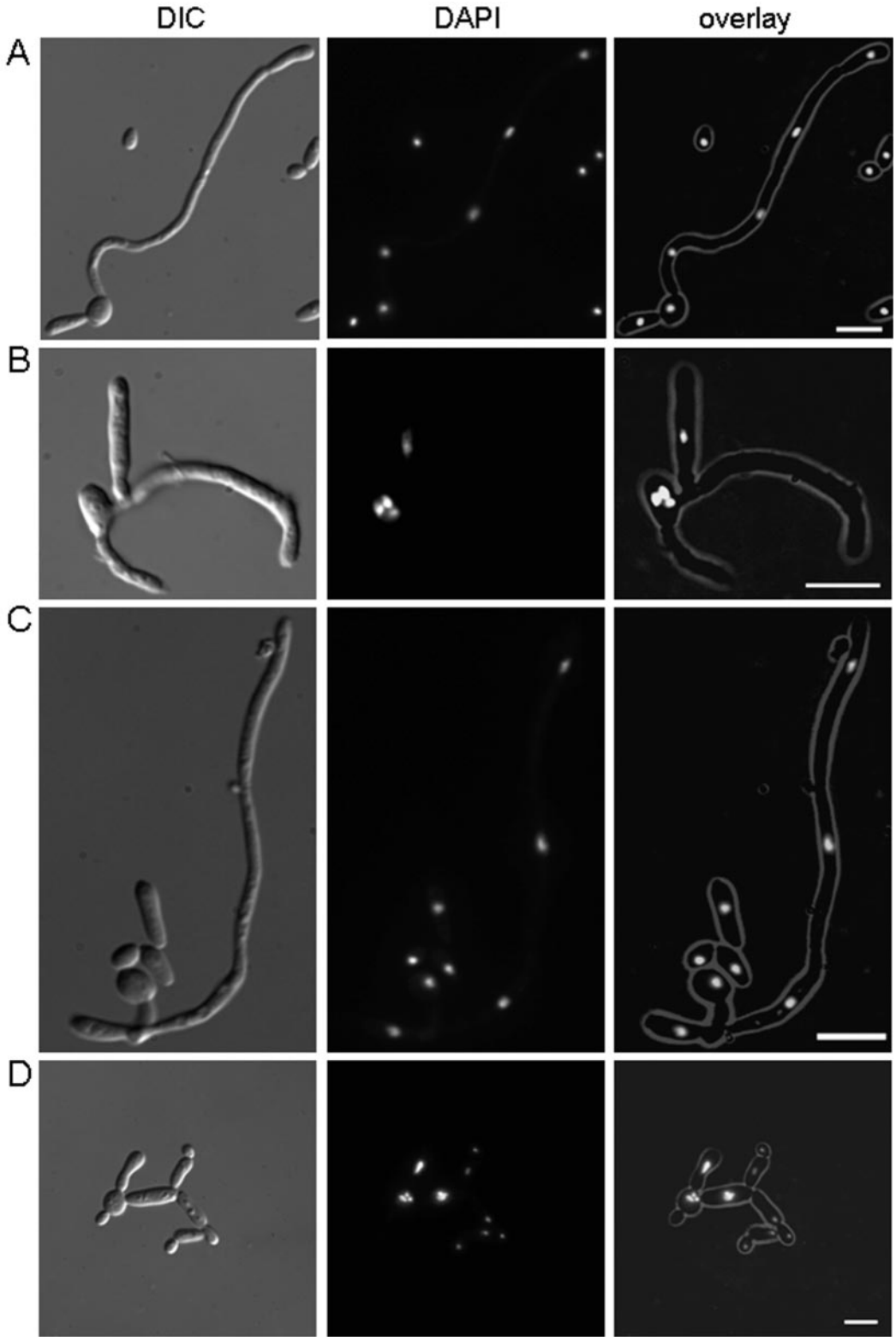

FIG. 8. Analysis of nuclear positioning in wild-type and *dyn1* mutant strains. Cells were incubated for 10 h under hypha-inducing conditions (CSM in the presence of 0.5 g of proline/liter). DIC images and images showing the DAPI fluorescence of stained nuclei were merged into an overlay. Characteristic nuclear positioning in the wild type (A) shows elongated hyphae with regular nuclear spacing, septal intervals, and one nucleus in the apical compartment, whereas inducing conditions resulted in germ tube formation in the *dyn1* mutant (B) in which nuclei were either trapped in the germ cell or did not migrate into the hyphal tip. (C) Hyphal induction using *C. albicans* strain CAT23 (*MAL2p-DYN1*:*HIS1*/*dyn1*::*URA3*) in maltose-containing medium shows wild-type-like nuclear positioning, whereas hyphal induction on CSM containing glucose (D) reveals the *dyn1* mutant phenotype.

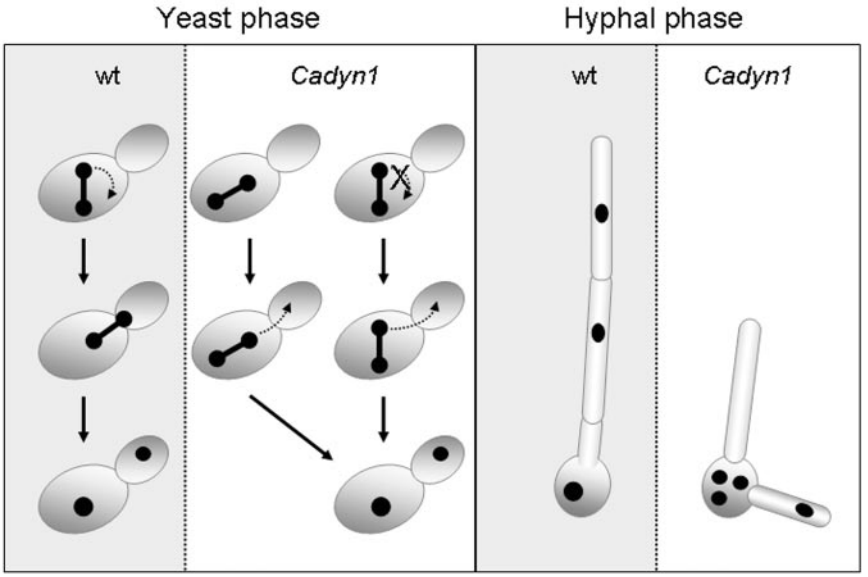

FIG. 9. Summary of nuclear migration defects in *dyn1* compared to migration of the wild type (wt). During the yeast phase, spindle realignment with the mother-bud neck occurs frequently in the wild type but is absent in *dyn1*. In the *dyn1* mutant, spindle elongation may occur in the mother-bud axis, resulting in correct nuclear migration, or else leads to mitosis in the mother cell. The generation of binucleate cells in *dyn1* is prevented (with high frequency) by postmitotic nuclear migration delivering one nucleus into the daughter cell (see also Table 4). Hyphal growth in the wild type results in nuclear migration and in evenly distributed nuclei along the hyphal segments. In *dyn1* cells induced for hyphal formation failure in nuclear migration leads to anucleate hyphal tips that cease growth and thus establish a filamentation defect.

frames that encode potential homologs of *S. cerevisiae* Bim1p (orf19.00676.prot) and Kar9p (YPL269w) (orf19.05011.prot) proteins were identified which allow further analysis of a similar mechanism in *C. albicans*.

Nuclear migration in the *C. albicans dyn1* mutant. The *dyn1* mutant exhibited a failure to move the nucleus to the bud site. On the other hand, only those nuclei that obtained a position close to the bud neck exhibited spindle elongation in the mother-bud axis, which then also resulted in correct nuclear distribution between mother and daughter cells during mitosis. Two striking defects of *dyn1* mutant yeast cells were the lack of any spindle realignment and the subsequent completion of mitosis in the mother cell in those cases were the spindle was not realigned (Fig. 9). As in *S. cerevisiae*, those *C. albicans* cells in which mitosis occurred in the mother cell still managed to distribute their nuclei evenly between mother and daughter cells. This is contrasted by *U. maydis* mutants deficient in dynein, in which mitosis aberrantly occurs in the mother cell but postmitotic nuclear migration is missing, resulting in lethality of the cells (23). Postmitotic nuclear migration in *Cadyn1* yeast cells largely prevents the generation of binucleate cells. As in *S. cerevisiae*, this nuclear migration may be triggered by a Kip3p homolog in *C. albicans* (see below). Under hypha-inducing conditions, however, nuclear migration defects became more dramatic in *C. albicans dyn1* cells. Mitotic divisions frequently took place in the *dyn1* mother cells even though germ tubes were formed. Therefore, the *C. albicans dyn1* defect resembles the *nudA1* phenotype in *A. nidulans*, which refers to clusters of nuclei in the germ cell (29). In *C. albicans* as in *A. nidulans*, these clusters are located in the germ cells, whereas in *A. gossypii* dynein mutant nuclei accumulate at the hyphal tips (2). Mitosis that took place in *dyn1* germ cells is in contrast to that of the *C. albicans* wild type, in which serum-induced cells predominantly undergo their first mitotic divisions in the germ tubes (24). Lack of long-range nuclear migration in *dyn1* hyphae finally results in the breakdown of polarized hyphal growth in *dyn1* cells (Fig. 9). Other microtubule-based motor proteins, for example, Kip2p and Kip3p, for which homologs exist in *Candida*, may be responsible for postmitotic nuclear migration in the *dyn1* mutant during yeast-like growth but fail to achieve a nuclear distribution that can support hyphal development in *C. albicans*. This indicates a dependency of polarized hyphal growth on the faithful delivery of a nucleus in the case of *C. albicans* (or nuclei in the case of true

TABLE 5. Analysis of polarized morphogenesis

Criterion	Wild-type SC5314 (%)	GC3 (*dyn1*/*dyn1*) (%)
Germ tube formation (after 3 h) of single cells/pseudohyphae/germ tubes	6/11/83 (n = 317)	6/16/78 (n = 234)
Hyphal growth (after 6 h) of single cells/pseudohyphae/germ tubes or hyphae	7/24/69 (n = 207)	5/39/56 (n = 200)

TABLE 6. Position of septa in germ tubes[a]

Distance (μm)	Wild-type SC5314 (%)	GC3 (*dyn1*/*dyn1*) (%)
No septum	8	19
0–5	16	23
6–20	73	51
>20	3	7

[a] $n > 170$.

filamentous ascomycetes, such as *A. nidulans*) to the tip compartment, even if establishment of polarized hyphal growth in ascomycetes may be solely a function carried out by the actin cytoskeleton (9). Efficient nuclear migration in *S. cerevisiae* is carried out by two partially redundant pathways centering on dynein and Kar9p (16). This is in line with the observation that deletion of *KAR9* in *S. cerevisiae* is synthetically lethal with deletions in *DYN1*. Analyses of the *C. albicans* set of motor proteins with respect to their contribution to nuclear migration, particularly during the hyphal growth stage, need to be performed in the future.

ACKNOWLEDGMENTS

We thank Judith Berman for discussions of the manuscript and for communicating results prior to publication. Sequence data for *C. albicans* were obtained from the Stanford Genome Technology Center website at http://www-sequence.stanford.edu/group/candida.

This research was supported by the Deutsche Forschungsgemeinschaft, the Friedrich-Schiller University, and the Hans-Knöll Institute. Sequencing of *Candida albicans* was accomplished with the support of the NIDR and the Burroughs Wellcome Fund.

REFERENCES

1. **Adames, N. R., and J. A. Cooper.** 2000. Microtubule interactions with the cell cortex causing nuclear movements in Saccharomyces cerevisiae. J. Cell Biol. **149:**863–874.
2. **Alberti-Segui, C., F. Dietrich, R. Altmann-Johl, D. Hoepfner, and P. Philippsen.** 2001. Cytoplasmic dynein is required to oppose the force that moves nuclei towards the hyphal tip in the filamentous ascomycete Ashbya gossypii. J. Cell Sci. **114:**975–986.
3. **Bloom, K.** 2001. Nuclear migration: cortical anchors for cytoplasmic dynein. Curr. Biol. **11:**R326–R329.
4. **Brachat, A., J. V. Kilmartin, A. Wach, and P. Philippsen.** 1998. Saccharomyces cerevisiae cells with defective spindle pole body outer plaques accomplish nuclear migration via half-bridge-organized microtubules. Mol. Biol. Cell. **9:**977–991.
5. **Desai, A., and T. J. Mitchison.** 1997. Microtubule polymerization dynamics. Annu. Rev. Cell Dev. Biol. **13:**83–117.

5a. **Fonzi, W. A., and M. Y. Irwin.** 1993. Isogenic strain construction and gene mapping in *Candida albicans*. Genetics **134:**717–728.

6. **Garnjobst, L., and E. L. Tatum.** 1967. A survey of new morphological mutants in Neurospora crassa. Genetics **57:**579–604.
7. **Gola, S., R. Martin, A. Walther, A. Dünkler, and J. Wendland.** 2003. New modules for PCR-based gene targeting in *Candida albicans*: rapid and efficient gene targeting using 100 bp of flanking homology region. Yeast **20:** 1339–1347.
8. **Gundersen, G. G., and A. Bretscher.** 2003. Cell biology. Microtubule asymmetry. Science **300:**2040–2041.
9. **Heath, I. B., G. Gupta, and S. Bai.** 2000. Plasma membrane-adjacent actin filaments, but not microtubules, are essential for both polarization and hyphal tip morphogenesis in *Saprolegnia ferax* and *Neurospora crassa.* Fungal Genet. Biol. **30:**45–62.
10. **Hoepfner, D., A. Brachat, and P. Philippsen.** 2000. Time-lapse video microscopy analysis reveals astral microtubule detachment in the yeast spindle pole mutant *cnm67*. Mol. Biol. Cell. **11:**1197–1211.
11. **Korinek, W. S., M. J. Copeland, A. Chaudhuri, and J. Chant.** 2000. Molecular linkage underlying microtubule orientation toward cortical sites in yeast. Science **287:**2257–2259.
12. **Lee, L., J. S. Tirnauer, J. Li, S. C. Schuyler, J. Y. Liu, and D. Pellman.** 2000. Positioning of the mitotic spindle by a cortical-microtubule capture mechanism. Science **287:**2260–2262.
13. **Li, Y. Y., E. Yeh, T. Hays, and K. Bloom.** 1993. Disruption of mitotic spindle orientation in a yeast dynein mutant. Proc. Natl. Acad. Sci. USA **90:**10096–10100.
14. **Liu, H., J. Kohler, and G. R. Fink.** 1994. Suppression of hyphal formation in Candida albicans by mutation of a STE12 homolog. Science **266:**1723–1726.
15. **Lo, H. J., J. Kohler, B. DiDomenico, D. Loebenberg, A. Cacciapuoti, and G. R. Fink.** 1997. Nonfilamentous *C. albicans* mutants are avirulent. Cell **90:**939–949.
16. **Miller, R. K., K. K. Heller, L. Frisen, D. L. Wallack, D. Loayza, A. E. Gammie, and M. D. Rose.** 1998. The kinesin-related proteins, Kip2p and Kip3p, function differently in nuclear migration in yeast. Mol. Biol. Cell **9:**2051–2068.
17. **Miller, R. K., D. Matheos, and M. D. Rose.** 1999. The cortical localization of the microtubule orientation protein, Kar9p, is dependent upon actin and proteins required for polarization. J. Cell Biol. **144:**963–975.
18. **Morris, N. R.** 2003. Nuclear positioning: the means is at the ends. Curr. Opin. Cell Biol. **15:**54–59.
19. **Plamann, M., P. F. Minke, J. H. Tinsley, and K. S. Bruno.** 1994. Cytoplasmic dynein and actin-related protein Arp1 are required for normal nuclear distribution in filamentous fungi. J. Cell Biol. **127:**139–149.
20. **Reck-Peterson, S. L., and R. D. Vale.** 2004. Molecular dissection of the roles of nucleotide binding and hydrolysis in dynein's AAA domains in *Saccharomyces cerevisiae*. Proc. Natl. Acad. Sci. USA **101:**1491–1495.
21. **Riquelme, M., G. Gierz, and S. Bartnicki-Garcia.** 2000. Dynein and dynactin deficiencies affect the formation and function of the Spitzenkorper and distort hyphal morphogenesis of *Neurospora crassa*. Microbiology **146:**1743–1752.
22. **Snyder, M., S. Gehrung, and B. D. Page.** 1991. Studies concerning the temporal and genetic control of cell polarity in *Saccharomyces cerevisiae*. J. Cell Biol. **114:**515–532.
23. **Straube, A., W. Enard, A. Berner, R. Wedlich-Soldner, R. Kahmann, and G. Steinberg.** 2001. A split motor domain in a cytoplasmic dynein. EMBO J. **20:**5091–5100.
24. **Sudbery, P. E.** 2001. The germ tubes of *Candida albicans* hyphae and pseudohyphae show different patterns of septin ring localization. Mol. Microbiol. **41:**19–31.
25. **Tinsley, J. H., P. F. Minke, K. S. Bruno, and M. Plamann.** 1996. p150Glued, the largest subunit of the dynactin complex, is nonessential in *Neurospora* but required for nuclear distribution. Mol. Biol. Cell **7:**731–742.
26. **Vierula, P. J., and J. M. Mais.** 1997. A gene required for nuclear migration in *Neurospora crassa* codes for a protein with cysteine-rich, LIM/RING-like domains. Mol. Microbiol. **24:**331–340.
27. **Walther, A., and J. Wendland.** 2003a. An improved transformation protocol for the human fungal pathogen *Candida albicans*. Curr. Genet. **42:**339–343.
28. **Walther, A., and J. Wendland.** 2004. Polarized hyphal growth in *Candida albicans* requires the WASP homolog Wal1p. Eukaryot. Cell. **3:**471–482.

28a. **Wilson, R. B., D. Davis, and A. P. Mitchell.** 1999. Rapid hypothesis testing with *Candida albicans* through gene disruption with short homology regions. J. Bacteriol. **181:**1868–1874.

29. **Xiang, X., S. M. Beckwith, and N. R. Morris.** 1994. Cytoplasmic dynein is involved in nuclear migration in *Aspergillus nidulans*. Proc. Natl. Acad. Sci. USA **91:**2100–2104.
30. **Xiang, X., and R. Fischer.** 2004. Nuclear migration and positioning in filamentous fungi. Fungal Genet. Biol. **41:**411–419.
31. **Xiang, X., and N. R. Morris.** 1999. Hyphal tip growth and nuclear migration. Curr. Opin. Microbiol. **2:**636–640.
32. **Xiang, X., and M. Plamann.** 2003. Cytoskeleton and motor proteins in filamentous fungi. Curr. Opin. Microbiol. **6:**628–633.
33. **Yamamoto, A., and Y. Hiraoka.** 2003. Cytoplasmic dynein in fungi: insights from nuclear migration. J. Cell Sci. **116:**4501–4512.
34. **Yeh, E., R. V. Skibbens, J. W. Cheng, E. D. Salmon, and K. Bloom.** 1995. Spindle dynamics and cell cycle regulation of dynein in the budding yeast, Saccharomyces cerevisiae. J. Cell Biol. **130:**687–700.

7

Ronny Martin *

Andrea Walther *

Jürgen Wendland

Ras1-induced hyphal development in *Candida albicans* requires the formin Bni1.

Eukaryot. Cell. (in Revision, 08.06.05).

Formine sind Effektorproteine von Rho-GTPasen. Die Deletion des Formin-Homologen *BNI1* in *C. albicans* resultierte in Defekten im polaren Wachstum während der Hefe- und der Hyphephase. Δ*bni1* Zellen waren zwar in der Lage, die Bildung von Keimhyphen zu iniitieren, die Aufrechterhaltung des polaren Wachstums war aber durch das Fehlen von Bni1p gestört und konnte auch nicht durch die konstitutive Aktivierung der übergeordneten Ras1-GTPase supprimiert werden.

* Beide Autoren lieferten gleichwertige Beiträge.

Ras1-induced hyphal development in Candida albicans requires the formin Bni1

Ronny Martin[1+], Andrea Walther[1+] and Jürgen Wendland[1,2,*]

[1]*Junior Research Group: Growth-control of Fungal Pathogens Leibniz Institute for Natural Products Research and Infection Biology-Hans-Knöll Institute- and* [2]*Dept. of Microbiology, Friedrich-Schiller University, Jena*

Received

Formins are downstream effector proteins of Rho-type GTPases and are involved in the organization of the actin cytoskeleton and actin cable assembly at sites of polarized cell growth. Here we show using *in vivo* time lapse microscopy that deletion of the *Candida albicans* formin homologue *BNI1* results in polarity defects during yeast growth and hyphal stages. Yeast *bni1* cells were swollen, showed increased random pattern and had a severe defect in cytokinesis with enlarged bud necks. Induction of hyphal development in *bni1* cells resulted in germ tube formation but was halted at the step of polarity maintenance. Introduction of a constitutively active *ras1G13V* allele in the *bni1* strain or addition of cAMP to the growth medium did not bypass *bni1* hyphal growth defects. Bni1-GFP is found persistently at the hyphal tip and colocalizes with a structure resembling the Spitzenkörper of true filamentous fungi. Deletion of the second *C. albicans* formin, *BNR1*, revealed only minor defects resulting in elongated yeast cells with cell separation defects but did not interfere with the ability of *bnr1* cells to initiate and maintain polarized hyphal growth. These results suggest that the maintenance of polarized hyphal growth in *C. albicans* requires two actin cytoskeletal pathways including the formin Bni1 and the secretory pathway as well as Wiskott-Aldrich Syndrome Protein (WASP)-homolg Wal1-mediated endocytosis.

Cell polarity establishment and maintenance of polarized secretion are essential for morphogenesis and development (9). Cell polarization is required in neuronal cells to establish a growth cone that maintains polarized growth direction in response to extracellular stimuli (8, 19). Cell polarization is also required for epithelium formation and in migrating cells. Similarly, in plant cells establishment and maintenance of cell polarity is used during root hair or pollen tube growth (30). Both actin and microtubule cytoskeletons play important roles in maintaining cell polarization and in providing cellular tracks for vesicle delivery. This requires complex processes of spatial and temporal coordination of protein localization and activation at sites of polarized growth (31). The actin cytoskeleton is involved in three basic structures: Actin patches, actin cables, and the cytokinetic ring at sites of cell cleavage in animal and fungal cells. Actin patches are found at sites of endocytosis, actin cables provide tracks for vesicle delivery and dynamic constriction of the actin ring is required for cytokinesis (31). Rho-type GTPases, such as Cdc42, are known regulators of the actin cytoskeleton by activating downstream effector proteins (10). Two major classes of conserved protein families are the Wiskott-Aldrich Syndrome Proteins or WASPs and the formins. WASP-like proteins are involved in endocytosis and play a role in Arp2/3-dependent actin assembly (7, 24, 42,). The *C. albicans* WASP-homolog, Wal1 was shown to be required for endocytosis, vacuolar morphology as well polarized hyphal growth (39). Formins represents the conserved family of Diaphanous-related proteins that control the assembly of actin cables (32, 33). Formins assemble linear actin cables in an Arp2/3-complex independent manner (11, 12, 32, 33). The sole *Aspergillus nidulans* formin, SEPA, is so far the only formin analyzed in a filamentous fungus. SEPA localizes to sites of polarized growth both at the hyphal tip and at septal sites. The tip-localization resembles the position of a phase-dark structure termed Spitzenkörper (16). In *Saccharomyces cerevisiae* the formin Bni1 co-localizes with Spa2, Bud6, and Pea2 at sites of polarised growth and forms a complex termed the polarisome (14, 35). In *C. albicans SPA2* has been analyzed recently and was found to localize to the tip of growing hyphae. Consistently, deletion of *SPA2* resulted in polarity and hyphal growth defects (43). In this study, we exploit the human fungal pathogen *Candida albicans* as a model to understand the role and contribution of formins in the regulation of polarized morphogenesis. In *C. albicans* the yeast-to-hypha transition contributes to its virulence and allows the penetration of epithelia and the evasion of the host cellular immune response (6). The genetic basis of morphogenetic switching in *C. albicans* relies on the activation of the Ras1-GTPase by extracellular signals which induce two downstream signal cascades: a MAP-kinase pathway and the cAMP-pathway. Both activate transcriptional regulators, Cph1 and Efg1, respectively, that induce hyphal specific gene expression (4). Deletions of *CPH1* and *EFG1* or *RAS1* yield viable mutant strains that are non-filamentous under most conditions and avirulent in animal models (13, 23). On the other hand, constitutive activation of *RAS1*, using a *ras1G13V* allele, enhances filamentous growth (13). To investigate the role of the actin cytoskeleton in hyphal growth we could show in a previous study that the *C. albicans* Wiskott-Aldrich Syndrome Protein homologue, Wal1, is important for endocytosis and maintenance of polarized cell growth (39). Here, we investigate the role of the *C. albicans* formins as part of a potential Spitzenkörper complex and present a model on the role of the actin cytoskeleton in hyphal morphogenesis in *C. albicans*.

* Corresponding author
Dr. Jürgen Wendland
Leibniz Institute for Natural Products Research and Infection Biology and Deptartment of Microbiology Friedrich-Schiller-University Beutenbergstr. 11a D-07745 Jena ,Tel.: +49-3641-65-6685
Fax: +49-3641-65-6620 email: juergen.wendland@uni-jena.de

MATERIALS AND METHODS

Strains and media. *C. albicans* strains used in this study are listed in Table 1. Media and the lithium acetate transformation procedure were used as described previously (38, 39).

Targeting of *C. albicans* genes. The *C. albicans* homologues of the *Saccharomyces cerevisiae* formins *BNI1* and *BNR1* were identified in the genomic sequence (http://www-sequence stanford.edu/group/candida). Deletions of the complete open reading frames of both alleles of *CaBNI1* or *BNR1* were

TABLE 1. Strains used in this study

Strain[a]	Genotype	Reference
SC5314	*Candida albicans* wild type	15
BWP17	*ura3::λimm34/ura3:λimm34, arg4::hisG/arg4::hisG, his1::hisG/his1::hisG*	41
CAT4	*WAL1/wal1::HIS1*	39
CAT6	*wal1::HIS1/wal1::URA3*	39
CAT37	*wal1::HIS1/wal1::SAT1*	This study
CAT40	*wal1::HIS1/wal1::SAT1 ADE2/ade2::MAL2p-ras1^{G13V}:URA3*	This study
GC11	*BNI1/bni1::URA3*	This study
GC13	*BNR1/bnr1::URA3*	This study
GC14	*bni1::URA3/bni1::HIS1*	This study
GC19	*bnr1::URA3/bnr1::HIS1*	This study
GC33	*MAL2p-BNI1::HIS1/bni1:URA3*	This study
GC40	*bni1::HIS1/bni1::ARG4*	This study
GC42	*ADE2/ade2::MAL2p-ras1^{G13V}:URA3*	This study
GC46	*bni1::HIS1/bni1::ARG4, ADE2/ade2::MAL2p-ras1^{G13V}:URA3*	This study
GC59	*BNI1/BNI1-GFP:URA3*	This study
GC60	*BNI1-GFP:URA3/bni1::HIS1*	This study

[a] All GC strains are derivates of BWP17 with the indicated genotypic alterations.

performed by PCR-generated *URA3* and *HIS1* disruption cassettes containing 100bp of target homology region at both ends of the cassettes as described (17). Similarly, regulatable expression of *BNI1* under the control of the *CaMAL2* promoter was achieved by amplifying *HIS1-MAL2p* cassettes in transformation of a *BNI1/bni1* strain so that the endogenous promoter of the only remaining copy of *BNI1* is exchanged for the *MAL2*-promoter. To reconstruct strains generating new marker combinations in the absence of a sexual cycle, a homozygous strain (in this case the *bni1::HIS1/bni1::URA3* strain) was used and transformed with PCR-amplified cassettes derived from the pFA-ARG4 plasmid. Upon double selection for histidine and arginine prototrophy transformants were selected which had replaced the *URA3* marker for the *ARG4* marker gene. Either this method or using a suitable heterozygous strain can result in generating the desired marker combinations. To increase the arsenal of available marker genes we generated a pFA-SAT1 plasmid which contains the SAT1 genes (kindly provided by Joachim Morschhäuser). In order to fuse *BNI1* with GFP, a fusion cassette was cloned. To this end a PCR-fragment was amplified from genomic DNA which contains the 3'-end of *BNI1*. The *in vivo* recombination machinery of *Saccharomyces cerevisiae* was used to fuse the *BNI1*-ORF to GFP. To this end a GFP-URA3 PCR-cassette was amplified from the standard set of modules. This cassette contains the *C. albicans URA3* which is also functional in *S. cerevisiae.* Gene targeting in *S. cerevisiae* requires shorter flanking homology regions to the target locus (45bp were used in our case). This detour via *S. cerevisiae* was used to generate a cassette and verify the correct in frame fusion after plasmid recovery from yeast and amplification in *Escherichia coli* by sequencing. This cassette was excised from the plasmid backbone and used for transformation of either the progenitor strain BWP17 or the heterozygous *BNI1/bni1* strain. In the latter, this generated a strain in which *BNI1-GFP* is the only form of *BNI1* expressed. The constitutively active *ras1G13V* was used as described previously which resulted into targeted integration of the *CaMAL2*-promoter driven alleles at the *C. albicans ADE2* locus (13). Primers used for the construction of the cassettes and the verification of the deletions are listed in Table 2 or were described previously (39). Disruptions were verified by PCR on whole yeast cells.

Hyphal induction of *C. albicans*. Different protocols were used to induce hyphae formation in *C. albicans* strains at 37°C. On solid plates hyphal induction was either done on Spider medium (22) or media containing 10% serum (Calf Serum, Sigma). Plates inoculated with different strains were incubated for 4-7 days prior to photography. In liquid culture next to serum also the addition of 10mM cAMP was used to induce filament formation.

Staining procedures: Chitin staining was done by directly adding 1µl calcofluor (1mg/ml) to a 100µl cell suspension followed by an incubation of 15min at room temperature and subsequent washing step to optimize the signal-to-noise ratio. Vacuolar staining of overnight cultures was done using the lipophilic dye FM4-64 (0.2µg/ml). Cells were stained for 30min at 30°C prior to photography. To monitor the uptake of FM4-64 by *in vivo* time lapse microscopy, cells in the exponential growth phase were transferred to deep-well microscopy slides containing the dye in the culture medium. Imaging of the Spitzenkörper-like structure was done by staining cells induced for germ tube formation with FM4-64 immediately prior to microscopy. Rhodamine-phalloidin staining of the actin cytoskeleton was done as described (27).

Time-lapse microscopy: Strains were grown to exponential phase, harvested, washed and resuspended in sterile water. Small aliquots of cells (1.5 µl) were applied on microscopy slides with deep-wells as described previously (37). Temperature control was achieved via a heat stage mounted on the microscope table. Microscopy was performed on an automated Zeiss AxioplanII-imaging microscope. Images acquisition using Metamorph software (Universal Imaging Corporation) and movie processing was done as described (39). Movies will be curated at the author's homepage at http://pinguin.biologie.uni-jena.de/phytopathologie/pathogenepilze/index.html.

TABLE 2. Oligonucleotide primers used in this study

Primer	Sequence[a]
#392 XFP verification	GAGTGCCATGCCCGAAGGTTATG
#599 U3	GGAGTTGGATTAGATGATAAAGGTGATGG
#600 U2	GTGTTACGAATCAATGGCACTACAGC
#601 H2	CAACGAAATGGCCTCCCCTACCACAG
#602 H3	GGACGAATTGAAGAAAGCTGGTGCAACCG
#797 S1-*BNI1*	ATCACAAACATCTTTTCATCATCCACTACTATCACCAGTGCTA GTGCAGTTTCAATTAATTACCATATTCTTCAACCTCATCCTCC CTTACCTCCTCCCTgaagcttcgtacgctgcaggtc
#798 S2-*BNI1*	CTTAACTTGTAAACTCACATGGTATATAATATGTAAATACAAC TTTGTACAGATATAAAAATTAATAGCTATATTTCATTTAAATA CATATACAAAAAAAAtctgatatcatcgatgaattcgag
#799 G1-*BNI1*	CTCTCTGAGGGAGACAACGC
#800 G4-*BNI1*	CAGGTTTCCAAATTGAATCGTCC
#801 G4-*BNI1-MAL2p*	GCACCCTTGTCGTATGGAC
#802 G1-*BNI1*-FP	CCGCCTGAAGGATGCTG
#804 S2-*BNI1-MAL2p*	GAGTTGAGTTCTGACTTGCTGATGATAATATACTAGCTGAGTC ATTGGAAGACATGTCGGACACACTGTCGGTGTTGTGCTTGTCT TTATGTCGTCTCCTcattgtagttgattattagttaaaccac
#805 S1-*BNR1*	GTTGTTTTTTTTTTTCAAACGCGACTTCTAAATCTCTAGCCAT ACCCGATCCAGAAACACTTGTTTTAAATTTTTTGGTTACCAC ACACACAAAAATATTCgaagcttcgtacgctgcaggtc
#806 S2-*BNR1*	AGAAAGTGAAAAAAAAGAAAAAAGAAAAAAAAAAAATAGTTGT TCTTTTTTAAGGAAGAGCATCACAAAATTTTTTAGACGTGTAT ATGCAGTATCGGTGTAGtctgatatcatcgatgaattcgag
#811 G1-*BNR1*	GTAAGCACCGAGTCTTGTCGC
#812 G4-*BNR1*	GGAAATTTCTACTCAACGAGCG
#1088 I1-*BNI1*	GGAAATCAAGAACCAGAGCCTTG
#1089 I2-*BNI1*	CTCTTGGCAAAGCCGGCAACAC
#1090 I1-*BNR1*	GAGATAGATTCCAGGAACACGAG
#1091 I2-*BNR1*	CACCAATGCCTTGACGACGTACAC
#1203 CaBNI1-BamHI-down	CGCGGATCCGCGGGCTCACCAACTAATGTCTCACC
#1204 CaBNI1-XbaI-up	CTTCATCTTCGTCATCATAAATAGAGTCGTGCTCTAGAGCA
#1242 *ADE2*-down	GGTCGTATGATTGTTGAAGCAGCAC
#1243 *ADE2*-up	CCAGAGTTGTGAGGTCTTGGTGC
#1244 *RAS1*-down	GGAAAGACAAGTTAGTTATCAAGATGG
# 1268 S1-BNI1-GFP	GTTCAAATAGATCTTGATGAAGTGGCTAAGAATAACAATAGTGAG ggtgctggcgcaggtgcttc
#1269 S2-BNI1-GFP	CTCGAATTCATCGATGATATCAGAGGCCTGCTAAGGAGAAGCACT ttttttgtatatgtatttaaatg

Uppercase sequences correspond to *C. albicans* genomic DNA. Lowercase sequences correspond to 3'-terminal annealing regions for the amplification of transformation cassettes. All sequences are written from 5' to 3'.

RESULTS

Functional analysis of *C. albicans* formins. *Candida* formins were identified in the *C. albicans* genome sequence using the *Saccharomyces cerevisiae* Bni1 protein. Two formins were found; *CaBNI1* and *CaBNR1* of 1732 and 1485 amino acids in length, respectively. *CaBNI1* is annotated as orf19.4927 and CaBNR1 as orf19.7537. Both formins correspond in their protein structure to the *A. nidulans* SEPA and other formins in that they possess an N-terminal G-protein binding domain (GBD), followed by a formin homology (FH) 3 domain and a C-terminal FH1-FH2-DAD (Diaphanous autoinhibitory domain) domain involved in actin filament assembly and regulation of formin activity by autoinhibition (29). Highest sequence identity of more than 50% between the *C. albicans* Bni1 and the *S. cerevisiae* Bni1 is found in the C-termini including the FH2 domains while the N-termini are less well conserved and show less than 30% identity on the amino acids level. The presence of a GDB and DAD indicates that similar regulatory mechanisms apply in *C. albicans* as have been described in other systems, particularly the direct binding to a Rho-type GTPase.

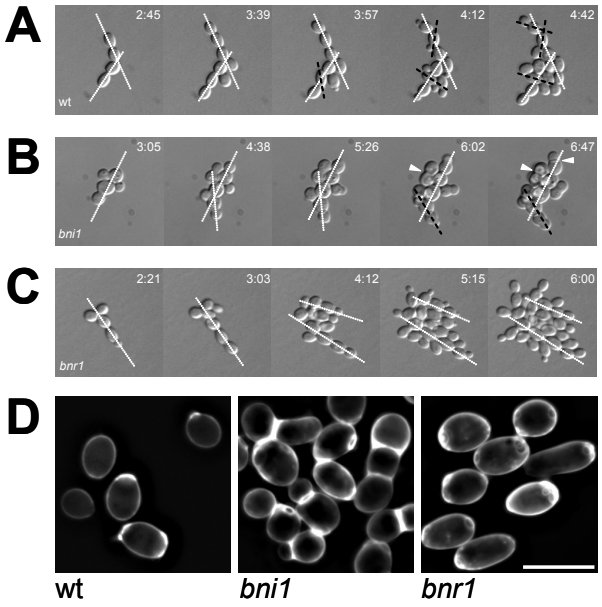

FIG. 1. Growth defects of *C. albicans* formin mutants during yeast growth. Growth of the wild type and formin mutant strains was monitored using time lapse microscopy over several hours (time scale in hrs:min) (A-C). In the wild type movies a characteristic change of cell axes after cytokinesis can be observed (previous mother-bud axes indicated as white dashed lines and newly established axes by black dashed lines in A-C). This results in lateral movement of cells such that wild type colonies form a single cell layer (A). In the *bni1* mutant growth was irregular and cells were dispatched in three dimensions. A shift of mother-bud axes occurs, but often only due to mechanical forces generated by new buds. The arrow denotes enlarged septal sites (B). In the *bnr1* mutant growth axes are kept over several cell cycles resulting in a linear array of mother and daughter cells (C). Cell shape and budding pattern of the indicated strains was analyzed after staining with calcofluor (D). Scale bar is 5µm.

To investigate the role of both *C. albicans* formins during yeast and hyphal growth, mutant strains were constructed in which the complete ORFs of both alleles of either *BNI1* or *BNR1* were sequentially replaced using PCR-based gene targeting methods (17). Homozygous mutant strains were generated from independent heterozygous strains for each formin and were phenotypically identical indicating that correct gene targeting had occurred as was verified by colony-PCR. Additionally, to provide further proof that the observed phenotypes described below were solely due to the disruption of *BNI1,* a heterozygous *BNI1/bni1* mutant strain was used to place the only remaining copy of the target gene under control of the regulatable *CaMAL2*-promoter. This generated strains with wild type like appearances including the ability to filament under permissive conditions during growth on maltose while shut down of the *MAL2*-promoter during a glucose growth regime restored mutant phenotypes (not shown).

TABLE 3 Yeast phase growth characterisitics.

Parameter	wild type SC5314	GC14 (*bni1/bni1*)	GC19 (*bnr1/bnr1*)
Cell cycle duration	71 ± 7 min	92 ± 15 min	99 ± 14 min
Cell length (n=500)	6.0 ± 0.5 µm	6.4 ± 0.6 µm	6.7 ± 0.5 µm
Cell width (n=500)	4.6 ± 0.7 µm	5.7 ± 0.4 µm	3.9 ± 0.4 µm
Bud scar diameter (n=200)	1.5 ± 0.3 µm	2.4 ± 0.9 µm	1.5 ± 0.4 µm

Polarized growth defects of formin mutants during the yeast growth phase. Cell cycle length of the wild type, the *bni1* and *bnr1* strains was determined using growth curves generated of cultures grown in liquid rich medium at 30°C and using *in vivo* time lapse microscopy recordings calculating as average cell cycle duration the time required between two consecutive bud emergence events. This revealed prolonged cell cycle durations of about 20min for both formin mutants compared to the wild type (Tab. 3). Wild type cells are characteristically ellipsoidal in cell shape and show a length vs width ratio of approximately 1.3. During growth on solid media, cytokinesis in the wild type is most obvious by a rotational movement of mother and daughter cells out of the mother bud axis (Fig. 1A). Heterozygous mutants of either *BNI1*/*bni1* or *BNR1/bnr1* were phenotypically like the wild type suggesting the absence of gene dosage effects.

Bud emergence in *bni1* cells was not inhibited. However, newly formed buds showed drastic defects in polarized growth. This resulted in formation of swollen and rounded yeast cells with a length/width index of 1.1, resembling mutant *wal1* cells bearing a deletion of the WASP-homolog *WAL1*. Strong defects were observed at the bud neck which was broadened and revealed enlarged septa (Tab. 3). Separation of mother and daughter cells did not take place as readily as in the wild type. Instead mother and daughter cells were separated by pushing forces generated by newly formed buds during growth on solid media as observed during *in vivo* time lapse recordings (Fig. 1B).

Characteristically *bnr1* cells were more elongated than the wild type which resulted in a length/width ratio of 1.7. Cell separation defects of *bnr1* cells were not as drastic as seen in *bni1* but still resulted in mother and daughter cells that were moved apart by colonial growth rather than by cytokinesis of mother and daughter cells itself (Fig. 1C).

To determine if the swollen morphology of *bni1* cells resulted also in an altered bud site selection pattern, cells were stained by calcofluor to visualize chitin rich septal rings (Fig. 1D). In the wild type and in *bnr1* cells a bipolar budding pattern was observed. In contrast *bni1* cells showed increased random

budding resembling *spa2* and *wal1* cells described in previous studies (Fig. 1D; Tab. 1) (39, 43).

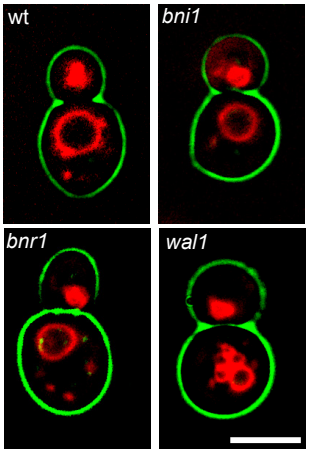

FIG. 2. Analysis of endocytosis. Endocytosis and vacuolar morphology of the indicated strains was analyzed by monitoring the uptake FM4-64. The figure shows images of cells that were grown over night and stained with FM4-64. The wild type and formin mutants generate a single large vacuole. In contrast the *wal1* cells exhibit fragmented vacuoles. Supplemental Movies 4-6 show the time course of uptake of FM4-64). Scale bar is 5µm.

***C. albicans* formin mutants do not show defects in endocytosis.** Since we found defects in endocytosis in *wal1* mutant cells in a previous study we wanted to determine any deficiencies in vacuolar morphology and transport to the vacuole in formin mutant strains. To this end we analyzed the uptake of the lipophilic dye FM4-64 by *in vivo* fluorescence time lapse microscopy. This revealed no vacuolar phenotypes in *bni1* and *bnr1* cells compared to the drastic defects in the *wal1* mutant suggesting that formins are not involved in endocytosis or in determining vacuolar morphology (Fig. 2B; movies M4-6).

The *C. albicans* formin Bni1 is required for the maintenance of polarized hyphal growth. To analyze growth defects during the hyphal growth phase formin mutants were germ tube formation was initiated under different inducing conditions. First we used *in vivo* time lapse microscopy we followed germ tube induction and polarized hyphal growth of the wild type and the formin mutant strains (Fig. 3; movies M7-9). The wild type and also the *bnr1* strain responded to serum as hyphal inducing cue with vigorous filamentation and the development of mycelia after several hours of growth. In contrast, *bni1* cells initiated germ tube induction but generated swollen germ tubes with widened diameters. These hyphal tubes were not able to maintain polarized cell growth, did not generate fast growing hyphal filaments and lateral branches and were thus not able to develop mycelia. Frequently, constrictions were observed at septal sites indicating the presence of pseudohyphal cells.

Growth on solid media plates containing either serum or on Spider plates revealed abundant filamentation at the edges of wild type and *bnr1* colonies while *bni1* colonies showed smooth edges generated by yeast cell growth supporting our time lapse data and indicating that even after prolonged incubation filamentation is crippled in *bni1* strains (Fig. 4).

Analysis of the actin cytoskeleton in formin mutants. Distribution of actin patches and cables was analyzed to

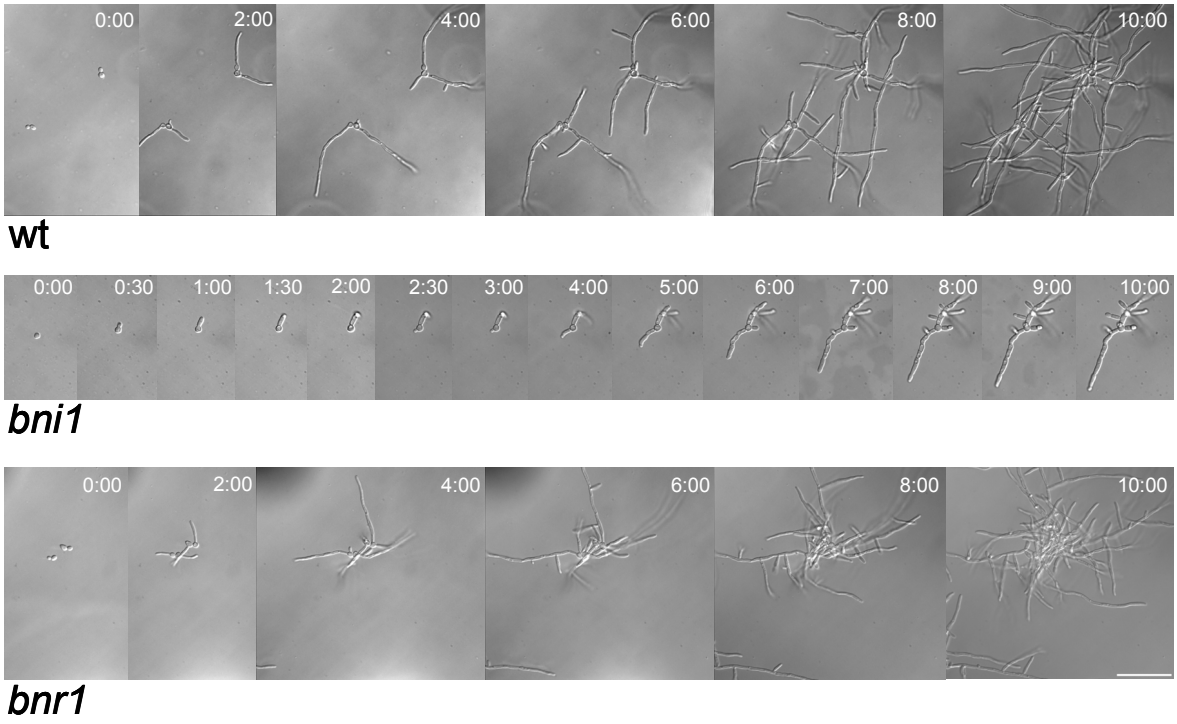

FIG. 3. Time lapse analysis of hyphal induction of formin mutants. *In vivo* time lapse microscopy was used to monitor the initial phases of germ tube induction in the wild type, the *bni1*, and the *bnr1* strains on solid media containing serum at 37°C (for full movies see supplemental movies M7-9). Images from these movies acquired at the indicated time points are shown.

determine if the morphological defects observed can be attributed to a disorganization of the actin cytoskeleton (Fig. 5). During wild type yeast growth cortical actin patches are accumulated in the growing bud and actin cables are found oriented in the mother-bud axis. This was also observed for the formin mutant strains although some partial delocalization

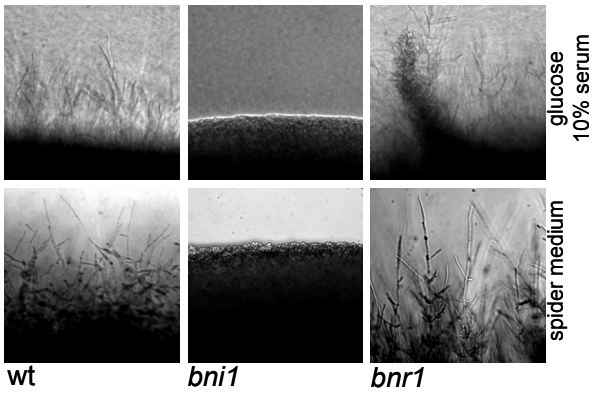

FIG. 4. Mycelial growth defects of the *bni1* mutant. The indicated strains were grown for four days at 37°C on plates containing either 10% serum or Spider medium prior to photography. Representative images of the edges of colony sectors are shown which demonstrate the mycelial growth defects of the *bni1* mutant.

of actin patches in *bni1* cells was found resulting in patch positioning in the mother instead of total accumulation of patches in the bud. This partial delocalization besides the prolonged cell cycle and the cytokinesis defect may attribute to the cell shape defects in *bni1* cells. In *bnr1* mutant cells elongated buds showed clustering of cortical actin patches at the broadened tip region (Fig. 5A). During germ tube induction the actin cytoskeleton in the wild type is strongly polarized towards the hyphal tip as in true filamentous fungi. Such an organization of the actin cytoskeleton was also found in the formin mutants (Fig. 5B). This was expected in *bnr1* hyphae since hyphal development is not blocked in this mutant. However, in the *bni1* germ tubes it was rather unexpected to find such a clearly polarized arrangement of the actin cytoskeleton. Since cortical actin patches are sites of endocytosis Bni1 may not be involved in the correct positioning of patches.

Subcellular localization of Bni1-GFP during hyphal growth. In *S. cerevisiae* Bni1 forms a polarisome complex with Spa2 and Bud6 (35). Since the Spa2 homolog in *C. albicans* was localized to the tip of growing hyphae we wanted to determine the subcellular localization of Bni1. To this end, a C-terminal fusion of GFP to Bni1 was employed both in a heterozygous background and in a strain expressing *BNI1*-GFP as sole variant of Bni1 which also demonstrated that the fusion protein was functional (Fig. 6A). Throughout polarized hyphal growth Bni1-GFP was found to localize to the hyphal tip as a punctuate spot. However, the label was too weak for prolonged time lapse series. Interestingly, during our studies on the uptake of FM4-64, we found that very short incubation periods of germ tube or hyphae with the dye resulted in a spot-like staining at the hyphal tip. Staining of Bni1-GFP expressing hyphae with FM4-64 showed that both spots co-localize (Fig. 6A). This suggests that in *C. albicans* hyphae a structure is present that resembles the Spitzenkörper of true filamentous fungi which on the molecular level can be described by the localization of Bni1 (16, 18). Such a Spitzenkörper was not found in yeast-like cells and thus represents a cellular marker that distinguishes the different cell types in *C. albicans*. Bni1-GFP was found to simultaneously localize to the hyphal tip as well as to a site of future septation in *C. albicans* (Fig. 6B).

Next, we determined if the Spitzenkörper is also present in *bni1* germ tubes. In contrast to the wild type which possesses a focussed, point-like Spitzenkörper, in the *bni1* germ tubes the Spitzenkörper was much broader and enlarged which indicates that the subcellular structure of the Spitzenkörper correlates with the hyphal diameter (Fig. 36).

***ras1G13V* does not suppress the *bni1* and *wal1* phenotypes.** Maintenance of polarized hyphal growth, but not the initiation of germ tube formation, was found to be blocked in both the *bni1* and wal1 germ tubes. Since morphogenetic switching depends on the activation of the Ras1-GTPase we wanted to determine if constitutive activation of Ras1 could bypass the *bni1* or *wal1* defects in polarized hyphal growth (Fig. 7A). To this end, the homozygous *bni1::HIS1/bni1::URA3* strain was used and its *URA3* marker was exchanged for the *ARG4* marker using a PCR-based approach. We then used an integrative cassette containing the *URA3* selectable marker gene which targets the *ras1G13V* allele under control of the *MAL2*-promoter to the *ADE2* locus and placed this cassette in the BWP17, *bni1*, and *wal1* backgrounds (13). Under inducing conditions (37°C and 10% serum) in the presence of maltose as carbon source wild type and BWP17 strains (with or without activated *ras1G13V* allele) filamented profusely both in liquid culture and on solid media (Fig. 7A). In contrast *bni1* germ tubes were phenotypically identical to those of strains harbouring the activated *ras1G13V*. Moreover, the constitutive *ras1G13V* allele in the *bni1* mutant background did not result in filamentation on solid media (insets in Fig. 7A). This indicates that *ras1G13V*, which in the wild type background induces filamentation even at 30°C in complete medium (not shown), is not able to bypass the *bni1* defect. Similarly, the *wal1* mutant phenotype which was previously shown to be defective in maintaining filamentous growth was also not bypassed (suppressed) by the constitutive *ras1G13V* allele. This suggests that both pathways including polarisome function and secretion as well as endocytosis are required for a stable hyphal growth phase in *C. albicans*.

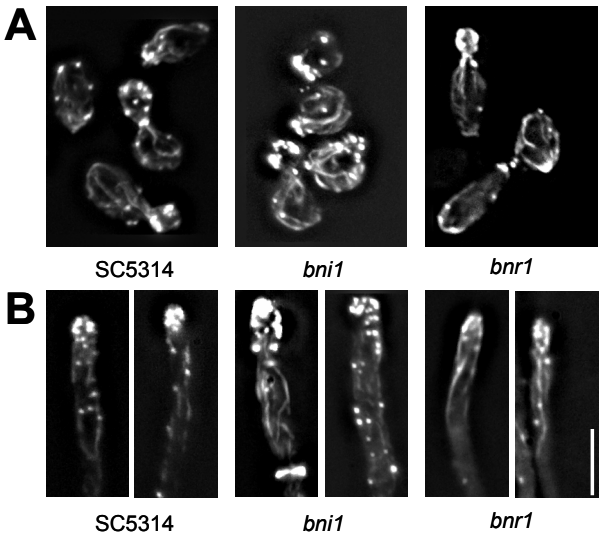

FIG. 5. Analysis of the actin cytoskeleton. Images of rhodamine-phalloidin stained cells of the indicated strains are shown. Cells were grown overnight in YPD at 30°C, inoculated into fresh YPD (A) or YPD+10% serum (B) and grown for three hours at 30°C (A) or 37°C (B) prior to fixation and staining. Bar represents 10µm.

Furthermore, as with the expression of the *ras1G13V* allele, addition of cAMP to the culture medium was not able generate mycelial growth neither in *bni1* nor in *wal1* cells but readily results in filamentation in the wild type strain (Fig. 7B).

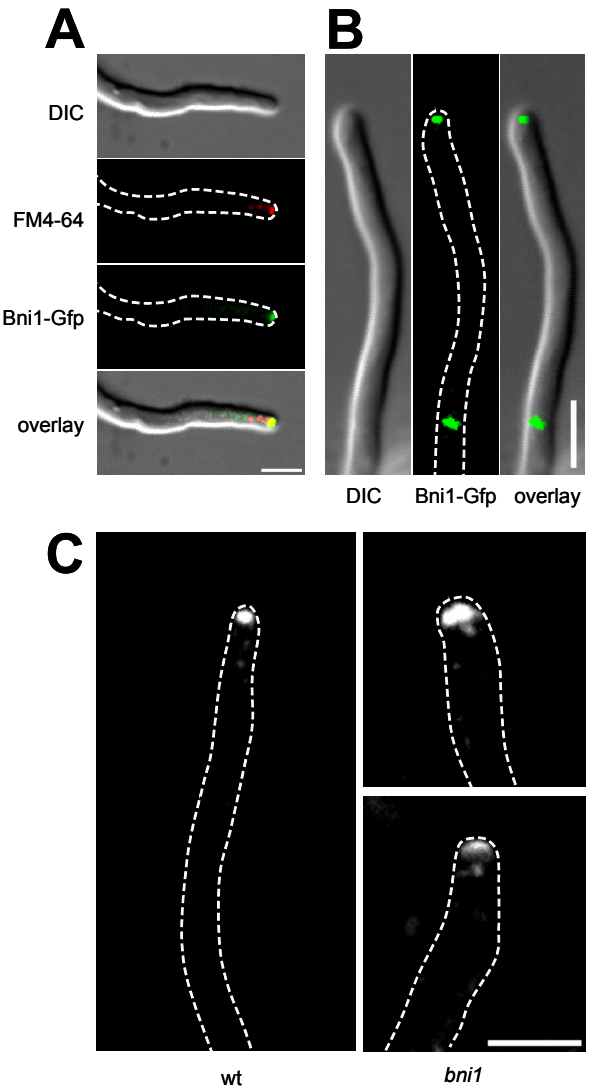

FIG. 6. Localization of Bni1-GFP and the Spitzenkörper. (A) A *BNI1-GFP* expressing strain was induced with serum and stained with FM4-64. GFP fluorescence and DIC images were used in an overlay showing co-localization with the FM4-64 stained Spitzenkörper. (B) Simultaneous localization of Bni1-GFP to the hyphal tip and to a future septal site. Note that in the DIC image no septum is apparent (compare with Fig. 3 or M7). (C) Comparison of Spitzenkörper morphology in wild type and bni1 strains using FM4-64. Images of FM4-64 stained germ tubes that were induced by serum at 37°C for three hours. Bars represent 5µm.

DISCUSSION

C. albicans is an opportunistic commensal mostly in our gastrointestinal tracts. On the other hand, patients with a crippled immune system can suffer from infections in which *C. albicans* colonizes and invades host tissue. In severe cases this may result in life threatening blood stream infections also affecting inner organs (4). An important aspect of *C. albicans* virulence is the ability to switch between yeast and hyphal stages (21, 28). Such a switch to the hyphal stage is dependent on a variety of extracellular stimuli and enables *C. albicans,* for example, to evade the host cellular immune response by killing phagocytes with outgrowing hyphae (6, 23).

Protein networks required for polarized growth. Although *C. albicans* can adopt a variety of morphologies, there are stable yeast and filamentous growth phases. The ability to induce hyphal growth in *Candida* allows its use as a model system to understand the underlying molecular mechanisms. One of the fascinating questions is, if hyphal growth of *C. albicans* relies on the same protein networks as does polarized growth of true filamentous fungi, for example, *Neurospora crassa, Aspergillus nidulans,* or *Ashbya gossypii* (5, 25, 40). In true filamentous fungi a apical body can be distinguished, that is phase dark and forms at growing hyphal tips and was found to be responsible for the growth direction of hyphal tips (1, 16, 18). This apical body or Spitzenkörper serves as vesicle supply center (VSC) in support of hyphal growth (2, 16). This Spitzenkörper can be stained by the lipophilic dye FM4-64 which stains endocytic vesicles (18). We have previously used this dye in the analysis of endocytosis in *C. albicans*. Deletion of the Wiskott-Aldrich Syndrome Protein homolog *CaWAL1* resulted in mutant strains that showed defects in the maintenance of polarized hyphal growth and we unable to form mycelia (39). Staining of yeast cells with FM4-64 did not reveal a prominent accumulation of vesicles but rather resulted in the delivery of the dye to and the visualization of vacuolar membranes (see also M4-6). Staining of germ tubes and hyphae resulted in almost immediate accumulation of the dye at the hyphal tip. This shows that *C. albicans* hyphae indeed resemble in this respect hyphae of other filamentous ascomycetes. In *A. nidulans* the formin SEPA was shown to localize to the hyphal tip either as a crescent at the tip or as a spot near the tip suggesting that SEPA is part of the Spitzenkörper (34). In *C. albicans* hyphae Bni1-GFP was found to colocalize with the FM4-64 stained Spitzenkörper and simultaneously at the latest septal site as was also observed for SEPA in *A. nidulans* suggesting mechanistic similarities. In *S. cerevisiae* Bni1 was shown to form a polarisome complex with Spa2, Bud6 and Pea2 (35). In *C. albicans* Spa2 was localized in a similar manner as Bni1-GFP in this study (43). This provides some further evidence for a conserved role of the polarisome in polarized hyphal growth. Interestingly, the *C. albicans* genome encodes a *BUD6* homolog (orf19.5087) but not a *PEA2* homolog (at least according to assembly 19) which suggests that there may be differences in the protein network between fungal species.

Function of formins. The function of formins in the assembly of linear actin filaments is conserved in nature and has elegantly been analyzed in several recent studies (11, 12, 32, 33). Our analysis of the actin cytoskeleton did not reveal any obvious phenotype in growing yeast cells or germ tubes. Double deletion of both formin genes, *BNI1* and *BNR1*, in *S. cerevisiae* results in synthetic lethality (36) suggesting overlapping functions of both formins. This may also suggest a surrogate mechanism in which Bnr1 partially takes over Bni1 functions in *C. albicans*. Since *bnr1* strains are able to form mycelia, Bnr1 does either not contribute to polarized morphogenesis or its function can be fulfilled by Bni1. Bni1, however, is required for the maintenance of polarized hyphal growth. This resembles the mutant phenotype of *SPA2* and *WAL1* deletions. In *bni1* and *wal1* cells polarized morphogenesis was initiated but after the formation of a germ tube hyphal growth ceased and mycelial development was abolished.

Role of the actin cytoskeleton for polarized hyphal growth. Morphogenetic switching in *C. albicans* was shown to be dependent on Ras1-signalling and the activation of the transcriptional regulators Cph1 and Efg1 by a MAP-kinase cascade and the cAMP-pathway, respectively (4, 20). In a

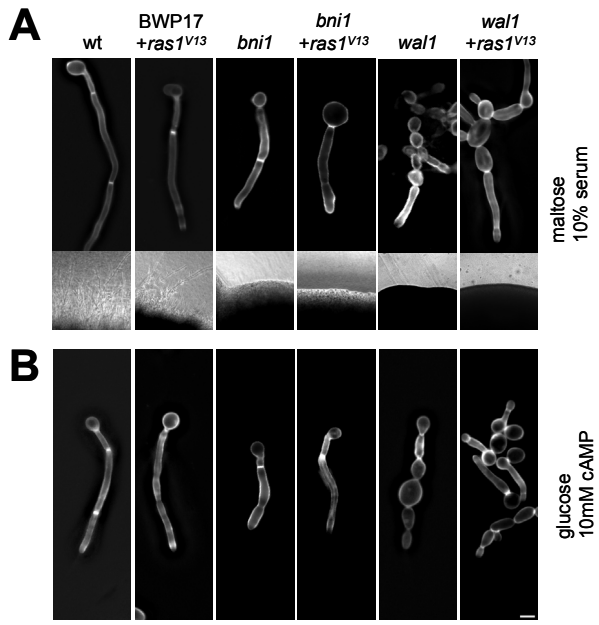

FIG. 7. Germ tube induction in *C. albicans* strains harboring the *ras1G13V* allele. Overnight cultures of the indicated strains were grown in liquid medium containing maltose as sole carbon source to allow for *MAL2*-promoter driven expression of the *ras1G13V* allele when applicable. Strains were then induced for 3h with either 10% serum (A) or 10mM cAMP (B) at 37°C and stained by calcofluor prior to photography. The insets of Fig. 7A depict microscopic images of colony edges of the strains grown on solid media plates containing serum. Expression of the constitutive *ras1G13V* allele did not enable mycelial growth in the *bni1* or *wal1* mutant strains.

previous study we showed that defects in endocytosis due to deletion of *WAL1* which encodes the *C. albicans* homologue of the human Wiskott-Aldrich Syndrome protein (WASP) crippled mycelial development (39). In this study we demonstrate a defect in the maintenance of hyphal growth due to the deletion of *BNI1*. Bni1 is a direct effector protein of Rho-protein signalling, whereas Wal1 lacks a G-protein binding domain (in contrast to its human homolog) and is activated by an as yet unknown mechanism. Tip-localization of both Bni1-GFP (this study) and Spa2-GFP (43), suggests the presence of a polarisome complex in *C. albicans* hyphae. The role of Bni1 as part of the *C. albicans* polarisome is, therefore, the targeted delivery of secretory vesicles. Another conserved function of Bni1 is the formation of the actin ring at septal sites and consistent with that Bni1-GFP was also found to localize to septal sites. In a recent study an explanation was provided how transcription via Efg1 could influence growth decisions and activate actin cytoskeleton dynamics. Under serum inducing conditions transcript levels of *CDC24*, encoding the guanine nucleotide exchange factor of Cdc42, transiently increase which could result in an increase in Cdc42 activity that could trigger germ tube formation (3). Other genes involved in the organization of the actin cytoskeleton, e.g. *RHO3* and *BEM2*, were found to be regulated in a similar manner (26). In summary, our results suggest that the organization of the actin cytoskeleton through multi-domain effector proteins of the WASP and formin families and thus the processes of endocytosis and secretion are both of central importance for the maintenance of polarized hyphal growth in *C. albicans* as presented in the model in Fig. 8. Deletion of key genes encoding parts of the actin cytoskeleton machinery will, therefore, provide means to specifically perturb the hyphal growth phase in *C. albicans*. This indicates that the protein network required for actin cytoskeletal organization may provide new targets for antifungal drug therapy. Further research will be required to elucidate how environmental signals relay their input mechanistically to the morphogenetic switch and need to define the dependencies of secretion and endocytosis to a balanced state of polarized cell growth. 17

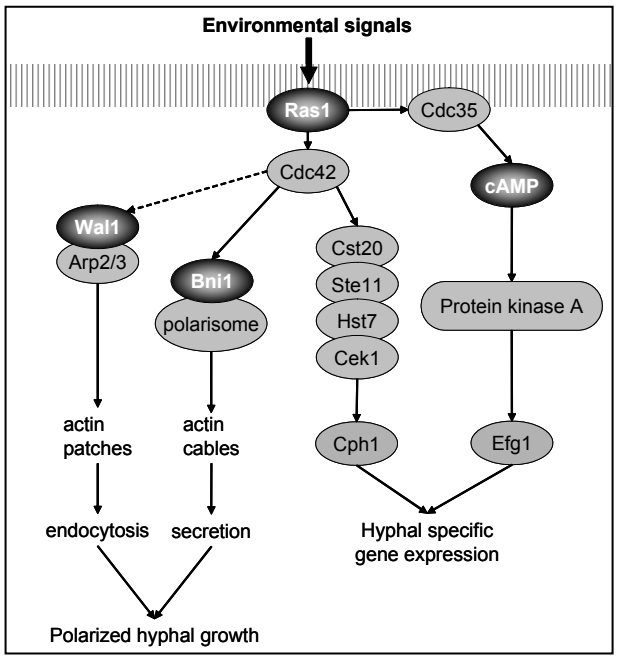

FIG. 8. The actin cytoskeleton as a downstream part of signal transduction in regulating polarized morphogenesis. A model is presented in which the central pathways to the actin cytoskeleton regulating endocytosis and secretion are incorporated via Cdc42 into the morphogenetic cascade of *C. albicans*. Ras1-induced signalling activates the cAMPpathway and a MAP-kinase cascade that activate hyphal specific gene expression. Defects in the actin cytoskeleton machinery affecting either endocytosis (e.g .via Wal1) or polarisome function (e.g. via Bni1 or Spa2) inhibit mycelial development indicating the relevance of membraneous vesicle transport and cycling for polarized growth. The dashed arrow connecting Cdc42 and Wal1 is to indicate the fact that Wal1 lacks a G-protein binding domain and can thus be activated only indirectly by Cdc42. Some othe rpathways regulating gene expression upon hyphal induction, e.g. the Tup1/Nrg1/Rbf1-pathway and the pH-Rim101-pathway, have been omitted for clarity.

ACKNOWLEDGMENTS

We thank Gerry Fink for providing the *ras1*-allele containing plasmids and Wang Yue for comments on the manuscript and communicating results prior to publication. This research was supported by the Deutsche Forschungsgemeinschaft, the Friedrich-Schiller University, and the Hans-Knöll Institute. Sequence data for *Candida albicans* was obtained from the Stanford Genome Technology Center website at http://www-sequence.stanford.edu/group/candida.

REFERENCES

1. **Bartnicki-Garcia, S., D. D. Bartnicki, G. Gierz, R. Lopez-Franco, and C. E. Bracker.** 1995. Evidence that Spitzenkörper behavior determines the shape of a fungal hypha: a test of the hyphoid model. Exp. Mycol. **19:**153-9.

2. **Bartnicki-Garcia, S., F. Hergert, and G. Gierz.** 1989. Computer simulation of fungal morphogenesis and the mathematical basis for hyphal tip growth. Protoplasma **153:**46–57.
3. **Bassilana, M., J. Hopkins, and R. A. Arkowitz.** 2005. Regulation of the Cdc42/Cdc24 GTPase module during *Candida albicans* hyphal growth. Eukaryot. Cell **4:**588-603.
4. **Berman, J., and P. E. Sudbery.** 2002. *Candida albicans*: a molecular revolution built on lessons from budding yeast. Nat. Rev. Genet. **3:**918-30.
5. **Borkovich, K. A., L. A. Alex, O. Yarden, M. Freitag, G. E. Turner, N. D. Read, S. Seiler, D. Bell-Pedersen, J. Paietta, N. Plesofsky, M. Plamann, M. Goodrich-Tanrikulu, U. Schulte, G. Mannhaupt, F. E. Nargang, A. Radford, C. Selitrennikoff, J. E. Galagan, J. C. Dunlap, J. J. Loros, D. Catcheside, H. Inoue, R. Aramayo, M. Polymenis, E. U. Selker, M. S. Sachs, G. A. Marzluf, I. Paulsen, R. Davis, D. J. Ebbole, A. Zelter, E. R. Kalkman, R. O'Rourke, F. Bowring, J. Yeadon, C. Ishii, K. Suzuki, W. Sakai, and R. Pratt.** 2004. Lessons from the genome sequence of *Neurospora crassa*: tracing the path from genomic blueprint to multicellular organism. Microbiol. Mol. Biol. Rev. **68:**1-108.
6. **Calderone, R. A., and W. A. Fonzi.** 2001. Virulence factors of *Candida albicans*. Trends Microbiol. **9:**327-35.
7. **Cory, G. O., R. Cramer, L. Blanchoin, and A. J. Ridley.** 2003. Phosphorylation of the WASP-VCA domain increases its affinity for the Arp2/3 complex and enhances actin polymerization by WASP. Mol. Cell **11:**1229-39.
8. **Dent, E. W., and F. B. Gertler.** 2003. Cytoskeletal dynamics and transport in growth cone motility and axon guidance. Neuron **40:**209-27.
9. **Drubin, D. G., and W. J. Nelson.** 1996. Origins of cell polarity. Cell **84:**335-44.
10. **Etienne-Manneville, S., and A. Hall.** 2002. Rho GTPases in cell biology. Nature **420:**629-35.
11. **Evangelista, M., D. Pruyne, D. C. Amberg, C. Boone, and A. Bretscher.** 2002. Formins direct Arp2/3-independent actin filament assembly to polarize cell growth in yeast. Nat. Cell Biol. **4:**32-41.
12. **Evangelista, M., S. Zigmond, and C. Boone.** 2003. Formins: signaling effectors for assembly and polarization of actin filaments. J. Cell Sci. **116:**2603-11.
13. **Feng, Q., E. Summers, B. Guo, and G. Fink.** 1999. Ras signaling is required for serum-induced hyphal differentiation in *Candida albicans*. J. Bacteriol. **181:**6339-46.
14. **Fujiwara, T., K. Tanaka, A. Mino, M. Kikyo, K. Takahashi, K. Shimizu, and Y. Takai.** 1998. Rho1p-Bni1p-Spa2p interactions: implication in localization of Bni1p at the bud site and regulation of the actin cytoskeleton in *Saccharomyces cerevisiae*. Mol. Biol. Cell **9:**1221-33.
15. **Gillum, A. M., E. Y. Tsay, and D. R. Kirsch.** 1984. Isolation of the *Candida albicans* gene for orotidine-5'-phosphate decarboxylase by complementation of *S. cerevisiae ura3* and *E. coli pyrF* mutations. Mol. Gen. Genet. **198:**179-82.
16. **Girbardt, M.** 1957. Der Spitzenkörper von *Polystictus versicolor*. Planta **50:**47–59.
17. **Gola, S., R. Martin, A. Walther, A. Dunkler, and J. Wendland.** 2003. New modules for PCR-based gene targeting in *Candida albicans*: rapid and efficient gene targeting using 100 bp of flanking homology region. Yeast **20:**1339-47.
18. **Harris, S. D., N. D. Read, R. W. Roberson, B. Shaw, S. Seiler, M. Plamann, and M. Momany.** 2005. Polarisome meets Spitzenkörper: microscopy, genetics, and genomics converge. Eukaryot. Cell **4:**225-9.
19. **Kiryushko, D., V. Berezin, and E. Bock.** 2004. Regulators of neurite outgrowth: role of cell adhesion molecules. Ann. N. Y. Acad. Sci. **1014:**140-54.
20. **Leberer, E., D. Harcus, D. Dignard, L. Johnson, S. Ushinsky, D. Y. Thomas, and K. Schroppel.** 2001. Ras links cellular morphogenesis to virulence by regulation of the MAP kinase and cAMP signalling pathways in the pathogenic fungus *Candida albicans*. Mol. Microbiol. **42:**673-87.
21. **Liu, H.** 2001. Transcriptional control of dimorphism in *Candida albicans*. Curr. Opin. Microbiol. **4:**728-35.
22. **Liu, H., J. Kohler, and G. R. Fink.** 1994. Suppression of hyphal formation in *Candida albicans* by mutation of a *STE12* homolog. Science **266:**1723-6.
23. **Lo, H. J., J. R. Kohler, B. DiDomenico, D. Loebenberg, A. Cacciapuoti, and G. R. Fink.** 1997. Nonfilamentous *C. albicans* mutants are avirulent. Cell **90:**939-49.
24. **Machesky, L. M., and K. L. Gould.** 1999. The Arp2/3 complex: a multifunctional actin organizer. Curr. Opin. Cell Biol. **11:**117-21.
25. **Momany, M.** 2002. Polarity in filamentous fungi: establishment, maintenance and new axes. Curr. Opin. Microbiol. **5:**580-5.
26. **Nantel, A., D. Dignard, C. Bachewich, D. Harcus, A. Marcil, A. P. Bouin, C. W. Sensen, H. Hogues, M. van het Hoog, P. Gordon, T. Rigby, F. Benoit, D. C. Tessier, D. Y. Thomas, and M. Whiteway.** 2002. Transcription profiling of *Candida albicans* cells undergoing the yeast-to-hyphal transition. Mol. Biol. Cell **13:**3452-65.
27. **Oberholzer, U., A. Marcil, E. Leberer, D. Y. Thomas, and M. Whiteway.** 2002. Myosin I is required for hypha formation in *Candida albicans*. Eukaryot. Cell **1:**213-28.
28. **Odds, F. C.** 1985. Morphogenesis in *Candida albicans*. Crit. Rev. Microbiol. **12:**45-93.
29. **Otomo, T., C. Otomo, D. R. Tomchick, M. Machius, and M. K. Rosen.** 2005. Structural basis of Rho GTPase-mediated activation of the formin mDia1. Mol. Cell **18:**273-81.
30. **Parton, R. M., S. Fischer-Parton, M. K. Watahiki, and A. J. Trewavas.** 2001. Dynamics of the apical vesicle accumulation and the rate of growth are related in individual pollen tubes. J. Cell Sci. **114:**2685-95.
31. **Pruyne, D., and A. Bretscher.** 2000. Polarization of cell growth in yeast. J. Cell Sci. **113:**571-85.
32. **Pruyne, D., M. Evangelista, C. Yang, E. Bi, S. Zigmond, A. Bretscher, and C. Boone.** 2002. Role of formins in actin assembly: nucleation and barbed-end association. Science **297:**612-5.
33. **Sagot, I., A. A. Rodal, J. Moseley, B. L. Goode, and D. Pellman.** 2002. An actin nucleation mechanism mediated by Bni1 and profilin. Nat. Cell Biol. **4:**626-31.
34. **Sharpless, K. E., and S. D. Harris.** 2002. Functional characterization and localization of the *Aspergillus nidulans* formin SEPA. Mol. Biol. Cell **13:**469-79.
35. **Sheu, Y. J., B. Santos, N. Fortin, C. Costigan, and M. Snyder.** 1998. Spa2p interacts with cell polarity proteins and signaling components involved in yeast cell morphogenesis. Mol. Cell Biol. **18:**4053-69.
36. **Tong, A. H., M. Evangelista, A. B. Parsons, H. Xu, G. D. Bader, N. Page, M. Robinson, S. Raghibizadeh, C. W. Hogue, H. Bussey, B. Andrews, M. Tyers, and C. Boone.** 2001. Systematic genetic analysis with ordered arrays of yeast deletion mutants. Science **294:**2364-8.
37. **Walther, A., and J. Wendland.** 2004. Apical localization of actin patches and vacuolar dynamics in *Ashbya gossypii* depend on the WASP homolog Wal1p. J. Cell Sci. **117:**4947-4958.
38. **Walther, A., and J. Wendland.** 2003. An improved transformation protocol for the human fungal pathogen *Candida albicans*. Curr. Genet. **42:**339-43.
39. **Walther, A., and J. Wendland.** 2004. Polarized hyphal growth in *Candida albicans* requires the Wiskott-Aldrich Syndrome protein homolog Wal1p. Eukaryot. Cell **3:**471-82.
40. **Wendland, J., and A. Walther.** 2005. *Ashbya gossypii*: a model for fungal developmental biology. Nat. Rev. Microbiol. **3:**421-9.
41. **Wilson, R. B., D. Davis, and A. P. Mitchell.** 1999. Rapid hypothesis testing with *Candida albicans* through gene disruption with short homology regions. J. Bacteriol. **181:**1868-74.
42. **Winter, D. C., E. Y. Choe, and R. Li.** 1999. Genetic dissection of the budding yeast Arp2/3 complex: a comparison of the in vivo and structural roles of individual subunits. Proc. Natl. Acad. Sci. USA **96:**7288-93.
43. **Zheng, X. D., Y. M. Wang, and Y. Wang.** 2003. *CaSPA2* is important for polarity establishment and maintenance in *Candida albicans*. Mol. Microbiol. **49:**1391-405.

8

Susanne Gola

Ronny Martin

Andrea Walther

Alexander Dünkler

Jürgen Wendland

New modules for PCR-based gene targeting in *Candida albicans*: Rapid and efficient gene targeting using 100bp of flanking homology region.

Yeast., 20(16): 1339-1347.

Die Verwendung PCR-basierter Methoden erlaubt die schnelle und basenpaargenaue Deletion von Genen in *C. albicans*. Für diesen Zweck wurden Module konstruiert, die neben der präzisen Deletion von offenen Leserastern (ORFs) durch ein Markergen auch die Fusion des ORFs mit GFP oder die Kontrolle von Genen durch regulierbare Promotoren ermöglicht. Durch den modulare Aufbau und die Verwendung einer minimalen Anzahl langer Oligonukleotide konnten erstmals effiziente Genveränderungen in *C. albicans* mit dieser Methode durchgeführt werden.

Yeast
Yeast 2003; **20**: 1339–1347.
Published online in Wiley InterScience (www.interscience.wiley.com). **DOI:** 10.1002/yea.1044

Yeast Functional Analysis Report

New modules for PCR-based gene targeting in *Candida albicans*: rapid and efficient gene targeting using 100 bp of flanking homology region

Susanne Gola[1], Ronny Martin[1,2], Andrea Walther[1,2], Alexander Dünkler[1,2] and Jürgen Wendland[1,2]*
[1]*Department of Microbiology, Friedrich-Schiller-University, Jena, Germany*
[2]*Junior Research Group: Growth-Control of Fungal Pathogens, Hans-Knöll Institut für Naturstoff-Forschung e.V., Winzerlaer Strasse 10, 07745 Jena, Germany*

**Correspondence to: Jürgen Wendland, Junior Research Group: Growth-Control of Fungal Pathogens, Hans-Knöll Institut für Naturstoff-Forschung e.V., Winzerlaer Strasse 10, 07745 Jena, Germany. E-mail: juergen.wendland@uni-jena.de*

Received: 25 May 2003
Accepted: 14 August 2003

Abstract

The use of PCR-based techniques for directed gene alterations has become a standard tool in *Saccharomyces cerevisiae*. In our efforts to increase the speed of functional analysis of *Candida albicans* genes, we constructed a modular system of plasmid vectors and successfully applied PCR-amplified functional analysis (FA)-cassettes in the transformation of *C. albicans*. These cassettes facilitate: (a) gene disruptions; (b) tagging of 3′-ends of genes with green fluorescent protein (GFP); and (c) replacements of endogenous promoters to achieve regulated expression. The modules consists of a core of three selectable marker genes, *CaURA3, CaHIS1* and *CaARG4*. Modules for C-terminal GFP-tagging were generated by adding GFP-sequences flanked at the 5′-end by a (Gly-Ala)$_3$-linker and at the 3′-end by the *S. cerevisiae URA3*-terminator to these selection markers. Promoter exchange modules consist of the respective marker genes followed by the regulatable *CaMAL2* or *CaMET3* promoters at their 3′-ends. In order to ensure a reliably high rate of homologous gene targeting, the flanking homology regions required a size of 100 bp of gene-specific sequences, which were provided with the oligonucleotide primers. The use of shorter flanking homology regions produced unsatisfactory results with *C. albicans* strain BWP17. With these new modules only a minimal set of primers is required to achieve the functional analysis of *C. albicans* genes and, therefore, provides a basic tool to increase the number of functionally characterized *C. albicans* genes of this human pathogen in the near future.

Keywords: ***Candida albicans*; human pathogen; functional analysis; polymerase chain reaction; GFP**

Introduction

Candida albicans is the most prevalent human fungal pathogen, which can cause superficial mucosal infections as well as life-threatening systemic infections in the immunocompromised host (Berman and Sudbery, 2002; Perea and Patterson, 2002; Sanglard and Odds, 2002). Due to the diploidy of *C. albicans*, molecular analysis of gene function requires the deletion of both alleles. For sequential or multiple rounds of gene disruptions the '*URA3*-blaster' strategy and its variations are commonly used (Alani and Kleckner, 1987; Fonzi and Irvin, 1993; for review, see De Backer *et al*., 2000; Berman and Sudbery, 2002). This technique is based on counter-selection with 5′-fluoro-orotic acid (5FOA) against the presence of the *URA3* gene product. It aims

at the isolation of transformants in which the selection marker has been excised by direct repeat induced recombination, which thus can be used again in a new round of transformation. The lack of a complete sexual cycle, despite recent demonstration of mating, does not allow genetic crosses with *C. albicans* (Hull *et al*., 2000; Magee and Magee, 2000; Miller and Johnson, 2002; Lockhart *et al*., 2003). Mutagenic screens in *C. albicans* are complicated by the diploid nature but, in principle, can be carried out using the *UAU1* construct (Enloe *et al*., 2000; Davis *et al*., 2002).

In conjunction with the *C. albicans* genome project (**http://www-sequence.stanford.edu/group/candida/**), many new genes have been discovered that await characterization. Recently, an important advance in the functional analysis of *C. albicans* genes was reported with the development of PCR-mediated techniques for gene deletion. It was shown that 50–60 bp homology regions to the target locus provided with PCR primers were sufficient to drive gene deletion in *C. albicans*, as was shown for *C. glabrata*, but with a low frequency (Wilson *et al*., 1999; Weig *et al*., 2001). Moreover, construction of strain BWP17, which bears deletions in three auxotrophic marker genes (*URA3, HIS1* and *ARG4*), enables sequential targeting events without the need to regenerate the *URA3* marker (Wilson *et al*., 1999). Regulatable gene expression from *MAL2* and *MET3* promoters was demonstrated previously and provided the basis for the choice of these promoters (Care *et al*., 1999; Backen *et al*., 2000). For visualization of proteins in living *C. albicans* cells, codon-optimized versions of the green, cyan and yellow fluorescent proteins are available that were also designed for a PCR-based targeting approach (Gerami-Nejad *et al*., 2001).

In order to increase the speed of comprehensive analysis of gene function in *C. albicans*, we constructed a set of modules designed for the application of PCR-based methodology. Moreover, these modules require a small set of primers and thus gene manipulations in *C. albicans* can be carried out in a time- and cost-efficient manner. In our hands, use of flanking homology regions of 100 bp provided with long oligonucleotide primers was required to produce a high percentage of transformants bearing the correctly targeted cassettes. Use of this technique, therefore, will rapidly increase our knowledge on the function of *C. albicans* genes in the future.

Materials and methods

Strains and media

C. albicans wild-type strain SC5314 (Gillum *et al*., 1984) was used to amplify the *MAL2* and *MET3* promoters and strain BWP17 (*ura3*Δ::λ*imm434*/*ura3*Δ::λ*imm434;his1::hisG/his1::hisG;arg4::hisG/arg4::hisG)* (Wilson *et al*., 1999) was used for all transformation experiments. Strains were grown as described previously (Walther and Wendland, 2003). Control of gene expression by carbon source and presence of methionine and cysteine was performed as described (Backen *et al*., 2000; Care *et al*., 1999). *Escherichia coli* strain DH5α was used for general recombinant techniques according to protocols described by Sambrook *et al*. (1989).

Construction of modules

Gene sequences used for the construction of the modules were amplified from plasmid-DNA with primers containing specific restriction sites, as indicated in Table 1. Integrity of open reading frames and correct cloning of all constructs was verified by sequencing (MWG-Biotech, Ebersberg, Germany). As a plasmid backbone, the pFA-vector was chosen, which has been used for functional analysis in *S. cerevisiae* (Wach *et al*., 1994). Marker genes were cloned as *Bam*HI–*Pme*I fragments into the *Bam*HI–*Pme*I sites of pFA. Fluorescent protein sequences (XFPs; source, Gerami-Nejad *et al*., 2001) were amplified using primers that introduced a 5′-linker encoding $(Gly\text{-}Ala)_3$. XFP fragments were subcloned into pGUG (a pFA-based plasmid; kindly provided by Philipp Knechtle and Peter Philippsen, Basel) using the *Pst*I and *Asc*I sites, which resulted in the combination of the XFPs with the *ScURA3* terminator. *Sun*I–*Bgl*II fragments from the pGUG–XFP plasmids that contained $(Gly–Ala)_3$–XFP–ScURA3term were cloned into the *Sun*I–*Bam*HI sites of plasmids pFA–URA3, pFA–HIS1 and pFA–ARG4, generating the pFA–XFP-marker modules. The second GFP variant incorporated in our set of modules was derived from pGFP-41 (Cormack *et al*., 1996; Morschhäuser *et al*., 1998; this GFP is based on the S65A, S68A and S72T mutations)

Table 1. Primers used for module construction

Sequence	Template	Primer sequence[a]
CaURA3	pGEM–URA3	5′URA GCGGGATCCGGATGGTATAAACGGAAAC 3′URA AGCTTGTTTAAACTAGAAGGACCACCTTTGATTG
CaHIS1	pGEM–HIS1	5′HIS CGCGGGATCCTGGAGGATG 3′HIS AAGGAAGTTTAAACGAGAATGCCTATTGAC
CaARG4	pRSARGΔSpe	5′ARG CGCGGATCCCCCCTTTAGTAAGATTTTTC 3′ARG AGCTTTGTTTAAACTATTGTAGTACAAGGTATCTC
GFP, CFP, YFP	pXFP–URA3	5′XFP AAACTGCAG**GGTGCTGGCGCAGGTGCT**TCTAAAG GTGAAGAATTATTCACTG 3′XFP CTGGCGCGCCTTATTTGTACAATTCATCCATACC
GFP$^{S65A, V68L, S72A}$	pGFP-41	AAACTGCAG**GGTGCTGGCGCAGGTGCT**TCTAAAGGAGAAG AACTTTTCACTGGAG
CaMAL2p	Genomic	5′MAL AGCTTTGTTTAAACTTTTGTCTAGTACCATCTGTACC 3′MAL GGCACTAGTCATTGTAGTTGATTATTAGTTAAACC
CaMET3p	Genomic	5′MET AAAATTGTTTAAACAATGACTATTGGTAGCGTGTTC 3′MET CCGACTAGTCATGTTTTCTGGGGAGGGTATTTAC

[a] Primer sequences are in the 5′ to 3′ direction. Restriction sites for *Bam*HI (GGATCC), *Pme*I (GTTTAAAC), *Pst*I (CTGCAG), *Asc*I (GGCGCGCC) and *Spe*I (ACTAGT) are underlined. The sequence representing the $(Gly–Ala)_3$ linker is in bold.

and is termed GFP$^{S65A, V68L, S72A}$ herein. The same $(Gly–Ala)_3$ linker was introduced via PCR and the resulting fragment was cloned via *Pst*I–*Asc*I sites into pFA–GFP–URA3, resulting in an exchange of the GFPs, thus creating pFA–GFP$^{S65A, V68L, S72A}$–URA3. Using the *Asc*I–*Pme*I sites, markers were replaced, generating pFA–GFP$^{S65A, V68L, S72A}$–HIS1 and pFA–GFP$^{S65A, V68L, S72A}$–ARG4 modules. The pFA-marker–promoter modules were generated in the following way. Promoter fragments of lengths 559 bp (*MAL2p*) and 1422 bp (*MET3*), containing the necessary sequence elements required for regulatable expression, were amplified from genomic DNA of *C. albicans* strain SC5314 and cloned as *PmeI–SpeI* fragments into the pFA-marker series. Both promoter fragments provide the initial ATG codon prior to the *SpeI* site. The sizes of the individual cassettes are summarized in Table 2. The original sequence annotation of pGEM–HIS1 (AF173955) contains a direct repeat sequence duplication of 203 bp (first position 3284–3486, repeat position 3481–3683), which upon sequencing was not detected in the original pGEM–HIS1 plasmid nor in our pFA–HIS1 marker constructs and is also absent in the Stanford Genome database annotation of *CaHIS1*.

Table 2. Fragment lengths of cassettes

Cassette	Length (bp)
pFA backbone	2513
pFA–URA3	1.351
pFA–HIS1	1.372
pFA–ARG4	1.960
pFA–URA3–MAL2p	1.892
pFA–HIS1–MAL2p	1.913
pFA–ARG4–MAL2p	2.501
pFA–URA3–MET3p	2.755
pFA–HIS1–MET3p	2.776
pFA–ARG4–MET3p	3.364
pFA–XFP–URA3	2.335
pFA–XFP–HIS1	2.356
pFA–XFP–ARG4	2.944

Cassette amplification and transformation

The pFA-marker cassettes were amplified by S1 and S2 primers, which each provide 100 bp sequence corresponding to the target regions at their 5′ end. For amplification of the pFA–XFP marker cassettes, S1–XFP served as the upstream primer with 100 bp sequence identity which ends at the last sense codon of the target ORF in combination with S2. The pFA marker–promoter cassettes are amplified by S1 and S2-Prom, which contains the 5′-end of the target gene ORF. The corresponding annealing regions to the pFA modules which need to be included with the primers are listed in Table 3. Purification of these approximately 120-mer primers at a low cost using HPLC is useful to ensure high quality primers and was found to further increase the yield of correctly targeted

Table 3. PCR primers used for amplification and verification

Primer	Primer sequence[a]
S1	(100 bp target sequence)-gaagcttcgtacgctgcaggtc
S2	(100 bp target sequence)-tctgatatcatcgatgaattcgag
S1–XFP	(100 bp target sequence)-**GGT GCT GGC GCA GGT GCT** TC
S2–Prom *MAL2*	(100 bp target sequence)-CATTGTAGTTGATTATTAGTTAAACCAC
S2–Prom *MET3*	(100 bp target sequence)-CATGTTTTCTGGGGAGGGTATTTAC
A2	AATGGATCAGTGGCACCGGTG
A3	GGGCCCATTGGTTAAGTTCATATGC
H2	CAACGAAATGGCCTCCCCTACCACAG
H3	GGACGAATTGAAGAAAGCTGGTGCAACCG
U2	GTGTTACGAATCAATGGCACTACAGC
U3	GGAGTTGGATTAGATGATAAAGGTGATGG
S1–HHF1–GFP	CTGTTACTTACACTGAACATGCTAAAAGAAAACCGTCACTTCATTGGATGTTGTTTACGCTTTG AAGAGACAAGGTAGAACCTTGTATGGTTTCGGTGGTggtgctggcgcaggtgcttc
S2–HHF1–GFP	GATAATGAACTTCAATGAATGACCATTTTATCTGACCAATAAAATCAAAATAGTAAAAAATTGGT GGAAATAAGATACCGAAAATAATTTGCTTGCCTTGtctgatatcatcgatgaattcgag
G1–HHF1	GGGTGTGTGTGTCTTTAGTGGTCG
G4–HHF1	CCACTCAAAGTCATACAGTCAAGC
S1–TUB1–GFP	AGAAGGTGAATTCACTGAAGCTAGAGAAGACTTGGCTGCTTTAGAGAGAGATTATATTGAAG TTGGTACTGATTCTTTCCCTGAAGAAGAAGAAGAATATggtgctggcgcaggtgcttc
S2–TUB1–GFP	CCCTCCTCTTAACCATTTGACACACCAAGAGAGTCAATTCCAAAAGTAAAAATTAAAAATC GGGCTTGGGAGTTCGGGTATATATGGTATATATATATAAGtctgatatcatcgatgaattcgag
G1–TUB1	GTTGTCTAACACTACTGCCATTGC
G4–TUB1	CGGTTTGAACAAAAGTAGGGATGC

[a] Primer sequences are given in the 5′ to 3′ direction. Sequence in bold corresponds to the $(Gly\text{-}Ala)_3$ linker, in which spaces indicate the reading frame. Underlined nucleotides correspond to the ATG start codons of *MAL2* and *MET3* promoters.

transformants. In this study all long-flanking primers were obtained from genaxxon/biomers (**http://www.biomers.net**). All pFA plasmids can be linearized by the restriction enzyme *Sca*I, which has a unique recognition site in the ampicillin resistance gene. However, transformation results did not vary with the use of linearized vs. uncut plasmid DNA template for PCR and subsequent transformation. In general, DNA from four or five 50 µl PCR reactions was pooled, precipitated and used for transformation without further processing, as described by Walther and Wendland (2003).

Our standard amplification protocol for the amplification of PCR cassettes with long-flanking primers uses the following PCR steps: initial denaturing, 94 °C for 5 min; 10 cycles using 93 °C for 1 min, 45 °C for 1 min, and 72 °C for 3–5 min; 30 cycles using 93 °C for 1 min, 52 °C for 1 min, and 72 °C for 3–5 min.

The roadmap to construct mutant strains includes the generation of independent heterozygous mutant strains with the *FA–URA3* and *FA–HIS1* cassettes. From these independent heterozygous strains individual homozygous strains are constructed in a second round of transformations. Correct insertion of the marker genes is verified by PCR. Diagnostic PCR includes the verification of both novel joints generated by the marker insertion as well as the absence of the target ORF using internal primers I1–I2 in the homozygous mutant strain (see Figure 2). Phenotypic defects (or testing of an essential gene) are substantiated with promoter shutdown experiments. To this end, the remaining copy of the target gene in one of the initial heterozygous mutant strains is placed under regulatable control using the pFA marker–promoter modules.

Microscopy

Cells were grown to logarithmic phase in complete or minimal media and washed with sterile water prior to observation. Differential interference contrast and fluorescence microscopy were performed as described (Wendland, 2003). Images were acquired and processed using Metamorph version 4.6 software.

Results and discussion

Module construction

For rapid elucidation of gene function in *C. albicans* we aimed at the construction of a modular set of plasmids that conveniently allows: (a) gene disruption; (b) promoter shut-down (in case a gene of interest proves to be essential or to demonstrate that a given phenotype is the result of the depletion of the target protein); and (c) the localization of a gene product bearing a C-terminal fusion with a fluorescent protein. As a plasmid backbone we chose the well-known pFA backbone which was used, for example, in pFA–kanMX4 as the standard selectable marker used in the EUROFAN deletion project (Wach *et al*., 1994). The choice of *C. albicans* selectable marker genes was guided by its application with *C. albicans* strain BWP17, which bears auxotrophic mutations in *URA3, HIS1* and *ARG4* (Wilson *et al*., 1999). Use of this strain was favoured because sequential transformation steps can be performed without the need to regenerate a single selection marker for the initial characterization of gene function.

To be as flexible as possible with the use of selection markers, combinations of marker genes with codon-optimized versions of the fluorescent protein encoding genes (Gerami-Nejad *et al*., 2001), another variant of GFP, termed GFP$^{S65A,\ V68L,\ S72A}$ (Cormack *et al*., 1996; Morschhäuser *et al*., 1998), and the regulatable promotors *MAL2*p and *MET3*p (Backen *et al*., 2000; Care *et al*., 1999) were generated. In this way, three pFA marker modules, twelve pFA–XFP marker modules, and six pFA marker–promoter modules were constructed (Figure 1). The pFA marker and pFA marker–promoter modules were cloned in a way that preserved the functional promoter and terminator sequences as described (Care *et al*., 1999; Wilson *et al*., 1999; Backen *et al*., 2000). The *XFP*-modules consist of a 5′ $(Gly–Ala)_3$ linker to provide a spacer region between the target protein and GFP, which should enhance correct folding of the fusion protein and contain the 251 bp heterologous *URA3* terminator sequence from *S. cerevisiae* (which previously has been used as a heterologous terminator in *A. gossypii*) instead of the 1.670 bp *CaADH1*

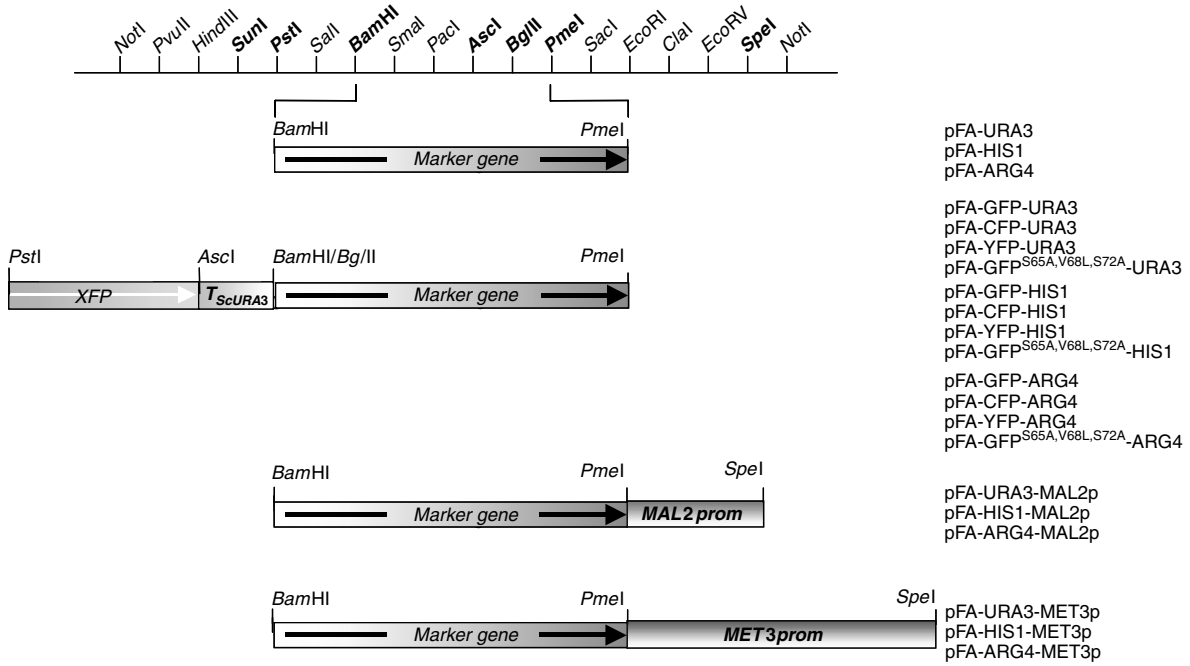

Figure 1. Map and nomenclature of modules cloned into the pFA vector background. For further details on the pFA backbone construction, see Wach *et al.* (1994). Restriction sites used for cloning are indicated in bold in the multiple cloning site. *URA3, HIS1* and *ARG4* were used as marker genes. The *XFP* and *GFP*$^{S65A,\ V68L,\ S72A}$ variants served as fluorescent protein-encoding ORFs and the *MAL2* and *MET3* promoter sequences as regulatable promoters

terminator sequence that was present in the published XFP cassettes (Gerami-Nejad *et al.*, 2001).

Minimal set of primers for the amplification of cassettes

Due to the modular nature of the pFA plasmids, a minimal set of four primers is required for the amplification of all pFA modules. Simple disruption experiments can be carried out with just two long-flanking primers. Cassettes for transformation were amplified by primers which included 100 bp of gene-specific sequences at their 5′-ends and the corresponding annealing regions to the pFA linker (Table 3). S1 and S2 primers were used for the amplification of two different markers from the pFA marker series. The generated disruption cassettes were used in parallel and in consecutive transformations. Homology regions were chosen such as to result in complete ORF deletions. S1-XFP and S2 primers were used for the amplification of cassettes for 3′-end tagging with a fluorescent protein. Similarly, S1 and S2-prom primers were used to generate cassettes for promoter exchanges.

In total, only four primers containing the 100 bp homology regions (S1, S2, S1-XFP and S2-prom *MAL2*/*MET3*) and four gene-specific verification primers (G1, G4, I1, and I2; plus the marker specific diagnostic primers) are needed for the comprehensive functional analysis of a single gene which encompasses the construction of homozygous null mutant strains, regulatable expression of the gene, and localization of the gene product in living cells.

Verification of correct gene targeting

During the course of testing the pFA marker modules, we constructed 18 independent homozygous null mutant strains in nine different genes, using all three markers. As a proof of principle we deleted, for example, the complete ORF of the *CaDHC1* gene, which is one of the largest genes in *C. albicans* encoding the dynein heavy chain (Martin *et al.*, in preparation). Phenotypic description of this and other gene deletions will be presented in detail elsewhere. It turned out that with the use of flanking homology regions of up to 75 bp, homologous integration was a rather rare event, yielding correctly targeted mutant strains with an efficiency of less than 1%. This requires a large amount of screening of primary transformants to isolate a desired mutant strain. Increasing the size of the homology region to 100 bp, however, increased the rate of homologous integration to 20–80%. We regularly achieved a rate of about 40% of correct gene targeting events. With our recently published improved lithium acetate transformation protocol (Walther and Wendland, 2003), we were able to isolate targeted transformants with a single transformation in all cases tested. The rather large region of homology required in *C. albicans* is in contrast to, for example, the 40 bp used in *S. cerevisiae* and 45 bp used in the filamentous fungus *Ashbya gossypii* (Wach *et al.*, 1994; Wendland *et al.*, 2000).

Correct integration of the cassettes was verified by PCR with two pairs of gene-specific and marker-specific primers, as shown in Figure 2. Both novel joints created by the marker insertion were analysed. The newly generated 5′-border was analysed using the gene-specific primer G1 in combination with a marker-specific primer (A2, H2, or U2) and the new 3′ border was verified with the G4 primer combined with either A3, H3, or U3, respectively (Figure 2). As a control, a gene-specific internal primer pair, I1 and I2, was used to monitor the presence or absence of the target ORF. This is important to exclude the presence of allelic triplications that where found to occur when deleting essential genes (Enloe *et al.*, 2000). In the same manner, insertion of the XFP marker or the promoter–marker cassettes was verified (which requires a set of verification primers close to the insertion event). To speed up the analysis of transformants, diagnostic PCR is generally performed directly on cells from growing colonies, which allows quick and efficient screening of transformants. PCR worked most reliably from several days old *C. albicans* colonies grown on minimal medium rather than from colonies grown on complex YPD medium. The size of the diagnostic PCR fragments was generally below 1000 bp.

Analysis of GFP-tagged transformants

We used the PCR-based gene targeting procedure to generate *CaHHF1GFP* and *CaTUB1GFP*. Use of the fluorescent protein tagging modules allows 3′-tagging of a gene with either of the fluorescent protein genes, using just one pair of primers per gene. In addition, the modular nature of the plasmids

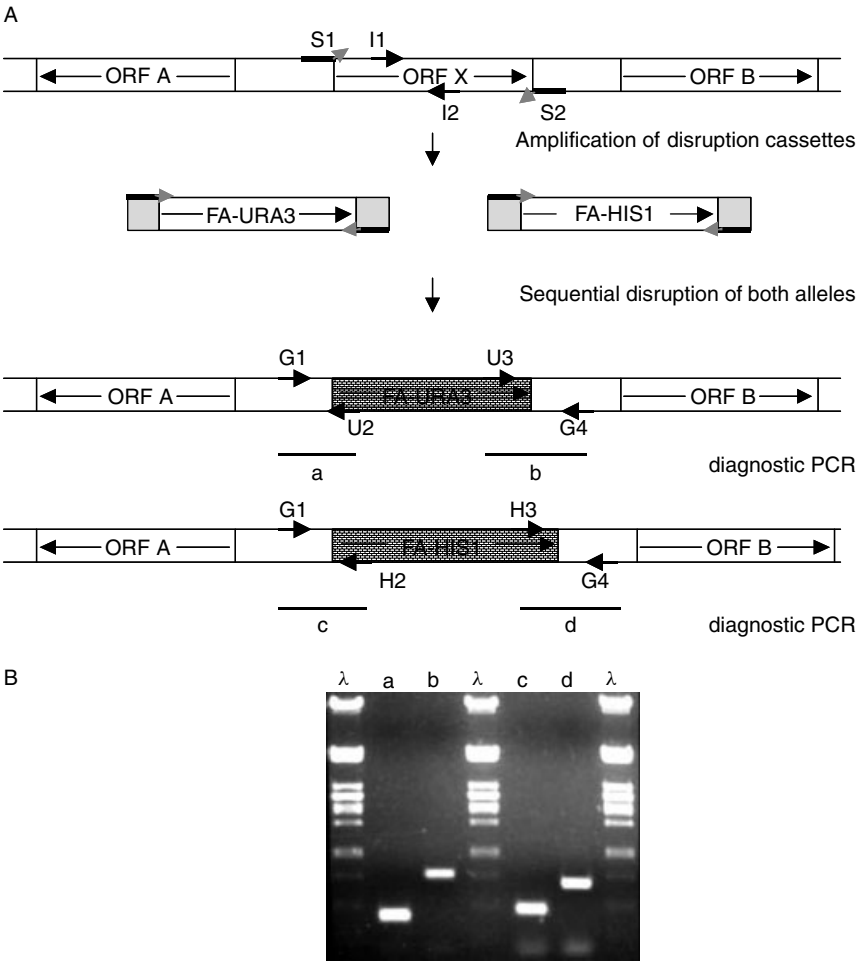

Figure 2. Transformation of *C. albicans* with functional analysis (FA)-constructs. (A) Design of chimeric primers bearing the homology regions and annealing sites for FA cassette amplification (see Table 3). Sequential disruption using these cassettes results in a homozygous mutant strain. Specific diagnostic PCR primers are positioned outside of the target ORF and within the FA cassette (for standard annealing regions within the FA cassettes, see Table 3). (B) Image of an ethidium bromide-stained gel showing the result of diagnostic PCR of a homozygous mutant strain, as described in (A). λ-DNA digested with *Pst*I was used as size marker

allows the addition of new and brighter fluorescent variants as they become available. Fluorescence was readily observed in transformants that carry the GFP constructs, indicating that in-frame fusion of the target gene with GFP had occurred (Figure 3). For the completion of our module series we have included the YFP and CFP variants of these previously reported XFP genes (Gerami-Nejad *et al*., 2001).

Regulated expression of *C. albicans* genes

Regulated gene expression by integration of pFA marker–promoter cassettes was tested by targeting a phenotypically characterized gene in a heterozygous mutant strain background. For this purpose we used the *C. albicans WAL1* gene, which encodes the Wiskott–Aldrich syndrome protein (WASP) homologue (Walther *et al*., submitted). Shut-down of the *MET3* promoter could be induced by addition of methionine and cysteine to the growth medium, as described by Care *et al*. (1999) and shut-down of the *MAL2* promoter was achieved by growth on glucose (Backen *et al*., 2000). As a result the mutant phenotypes of the homozygous deletion strain could be obtained with the heterozygous strains, in which the regulatable promoters

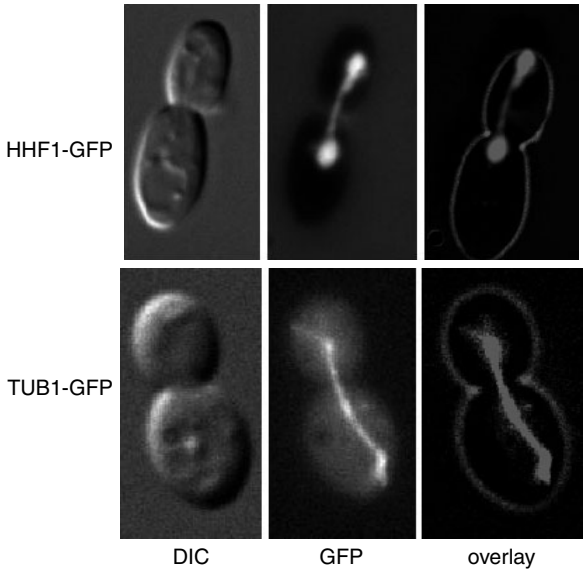

Figure 3. Examples of PCR-based targeting of GFP–reporter cassettes. Primers were designed using the Stanford Genome database to construct in-frame C-terminal fusions to the *HHF1* gene encoding histone H4 and the *TUB1* gene encoding α-tubulin (see also Table 3). Heterozygous tagged strains were generated and verified as shown in Figure 2. Strains were observed with differential interference contrast (DIC) and with fluorescence microscopy, using the GFP filter set as indicated. Both images were used to construct an overlay as shown

driving the only remaining copy of the gene had been turned off. Thus, evidence for the functionality of the pFA marker–promoter cassettes was obtained, which was subsequently verified with other *C. albicans* genes in our group.

Conclusions

We have constructed a set of modules for PCR-based functional analysis of *C. albicans* genes. To achieve a high rate of correct gene targeting, the size of the homology region was increased to 100 bp. Our system allows the generation of homozygous mutants for a gene of interest, while at the same time the heterozygous mutant can be used for promoter shut-down experiments to reproduce the knockout phenotype of the gene without the need for marker recycling. The localization of the gene product may be monitored by tagging with GFP. Since only four different long-flanking oligonucleotides are needed for gene disruption, expression and localization studies, this system provides a rapid and cost-efficient method to assay the function of *C. albicans* genes. Up to now, we have tested this set of PCR modules successfully in more than 50 independent targeting experiments. Therefore, these modules will undoubtedly facilitate characterization of the many previously unknown genes present in the *C. albicans* genome and will help to isolate target genes for antifungal drug therapy in this important human fungal pathogen. To promote this effort, all modules will be made freely available to the scientific community. Requests for materials should be made to the corresponding author.

Acknowledgements

We thank Judith Berman, Cheryl Gale, Aaron Mitchell, Joachim Morschhäuser, Peter Philippsen and Philipp Knechtle for providing strains and/or plasmids. Diana Schade contributed to the project with her expert technical assistance and Daniela Hellwig participated in a practical course during her undergraduate studies. J.W. is supported by the Deutsche Forschungsgemeinschaft (We2634/3-1 and We2634/4-1), the Hans-Knöll Institute, and the Friedrich-Schiller University, Jena.

References

Alani E, Kleckner N. 1987. A new type of fusion analysis applicable to many organisms: protein fusions to the *URA3* gene of yeast. *Genetics* **117**: 5–12.

Backen AC, Broadbent ID, Fetherston RW, *et al*. 2000. Evaluation of the *CaMAL2* promoter for regulated expression of genes in *Candida albicans*. *Yeast* **16**: 1121–1129.

De Backer MD, Magee PT, Pla J. 2000. Recent developments in molecular genetics of *Candida albicans*. *Ann Rev Microbiol* **54**: 463–498.

Berman J, Sudbery PE. 2002. *Candida albicans*: a molecular revolution built on lessons from budding yeast. *Nature Rev Genet* **3**: 918–930.

Care RS, Trevethick J, Binley KM, Sudbery PE. 1999. The *MET3* promoter: a new tool for *Candida albicans* molecular genetics. *Mol Microbiol* **34**: 792–798.

Cormack BP, Valdivia RH, Falkow S. 1996. FACS-optimized mutants of the green fluorescent protein (GFP). *Gene* **173**: 33–38.

Davis DA, Bruno VM, Loza L, Filler SG, Mitchell AP. 2002. *Candida albicans* Mds3p, a conserved regulator of pH responses and virulence identified through insertional mutagenesis. *Genetics* **162**: 1573–1581.

Enloe B, Diamond A, Mitchell AP. 2000. A single-transformation gene function test in diploid *Candida albicans*. *J Bacteriol* **182**: 5730–5736.

Fonzi WA, Irwin MY. 1993. Isogenic strain construction and gene mapping in *Candida albicans*. *Genetics* **134**: 717–728.

Gerami-Nejad M, Berman J, Gale CA. 2001. Cassettes for PCR-mediated construction of green, yellow, and cyan fluorescent protein fusions in *Candida albicans*. *Yeast* **18**: 859–864.

Gillum AM, Tsay EY, Kirsch DR. 1984. Isolation of the *Candida albicans* gene for orotidine-5′-phosphate decarboxylase by complementation of *S. cerevisiae ura3* and *E. coli pyr*F mutations. *Mol Gen Genet* **198**: 179–182.

Hull CM, Raisner RM, Johnson AD. 2000. Evidence for mating of the 'asexual' yeast *Candida albicans* in a mammalian host. *Science* **289**: 307–310.

Lockhart SR, Daniels KJ, Zhao R, Wessels D, Soll DR. 2003. Cell biology of mating in *Candida albicans*. *Eukaryot Cell* **2**: 49–61.

Magee BB, Magee PT. 2000. Induction of mating in *Candida albicans* by construction of MTL**a** and MTLα strains. *Science* **289**: 310–313.

Miller MG, Johnson AD. 2002. White–opaque switching in *Candida albicans* is controlled by mating-type locus homeodomain proteins and allows efficient mating. *Cell* **110**: 293–302.

Morschhäuser J, Michel S, Hacker J. 1998. Expression of a chromosomally integrated, single-copy GFP gene in *Candida albicans*, and its use as a reporter of gene regulation. *Mol Gen Genet* **257**: 412–420.

Perea S, Patterson TF. 2002. Antifungal resistance in pathogenic fungi. *Clin Infect Dis* **35**: 1073–1080.

Sambrook J, Fritsch EF, Maniatis T. 1989. *Molecular Cloning. A Laboratory Manual*, 2nd edn. Cold Spring Harbor Laboratory Press: New York.

Sanglard D, Odds F. 2002. Resistance of *Candida* species to antifungal agents: molecular mechanisms and clinical consequences. *Lancet Infect Dis* **2**: 73–85.

Wach A, Brachat A, Pöhlmann R, Philippsen P. 1994. New heterologous modules for classical or PCR-based gene disruptions in *Saccharomyces cerevisiae*. *Yeast* **10**: 1793–1808.

Walther A, Wendland J. 2003. An improved transformation protocol for the human fungal pathogen *Candida albicans*. *Curr Genet* **42**: 339–343.

Weig M, Haynes K, Rogers TR, *et al*. 2001. A GAS-like gene family in the pathogenic fungus *Candida glabrata*. *Microbiology* **147**: 2007–2019.

Wendland J. 2003. Analysis of the landmark protein Bud3 of *Ashbya gossypii* reveals a novel role in septum construction. *EMBO Rep* **4**: 200–204.

Wendland J, Ayad-Durieux Y, Knechtle P, Rebischung C, Philippsen P. 2000. PCR-based gene targeting in the filamentous fungus *Ashbya gossypii*. *Gene* **242**: 381–391.

Wilson RB, Davis D, Mitchell AP. 1999. Rapid hypothesis testing with *Candida albicans* through gene disruption with short homology regions. *J Bacteriol* **181**: 1868–1874.

9

Andrea Walther

Jürgen Wendland

Septation and cytokinesis in fungi.

Fungal Genet. Biol., 40(3): 187-196.

Die Zytokinese ist der letzte Schritt des Zellzyklus. In Pilzen erfolgt nach der Auswahl einer Teilungsstelle die geordnete Assemblierung von Proteinkomplexen an diese Stelle und anschließend die dynamische Konstriktion eines kontraktilen Ringes, die mit der Bildung eines Septums verbunden ist.

Available online at www.sciencedirect.com
SCIENCE DIRECT®
Fungal Genetics and Biology 40 (2003) 187–196
FUNGAL GENETICS AND BIOLOGY
www.elsevier.com/locate/yfgbi

Review

Septation and cytokinesis in fungi

Andrea Walther and Jürgen Wendland*

Junior Research Group, Growth-Control of Fungal Pathogens, Department of Microbiology, Hans-Knöll Institute, Friedrich-Schiller University Jena, Winzerlaer Str. 10, D-07745, Jena, Germany

Received 9 July 2003; accepted 26 August 2003

Abstract

Cytokinesis is the ultimate step of a cell cycle resulting in the generation of two progeny. Failure of correct cell division may be lethal for both, mother and daughter cells, and thus such a process must be tightly regulated with other events of the cell cyle. Differing solutions to the same problem have been developed in bacteria and plants while cytokinesis in animal and fungal cells is highly similar and requires a contractile ring containing actomyosin. Cytokinesis in fungi can be viewed as a three-stage process: (i) selection of a division site, (ii) orderly assembly of protein complexes, and finally (iii) dynamic events that lead to a constriction of the contractile ring and septum construction. Elaborate mechanisms known as the Mitotic Exit Network (MEN) and the Septation Initiation Network (SIN) have evolved to link these events, particularly the final steps of cytokinesis, with nuclear division. The purpose of this review was to discuss the latest developments in the fungal field and to describe the central known players required for key steps on the road to cell division. Differences in the cytokinesis of yeast-like fungi that result in complete cell separation in contrast to septation which leads to the compartmentalization of fungal hyphae are highlighted.

Keywords: Morphogenesis; Cell cycle; Septins; Septum formation; Actomyosin ring constriction; Mitotic Exit Network; Septation Initiation Network

1. Introduction

The ultimate goal of cell division is to separate mother and daughter cells into two individual units with appropriately segregated sets of chromosomes, organelles, and vesicles. Once all mitotic events have been completed, protein complexes at the division site act in a dynamic way to complete cell division. The basic idea of this process has been conserved from bacteria to plants, animals, and fungi (Nanninga, 2001). In general, the involvement of micotubules and actin is found. Even bacterial cells contain ancestral tubulin and actin, encoded by FtsZ and FtsA, respectively (Errington et al., 2003; Guertin et al., 2002). In plant cells, the division site is marked by the preprophase band. Upon division, microtubule-directed vesicle transport to the phragmoplast (a dense structure that contains microtubules and actin) provides the material to generate a cell plate, which grows outward and fuses with the cell wall at the sites marked by the preprophase band. In all other cell systems, contractile rings are employed to result in a constriction at the division site. Beyond this mechanistic similarities, conservation of macromolecular complexes is difficult to find. Cell division in fungal and animal cells, however, is highly conserved. A fact that has made *Schizosaccharomyces pombe* a simple model system to study these events in a very tractable organism (Feierbach and Chang, 2001). A major difference in fungal and animal cell division is that fungal cells construct a chitin rich septum at the division site.

Execution of the dynamic processes of cell division requires the integration and evaluation of signals coming from diverse cellular programs and is thus a highly complex process. In the following sections, the major events required for fungal cytokinesis are discussed including the coordination of cytokinesis with the completion of the nuclear cycle. Recent reviews have strengthened the view of similarities in cell division between prokaryotes and eukaryotes (Hales et al., 1999; Nanninga, 2001). In this review, every section will discuss differences between cytokinesis of yeast-like cells

* Corresponding author. Fax: +49-3641-65-7633.
E-mail address: juergen.wendland@uni-jena.de (J. Wendland).
URL: http://pinguin.biologie.uni-jena.de/phytopathologie/pathogenepilze/index.html.

1087-1845/$ - see front matter © 2003 Elsevier Inc. All rights reserved.
doi:10.1016/j.fgb.2003.08.005

and septation in filamentous fungi but also present homologs of conserved proteins found in the newly finished genome sequence of the filamentous fungus *Neurospora crassa* (Galagan et al., 2003; Hynes, 2003).

2. Selection of a division site

Two different mechanisms for the selection of a division site can be found in the budding yeast *Saccharomyces cerevisiae* and the fission yeast *S. pombe* (Fig. 1). In *S. cerevisiae* the cleavage plane is predetermined by the cell-type specific choice of a bud-site on the cell cortex (Chant, 1996). Haploid cells (either **a** or α) show an axial budding pattern in which the new site of bud emergence is chosen immediately adjacent to its previous division site, thus restricting budding events to the proximal cell pole. Diploid cells (**a**/α) exhibit a bipolar budding pattern, which allows the use of both poles for budding (Chant and Pringle, 1991, 1995; Freifelder, 1960). Similar to plant cells, where positioning of the preprophase band is thought to occur via landmark proteins, in yeast cortical proteins may provide the positional information to direct future budding events (Chant et al., 1991; Snyder et al., 1991). In case of the axial budding pattern, specific marker proteins such as Bud3p, Bud4p, or Axl2p/Bud10p appear to be transiently localized at the cortex (Chant and Herskowitz, 1991; Halme et al., 1996; Roemer et al., 1996; Sanders and Herskowitz, 1996). In contrast, the bipolar budding pattern relies on persistent cellular cues (Madden and Snyder, 1998; Ni and Snyder, 2001). Deletion of genes required for the axial budding pattern in haploid cells converts bud-site selection towards the the bipolar budding pattern whereas deletion of, for example, *BUD3* in diploid cells has no discernible phenotype. To establish the bipolar budding pattern different proteins, Bud8p and Bud9p, are used to mark either cell pole (Harkins et al., 2001; Zahner et al., 1996). Upon deletion of both alleles of *BUD8*, diploid cells use the proximal pole (the side of the cell that was connected to the mother cell) for budding. This is consistent with Bud8p localizing to the distal pole (Taheri et al., 2000; Harkins et al., 2001). Conversely, diploid *bud9*/*bud9* yeast cells bud at the distal pole (Zahner et al., 1996). Next to the landmark proteins, a GTPase module consisting of Bud1p-GTPase, Bud2p (GTPase activating protein), and Bud5p (guanine-nucleotide exchange factor) plays a central role for bud-site selection in yeast. Deletion of either of the genes of this module leads to a randomization of budding pattern in either cell-type (Chant and Herskowitz, 1991; Chant et al., 1991; Park et al., 1993). It is still largely unclear how these landmark proteins are positioned and signal to the Bud1p-module. Bud3p may use the spatial information provided by the septin ring (see below) for its localization (Chant et al., 1995). Axl2p, required for axial budding, directly interacts with Bud5p (Kang et al., 2001; Roemer et al., 1996). Activated Bud1p (Bud1p-GTP) may then recruit the cell polarity establishment Cdc42-module, which results in bud formation (Pruyne and Bretscher, 2000). Bud-site selection in yeast occurs prior to spindle formation. This requires a spatial coordination and realignment of spindle position with the mother-bud axis (Lee et al., 1999; Miller et al., 1999).

Selection of the division site in *S. pombe* is much more similar to animal cell. In *S. pombe*, the nucleus plays an essential role for the selection of the position of the division plane. Through interactions with the microtubule cytoskeleton nuclear position is kept in the

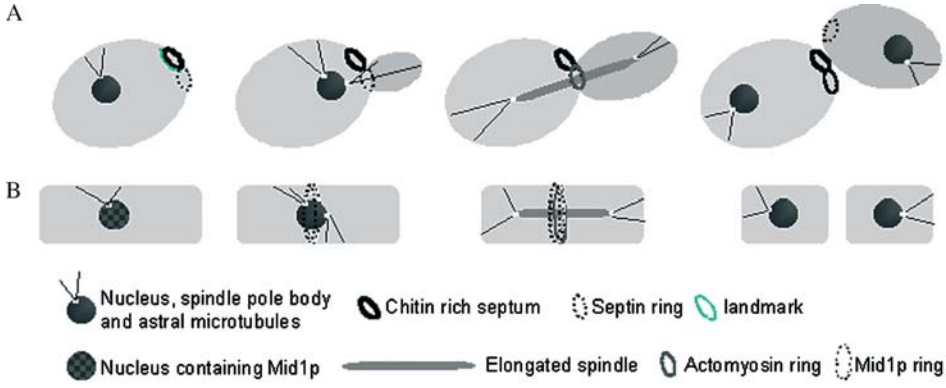

Fig. 1. Different mechanisms for the selection of a new division site. (A) In *S. cerevisiae*, the bud site selection machinery is involved in directing the septin ring at the incipient bud site. The division plane is thereby determined prior to spindle elongation. Although Myo1p localizes early to the bud neck, the complete actomyosin ring assembles much later. Upon bud emergence astral microtubules emanating from one spindle pole body (SPB) interact with the cell cortex of the daughter cell while microtubules from the other SPB interact with the mother cell cortex. This enables correct spindle positioning. After completion of nuclear division, the septin ring splits into two and the actomyosin ring constricts, which results in cytokinesis. (B) In the fission yeast *S. pombe*, the nucleus is positioned in the cell center by microtubule associated motor proteins using astral microtubules as well as microtubules that span the cytoplasm. Mid1p is localized to the nucleus and then exits the nucleus to form a ring that recruits the actomyosin ring. Spindle elongation occurs in the long axis of the cell. Actomyosin ring constriction and septum formation occur simultaneously. See text for details.

center of the cell (Tran et al., 2001). This is of importance, since mispositioning of the nucleus results in aberrant localization of the division plane (Chang et al., 1996). During interphase, the landmark protein Mid1p is localized in the nucleus. Upon phosphorylation, Mid1p exits from the nucleus and marks the cell cortex in the vicinity of the nucleus (potentially via a Pleckstrin homology (PH)-domain), thereby determining the site of division (Bahler and Pringle, 1998; Sohrmann et al., 1996). This rather simple mechanism of site selection may be conserved in higher eukaryotes, since Mid1p related proteins play an essential role in cytokinesis in *Drosophila* and human (Field and Alberts, 1995; Oegema et al., 2000).

The search for homologs of either Bud-proteins or Mid1-related proteins in dimorphic and filamentous fungi has revealed the presence of *BUD* genes in the dimorphic human fungal pathogen *Candida albicans* and in the filamentous fungus *Ashbya gossypii* (Wendland, 2003). This may be expected for species that are closely related to *S. cerevisiae*. During filamentous growth, however, bud-site selection may occur via different pathways. In *Aspergillus nidulans*, it was found that the microtubule motor protein nudA, encoding a dynein heavy chain, plays a role for nuclear positioning and for correct septum placement (Xiang et al., 1994). However, the underlying mechanism is still unknown. After spore germination, the position of the first septum was found to be at the bud neck separating germ cell and germ tube (the first hypha) in *A. gossypii* and *A. nidulans* (Wendland and Philippsen, 2000; Wolkow et al., 1996). In *C. albicans*, induction of hyphal growth has been shown to result in an altered position of the first septum, which is not placed at the bud neck but rather some distance away from the bud neck in the hyphal tube (Hazan et al., 2002). The hyphal tip has been speculated to be involved in determining septal sites in *A. nidulans* (Kaminskyj, 2000). In *A. gossypii*, it was recently shown that the growth speed of the hyphal tip is decreased during the formation of a lateral branch or a septum (Knechtle et al., in press). This may be explained by redirecting vesicle flow from a tip-ward direction to these sites. Interestingly, the decrease of tip growth generated positional information to produce a septum at this site once the hyphal tip had resumed growth and extended away from that position (Knechtle et al., in press). This argues in favor of a model in which a landmark protein for septation is positioned by the hyphal tip. The *A. gossypii* Bud3 protein may be one of these landmark proteins (Wendland, 2003). AgBud3p was found to be localized close to hyphal tips in a transient manner and was also found at future septal sites ahead of chitin depositioning (Wendland, 2003). Similarly, the branching frequency in *A. nidulans* was found to be increased when hyphal tip growth was reduced (Dynesen and Nielsen, in press).

Beyond these similarities between *A. gossypii* and *A. nidulans*, there may be evolutionary differences in the way hyphal growth is brought about. This centers around the questions whether hyphal growth is an ancient trait over yeast-like growth and if hyphal growth may have evolved independently several times. With our current knowledge we find that the closest relative to *A. gossypii* within the hemiascomycetous yeasts is the dimorphic plant pathogen *Holleya sinecauda* (Prillinger et al., 1997). This may open the possibility of an evolutionary developmental genetics approach to morphogenesis within this group of fungi (Schade et al., 2003).

Searching the *N. crassa* genome database (http://www-genome.wi.mit.edu/annotation/fungi/neurospora/) reveals several proteins with homology to bud site selection genes of *S. cerevisiae* (Table 1). Interestingly, within the *N. crassa* genome *S. cerevisiae* homologs were found that in yeast are required either for the haploid or the diploid budding pattern. The presence of *N. crassa* genes coding for proteins with strong amino acids identity to *S. cerevisiae* Rsr1p and Bud2p, belonging to the Bud1p-GTPase module, suggests a similar molecular mechanism for the selection of new hyphal branches (Table 1). In haploid *S. cerevisiae* cells, axial budding results in a spiral of bud scars. A new bud is generated adjacent to the bud scar of the previous cell cycle (Fig. 2A). Diploid yeast cells use both poles for budding but also generate these spirals (Fig. 2B). Diploid *C. albicans* cells also show bipolar budding pattern as their yeast relatives (Fig. 2C). *C. albicans* forms lateral branches under hyphae inducing conditions preferentially at sites of previous septation (Fig. 2D). Directing lateral branches at sites of septation also occurs in other

Table 1
N. crassa proteins with similarity to *S. cerevisiae* bud-site selection proteins[a]

Protein identifier	Best *S. cerevisiae* match	Blastp score
NCU04601.1	Axl2p	2e – 027
NCU02167.1	Bud1p/Rsr1p	2e – 048
NCU03852.1	Bud2p	4e – 044
NCU06579.1	Bud3p	5e – 006
NCU00152.1	Bud4p	3e – 019
NCU08469.1	Bud6p	2e – 046
NCU04511.1	Bud7p	1e – 065
NCU06649.1	Bud9p	0.034
NCU04362.1	Bud13p	3e – 009
NCU00006.1	Bud14p	8e – 012
NCU02364.1	Bud20p	8e – 015
NCU00777.1	Bud23p	4e – 074
NCU00417.1	Bud31p	4e – 044
NCU04595.1	Bud32p	3e – 019
NCU07090.1	Spa2p	3e – 019

[a] Tables 1–3 are intended to facilitate comparison between *N. crassa* and *S. cerevisiae*. It is a list of the major players in *S. cerevisiae* that were shown to be involved in the described processes and their respective closest match in *N. crassa* based on the *N. crassa* genome database (http://www-genome.wi.mit.edu/annotation/fungi/neurospora/).

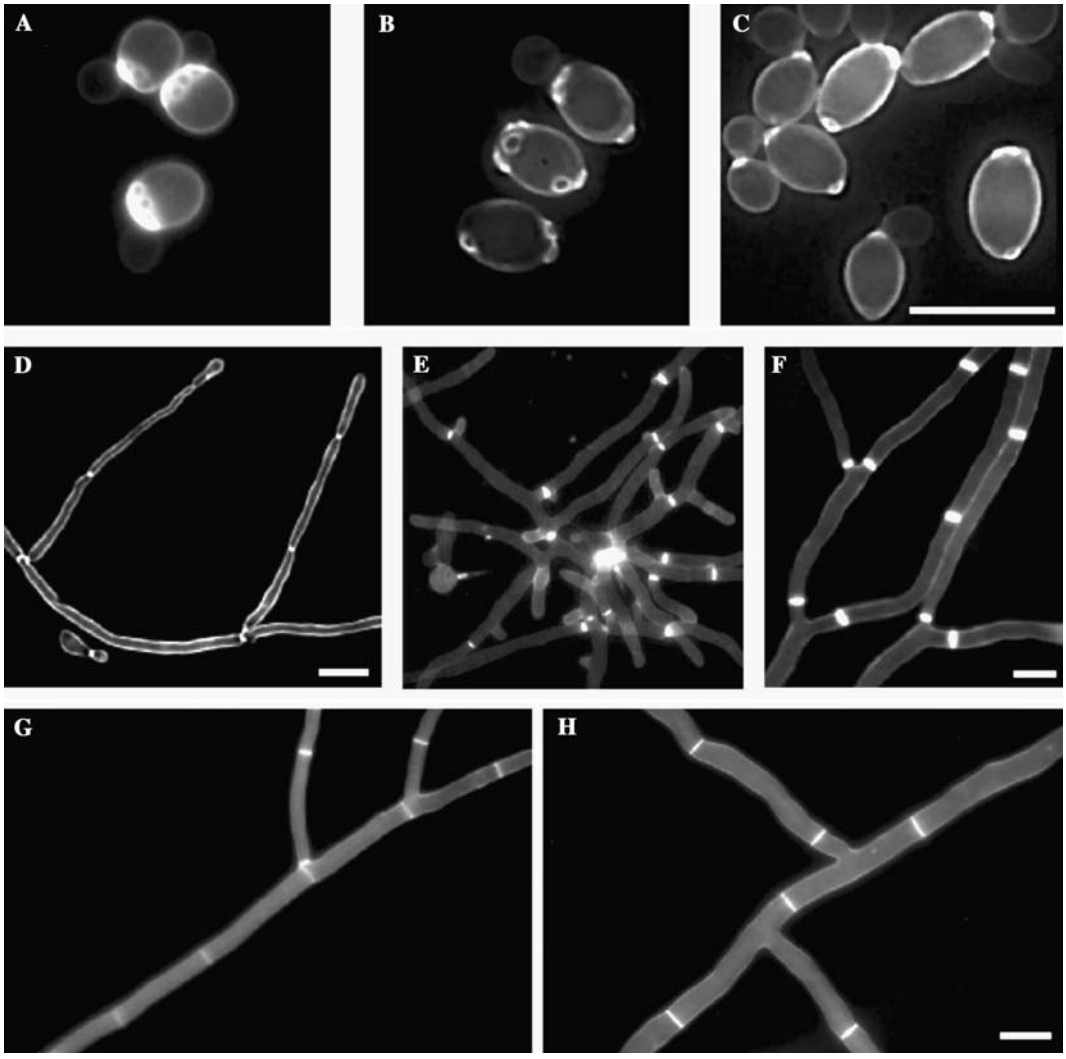

Fig. 2. Budding and branching pattern in ascomycetous fungi. Fungal strains were grown in complete media (in case of *C. albicans* supplemented with serum to induce hypha formation), stained with calcofluor, and photographed as described previously (Wendland and Philippsen, 2000). Images show haploid and diploid *S. cerevisiae* cells (A,B) with axial and bipolar budding patterns, respectively, *C. albicans*, which is a functional dipoid, also uses bipolar bud site selection during the yeast growth phase (C). Upon hyphal induction, a lateral branching pattern is evident in *C. albicans* in which branches occur at sites of previous septation (D). This is similar to the branching pattern in young *A. gossypii* mycelia (E) whereas adult mycelia proliferate via tip-branching (F). In *A. nidulans*, lateral branching can also be found at septal sites but may also occur at internal positions (G). In *N. crassa*, lateral branches generally occur in the middle of a hyphal compartment (H).

ascomycetous fungi, for example in *A. gossypii* (Fig. 2E). Lateral branching in *A. gossypii* is active in young mycelia whereas mature mycelia exhibit a dichotomous tip branching pattern (Fig. 2F) (Wendland and Philippsen, 2000). In *A. nidulans*, about 50% of lateral branches ($n = 500$) occur in the vicinity of septa whereas the other half seems to emerge in a random fashion (Fig. 2G). In *N. crassa*, lateral branching does not occur to be connected with septation, since lateral branches are generally formed in the middle of a cell compartment ($n = 500$) (Fig. 2H). In, depth analysis regarding the function of *BUD*-homologs in other filamentous fungi has yet to be initiated, since only the *A. gossypii BUD3* has been studied in detail (see below).

3. Assembly of protein complexes at the division site

Although quite different mechanisms operate in the selection of a new division site, subsequent events appear to be much more conserved in animal and fungal cells (Table 2). One aspect in which animal and fungal cells, however, differ from each other is the formation of a chitin rich septum in fungal cells, which is absent in animal cells. This is of particular interest to scientists studying human fungal, pathogens since this might present ideal opportunities for antifungal drug therapy.

In *S. cerevisiae*, the Cdc42-GTPase module initiates the assembly of a ring structure at the site of the next bud emergence. This is composed of septin family pro-

Table 2
N. crassa proteins with similarity to *S. cerevisiae* septation proteins

Protein identifier	Best *S. cerevisiae* match	Blastp score
NCU08297.1	Cdc3p (septin)	e – 104
NCU01998.1	Cdc3p (potential septin)	1e – 012
NCU03515.1	Cdc10 (septin)	e – 109
NCU02464.1	Cdc11 (septin)	2e – 072
NCU03795.1	Cdc12 (septin)	e – 127
NCU06454.1	Cdc42p	1e – 082
NCU00406.1	Cla4p	e – 105
NCU01431.1	Bni1p (formin)	3e – 085
NCU06617.1	Mlc1p (myosin light chain)	6e – 024
NCU03116.1	Cyk1p/Iqg1p (IQGAP-related protein)	4e – 048
NCU00551.1	Myo1p (myosin II heavy chain)	0.0
NCU04763.1	Cyk2p/Hof1p	9e – 017
NCU04095.1	Cyk3p	3e – 045

teins encoded by the *CDC3*, *CDC10*, *CDC11*, and *CDC12* genes (Gladfelter et al., 2001; Sanders and Field, 1994). The septin ring may serve several functions: (i) as a scaffold upon which numerous other proteins co-assemble to form a septum formation complex, (ii) as a rigid backbone that stabilizes the bud neck (Faty et al., 2002), (iii) as a barrier to maintain exocytosis and other factors directed to the daughter (Barral et al., 2000; Takizawa et al., 2000), and finally (iv) septins may play a role in the positioning of the spindle in the mother–daughter cell axis (Kusch et al., 2002). In *S. cerevisiae*, the Cdc42p-effector Cla4p (which shares some functions with Ste20p) is required for the maintenance of the architecture of the septin ring (Schmidt et al., 2003).

A central role in animal and fungal cytokinesis plays the contractile actomyosin ring (Mulvihill and Hyams, 2002; Straight et al., 2003). Some differences, however, exist in the timing of ring assembly between yeast and mammalian cells: in yeast, Myo1p is located at the bud neck prior to bud emergence and actin arrives there only at anaphase to assemble a functional actomyosin ring (Bi et al., 1998; Lippincott and Li, 1998). In animal cells, both proteins arrive at the same time in anaphase (Satterwhite and Pollard, 1992). In animal cells, the actomyosin ring is essential for viability whereas in *S. cerevisiae* viable strains were presented that lacked a functional actomyosin ring but were viable and produced separated cells (Bi et al., 1998). This is a feature rather specific to *S. cerevisiae* and may correlate to the small bud neck region that needs to be sealed. And, of course, actomyosin ring contraction and septum formation need to be coordinated in yeast whereas no septum formation occurs in animal cells (Bi, 2001). Two conserved classes of proteins, formins (encoded in *S. cerevisiae* by *BNI1* and *BNR1* and in *S. pombe* by *cdc12)* and IQGAP-related proteins (*ScCYK1*/*IQG1* and *Sprng2*), are essential for ring formation (Bi, 2001). Members of these protein classes were shown to interact with numerous other proteins. Formins are activated by the Rho1-GTPase and direct actin ring assembly (Tolliday et al., 2002). Cyk1p is a multidomain protein consisting of an N-terminal Calponin-homology domain, central "IQ"-repeats, and a C-terminal GTPase-activating protein domain (Shannon and Li, 1999). Fungal IQGAP-related proteins carry different numbers of these "IQ"-repeats, which share a basic consensus sequence of "$Q–X_3–RG–X_3–R$" (Wendland and Philippsen, 2002). In *S. cerevisiae*, *IQG1*/*CYK1* is an essential gene and is required for actin ring formation and cytokinesis (Epp and Chant, 1997; Lippincott and Li, 1998). In yeast, it appears that the septin ring recruits a myosin light chain, encoded by the *MLC1* gene, to the bud neck. Mlc1p localizes to the bud neck prior to Cyk1p/Iqg1p, interacts with Cyk1p/Iqg1p, and thus helps to localize Cyk1p/Iqg1p. In turn, Cyk1p/Iqg1p is required for actomyosin ring assembly and constriction. Another yeast protein that belongs to the conserved cdc15/PSTPIP family is encoded by *CYK2*. Deletion of *CYK2* leads to a cytokinesis defect (see below).

Fungal cells produce chitin rich septa upon cytokinesis/septation. Therefore, both processes need to be regulated in a temporal as well as spatial manner. In *S. cerevisiae*, chitin synthase III (Chs3p) synthesizes the chitin ring, which will remain after cytokinesis. This chitin ring represents the septum and is also referred to as the "bud scar" (Chuang and Schekman, 1996). Chitin ring formation starts early in the cell cycle. In *S. cerevisiae*, Bni4p interacts both with a septin (Cdc10p) and Chs4p, which is an activator of Chs3p (DeMarini et al., 1997). *CHS3* encodes the catalytic subunit of chitin synthase III.

The assembly of protein complexes is conserved in yeast-like and animal cells. Similar protein complexes (excluding the chitin synthesis machinery) are assembled at the cleavage site. Therefore, the search for homologous proteins belonging to the septin, formin, and IQGAP-related families should result in the identification of these genes in any filamentous fungus. Neither of these genes has been studied so far in *N. crassa*. However, with the genome sequence at hand it is straightforward to look at the repertoire of these homologs in this organism (Table 2). Interestingly, no Bnr1 homolog appeared in the database and only one copy of a *N. crassa* Bni1p occurred in addition to the septins, an IQGAP-related protein and others (Table 2). Furthermore, several sequences with a high degree of amino acids sequence identity to the *S. cerevisiae* Chs3p were found in the *N. crassa* database, which represents different classes of chitin synthases more similar to the situation found in *A. nidulans* (Horiuchi and Takagi, 1999).

Cdc42p is a highly conserved protein amongst eukaryotes (Johnson, 1999). *A. gossypii* Cdc42p serves similar functions of polarity establishment as its *S. cerevisiae* Cdc42p homolog (Wendland and Philippsen, 2001). In *Suillus bovinus*, Cdc42p was found to localize at growing hyphal tips indicating the constant

requirement of Cdc42p for hyphal growth (Gorfer et al., 2001). Septin genes are also well conserved in animal and fungal cells (Table 2) (Fares et al., 1995; Momany et al., 2001). In *A. gossypii*, several septin homologs were isolated by degenerate PCR. One of these, the *AgCDC3* gene, was deleted. The *Agcdc3* mutant strain was found to be viable but slowly growing and exhibited an inability to form septa (Wendland and Philippsen, unpublished). This is in contrast to the *A. nidulans CDC3* homolog, aspB, which could not be deleted and is therefore an essential gene (Momany and Hamer, 1997). Among *A. gossypii* mutants that fail to produce actin rings at septal sites are strains carrying a deletion of either of the *CLA4* or *CYK1* genes (Ayad-Durieux et al., 2000; Wendland and Philippsen, 2002). The analysis of *AgCLA4* indicates that Cdc42p-signaling is not only required for hyphal tip growth but is also essential for septation. Similarly, it was found in *A. nidulans* that another Rho-protein effector, the formin homolog SEPA, is required for actin ring formation and septation (Harris et al., 1997; Sharpless and Harris, 2002). The *A. gossypii CYK1* gene was studied in more detail (Wendland and Philippsen, 2002). Mutant *Agcyk1* strains were viable and tip growth occurred with a wildtype rate. However, mutant hyphae did not assemble any actin rings nor did they accumulate any chitin at presumptive septal sites. The inability to compartmentalize the hyphae resulted in an increased rate of loss of hyphae due to lysis at hyphal tips. This decreased the rate of survival of these hyphae leading to a much slower accumulation of biomass as compared to the wildtype (Wendland and Philippsen, 2002). Analysis of the *AgBUD3* gene showed that Bud3p may act as a landmark protein. Additionally, Bud3p has an important function for the construction of septa in *A gossypii* due to its role in correctly localizing Cyk1p. Loss of *BUD3* results in aberrantly localized Cyk1p, which was shown to form linear cables instead of rings resulting in the assembly of linear actin filaments instead of correct actin rings. Moreover, these linear actin structures were sufficient to direct targeted delivery of chitin rich vesicles to these sites, leading to the formation of chitin aggregates rather than septa (Wendland, 2003). This is in contrast to *S. cerevisiae* where deletion of *BUD3* has no phenotype in diploid cells and only alters the axial budding pattern in haploids to bipolar bud-site selection (Chant et al., 1995). Basically, a redundant system of proteins directing septum construction could be operational in yeast, which would compensate for a loss of *BUD3*. Further studies in these organisms will clarify the role of Bud3p in septation, particularly, defining the mode of localization of Bud3p to septal sites and determining other interacting proteins. Studies in filamentous fungi indicate that within hyphal tip compartments multiple sites of future septation can be marked. Actin rings are formed at these sites and septation complexes are formed that become activated in a spatially and temporally regulated manner (Wendland, 2003; Westfall and Momany, 2002).

4. Dynamic events leading to septum formation

In the previous chapters, proteins were discussed that play a role in actomyosin ring constriction and chitin accumulation. This chapter deals with the temporal and spatial coordination of these processes. The basic questions are: who arrives first, recruits the others, and finally initiates septum completion? Most of the proteins that localize to septal sites do so in a ring shape. In haploid *S. cerevisiae* cells, an interplay between the septin ring and Bud3p has been described. The septin ring assembles at the incipient bud site, remains there during bud growth, is split into two rings late in mitosis, and disappears after cytokinesis. Ring separation is dependent, for example, on Cdc15p, which is a proten kinase of the mitotic exit network (see below) (Cid et al., 2001; Li, 2000). Bud3p localizes in a very similar way as the septins and also undergoes ring separation. It was therefore proposed that localization of Bud3p and the septin ring is interconnected: first septins localize into a ring, which recruits Bud3p. After cytokinesis, it is the Bud3p ring that recruits the septins to the axial bud site in the next cell cycle (Chant et al., 1995). Conversely, the Cyk2p/Hof1p double rings merge into a single ring upon cytokinesis (Vallen et al., 2000). Of central importance is, of course, the dynamic constriction of the actomyosin ring. The N-terminal calponin homology domain of Cyk1p is responsible for actin ring assembly, whereas the C-terminal GAP-domain of Cyk1p is required for ring constriction. Ring constriction has been visualized by in vivo fluorescence time lapse microscopy and takes less than 5 min (Shannon and Li, 1999). Cyk1p is required for the constriction of the actomyosin ring, since deletion of *CYK1* results in a failure of Myo1p to constrict (Shannon and Li, 1999). The function of Hof1p (and that of Cyk3p for the same reasons) may link ring constriction with septum formation. Both proteins are multicopy suppressors of *cyk1*, even if they are not able to restore actin ring formation in *cyk1* mutant cells (Korinek et al., 2000).

In *A. gossypii*, Bud3p plays a more prominent role than in *S. cerevisiae*. It is participating in the localization of AgCyk1p to septal sites and provides positional information of where to form actin rings. This positional cue is somewhat redundant, since in *bud3* mutant hyphae occasional actin ring formation takes place (Wendland, 2003). In these cases, actin ring formation is then sufficient to trigger constriction and septum formation in the absence of Bud3p. Therefore, the role of Bud3p for septum construction lies in correct positioning of proteins. AgBud3p shares the dynamic features of its yeast homolog: it does not constrict but separates

into a double ring at septal sites concomitantly with chitin accumulation and septum completion (Wendland, 2003). The dynamics of AgCyk1p result in the constriction of the actomyosin ring. This dynamic behavior is the starting signal for chitin accumulation at septal sites that results in septum formation (Wendland and Philippsen, 2002). Basic differences in the timing of events are evident when comparing *A. nidulans* with *S. cerevisiae*. It was shown that the *A. nidulans* septin ASPB assembles downstream of the *A. nidulans* formin SEPA but also downstream of SEPH, which represents a *S. cerevisiae* Cdc15p homolog whose role will be discussed in the next chapter (Bruno et al., 2001; Westfall and Momany, 2002). Since the localization of SEPA is dependent on SEPH function, the order of events in *A. nidulans* requires SEPH, followed by the assembly of the formin SEPA and of the septin ring (Sharpless and Harris, 2002). SEPA-GFP was shown to localize to the septum as a ring. SEPA is required for actin ring formation and contraction of the SEPA ring was followed by chitin accumulation (Sharpless and Harris, 2002).

Finally, cytokinesis in yeast-like fungi results in the complete separation of mother and daughter cells. In contrast, septation in filamentous fungi leads to the generation of individual compartments within the hyphae. As a result, septal sites are not closed but contain septal pores, which interconnect the cytoplasm and even allow the passage of organelles. The passage of nuclei through septal sites has been observed in *A. gossypii* hyphae showing that septal sites are not closed, indicating that *A. gossypii* shows true hyphal growth (Alberti-Segui et al., 2001). Closure of the septal pore can be achieved by Woronin bodies (Jedd and Chua, 2000; Muller et al., 2000; Tenney et al., 2000; Yuan et al., 2003). This is important to the biology of filamentous fungi, since it may help us to preserve the integrity of hyphae once a hypha has been damaged lysis of the hyphal tip occurred (Bartnicki-Garcia and Lippman, 1972). Woronin bodies are not only found near septa but they (or their precursors) are also found at apical regions of *A. nidulans* hyphal tips (Momany et al., 2002). The mechanism of construction of the septal pore, either during septum formation or after septum completion, is at present unclear.

5. Coordination of cytokinesis with nuclear division

The central issue is that cytokinesis must not occur prior to the replication and segregation of the chromosomes (and also other essential organelles). Therefore, monitoring nuclear distribution and coupling it with the onset of cytokinesis is an efficient mechanism to ensure proper cell division. Cell cycle events in eukaryotic cells are controlled by the activity of cyclin dependent kinases (CDKs). Regulation of CDKs occurs at several levels, by their association with different cyclin subunits, by phase specific destruction of cyclins, and by phosphorylation of CDKs (Mendenhall and Hodge, 1998). In *A. nidulans*, for example, the CDK–cyclin complex of $NIMX^{cdc2}$–$NIME^{cyclinB}$ is inactivated by proteolysis of the cyclin at the exit of mitosis (Osmani and Ye, 1996). Next to CDKs, Polo kinase homologs have been shown to function not only in mitosis but also in cytokinesis (Song and Lee, 2001). In *S. pombe* and *S. cerevisiae*, GTPase modules linked to kinase cascades have been described that function to coordinate nuclear division with cytokinesis and are called SIN (Septation Initiation Network) and MEN (Mitotic Exit Network), respectively (Balasubramanian et al., 2000; McCollum and Gould, 2001). The basic function of SIN and MEN is the degradation of mitotic cyclins and/or the inhibition of CDK (Li, 2000). The timing of events, however, is not linear and individual proteins, such as the Polo kinase homologs Plo1p in *S. pombe* and Cdc5p in *S. cerevisiae*, may exercise multiple functions in the cell cycle (Guertin et al., 2002).

In *S. cerevisiae*, the GTPase module consists of the GTPase Tem1p, which is localized to the spindle pole body (SPB) and it is preferentially found at the SPB, which is targeted into the daughter cell (Bardin et al., 2000). Tem1p activity is controlled by GTPase activating proteins (GAP) and a guanine-nucleotide exchange factor (GEF). The GAP is composed of two proteins, encoded by the *BUB2* and *BFA1* genes (Furge et al., 1998; Pereira et al., 2000). The potential GEF is encoded by *LTE1*, which acts as a downstream effector protein of activated Ras (Shirayama et al., 1994; Yoshida et al., 2003). Whereas the GAPs also localize to the SPB, the Tem1p-GEF localizes to the daughter cell cortex (Pereira et al., 2000). This suggests a model in which the GTPase switch is turned on as soon as the SPB passes through the bud neck and reaches the daughter cell cortex after proper spindle elongation (Pereira et al., 2000). Once Tem1p is activated and GTP bound, it recruits Cdc15p. Cdc15 belongs to a set of kinases, which also includes Cdc5p and Dbf2p, which interacts with Mob1p (Luca and Winey, 1998). This cascade triggers release of Cdc14p phosphatase from the nucleolus that results in dephosphorylation of the target genes Cdh1p and Sic1p, which control cyclin destruction and CDK inactivation, respectively (Jaspersen et al., 1998; Shou et al., 1999; Visintin et al., 1999). How is the exit of mitosis then linked with cytokinesis? Localization studies have provided some further insight into *S. cerevisiae*. The kinases have all been found to localize to the bud neck in yeast (Guertin et al., 2002). More importantly, MEN also functions in septin ring division and actomyosin ring constriction (Lippincott et al., 2001). The exact mechanism, however, remains to be resolved.

Although SIN and MEN components are highly conserved and can be readily identified in fungi as is shown for *N. crassa* (see Table 3), only one MEN component has recently been studied in a filamentous fungus.

Table 3
N. crassa proteins with similarity to *S. cerevisiae* Mitotic Exit Network proteins

Protein identifier	Best *S. cerevisiae* match	Blastp score
NCU008878.1	Tem1p	2e – 065
NCU03379.1	Lte1p	2e – 041
NCU03237.1	Bub2p	1e – 050
NCU01584.1	Bfa1p	9e – 006
NCU01335.1	Cdc15p	3e – 053
NCU09258.1	Cdc5p	2e – 063
NCU09071.1	Dbf2p	e – 135
NCU01605.1	Mob1p	5e – 051
NCU03246.1	Cdc14p	2e – 098
NCU01269.1	Cdh1p	e – 105

SepH was shown to encode a protein homologous to Cdc15p of *S. cerevisiae*. Here, surprisingly, SEPH functions upstream of actin ring formation (Bruno et al., 2001). Several other temperature sensitive *sep* mutants were isolated of which only the formin *sepA* has been characterized in detail (Harris et al., 1994; Harris et al., 1997; Sharpless and Harris, 2002). And given the phenotypic similarity of certain alleles of *sepD* and *sepG* with *sepH* mutants, these genes may encode other components of the SIN/MEN network in *A. nidulans* (Harris, 2001). Cytokinesis in *A. nidulans* is dependent on nuclear positioning and mitosis (Wolkow et al., 1996; Westfall and Momany, 2002). Recently, it has been shown that septation follows the mitotic wave in a hyphal tip to base like manner in *A. nidulans* (Westfall and Momany, 2002). The opposite, however, has been found in *A. gossypii* in which septation in the hyphal tip compartment starts at the basal septum of the tip compartment and progresses towards the hyphal tip (Wendland and Philippsen, 2002). This might reflect different states of mitosis in these two fungi. Interestingly, opposite phenotypes were also demonstrated in these two fungal species regarding the dynein heavy chain mutants (Alberti-Segui et al., 2001; Xiang et al., 1994).

6. Conclusions

Septation and cytokinesis of filamentous and yeast-like fungi bear key similarities, particularly in the assembly of septation complexes and the dynamic events of splitting septin rings and of actomyosin ring constriction. Central players are conserved not only in fungi but also in animal cells. Differences occur in the mechanism of selecting future sites of septation and in the coordination of septation with other cellular events. Therefore, future studies in filamentous fungi will have to solve these puzzles at the molecular level and may likely come up with new solutions to the general problem of how to divide. Since these processes are dynamic and cell cycle regulated, modern cell biology and in vivo protein localization studies will be most valuable tools in this research area.

Acknowledgments

We thank Yasmina Bauer and Novartis AG for providing the *N. crassa* and *A. nidulans* strains. J.W. is supported by the Deutsche Forschungsgemeinschaft (We2634/2-4-1).

References

Alberti-Segui, C., Dietrich, F., Altmann-Johl, R., Hoepfner, D., Philippsen, P., 2001. Cytoplasmic dynein is required to oppose the force that moves nuclei towards the hyphal tip in the filamentous ascomycete *Ashbya gossypii*. J. Cell Sci. 114, 975–986.

Ayad-Durieux, Y., Knechtle, P., Goff, S., Dietrich, F., Philippsen, P., 2000. A PAK-like protein kinase is required for maturation of young hyphae and septation in the filamentous ascomycete *Ashbya gossypii*. J. Cell Sci. 113, 4563–4575.

Bahler, J., Pringle, J.R., 1998. Pom1p, a fission yeast protein kinase that provides positional information for both polarized growth and cytokinesis. Genes Dev. 12, 1356–1370.

Balasubramanian, M.K., McCollum, D., Surana, U., 2000. Tying the knot: linking cytokinesis to the nuclear cycle. J. Cell Sci. 113, 1503–1513.

Bardin, A.J., Visintin, R., Amon, A., 2000. A mechanism for coupling exit from mitosis to partitioning of the nucleus. Cell 102, 21–31.

Barral, Y., Mermall, V., Mooseker, M.S., Snyder, M., 2000. Compartmentalization of the cell cortex by septins is required for maintenance of cell polarity in yeast. Mol. Cell 5, 841–851.

Bartnicki-Garcia, S., Lippman, E., 1972. The bursting tendency of hyphal tips of fungi: presumptive evidence for a delicate balance between wall synthesis and wall lysis in apical growth. J. Gen. Microbiol. 73, 487–500.

Bi, E., 2001. Cytokinesis in budding yeast: the relationship between actomyosin ring function and septum formation. Cell Struct. Funct. 26, 529–537.

Bi, E., Maddox, P., Lew, D.J., Salmon, E.D., McMillan, J.N., Yeh, E., Pringle, J.R., 1998. Involvement of an actomyosin contractile ring in *Saccharomyces cerevisiae* cytokinesis. J. Cell Biol. 142, 1301–1312.

Bruno, K.S., Morrell, J.L., Hamer, J.E., Staiger, C.J., 2001. SEPH, a Cdc7p orthologue from *Aspergillus nidulans*, functions upstream of actin ring formation during cytokinesis. Mol. Microbiol. 42, 3–12.

Chang, F., Woollard, A., Nurse, P., 1996. Isolation and characterization of fission yeast mutants defective in the assembly and placement of the contractile actin ring. J. Cell Sci. 109, 131–142.

Chant, J., 1996. Generation of cell polarity in yeast. Curr. Opin. Cell Biol. 8, 557–565.

Chant, J., Herskowitz, I., 1991. Genetic control of bud site selection in yeast by a set of gene products that constitute a morphogenetic pathway. Cell 65, 1203–1212.

Chant, J., Pringle, J.R., 1991. Budding and cell polarity in *Saccharomyces cerevisiae*. Curr. Opin. Genet. Dev. 1, 342–350.

Chant, J., Pringle, J.R., 1995. Patterns of bud-site selection in the yeast *Saccharomyces cerevisiae*. J. Cell Biol. 129, 751–765.

Chant, J., Corrado, K., Pringle, J.R., Herskowitz, I., 1991. Yeast BUD5, encoding a putative GDP–GTP exchange factor, is necessary for bud site selection and interacts with bud formation gene *BEM1*. Cell 65, 1213–1224.

Chant, J., Mischke, M., Mitchell, E., Herskowitz, I., Pringle, J.R., 1995. Role of Bud3p in producing the axial budding pattern of yeast. J. Cell Biol. 129, 767–778.

Chuang, J.S., Schekman, R.W., 1996. Differential trafficking and timed localization of two chitin synthase proteins, Chs2p and Chs3p. J. Cell Biol. 135, 597–610.

Cid, V.J., Adamikova, L., Sanchez, M., Molina, M., Nombela, C., 2001. Cell cycle control of septin ring dynamics in the budding yeast. Microbiology 147, 1437–1450.

DeMarini, D.J., Adams, A.E., Fares, H., De Virgilio, C., Valle, G., Chuang, J.S., Pringle, J.R., 1997. A septin-based hierarchy of proteins required for localized deposition of chitin in the *Saccharomyces cerevisiae* cell wall. J. Cell Biol. 139, 75–93.

Dynesen, J., Nielsen, J., in press. Branching is coordinated with mitosis in the growing hyphae of *A. nidulans*. Fungal Genet. Biol.

Epp, J.A., Chant, J., 1997. An IQGAP-related protein controls actin-ring formation and cytokinesis in yeast. Curr. Biol. 7, 921–929.

Errington, J., Daniel, R.A., Scheffers, D.J., 2003. Cytokinesis in bacteria. Microbiol. Mol. Biol. Rev. 67, 52–65, table of contents.

Fares, H., Peifer, M., Pringle, J.R., 1995. Localization and possible functions of *Drosophila* septins. Mol. Biol. Cell 6, 1843–1859.

Faty, M., Fink, M., Barral, Y., 2002. Septins: a ring to part mother and daughter. Curr. Genet. 41, 123–131.

Feierbach, B., Chang, F., 2001. Cytokinesis and the contractile ring in fission yeast. Curr. Opin. Microbiol. 4, 713–719.

Field, C.M., Alberts, B.M., 1995. Anillin, a contractile ring protein that cycles from the nucleus to the cell cortex. J. Cell Biol. 131, 165–178.

Freifelder, D., 1960. Bud position in *Saccharomyces cerevisiae*. J. Bacteriol. 80, 567–580.

Furge, K.A., Wong, K., Armstrong, J., Balasubramanian, M., Albright, C.F., 1998. Byr4 and Cdc16 form a two-component GTPase-activating protein for the Spg1 GTPase that controls septation in fission yeast. Curr. Biol. 8, 947–954.

Galagan, J.E., Calvo, S.E., Borkovich, K.A., Selker, E.U., Read, N.D., Jaffe, D., FitzHugh, W., Ma, L.J., Smirnov, S., Purcell, S., Rehman, B., Elkins, T., Engels, R., Wang, S., Nielsen, C.B., Butler, J., Endrizzi, M., Qui, D., Ianakiev, P., Bell-Pedersen, D., Nelson, M.A., Werner-Washburne, M., Selitrennikoff, C.P., Kinsey, J.A., Braun, E.L., Zelter, A., Schulte, U., Kothe, G.O., Jedd, G., Mewes, W., Staben, C., Marcotte, E., Greenberg, D., Roy, A., Foley, K., Naylor, J., Stange-Thomann, N., Barrett, R., Gnerre, S., Kamal, M., Kamvysselis, M., Mauceli, E., Bielke, C., Rudd, S., Frishman, D., Krystofova, S., Rasmussen, C., Metzenberg, R.L., Perkins, D.D., Kroken, S., Cogoni, C., Macino, G., Catcheside, D., Li, W., Pratt, R.J., Osmani, S.A., DeSouza, C.P., Glass, L., Orbach, M.J., Berglund, J.A., Voelker, R., Yarden, O., Plamann, M., Seiler, S., Dunlap, J., Radford, A., Aramayo, R., Natvig, D.O., Alex, L.A., Mannhaupt, G., Ebbole, D.J., Freitag, M., Paulsen, I., Sachs, M.S., Lander, E.S., Nusbaum, C., Birren, B., 2003. The genome sequence of the filamentous fungus *Neurospora crassa*. Nature 422, 859–868.

Gladfelter, A.S., Pringle, J.R., Lew, D.J., 2001. The septin cortex at the yeast mother-bud neck. Curr. Opin. Microbiol. 4, 681–689.

Gorfer, M., Tarkka, M.T., Hanif, M., Pardo, A.G., Laitiainen, E., Raudaskoski, M., 2001. Characterization of small GTPases Cdc42 and Rac, and relationship between Cdc42 and actin cytoskeleton in vegetative and ectomycorrhizal hyphae of *Suillus bovinus*. Mol. Plant Microbe Interact. 14, 135–144.

Guertin, D.A., Venkatram, S., Gould, K.L., McCollum, D., 2002. Dma1 prevents mitotic exit and cytokinesis by inhibiting the septation initiation network (SIN). Dev. Cell 3, 779–790.

Hales, K.G., Bi, E., Wu, J.Q., Adam, J.C., Yu, I.C., Pringle, J.R., 1999. Cytokinesis: an emerging unified theory for eukaryotes? Curr. Opin. Cell Biol. 11, 717–725.

Halme, A., Michelitch, M., Mitchell, E.L., Chant, J., 1996. Bud10p directs axial cell polarization in budding yeast and resembles a transmembrane receptor. Curr. Biol. 6, 570–579.

Harkins, H.A., Page, N., Schenkman, L.R., De Virgilio, C., Shaw, S., Bussey, H., Pringle, J.R., 2001. Bud8p and Bud9p, proteins that may mark the sites for bipolar budding in yeast. Mol. Biol. Cell 12, 2497–2518.

Harris, S.D., 2001. Septum formation in *Aspergillus nidulans*. Curr. Opin. Microbiol. 4, 736–739.

Harris, S.D., Hamer, L., Sharpless, K.E., Hamer, J.E., 1997. The *Aspergillus nidulans* sepA gene encodes an FH1/2 protein involved in cytokinesis and the maintenance of cellular polarity. EMBO J. 16, 3474–3483.

Harris, S.D., Morrell, J.L., Hamer, J.E., 1994. Identification and characterization of *Aspergillus nidulans* mutants defective in cytokinesis. Genetics 136, 517–532.

Hazan, I., Sepulveda-Becerra, M., Liu, H., 2002. Hyphal elongation is regulated independently of cell cycle in *Candida albicans*. Mol. Biol. Cell 13, 134–145.

Horiuchi, H., Takagi, M., 1999. Chitin synthase genes of *Aspergillus species*. Contrib. Microbiol. 2, 193–204.

Hynes, M.J., 2003. The *Neurospora crassa* genome opens up the world of filamentous fungi. Genome Biol. 4, 217.

Jaspersen, S.L., Charles, J.F., Tinker-Kulberg, R.L., Morgan, D.O., 1998. A late mitotic regulatory network controlling cyclin destruction in *Saccharomyces cerevisiae*. Mol. Biol. Cell 9, 2803–2817.

Jedd, G., Chua, N.H., 2000. A new self-assembled peroxisomal vesicle required for efficient resealing of the plasma membrane. Nat. Cell Biol. 2, 226–231.

Johnson, D.I., 1999. Cdc42: an essential Rho-type GTPase controlling eukaryotic cell polarity. Microbiol. Mol. Biol. Rev. 63, 54–105.

Kaminskyj, S.G., 2000. Septum position is marked at the tip of *Aspergillus nidulans* hyphae. Fungal Genet. Biol. 31, 105–113.

Kang, P.J., Sanson, A., Lee, B., Park, H.O., 2001. A GDP/GTP exchange factor involved in linking a spatial landmark to cell polarity. Science 292, 1376–1378.

Knechtle, P., Dietrich, F., Philippsen, P., in press. Maximal polar growth potential depends on the polarisome component AgSpa2 in the filamentous fungus *Ashbya gossypii*. Mol. Biol. Cell.

Korinek, W.S., Bi, E., Epp, J.A., Wang, L., Ho, J., Chant, J., 2000. Cyk3, a novel SH3-domain protein, affects cytokinesis in yeast. Curr. Biol. 10, 947–950.

Kusch, J., Meyer, A., Snyder, M.P., Barral, Y., 2002. Microtubule capture by the cleavage apparatus is required for proper spindle positioning in yeast. Genes Dev. 16, 1627–1639.

Lee, L., Klee, S.K., Evangelista, M., Boone, C., Pellman, D., 1999. Control of mitotic spindle position by the *Saccharomyces cerevisiae* formin Bni1p. J. Cell Biol. 144, 947–961.

Li, R., 2000. Mitosis: shutting the door behind. Curr. Biol. 10, 781–784.

Lippincott, J., Li, R., 1998. Sequential assembly of myosin II, an IQGAP-like protein, and filamentous actin to a ring structure involved in budding yeast cytokinesis. J. Cell Biol. 140, 355–366.

Lippincott, J., Shannon, K.B., Shou, W., Deshaies, R.J., Li, R., 2001. The Tem1 small GTPase controls actomyosin and septin dynamics during cytokinesis. J. Cell Sci. 114, 1379–1386.

Luca, F.C., Winey, M., 1998. MOB1, an essential yeast gene required for completion of mitosis and maintenance of ploidy. Mol. Biol. Cell 9, 29–46.

Madden, K., Snyder, M., 1998. Cell polarity and morphogenesis in budding yeast. Annu. Rev. Microbiol. 52, 687–744.

McCollum, D., Gould, K.L., 2001. Timing is everything: regulation of mitotic exit and cytokinesis by the MEN and SIN. Trends Cell Biol. 11, 89–95.

Mendenhall, M.D., Hodge, A.E., 1998. Regulation of Cdc28 cyclin-dependent protein kinase activity during the cell cycle of the yeast *Saccharomyces cerevisiae*. Microbiol. Mol. Biol. Rev. 62, 1191–1243.

Matheos, D., Rose, M.D., 1999. The cortical localization of the microtubule orientation protein, Kar9p, is dependent upon actin and proteins required for polarization. J. Cell Biol. 144, 963–975.

Momany, M., Zhao, J., Lindsey, R., Westfall, P.J., 2001. Characterization of the *Aspergillus nidulans* septin (asp) gene family. Genetics 157, 969–977.

Momany, M., Hamer, J.E., 1997. Relationship of actin, microtubules, and crosswall synthesis during septation in *Aspergillus nidulans*. Cell Motil. Cytoskeleton 38, 373–384.

Momany, M., Richardson, E.A., VanSickle, C., 2002. Mapping Woronin body position in *Aspergillus nidulans*. Mycologia 94, 260–266.

Muller, C., Spohr, A.B., Nielsen, J., 2000. Role of substrate concentration in mitosis and hyphal extension of *Aspergillus*. Biotechnol. Bioeng. 67, 390–397.

Mulvihill, D.P., Hyams, J.S., 2002. Cytokinetic actomyosin ring formation and septation in fission yeast are dependent on the full recruitment of the polo-like kinase Plo1 to the spindle pole body and a functional spindle assembly checkpoint. J. Cell Sci. 115, 3575–3586.

Nanninga, N., 2001. Cytokinesis in prokaryotes and eukaryotes: common principles and different solutions. Microbiol. Mol. Biol. Rev. 65, 319–333.

Ni, L., Snyder, M., 2001. A genomic study of the bipolar bud site selection pattern in *Saccharomyces cerevisiae*. Mol. Biol. Cell 12, 2147–2170.

Oegema, K., Savoian, M.S., Mitchison, T.J., Field, C.M., 2000. Functional analysis of a human homologue of the *Drosophila* actin binding protein anillin suggests a role in cytokinesis. J. Cell Biol. 150, 539–552.

Osmani, S.A., Ye, X.S., 1996. Cell cycle regulation in *Aspergillus* by two protein kinases. Biochem. J. 317, 633–641.

Park, H.O., Chant, J., Herskowitz, I., 1993. *BUD2* encodes a GTPase-activating protein for Bud1/Rsr1 necessary for proper bud-site selection in yeast. Nature 365, 269–274.

Pereira, G., Hofken, T., Grindlay, J., Manson, C., Schiebel, E., 2000. The Bub2p spindle checkpoint links nuclear migration with mitotic exit. Mol. Cell 6, 1–10.

Prillinger, H., Schweigkofler, W., Breitenbach, M., Briza, P., Staudacher, E., Lopandic, K., Molnar, O., Weigang, F., Ibl, M., Ellinger, A., 1997. Phytopathogenic filamentous (*Ashbya*, *Eremothecium*) and dimorphic fungi (*Holleya*, *Nematospora*) with needle-shaped ascospores as new members within the *Saccharomycetaceae*. Yeast 13, 945–960.

Pruyne, D., Bretscher, A., 2000. Polarization of cell growth in yeast. I. Establishment and maintenance of polarity states. J. Cell Sci. 113, 365–375.

Roemer, T., Madden, K., Chang, J., Snyder, M., 1996. Selection of axial growth sites in yeast requires Axl2p, a novel plasma membrane glycoprotein. Genes Dev. 10, 777–793.

Sanders, S.L., Field, C.M., 1994. Cell division. Septins in common? Curr. Biol. 4, 907–910.

Sanders, S.L., Herskowitz, I., 1996. The Bud4 protein of yeast, required for axial budding, is localized to the mother/BUD neck in a cell cycle-dependent manner. J. Cell Biol. 134, 413–427.

Satterwhite, L.L., Pollard, T.D., 1992. Cytokinesis Curr. Opin. Cell Biol. 4, 43–52.

Schade, D., Walther, A., Wendland, J., 2003. The development of a transformation system for the dimorphic plant pathogen *Holleya sinecauda* based on *Ashbya gossypii* DNA elements. Fungal Genet. Biol. 40, 65–71.

Schmidt, M., Varma, A., Drgon, T., Bowers, B., Cabib, E., 2003. Septins, under Cla4p regulation, and the chitin ring are required for neck integrity in budding yeast. Mol. Biol. Cell 14, 2128–2141.

Shannon, K.B., Li, R., 1999. The multiple roles of Cyk1p in the assembly and function of the actomyosin ring in budding yeast. Mol. Biol. Cell 10, 283–296.

Sharpless, K.E., Harris, S.D., 2002. Functional characterization and localization of the *Aspergillus nidulans* formin SEPA. Mol. Biol. Cell 13, 469–479.

Shirayama, M., Matsui, Y., Tanaka, K., Toh-e, A., 1994. Isolation of a *CDC25* family gene, *MSI2/LTE1*, as a multicopy suppressor of *ira1*. Yeast 10, 451–461.

Shou, W., Seol, J.H., Shevchenko, A., Baskerville, C., Moazed, D., Chen, Z.W., Jang, J., Charbonneau, H., Deshaies, R.J., 1999. Exit from mitosis is triggered by Tem1-dependent release of the protein phosphatase Cdc14 from nucleolar RENT complex. Cell 97, 233–244.

Snyder, M., Gehrung, S., Page, B.D., 1991. Studies concerning the temporal and genetic control of cell polarity in *Saccharomyces cerevisiae*. J. Cell Biol. 114, 515–532.

Sohrmann, M., Fankhauser, C., Brodbeck, C., Simanis, V., 1996. The *dmf1/mid1* gene is essential for correct positioning of the division septum in fission yeast. Genes Dev. 10, 2707–2719.

Song, S., Lee, K.S., 2001. A novel function of *Saccharomyces cerevisiae CDC5* in cytokinesis. J. Cell Biol. 152, 451–469.

Straight, A.F., Cheung, A., Limouze, J., Chen, I., Westwood, N.J., Sellers, J.R., Mitchison, T.J., 2003. Dissecting temporal and spatial control of cytokinesis with a myosin II inhibitor. Science 299, 1743–1747.

Taheri, N., Kohler, T., Braus, G.H., Mosch, H.U., 2000. Asymmetrically localized Bud8p and Bud9p proteins control yeast cell polarity and development. EMBO J. 19, 6686–6696.

Takizawa, P.A., DeRisi, J.L., Wilhelm, J.E., Vale, R.D., 2000. Plasma membrane compartmentalization in yeast by messenger RNA transport and a septin diffusion barrier. Science 290, 341–344.

Tenney, K., Hunt, I., Sweigard, J., Pounder, J.I., McClain, C., Bowman, E.J., Bowman, B.J., 2000. *Hex-1*, a gene unique to filamentous fungi, encodes the major protein of the Woronin body and functions as a plug for septal pores. Fungal Genet. Biol. 31, 205–217.

Tolliday, N., VerPlank, L., Li, R., 2002. Rho1 directs formin-mediated actin ring assembly during budding yeast cytokinesis. Curr. Biol. 12, 1864–1870.

Tran, P.T., Marsh, L., Doye, V., Inoue, S., Chang, F., 2001. A mechanism for nuclear positioning in fission yeast based on microtubule pushing. J. Cell Biol. 153, 397–411.

Vallen, E.A., Caviston, J., Bi, E., 2000. Roles of Hof1p, Bni1p, Bnr1p, and myo1p in cytokinesis in *Saccharomyces cerevisiae*. Mol. Biol. Cell 11, 593–611.

Visintin, R., Hwang, E.S., Amon, A., 1999. Cfi1 prevents premature exit from mitosis by anchoring Cdc14 phosphatase in the nucleolus. Nature 398, 818–823.

Wendland, J., 2003. Analysis of the landmark protein Bud3 of *Ashbya gossypii* reveals a novel role in septum construction. EMBO Rep. 4, 200–204.

Wendland, J., Philippsen, P., 2002. An IQGAP-related protein, encoded by *AgCYK1*, is required for septation in the filamentous fungus *Ashbya gossypii*. Fungal Genet. Biol. 37, 81–88.

Wendland, J., Philippsen, P., 2001. Cell polarity and hyphal morphogenesis are controlled by multiple Rho-protein modules in the filamentous ascomycete *Ashbya gossypii*. Genetics 157, 601–610.

Wendland, J., Philippsen, P., 2000. Determination of cell polarity in germinated spores and hyphal tips of the filamentous ascomycete *Ashbya gossypii* requires a rhoGAP homolog. J. Cell Sci. 113, 1611–1621.

Westfall, P.J., Momany, M., 2002. *Aspergillus nidulans* septin AspB plays pre- and postmitotic roles in septum, branch, and conidiophore development. Mol. Biol. Cell 13, 110–118.

Wolkow, T.D., Harris, S.D., Hamer, J.E., 1996. Cytokinesis in *Aspergillus nidulans* is controlled by cell size, nuclear positioning and mitosis. J. Cell Sci. 109, 2179–2188.

Xiang, X., Beckwith, S.M., Morris, N.R., 1994. Cytoplasmic dynein is involved in nuclear migration in *Aspergillus nidulans*. Proc. Natl. Acad. Sci. USA 91, 2100–2104.

Yoshida, S., Ichihashi, R., Toh-e, A., 2003. Ras recruits mitotic exit regulator Lte1 to the bud cortex in budding yeast. J. Cell Biol. 161, 889–897.

Yuan, P., Jedd, G., Kumaran, D., Swaminathan, S., Shio, H., Hewitt, D., Chua, N.H., Swaminathan, K., 2003. A HEX-1 crystal lattice required for Woronin body function in *Neurospora crassa*. Nat. Struct. Biol. 10, 264–270.

Zahner, J.E., Harkins, H.A., Pringle, J.R., 1996. Genetic analysis of the bipolar pattern of bud site selection in the yeast *Saccharomyces cerevisiae*. Mol. Cell Biol. 16, 1857–1870.

12. Anhang

12.1. CD-ROM der Dissertation

Im Bucheinband dieser Arbeit sind auf einer CD-ROM alle Zeitrafferaufnahmen dieser Arbeit, die Originalpublikationen und die Dissertation im PDF-Format enthalten.
Die Zeitrafferaufnahmen können durch Starten der Datei **start.html** ausgewählt werden. Sie befinden sich außerdem nach Publikationen sortiert im MPG-Format auf der CD. Sollten die Filme nicht abspielbar sein, sollte der Quicktime-Player zusätzlich installiert werden. Dieser befindet sich in einem separaten Ordner auf dieser CD.